DEPARTAMENT DE MICROBIOLOGIA I ECOLOGIA

ECOLOGÍA Y GEOQUÍMICA DE OSTRÁCODOS COMO INDICADORES PALEOAMBIENTALES EN AMBIENTES MARGINALES MARINOS: UN EJEMPLO DE ESTUDIO, LA ALBUFERA DE VALENCIA.

JAVIER MARCO BARBA

UNIVERSITAT DE VALÈNCIA
Servei de Publicacions
2010

Aquesta Tesi Doctoral va ser presentada a València el dia 23 d'abril de 2010 davant un tribunal format per:

- Dr. Blas Valero Garcés
- Dr. Eduardo Vicente Pedrós
- Dr. Pere Anadón Monzón
- Dr. Carlos de Santisteban Bové

Va ser dirigida per:
Dra. Rosa Miracle Solé
Dr. Francesc Mezquita i Juanes

©Copyright: Servei de Publicacions
Javier Marco Barba

Dipòsit legal: V-2102-2011
I.S.B.N.: 978-84-370-7865-6
Edita: Universitat de València
Servei de Publicacions
C/ Arts Gràfiques, 13 baix
46010 València
Spain
Telèfon:(0034)963864115

Instituto Cavanilles de Biodiversidad y Biología Evolutiva

Ecología y geoquímica de ostrácodos como indicadores paleoambientales en ambientes marginales marinos: un ejemplo de estudio, la Albufera de Valencia

Freshwater ostracods ecology and geochemistry as paleoenvironmental indicators in marginal marine ecosystems: a case of study, the Albufera de Valencia

Tesis doctoral presentada por

Javier Marco Barba

2010

Dirigida por

Dra. M^{a}Rosa Miracle

Dr. F. Mezquita

Tesis presentada por JAVIER MARCO BARBA para optar al grado de Doctor en Ciencias Biológicas por la Universidad de Valencia.

Firmado: Javier Marco Barba

Tesis dirigida por los Doctores en Ciencias Biológicas por la Universidad de Valencia, MARIA ROSA MIRACLE SOLÉ Y FRANCESC MEZQUITA I JUANES.

Firmado: Mª Rosa Miracle Solé

Catedrática de Ecología

Universidad de Valencia

Firmado: F. Mezquita i Juanes

Profesor Titular de Ecología

Universidad de Valencia

A mis padres, mis abuelos y mi hermana

Agradecimientos

Cuando empiezas no sabes cuando acabarás, cuando vas por la mitad crees que estás acabando y cuando estás llegando al final piensas en la multitud de nuevas ideas que te gustaría emprender, pero un buen trabajo no lo es si no lo cierras del todo. De hecho nunca visualizaba este momento, el momento en el que empiezas a escribir tus agradecimientos y ves la cantidad de gente que ha pasado por tu vida, y que de alguna manera han sido partícipes de tu entusiasmo, de tu desesperación, de tus cambios de humor y de tu evolución personal en esta etapa de tu vida. En esta mañana lluviosa, como hacía años que no sucedía en el mes de marzo, empiezo mis agradecimientos.

Me gustaría agradecer a mi directora de tesis, Mª Rosa Miracle la dirección de la tesis durante todos estos años, la confianza que depositó en mi y la oportunidad que me brindó para realizar mi tesis doctoral, que no es poco, cuando yo era un total desconocido. Gracias por el apoyo prestado todos estos años, tanto a nivel científico como a nivel personal, en todas las decisiones de la presente tesis doctoral. Por apoyarme en los momentos de crisis buscando las soluciones necesarias para poder seguir financiando mi trabajo científico. Pero sin duda, por demostrarme que todavía quedan personas en este mundo que luchan por defender los derechos de la naturaleza, sin personas así ya nos habríamos quedado sin entornos naturales de los que disfrutar. Agradecer de todo corazón a Francesc Mezquita que al poquito de incorporarme en este proyecto acepto ser co-director de este trabajo científico, ante todo decirle gracias, por su apoyo incondicional en todo momento, su esfuerzo diario y su saber estar. Esto no hubiese sido lo mismo sin sus sugerencias científicas, sus correcciones y en definitiva su forma de ser.

Agradecer al Ministerio de Educación y Ciencia (MEC) que me dio la oportunidad de trabajar en investigación proporcionándome una beca (BES-2003-2759) para realizar este trabajo, incluida dentro del proyecto VARECOMED (Variabilidad ambiental del ecosistema mediterráneo Español durante el Holoceno), financiado por el Ministerio de Ciencia y Tecnología (REN2002-03272) y del cual se han sufraguado los costes de este trabajo. Al proyecto INCAMEDSELAR (Indicadores de Cambios medioambientales en registros sedimentarios lacustres de alta resolucion) financiado por el MEC (CGL2005-04040/BOS), y a su líder Eduardo Vicente por la colaboración activa en el proyecto y especialmente en la extracción de los sondeos del presente

trabajo. Y al proyecto ECOINVADER (Ecology of exotic aquatic invertebrates with invading potential in the Iberian Peninsula: the case of Ostracoda) subvencionado por el Ministerio de Ciencia e Innovación (CGL2008-01296/BOS), por sufragar los costes de impresión de la presente tesis.

A Jonathan Holmes porque fue el primero que me aceptó en su centro de investigación, y que siendo yo un novato en todo esto, tuvo la paciencia necesaria tanto con mi inglés del aquel entonces, como para enseñarme todo aquello que debía saber sobre la geoquímica de ostrácodos. Agradecerle sus correcciones científicas y del inglés del segundo capitulo de la presente tesis, del cual ha sido partícipe. En definitiva agradecer a toda la gente del ECRC que conocí en Londres y que me apoyó en mi primera estancia en el extranjero.

Muy especialmente a una gran científica Emi Ito, que aparte de ser una de las mejores científicas que conozco, ha sido una de las personas más llanas y humildes que haya podido conocer en mi vida. Gracias por tus correcciones y comentarios del primer capitulo de la presente tesis, por aceptarme en tu centro de investigación tres años consecutivos, por enseñarme todo lo que no sabía acerca de la geoquímica de ostrácodos y por mostrarme lo que verdaderamente es investigación. Gracias por enseñarme a pensar y a luchar al máximo por aquello que deseas, sea lo que sea.

Gracias a toda la gente del Limnological Research Center (LRC) y especialmente a la gente del LacCore, que me enseñaron todas las técnicas para trabajar con sondeos lacustres: Anders Noren, Amy Myrbo y Kristina Brady. A Daniel Engstrom de St. Croix Watershed Research Station, por su profesionalidad, sus comentarios y sugerencias a la hora de datar mis sondeos con ^{210}Pb y ^{137}Cs. A Erik Brown de Large Lakes Observatory (Duluth, MN) por enseñarme a utilizar un XRF y por agilizar el análisis de mis sondeos. Y muy especialmente a Maniko Solheid del Stable Isotope Lab., que tuvo la paciencia de enseñarme todo lo que se acerca de analizar muestras de calcita y utilizar un AMS, y sobre todo por aguantarme durante la mayor parte del tiempo que me pasé en Minneapolis encerrado en el Isotope Lab.

Tengo que agradecer a la gente del Instituto Pirenaico de Ecología su colaboración en muchos aspectos del presente trabajo. Muy especialmente a dos grandes científicos y dos grandes personas: Blas Valero y Ana Moreno. A Blas por su accesibilidad y por su colaboración en la extracción de parte de los sondeos del presente trabajo. A Ana Moreno por su compañerismo en Estados Unidos y

por su apoyo y sus comentarios en algunos de los puntos de esta tesis.

A Pere Anadón por su revisión preliminar del primer capitulo y sus comentarios. A Carlos Santiesteban por su colaboracion activa como miembro del proyecto en las descripciones sedimentologicas de los sondeos y sus interpretaciones finales. A Francesc Burjachs por su ayuda en las dataciones de los sondeos y sus interpretaciones. A los miembros del Servicio de Microscopía del SCSIE de la U.V. A los profesores del Dpto. de Ecología de la U.V., Toni Camacho por su paciencia a la hora de escuchar y dar consejos. Susana Romo por sus comentarios finales de la tesis y por su pasión y lucha constante por salvar este bien tan preciado, el cual perderemos si no hacemos piña y luchamos por ello: la Albufera de Valencia. Juan Soria por aportar datos hidrométricos que perfilasen este trabajo. A Javier Armengol, Antonio Sanz, Juan Monrós y José A. Gil-Delgado por esos cafés y esas risas del almuerzo.

A mis compañeros de laboratorio. A Laia Zamora por poner siempre ese punto agradable en todo este proceso y por su apoyo llueva o nieve. A Sara Morata, por compartir todos esos momentos de incertidumbre y poner su hombro cuando hacía falta. Gracias Lidia Romero-Viana por tu ayuda en la extracción de parte de los sondeos de este trabajo. A María Sauquillo, por compartir esta pasión por la biología y por todos esos buenos ratos en el "69" mirando bichitos, escuchando música y solucionando el mundo. A las Mexicans, Maru y Nayeli por poner ese toque picante en todos esos momentos agri-dulces. A Olivier por saber que siempre esta ahí. A Antonio Picazo por su constancia, sus programas informáticos (que haríamos sin ellos), su paciencia y su disponibilidad en todo momento a ayudar a los demás. A Carlos Rochera, por su ayuda en algun parrafito de la tesis y por su predisposición a colaborar en todo momento. A Evarist Carbonell porque fue uno de los precursores de este trabajo, realizando los muestreos y el análisis de las muestras del primer capítulo. A Nieves, Yolanda, Esther, Cris, María Antón y un largo etc. de compañeros que han colaborado en todo y han estado en los buenos y malos momentos.

Me gustaría dedicarle esta tesis a la gente que conocí en Estados Unidos, y que hoy por hoy siguen siendo unos grandes amigos. Renne Domain, mi amigo palinólogo que me enseño a disfrutar de este trabajo, por todos esos conciertos a los que fuimos juntos en Minneapolis, cervezas, risas, y esa buena amistad que surgió desde aquel entonces. A Tiff y Jon Hester por hacer más agradable mi estancia en todas mis visitas a las Twin Cities y por compartir conmigo mi otra pasión, la música.

Gracias a todos mis amigos, perdonad si me dejo alguno, porque realmente no sé por donde empezar. A los Kukulundrucus (ostrácodos en jerga amiguil), Marieta, Asier, Isma, Pauli, Berni, Alex, Talia, Ana, Fede (Polps), Nikoo, David, Edu, Clara y un largo etc de personas, que han estado o están, y que me han apoyado y se han interesado en conocer un poquito todo este mundo de los ostrácodos. A Patri, por conocerme y apoyarme en todo este proceso desde el principio, que sería yo sin tus buenos consejos y esos viernes por las tardes de cubatas, que por cierto hay que recuperarlos. A Amparo, porque siempre ha estado ahí y por ser una buena amiga. A Jesús (Chusfor), je,je... por tenerlo otra vez a mi lado y poder disfrutar con él este momento de nuestras vidas. Y como no...a Iker por....eh Joe!! nos hacemos otro y me voy pa casa?!...por parte de las fotos de la tesis, y principalmente por su posición crítica y su saber estar, pedazo de amigo (pon un vasco en tú vida!). A Rafa (Makeinsh!) por haber puesto ese granito de arena cuando hacía falta, por su paciencia, su música y por ser un gran amigo. A Antonio (Thorazine), por enseñarme que una palabra es una palabra, un párrafo es un párrafo y porque el diseño final de la tesis no habría sido lo mismo sin el. Y como no,a Framebeard, esto no tendría sentido sin ti, gracias por tu apoyo diario, por compartir nuestra gran afición y por todos esos buenos momentos musicales, nadie me entiende como tú. Me gustaría realizar una especial dedicación a los Joes.....A Old Joe (Jorge), por ser uno de los mejores amigos que tengo y porque me ayudó en una fase muy crítica de este trabajo y de mi vida, un capítulo debería tener tú nombre Joe. A Mad Joe (Esteban), por poner esa locura-cuerda y toda esa alegría en este proceso. A Xim Joe (Ximet), por sus idas y venidas y claro está por su: Fuerza y Honor Javier! Fuerza y Honor Javier! En definitiva....a los Joes.

A mi familia. A mis padres por ser, estar y darme todo su apoyo en todo momento. A mis abuelos por su alegría de cuando apareces por su casa, por esas comidas revitalizantes de entre semana, por su paciencia y por intentar entender lo que hacía y porque lo hacía. A mi hermana Sandra, joder! que sería yo sin mi hermana! gracias por ser como eres, por tu paciencia en...ahora luego te llamo.... y convertirse en un mes sin hablar, pero que sepas que aunque ahora estés un poquito lejos siempre te llevo en mi corazón, esto te lo dedico.

Y por último me gustaría dedicarle este trabajo a una persona muy especial, a Stella por compartir este último año conmigo, por entenderme (que no es fácil), por su paciencia, por enseñarme muchas cosas sobre la vida y por ser una de las pocas personas que me ha demostrado que me quiere. Para ti pequeña.

Index

Abstract

We undertook a paleolimnological study on the Holocene evolution of the Albufera de Valencia, the largest coastal oligohaline lake in the Iberian Peninsula, enclosed in the Albufera Natural Park. The lake has been the focus of many studies during the last century; however, the origin and the evolution of the lake remained unknown. Subfossil ostracod remains preserved in lake sediments were considered as the most suitable bioindicators owing to the significant relationships between the species distribution and shell chemistry (trace elements and isotopes) of ostracods and water physical and chemical variables. The paleolimnology of coastal lakes is a complex and difficult task; hence, prior to this we undertook a study to calibrate the euryhaline ostracod target species *Cyprideis torosa* as a quantitative paleoenvironmental proxy. The results showed that the combination of both shell nodes and $\delta^{18}O$ provided an accurate quantitative model for salinity reconstruction. On the other hand, *C. torosa* shell Sr/Ca was highly correlated with water Sr/Ca, allowing the possibility to reconstruct past water Sr/Ca in a quantitative manner. Additionally, we support the previous findings that $\delta^{13}C_{DIC}$ can be inferred from ostracod shell $\delta^{13}C$. These results, together with classical paleoecological analyses and interpretations based on ostracod paleoassemblages and sediment characteristics were applied to study three sedimentary sequences from lake Albufera of various lengths (850 cm, 240 cm and 63 cm). The longest two cores provided information about the main transgressive phases occurred during the mid to late Holocene. However, a typical marine ostracod fauna was not recorded at a certain unit of the core, suggesting that the lake was not totally open to the sea during this period. The highest resolution of the shorter two cores, allowed to establish that the main desalinization of the Albufera took place later than thought before, probably in the last quarter of the XIXth century, when an important rice field expansion took place around the lake. The untreated sewage waters and the change of rice cultivation methods from surrounding towns increased the nutrient load onto the lake favoring a drastic eutrophication process during the mid to late XX century. The dense macrophyte cover disappeared from the lake by the end of 1960 resulting in marked sediment differences (disturbed and anoxic sediment layer). Furthermore, the uncontrolled spills from the nearby industries and probably also the increasing hunting activities since the beginning of the XIXth century increased the heavy metals load remaining in the sediment.

Resumen

El presente estudio paleolimnológico se centra en la evolución Holocena de la Albufera de Valencia, el mayor lago costero oligohalino de la Península Ibérica, enclavado en el Parque Natural de la Albufera. Este lago costero ha sido el punto de mira de numerosos estudios durante el último siglo, sin embargo, se sabía muy poco sobre el origen y evolución del mismo. Se utilizaron los restos subfósiles de ostrácodos como los mejores bioindicadores ambientales debido a sus conocidas relaciones entre la distribución de las especies, la composición geoquímica de sus valvas (metales traza e isótopos) y las variables físico-químicas del agua. Los estudios paleolimnológicos en lagos costeros son complicados y difíciles de interpretar, por ello, primero se emprendió un estudio basado en la calibración de una especie de ostrácodo euribalino clave, Cyprideis torosa, *como indicador paleoambiental. Los resultados mostraron que la combinación de los nodos de las valvas junto con los isotopos de oxígeno ($\delta^{18}O$), nos proporcionaba un modelo cuantitativo certero para reconstruir salinidades. Por otro lado, el Sr/Ca de las valvas de* C. torosa *estaba altamente correlacionado con el Sr/Ca del agua, permitiendo así la posibilidad de reconstruir el Sr/Ca de aguas pasadas de una manera cuantitativa. Además, se reafirmó que el $\delta^{13}C_{DIC}$ puede ser inferido a partir del $\delta^{13}C$ del ostrácodo, como mostraban estudios previos. Estos resultados, junto con las técnicas de análisis paleoecológicos se aplicaron en tres secuencias sedimentarias de la Albufera con distintas longitudes (850 cm, 240 cm y 63 cm). Los sondeos más largos aportaron información sobre las principales transgresiones marinas que se produjeron durante el Holoceno. Sin embargo, no se encontró ninguna asociación típicamente marina, sugiriendo así que el lago no estuvo totalmente abierto al mar durante este periodo. Los sondeos cortos se estudiaron con una alta resolución, permitiendo ajustar mucho más en eventos puntuales. Los resultados mostraron que la desalinización de la Albufera se produjo más tarde de lo postulado en estudios previos, probablemente en el último cuarto del siglo XIX, época en la que se produjo la gran expansión del cultivo del arroz en los alrededores del lago de la Albufera. Las aguas no tratadas de la de las ciudades de alrededor y el cambio de los métodos de cultivo del arroz incrementaron la carga de nutrientes en el lago provocando un proceso drástico de eutrofización durante la mitad y la parte final del siglo XX. La densa pradera de macrófitos que poblaba el lago desapareció hacia finales de los años 60, produciendo un cambio en el registro sedimentario (capa de sedimento anóxico). Así mismo, los vertidos incontrolados de las industrias de alrededor del lago y probablemente el incremento de las actividades cinegéticas en el lago, desde principios del siglo XIX, incrementaron la carga de metales pesados que todavía hoy permanecen en los sedimentos de la Albufera*

General introduction and obejectives

I. General introduction

General context: Mediterranean climate, vegetation and limnological changes

The mathematician M. Milankovitch suggested that variations in eccentricity axial tilt, and precession of the Earth's orbit determined climatic patterns on Earth, resulting in 100000-year ice age cycles (Berger, 1988). The Holocene is the most recent period of the Earth's history which encompasses the last 12000 years BP and it is considered, in general trends, a much milder period than the most part of the previous glacial one, the Pleistocene. During the late Pleistocene, the ice caps covered most part of northern North America and Europe. At the end of this period, the rapid warming drove the consequent ice cover melting, however, it was interrupted by a brief cold period (between 12.7 and 11.5 kyrs BP) called Younger Dryas (Lambeck *et al*., 2002), that was characterized by cold-dry weather. In general trends, the beginning of the Holocene started with a sub-humid climate characterized by the arboreal expansion of *Betula* and *Pinus* (between 10 and 9,5 kyrs BP) and deciduous *Quercus* later on (between 9,5 and 8,6 kyrs BP). *Pinus* and mixed forests were progressively displaced by deciduous forests between 8,5 and 6 kyrs BP. This is the case of the north-western Mediterranean and particularly in the Gulf of Lyon area, where temperate deciduous forests dominated the region including *Alnus*, *Betula*, *Populus*, *Salix*, *Carpinus* and *Fagus* (Jalut *et al*., 1997). There was a decline in vegetation at around 6 kyrs BP for most of the species, accompanied by an increase of herbaceous taxa. At 4.2 kyrs BP the climate changed abruptly, dryness increased in general, but with imbedded short wetter periods. Generally, deciduous forests were successively replaced by garrigue (Jalut *et al*., 2000) and the first traces of desertification, arid soils and salinity increases were observed at the irrigated lands. Different data point to the period at around 4 kyrs BP as the begging of the anthropogenic degradation for most part of the eastern Iberian Peninsula (Carrión *et al*., 2000).

At present, the Mediterranean climate is characterized by two main seasons: wet winters, where most of the precipitation is concentrated (rainfalls occur mostly in spring and autumn) and dry arid summers with almost no precipitations (Bolle, 2003). The sustainability of Mediterranean aquatic

ecosystems depends largely of rainfall seasonality, because the functioning of many aquatic ecosystems is controlled by groundwaters, which are feed by these local rainfalls (Álvarez-Cobelas *et al*., 2005; Naselli-Flores and Barone, 2005). Changes in rainfall mark the water level changes suffered by these systems, which may cause heavy disturbances, leading to state shifts and affecting the functioning of the biotic components of the aquatic systems (Naselli-Flores and Barone, 2005; Romo *et al*., 2005; Beklioglu *et al*., 2006). Particularly, dry summers or summer drought may cause stress in shallow lakes, increasing evapotranspiration and reducing water discharges into the lakes (Álvarez-Cobelas *et al*., 2005; Beklioglu *et al*., 2007). Additionally, the complex Mediterranean orography induce other extreme climate characteristics, such as flood events and heavy storms that are commonly observed (Sánchez *et al*., 2004), or heat or cold waves (Easterling *et al*., 2000), which can highly affect the functioning of the biotic components of the aquatic systems (Bolle, 2003).

Sea level changes during the last glacial maximum and the Holocene

Sea level is not static and has experienced wide variations along the Earth's history. The available geomorphological, sedimentological, palaeontological, archaeological and geochronological data from different Mediterranean locations: Israel (Sivan *et al*., 2001), Nile (Omran, 1992), Tunisia (Jedoui *et al*., 1988), Ebro delta (Somoza *et al*., 1998) and Atlantic-Mediterranean Spanish linkage area (Zazo *et al*., 2008), suggest successive melting pulses and sea level rising along the Holocene.

Around 21 kyrs BP, during the period of maximum ice cover of the last glaciations, the sea level was much lower (≈-130 m) than at present (Pirazzoli, 2005; Zazo *et al*., 2008). The melting of ice caps drove several episodes of rapid rising sea level, known as melt water pulses, which have been happening since the last glacial period (Zazo *et al*., 2008). Particularly a short duration plateau in sea level rise may have occurred at 12.5–11.5 cal kyrs BP, corresponding to the Younger Dryas (Lambeck *et al*., 2002). The sea level increased at different rates, but generally it started slowly (3 mm y^{-1}) and increased the rate during the last pulses (16 mm y^{-1}). Around 7 kyrs BP, the ocean level was approaching the actual one (Lambeck *et al*., 2002). According to Pirazzoli (2005), who studied different Mediterranean areas (France, Sardinia, Tunisia, Italy, Greece, Turkey, Syia and Lebanon), the maximum sea level occurred around 6000–5000 radiocarbon years

BP (2 meters above the actual sea level) and was probably followed by a gradual sea-level fall to the present situation (at a rate of 0.4 mm y^{-1}). Zazo *et al*. (2008) based on coastal archives of the last 15 kyrs BP in the Atlantic–Mediterranean Spanish linkage area suggested that the postglacial rise of sea level took place in two phases: a rapid rise until 6500 cal BP, and a second phase, later on, with minor oscillations, when sea level fell. High frequency sea-level fluctuations during the last 4000 years were relatively minor, fluctuating by less than 1 m.

Coastal lagoons origin and human impacts

According to Kjerfve (1994), "coastal lagoons are inland water bodies, found on all continents, usually oriented parallel to the coast, separated from the ocean by a barrier connected to the ocean by one or more restricted inlets...A lagoon may or may be not subject to tidal mixing, and salinity can vary from that of a coastal fresh-water lake to hypersaline lagoon depending on the hydrological balance".

These systems are highly influenced by climatic forcing factors (flood events, storms, river runoff, droughts) that can alter their ecological characteristics (Viaroli *et al*., 2007). Despite the multitude of coastal zones around the world and their particular histories, all systems have suffered similar trajectories along the last 2500 ys BP (Halpern *et al*., 2008). During the last 100 years, these systems have been subject to human impacts through fishing, aquaculture, agriculture, hydrology management and tourism and urban development (Lotze *et al*., 2006; Halpern *et al*., 2008). These human activities varied in their intensity of pressure on the ecological communities, being the coastal zones near the Poles largy unaffected (Halpern *et al*., 2008).

The human influence by hidrological modifications, industrial discharges and/or domestic sewage onto shallow Mediterranean lakes appears to increase southward in Europe (Moss *et al*., 2004). The nutrient balance in these perturbed ecosystems may disrupt the macrophytes dominance to phytoplankton dominance (Romo *et al*., 2004). Eutrophication and the deterioration of water quality in Mediterranean coastal wetlands are the main consequences of human activities in these ecosystems (Álvarez-Cobelas *et al*., 2005; Beklioglu *et al*., 2007). The eutrophication of coastal lakes drives the consequent habitat degradation and loss of biodiversity (Poquet *et al*., 2008). Research on the changes of state in aquatic systems has been really productive in the last decade and, indeed, general advances on theoretical ecology have been postulated in relation to the

system stability properties (Jeppensen *et al*., 1998, Scheffer, 1998). One of the ideas that emerged from these studies is the theory that these lakes can show in two alternative states: clear with macrophytes dominance or turbid without submerged plants (Scheffer *et al*., 1993; Scheffer and van Nes, 2007). However, numerous restoration attemps during the last decade trying to recover the previous clear states with macrophyte dominance in shallow lakes, showed that this is an extremely difficult task.

Palaeolimnology in coastal lagoons

Humans try to organize and archive all kind of information. Since the origin of the human culture, highly increased recently with the outset of the new technologies, we try to collect, to organize and to order all kind of information that we have around us. But this kind of task is not new; it has been done by lakes since lakes origin. Lakes store highly valuable old Earth's information, encompassing some millions of years of source information. The lakes receive the information and the sediments hold the archives where this information is saved (Cohen, 2003). All lakes are under diverse influencing factors, extrinsic or intrinsic variables which regulate the history of the Lake (Cohen, 2003), including climate, water composition, watershed bedrock, tectonics, vegetation, aquatic biota and human activities among others. The history of all these variables is commonly approached using paleolimnological techniques.

Sediment coring is the most common technique to obtain paleolimnological information in the vertical dimension. A wide array of questions can be studied using paleolimnological approaches. Additionally, monitoring recent systems helps us to better understand the old systems functioning, particularly using transfer functions to reconstruct different variables such as temperatures, sea level changes and many other climatic and biotic variables (Birks and Gordon, 1985). From biological proxies (pollen, diatoms, ostracods, lipids...) to geological ones (mineralogy, isotopes, sedimentology...), we can approach with relatively high detail on dilated time scales, records of climate, tectonic and biotic evolution.

The study of the evolution of coastal systems is a complicated task, because there are many factors that can affect the information that sediments keep. Coastal lake sediments can be influenced by wind effects, wash of sediments by heavy rains or flood events, high sedimentation rates, burrowing activities by animals and human's activities, among others. Paleolimnological studies

on coastal lakes have been especially applied to reconstruct sea level changes, hydrological dynamics and eutrophication processes during the last decades (Cohen, 2003).

Ostracods

Ostracods are huge sources of biological and chemical information on their surrounding habitats. They are bivalved crustaceans that are found in many aquatic systems, from ponds to deep lakes to marine waters (Meisch, 2000) and even some species have semi-terrestrial abilities (Schornikov, 1969). All ostracods secrete a carapace composed of low-magnesium calcite. Their shells are commonly found as fossils or subfosils in Quaternary sediments giving an extraordinary potential as paleoenvironmental indicators (Griffiths and Holmes, 2000). For that reason the study of paleoecological ostracod assemblages and geochemistry can give essential information about past environments.

In fact, several studies were carried out to build transfer functions based on ostracods on the last decade, mainly focused on temperature and water chemistry (Mezquita *et al.*, 2005; Viehberg, 2006; Mischke *et al.*, 2007; Horne and Mezquita 2008) and the relationships between geochemical (trace elements and isotopical ratios) and environmental data (Xia *et al* 1997a,b; von Grafenstein *et al.*, 1999). Water chemistry (solute composition and concentration) and temperature are some of the factors to which non-marine ostracod species respond in a more clear and consistent way (Mezquita *et al.*, 2005; Horne and Mezquita, 2008). Thus, ostracod paleoassemblages can provide useful information about the water chemistry and solute composition at the time they lived. Trace elements ratios, especially Mg/Ca and Sr/Ca, have been used to infer variations in water salinity and ionic composition (Chivas *et al.*, 1985, 1986a,b; Ensgtrom and Nelson, 1991; De Deckker *et al.*, 1999; Holmes and Chivas, 2002) and temperatures (Chivas *et al.*, 1986a,b; Wansard, 1996a,b; Xia *et al.*, 1997b). However, the conventional application of these proxies in paleolimnology studies most frequently overlooked the complex processes involved with the solute evolution, hydrological changes, physical chemistry and ostracod biological aspects, for that reason, the interpretation of those results should be done carefully (Ito and Forester, 2009). Isotopical ratios ($^{18}O/^{16}O$ and $^{13}C/^{12}C$) from ostracod shells can provide information about hydrology of the lake (from oxygen isotopes), affected by P/E processes and salinity changes (Chivas *et al.*, 2002) and about the carbon cycle from carbon isotopes (Durazzi, 1977; Von Grafenstein *et al.*, 1992,1999; Xia *et al.* 1997b).

II. Thesis structure and objectives

This thesis is structured in two main parts. In the first part (Chapter I) we test the possibility to use ostracods of the species *C. torosa* as a quantitative paleoenvironmental proxy based on various shell characteristics. The second part is divided in three chapters (Chapters II, III, and IV) where we reconstruct the Holocene history of Albufera de Valencia (sea level influences, salinity and hydrological changes, increasing pollution and other human impacts).

In the first chapter (**Chapter I**) we try to test if ostracod shell morphological and geochemical variables could be good indicators of water chemical changes. We therefore study recent *Cyprideis torosa* specimens to test if salinity or other physical and chemical variables have some intra-specific influence on its life cycle, shell morphology and geochemical composition. We chose *Cyprideis torosa* because it is a common euryhaline ostracod, well distributed in the study area and in the fossil record. We undertake an extensive study that covers 17 places (sampled once) where the same species is found, but with different water chemistry characteristics. These sites are distributed over a wide salinity and environmental gradient, covering from springs to coastal lagoons and hypersaline salt pans, allowing the use of the obtained data in a statistical procedure to build regressions that could be used as transfer functions to reconstruct past environmental variables from subfossil *C. torosa* ostracod shells, as we did in the next chapters.

In addition, we monitored *C. torosa* populations in three different coastal lakes (in a salinity gradient) monthly for a year analyzing its life cycle, shell morphology, and the geochemical composition of the shells (trace elements and isotopical ratios). *Cyprideis torosa* shell variables were compared with changes in water chemistry, temperature, water isotopes and other environmental factors to find out if any significant pattern emerges that could relate ostracod shell traits to environmental features.

The second part of the thesis is subdivided in three chapters. We chose the Albufera de Valencia system as an example of a coastal lagoon that has been formed during the Holocene due to sea level rising and has suffered from human impact in the last decades.

In **Chapter II**, we analyze a long core (850 cm) extracted from the sandy littoral bar (Palmar core) that allows us to interpret the mid Holocene history of

Albufera de Valencia and the beach barrier system evolution (sea level changes, P/E processes and sand bar evolution). However, the most detailed recent evolution of the lake is best recorded at the central lake sediments. In **Chapter III**, we present the study of a two meters long core (core Center) extracted from the center of Lake Albufera. Core Center encompasses the last 3400 yrs BP, *i.e.*, the late Holocene evolution of the lake. We undertook a multidisciplinary study of this sequence, including image analysis, sediment geochemical analyses, nutrients analysis and ostracod paleoecology and geochemistry to approach sea level changes, salinity variations, and flood and storm events. According to historical sources, the recent evolution of the lake was highly influenced by humans, at least during the last 100 years. In **Chapter IV**, we study L'Antina core, a short core (63 cm) extracted in a central location different than the previous one. Ostracod paleoecology and geochemistry techniques were applied with higher resolution than in the case of core Center. Correlations with the previous core support the previous results about hydrological lake changes, salinity variations and eutrophication processes, detected with more accuracy in the study of this shorter core.

PART I

Calibrating ostracod species

CHAPTER I

Emprical shell morphology and chemistry calibration of Cypridies torosa *(Jones, 1850) (Crustacea: Ostracoda)*

1. Introduction

Since the first suggestion made by Chivas *et al.* (1983), numerous attempts have been made to use the stable isotope and cation chemistry of ostracod valves to reconstruct paleoclimate and to delineate relation between water and shell chemistry (e.g., Griffiths and Holmes, 2000; Ito *et al.*, 2003). In particular, multiple experimental and empirical studies have sought to calibrate the uptake of ^{18}O, Mg and Sr by different species of ostracods into low-Mg calcite valves (Engstrom and Nelson, 1991; Von Grafenstein *et al.*, 1992, 1999; Xia *et al.*, 1997a, b; Wansard *et al.*, 1998; Palacios-Fest and Dettman, 2001; Ito *et al.*, 2002). Based mainly on the observed relation between non-marine ostracod valve chemistry and water chemistry of Australian saline lakes coupled with the consideration of Mg and Sr incorporation into inorganic calcite, Chivas *et al.* (1983, 1985, 1986a, b, 2002), and De Deckker *et al.* (1988, 1999) suggested that for each different species or genus there may be a systematic fractionation of Mg and Sr as functions of water chemistry and for Mg also as a function of temperature. Additionally, these authors suggested that there may be a similar systematic fractionation of oxygen isotopes as functions of temperature and $\delta^{18}O$ of water in which the ostracod moulted and hence the tandem use of $\delta^{18}O$, Mg/Ca and Sr/Ca of fossil ostracod valves may enable both the paleotemperature and paleosalinity of water to be reconstructed.

During the last 20 years, a few studies have pointed out that ostracods calcify low-Mg calcite valves even in waters that are endogenically precipitating aragonite or high-Mg calcite, so that considerable metabolic costs must be involved (Xia *et al.*, 1997a, b; Wansard *et al.*, 1998; Ito *et al.*, 2003) and because of that Mg, Sr and $\delta^{18}O$ incorporation may not be systematic. De Deckker *et al.* (1999) studied the species *Cyprideis australiensis* in *in vitro* experiments and suggested that there is not a systematic one-to-one relationship between salinity and the shell Mg/Ca and Sr/Ca ratios. For example, Mg uptake by *C. australiensis* shows systematic temperature dependence within a certain range of Mg/Ca of host water, but in waters of low (<1) or high (>30) Mg/Ca, *C. australiensis* will not take up Mg in accordance with the calculated temperature dependent $Mg/Ca_{ostracod}/Mg/Ca_{water}$ ratio. Ito and Forester (2009) showed that temperature dependence of the Mg uptake by *Cypridopsis vidua* deduced from a study of a Mexican irrigation pond gave unreasonable (negative) temperatures when applied to *C. vidua* living in water of similar Mg/Ca but very different Ca concentration. These recent studies suggest that the uptake of Mg and Sr

by ostracods is more complex than originally thought and that vital effects or the effects that depend on the metabolic cost of shell calcification may exert significant control. Hence, if shell chemistry of ostracods is to remain useful in reconstructing paleoenvironment and paleoclimate, all factors that affect the calcification process may need to be examined to distinguish those that are significant and must be considered in interpreting (fossil) shell chemistry from other that may be minor and thus can be ignored. However, further delineation of effects of various factors on ostracod valve chemistry has been hampered by lack of calibration studies that involve time-series monitoring of several sites with widely differing salinities and ionic compositions. A time-series monitoring at sufficient temporal resolution is necessary because ostracods moult and calcify valves in less than 24 hours (Turpen and Angell, 1971) to a few days (Chivas *et al*., 1983; Roca and Wansard, 1997) and many non-marine water bodies undergo significant seasonal temperature and salinity changes.

Under certain circumstances, deep lake water $\delta^{18}O$ ($\delta^{18}O_L$) can be reconstructed by benthic ostracod shell and information gained can be combined with endogenic carbonate $\delta^{18}O$ to reconstruct $\delta^{18}O_L$ and temperatures (Von Grafenstein *et al*., 1999). However, the full potential of this proxy cannot be exploited so far, because how ostracod shell calcification process (e.g. calcification rate, cation uptake (and elimination), C and O isotope fractionation) changes in different physicochemical conditions is not fully understood.

Given the inconsistent results on ostracod valve chemistry investigations found at present in the literature, we planned a field survey encompassing a hydrochemical gradient as wide as possible but controlling for species effect by using a single taxa that is also common in sedimentary records. Target species *Cyprideis torosa* (Jones, 1850), is both widely distributed and commonly found in the paleoecological literature (e.g. Bronshtein, 1947; Mischke, 2001; Meisch, 2000) and tolerant of a wide range of salinities from dilute springs to estuaries and salt evaporation ponds (Heip, 1976; Van Harten 1975, 1996, 2000; Mezquita, *et al*., 2000).

2. Material and Methods

2.1 Study sites

Twenty coastal water bodies were sampled on the eastern Iberian Peninsula (Fig. 1.1). Seventeen of these 20 were sampled just once during March 2004 and will be referred as broad-survey samples (BSS). Three sites were sampled monthly for 1 year, from March 2001 to March 2002, and will be referred as monthly survey samples (MSS).

Hot (> 24°C) dry summers (July and August) and mild (9~11°C) dry winters (January and February) characterize the climate of the region. Annual precipitation varies between 200 mm south of Alicante and as high as 800 mm near Gandía, with most of precipitation occurring between September to November (Fig. 1.2). A secondary, much weaker wet season occurs in spring (March to May). Single storm events can bring nearly 50% of annual precipitation (Martin-Vide and Lopez-Bustins, 2006).

Most of the study sites are located in Quaternary and Neogene basin fills except in the areas between Gandía and Alicante where Cretaceous and Tertiary carbonate rocks (part of the External Betics deformed by the Alpine Orogeny) crop out or are very close to the surface (Gibbons and Moreno, 2002). Most river waters and ground waters of the region are hard water and originate in Cretaceous and Tertiary carbonate-rich rocks, but in some cases Tertiary evaporites strongly influence the ionic composition of aquifers.

The majority of the sampled sites are part of wider wetland systems protected as Natural Parks (Fig. 1.1). Five sites are natural springs (E01, E07, E28, E70 and U1). E53 and E58 are located in the Natural Park "Prat de Cabanes-Torreblanca wetland"; E01, E02, E06, and E08 are in the "Pego-Oliva wetland Natural Park"; and E21, E28 and RA05 are in "Albufera de Valencia Natural Park". Eight of the sampled sites, E38, E38bis, E39, E39bis, E45, E46, P5 and P7 are in the Natural Park of "Santa Pola wetland"; many of the Santa Pola wetlands are associated with coastal evaporative systems used for salt production.

Monthly survey samples were collected from sites P5, P7, and U1 (Fig. 1.1). U1 (Ullal Fosc), located near Gandía is a spring (area: 225 m^2; depth: 1,5 to 2m) discharging ground water probably originating in karstic Massif Mondúver immediately to the west. Because ground water in karsts typically flows through

dissolution features in limestone and because the massif is close-by, its residence time is expected to be short and to show some seasonal variation. P5 (Charco Lis, Santa Pola) is in the middle of a chain of coastal evaporation ponds used for sea salt production. P7 (Las Cuadretas, Santa Pola) although close to P5, is not part of this chain and mainly receives water from a canal that originates in another series of inner wetlands (Fondo d'Elx) related to the hydrological system of River Vinalopó. The water levels in these wetlands are artificially controlled. Both P5 and P7 are on the average about 50cm-deep but have large surface areas (ca. 96 hectares and 17 hectares, respectively).

2.2 Water Samples

Field water variables were measured in situ at all the sampling sites. Conductivity, salinity, pH, dissolved oxygen and water temperature were measured with a multi-sensor (Multiline P4; WTW®) probe. Water samples were taken at the same time. Filtered water (0.7μm Whatman®GF/F) for ionic composition was taken in 100ml HDPE (high density polyethylene) bottles. Cation water samples were fixed with 1 ml 60% HNO_3 and bottles were kept at 4°C. Cation analyses for major and minor elements (Na, Mg, Ca, Sr), were performed by ICP-MS (Thermo Elemental PQ-Excell) with an accuracy of 2%. Anions (Cl, SO_4^{-2}) were analyzed by ion chromatography on a Dionex instrument calibrated daily to 5 standard solutions per ion at the University of Minnesota. Total inorganic carbon (TIC) was measured in the field by titration to pH of 4.5 and speciated to HCO_3^- and CO_3^{-2} according to field measured pH.

Between 100 and 1000 ml of water was filtered in the field using Whatman®GF/F filter (0.7μm) and filters were stored at -20°C until being used for chlorophyll extractions (following Shoaf and Lium, 1976). Chlorophyll *a* concentration was calculated following Jeffrey and Humphrey (1975). Unfiltered water was kept in 50 ml borosilicate Polyseal®-capped bottles for $\delta^{18}O$, $\delta^{2}H$ and $\delta^{13}C$ analyses. These water isotopic values were measured at Mountain Mass Spectrometry (Boulder, CO, USA). Each sample was analyzed twice and average values are reported in δ notation relative to the VSMOW (Vienna Standard Mean Ocean Water) standard. The total analytical error is ±1‰ for $\delta^{2}H$ and ±0.1‰ for $\delta^{18}O$. PhreeqcI program (version 2.14.2) with Waterq4F (for diluted waters) and Pitzer (for saline and hypersaline waters) databases, was used to calculate free ions concentration, ions activities and saturation indices.

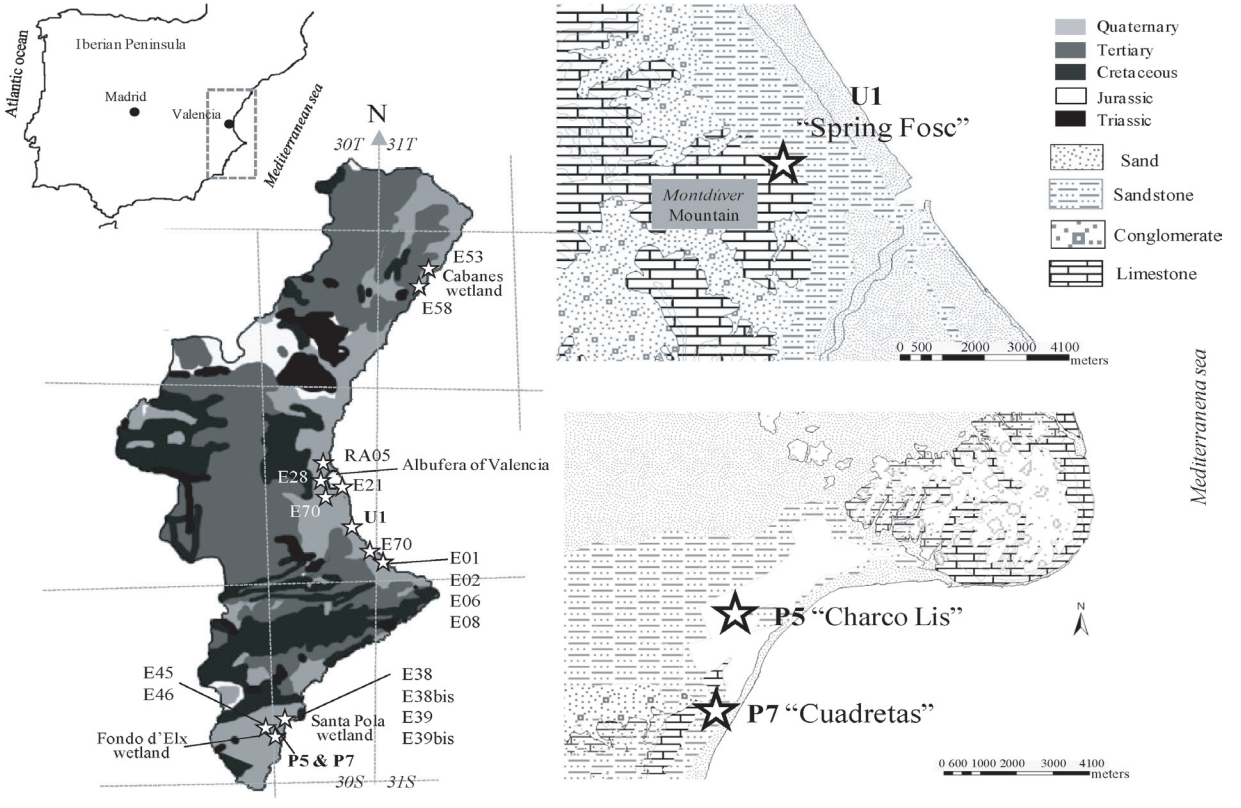

Figure 1.1: Map location of the 20 studied sites, for broad survey samples (BSS) and monthly survey samples (MSS). P5, P7 and U1 (MSS) locations are show with more detail on the right. Legend shows geological deposits age and lithological composition.

Figura 1.1: *Mapa geológico y litológico de los 20 puntos estudiados, tanto para las muestras del estudio extensivo (BSS) como los puntos muestreados mensualmente en el estudio intemsivo (MSS). P5, P7 and U1 (MSS) se muestran con más detalle a la derecha. La leyenda muestra la edad de los depósitos geológicos y la composición litológica.*

2.3 Ostracods

Ostracod samples were collected at each site with a 100 μm mesh size hand-net, sampling the superficial area of the sediment to a maximum substrate depth of 2 cm. For the MSS, the samples were taken from the same especific sampled point, sampling the same area (aprox. 600 cm^2) and the same particular habitat every month. The samples were fixed in the field with ethanol (70%). Live-collected ostracods belonging to the species *Cyprideis torosa* (Jones, 1850) were picked under a binocular microscope using a fine-tipped paintbrush. For identification of juvenile stages we followed Heip (1976), Weygoldt (1960) and Mezquita *et al.* (2000). Ostracod were counted and abundances expressed as individuals/100 cm^2. In the case that ostracods were highly abundant subsamples were taken, otherwise the whole sample was processed.

Cyprideis torosa morphological variables were taken into account for the different analyses. Lengths for females and males were measured for this study. Heip (1976), Van Harten (1975, 1996), and Mezquita, *et al.* (2000) studied *C. torosa* in different ecosystems and found that adults have smaller shells sizes in waters with high salinities. Moreover, Mezquita *et al.* (2000) observed shells size variations along the year and suggested that this may be due to low temperatures and/or by seasonal salinity variations during the year

Additionally *C. torosa* noding was measured for females, males and juveniles, as a categorical variable, noded or not noded, and expressed as the frequency of noded valves per sample (*Pn*). Adults of both sexes and all juvenile stages were considered together. One-sample Kolmogorov-Smirnov test indicated that data on frequency of noded individuals (*Pn*) were not normally distributed. *Pn* was transformed to Arcsin($\sqrt{Pn}$) with the objective to normalize the data. Non-parametric bivariate correlation (Spearman) was calculated between arcsin($\sqrt{Pn}$) and the physico-chemical variables. Many authors have studied this phenomenon in the literature (see Sandberg, 1964; Kilenyi, 1972; Vesper; 1972a,b, 1975; Van Harten, 1975, 1996, 2000; Keyser, 2005). This variable was well studied by Vesper (1972b) and Van Harten, (1975), their findings showed the negative effect of salinity on noding. However, Keyser (2005) demonstrated that nodes appear when a deficiency of calcium in the surrounding waters.

Ostracods were separated according to sex and developmental instars: adult females (f), adult males (m) and juveniles (j: from A-8 to A-1), and a subset of each group was measured for shell length. Only adults and late-instar juveniles

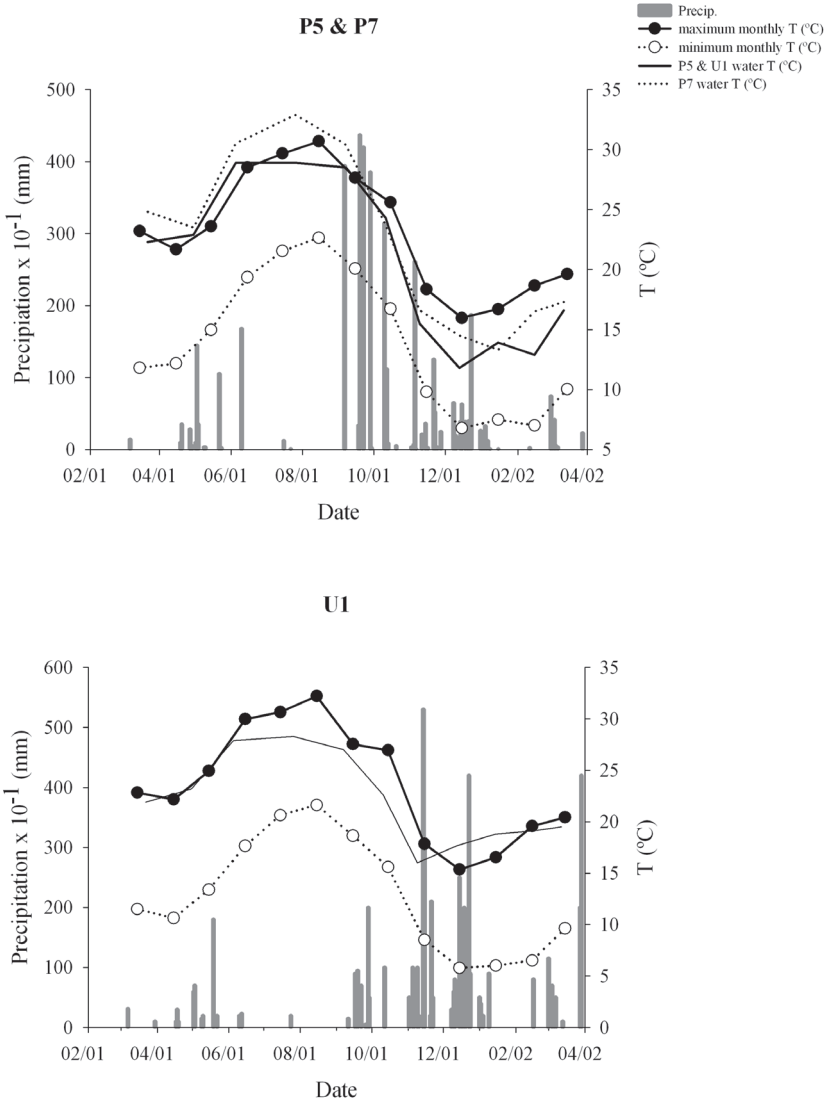

Figure 1.2: Daily precipitation (Bars), maximum and minimum monthly average temperatures (°C) and water temperatures (°C) for the three sites sampled monthly (MSS). Meteorological data from observatories in Alicante (P5 and P7) and Gandía (U1) during March-01 to April-02.

Figura 1.2*: Precipitaciones diarias (barras), temperaturas medias máximas y mínimas del aire (°C) y temperaturas del agua para los tres puntos muestreados mensualmente (MSS). Datos mensuales de los observatorios de Alicante (P5 and P7) y Gandía (U1) desde Marzo-01 hasta Abril-02.*

(A-1 and A-2) were used for geochemical analyses. For samples collected monthly from P5, P7 and U1 the number of individuals belonging to each different growth instar of *C. torosa* was counted in order to assess population dynamics that might indicate the main calcification period for each stage.

About 25 ostracod geochemical analyses were usually performed per MSS collection. One adult carapace (2 valves) or 2 late-instar juvenile carapaces (4 valves) were used for each analysis. Out of these 25 analyses, 9-10 analyses were carried out on females, 9-10 analyses on males and 5 analyses on juveniles (A-1 and A-2). Five to nine analyses were carried out on ostracod samples collected from BSS. For each analysis, 1 to 2 adult animals or 2 to 3 late-instars juvenile animals were used. Juveniles were only used when the number of adults collected was not sufficient to obtain 5 analyses per site. Adult and juvenile valves were never mixed together to obtain an analysis, and neither were male and females valves. At 3 sites (E01, E02, E70), sample collection was undertaken on several visits because of very low abundance of living animals. Even then, it was not possible to obtain more than 1 analysis each from E01 and E02, and 2 from E70.

Ostracod valves were cleaned for geochemical analysis using the method described in Ito (2001). Cleaned valves were analyzed using a Kiel-II online carbonate preparation device coupled to a Finnigan MAT 252 stable isotope ratio mass spectrometer at the University of Minnesota. The isotope results are reported in standard δ notation with respect to VPDB (Vienna Pee Dee Belemnite) and the analytical error (1σ) is <0.1‰ for both oxygen and carbon.

Carbonate dissolution was accomplished with ultra-pure H_3PO_4 and the acid-residue remaining after the isotope analysis was analyzed for Ca, Mg and Sr concentrations by a Thermo Elemental PQ-Excel Quadrupole ICP-MS at the University of Minnesota with a mean precision of 2%. Because the acid–reaction residue was diluted to a known mass, it allowed us to calculate the weight of $CaCO_3$ in each sample which in turn allowed us to estimate Ca content per carapace (Ca_{SHELL}). Mg/Ca and Sr/Ca ratios are presented as molar ratios.

2.4 Statistical methods

Bivariate correlations were calculated between ostracod variables and water physico-chemical data. Parametric (Pearson) and non-parametric correlations (Spearman) were used when appropriate. Two-way ANOVA and the parametric Games-Howell analyses, specific for lack of homogeneity

between variances were also performed for comparison of lengths (CL), calcium content per carapace (Ca_{SHELL}), Mg/Ca, Sr/Ca, ostracod molar ratios, $\delta^{18}O_{VPDB}$ and $\delta^{13}C_{VPDB}$ between samples. Multiple comparisons (with Bonferroni correction) so as comparisons within the subcategories (females-males) and comparisons between sexes and samples were also performed. The normality of data was checked with Kolmogorov-Smirnov tests. In order to compare our ostracod data between and within water bodies, we selected only water bodies with ≥4 measured shells (consequently E01, E02 and E38 were removed from the analysis) to minimize the influence of samples with low number of analysis. In addition, for these comparisons, juvenile data was not considered because we did not analyze juvenile shells in most of the BSS sites. The geochemistry data of one of the main moulting periods for MSS (P5-P7-U1) were used considering that those results will reflect better the water chemistry for those places, when compared with the BSS samples. Particularly, 13 samples of the 20 sampled places (BSS + MSS) were selected for statistical comparisons. In the case of CL comparisons, animals measured from July-01 of P5 and April-01 of P7 were used for the analysis. Data on U1 shell lenght was lost, then, it was not possible to use it to do any comparison.

To assess the possibility of using geochemical ostracod variables as paleoenvironmental tools for the paleolimnological reconstruction of hydrochemical variables of interest, we carried out (multivariate) regressions using the best subsets of ostracod explanatory variables, as evaluated with the Akaike Information Criteria (AIC) implemented in Statistica v.7.0. These multivariate regressions were carried out using our BSS data set to calculate equations for the reconstruction of salinity, TDS, Sr/Ca, Mg/Ca, pH, Alkalinity, SO_4^{2-} and $\delta^{18}O$. The multivariate regressions used water hydrochemistry variables as dependent variables and ostracod shell data (trace elements, isotope ratios, length, nodes) as independent variables. Finally, we used our MSS dataset (using the averages of adults) to apply these equations and validate the best fitted regression models obtained.

3. Results

3.1. Water Chemistry

The TDS (total dissolved salts) range represented by sampled sites (Appendixes 1.1 and 1.2) is large, from (0.2 to 65.9 g/L). Due mainly to either direct sea water influences or geological setting, chloride was the most dominant anion in all waters, except in the two most dilute samples (E70 and U1) which were dominated by bicarbonate (Appendixes 1.1 and 1.2; Figure 1.3). Waters of all 20 study sites lie on the carbonate alkalinity-depletion trend of Eugster and Jones (1979) and span a wide range of ionic and stable isotopic compositions (Appendixes 1.1 and 1.2, Figures 1.3 and 1.4).

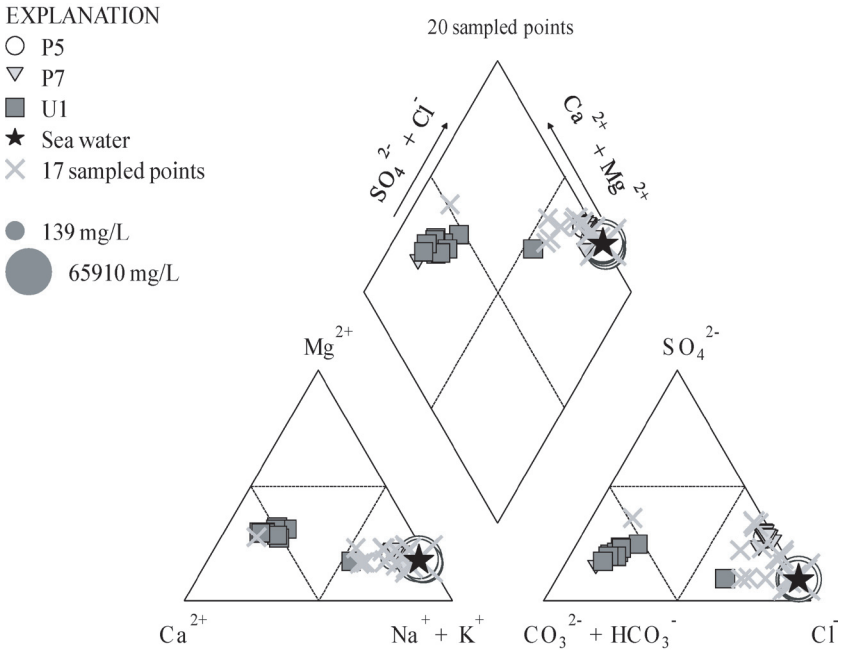

Figure 1.3: Ionic composition of the 20 sampled sites, including P5-P7-U1. Symbol size is proportional to the total dissolved solids concentration (TDS).

Figure 1.3*: Composición iónica de los 20 puntos muestreados, incluyendo P5, P7 y U1. El tamaño del símbolo es proporcional al valor de concentración de los sólidos disueltos totales (TDS).*

The alkalis ($Na^+ + K^+$) were more abundant than the alkali metals ($Ca^{2+} + Mg^{2+}$) (in meq) except in E70 and U1 (Fig. 1.3 and Appendixes 1.1 and 1.2). The range of Mg/Ca molar ratios was between 0.5 and 6.4 and Sr/Ca was between 1.2

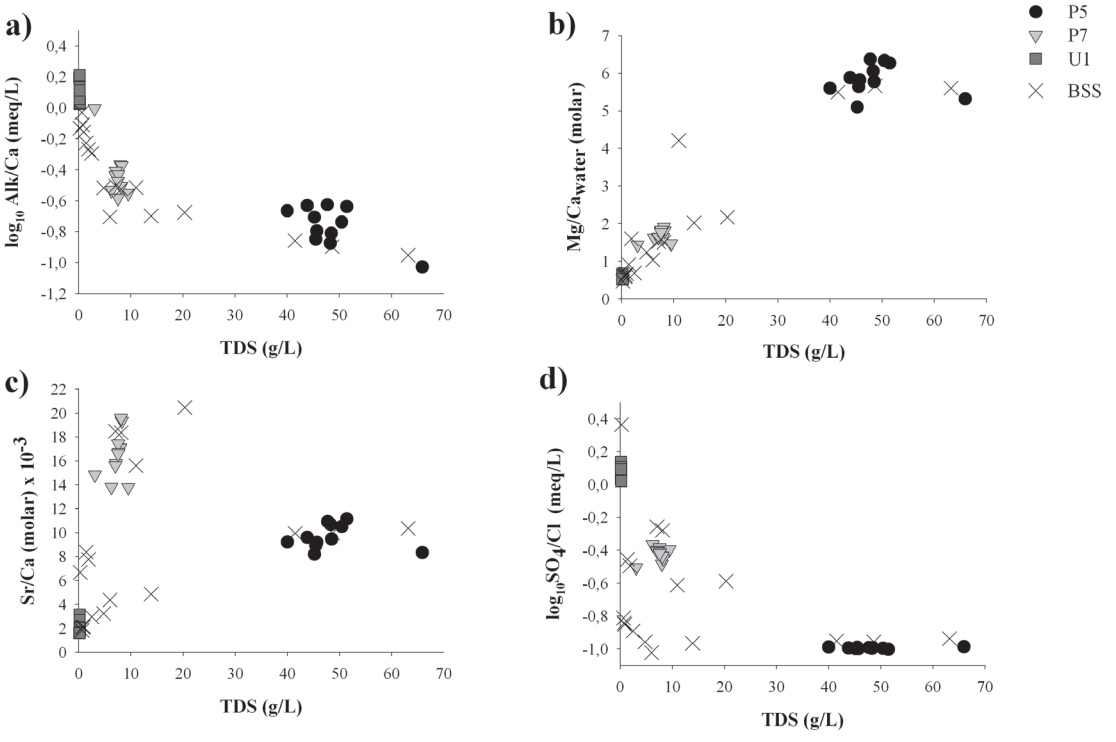

Figure 1.4: Different ionic evolution ratios with respect to TDS (g/L) for the 20 sampled places. P5, P7 and U1 values represent the monthly results for the sampled period during 2001-02. a) Log_{10}Alk/Ca is depleted with TDS evolution; b) water Mg/Ca increase with TDS evolution; c) water Sr/Ca seems to increase at low TDS but not for high TDS waters; d) $Log_{10}SO_4$/Cl decreases with TDS increase.

Figura 1.4: *Evolución de las variables iónicas respecto al TDS (g/L) para los 20 puntos muestreados. Los valores de P5, P7 y U1 representan los resultados mensuales para el periodo estudiado de 2001-02. a) Log_{10}Alk/Ca se reduce con la evolución del TDS; b) Mg/Ca del agua se incrementa con la evolución del TDS; c) Sr/Ca del agua parece aumentar a bajos TDS pero no en aguas con alto TDS; d) Reducción de $log_{10}SO_4$/Cl con el aumento del TDS.*

x 10^{-3} and 20 x 10^{-3}. Mg/Ca increases with TDS (Figure 1.4b) and SO_4/Cl decreases with TDS (Fig. 1.4d). The range of water $\delta^{18}O$ was between -6.9 and 3.9‰ and $\delta^{2}H$ between -51 and 15‰ (Appendix 1.1 and 1.2, Figure 1.6a). Water temperature at the time of sampling varied between 9 and 33°C. The monthly values for MSS water samples are shown in Appendix 1.2 and Fig. 1.2. Water temperatures during the sampling period in P5 varied between 11.8 and 28.9 °C, in P7 between 13.3 and 32.9°C and in U1 between 16 and 28.3°C. TDS varied between 40 and 65,9 g/L for P5, between 3,1 and 9,5 in P7 and between 0,14 and 0,23 in U1.

P5 showed peaks of Mg/Ca and Sr/Ca in April-September during the hot and dry late spring summer period and low values from November to March during the cooler and wetter months (Appendix 1.2). In P7, Mg/Ca and Sr/Ca also increased from spring to summer recording the highest values in July and August. Highest ratios of Mg/Ca and Sr/Ca in U1 occur during June through August, but salinity maintained low values suggesting precipitation of carbonates due to photosynthetic activities of macrophytes. The $\delta^{2}H$ for P5 varied between 0 and 32‰ and $\delta^{18}O$ between 0.2 and 3.9‰. In P7 $\delta^{2}H$ and $\delta^{18}O$ were lower than in P5, ranging between -30 and -8‰ and -4.5 and -2.9‰, respectively. U1 had the lowest values with $\delta^{2}H$ between -51 and -26‰ and $\delta^{18}O$ between -7.0 and -5.5‰. $\delta^{13}C$ of DIC (Dissolved Inorganic Carbon) for P5 varied from -5.3 to -0.3‰, for P7 from -10.9 to -3.5‰, and for U1 from -12.2 to -9.3‰. The annual range of Mg/Ca molar ratio in P5 was between 5.1 and 6.4, between 1.4 and 1.9 in P7, and between 0.5 and 0.7 in U1. The Sr/Ca molar ratios for P5 were between 8.2x10^{-3} and 11.2x10^{-3}, between 13.8x10^{-3} and 19.6x10^{-3} for P7, and between 1.6x10^{-3} to 3.2x10^{-3} for U1.

Principal Component Analysis (PCA) was carried out to summarize the hydrochemistry of 20 sampled sites (Fig. 1.5). P5, P7 and U1 were included using the annually averaged values. The first PCA axis (**Factor 1**; 59% of variance explained) relates to a gradient from low Mg/Ca, low TDS waters to chloride-dominated, high Mg/Ca, $\delta^{18}O$, $\delta^{2}H$ and TDS. The second PCA axis (**Factor 2**; 18%) singled out the two carbonate- and sulphate-dominated dilute spring waters. Overall, the sampled sites can be separated into 3 groups. Group I: dilute carbonate and sulphate dominated springs (E70 and U1), Group II: high TDS, high Mg/Ca seawater evaporation ponds of "Salinas de Santa Pola" (E38, E38bis, E39, and P5), and Group III: comprised of the remaining 14 sites, all of which are located on Quaternary alluvial deposits, with relatively low TDS, low Mg/Ca, and relatively high-medium Alk/Ca.

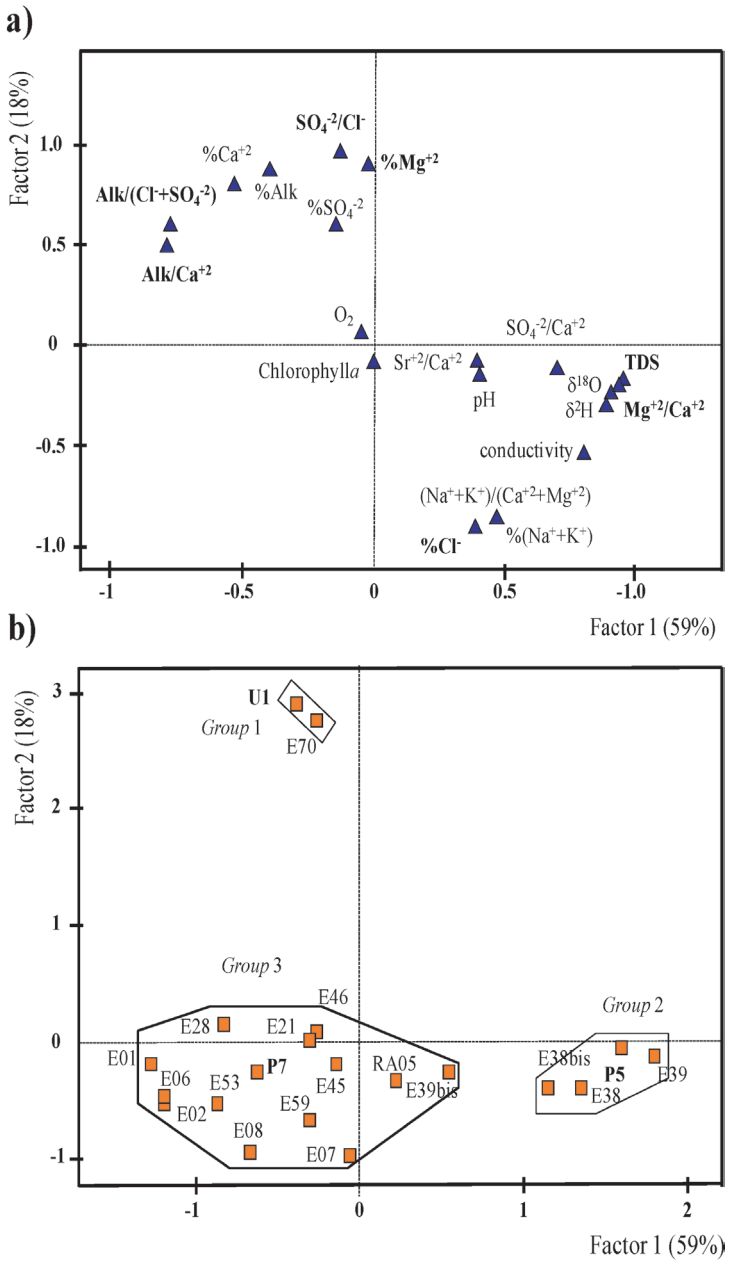

Figure 1.5: PCA (Principal Component Analyses) results for the twenty coastal places and all the physico-chemical variables. a) the physico-chemical variables; b) PCA samples scores.

Figure 1.5*: PCA (Análisis de Componentes Principales) de los 20 puntos estudiados y sus variables físico-químicas. a) Ordenación de las variables físico-químicas; b) Resultados del PCA para las muestras.*

The oxygen and hydrogen isotope analyses of the waters are presented as a $\delta^{18}O$– δD plot (Fig. 1.6a). The studied lakes and ponds are mainly fed by meteoric precipitation. The samples that are located on an evaporation trend line below

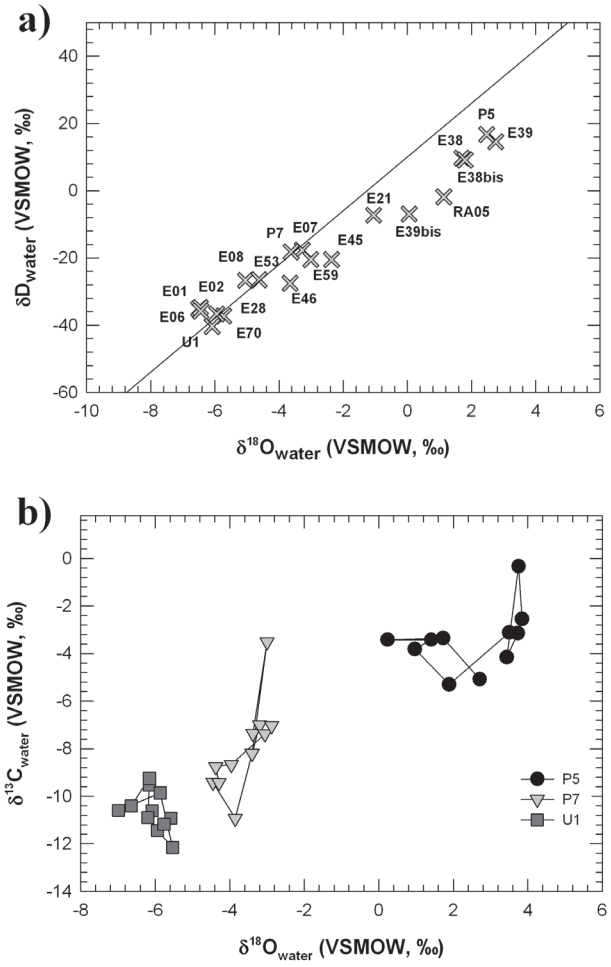

Figure 1.6: Isotopic composition in natural waters corresponding to BSS and MSS samples. a) Plot of oxygen and hydrogen isotopes ($\delta^{18}O$ and $\delta^{2}H$) in the BSS and MSS. The values used for MSS correspond to the average value for all year. The line indicates the Meteoric water line obtained by Craig and Gordon (1961); b) Plot of oxygen and carbon isotopes ($\delta^{18}O$ and $\delta^{13}C$) in MSS.

Figure 1.6*: Composición isotópica de las aguas correspondientes al BSS y MSS. a) Isótopos de oxígeno e hidrógeno ($\delta^{18}O$ and $\delta^{2}H$) en BSS y MSS. Los valores usados para el MSS corresponden con el valor medio anual. La línea indica la línea Meteórica del agua obtenida por Craig y Gordon (1961); b) Isótopos de oxígeno y carbono ($\delta^{18}O$ y $\delta^{13}C$) del MSS.*

the Global Meteoric Water Line correspond with the Group II waters. The samples associated with Group III are above or on the GMWL indicating they are little affected by evaporation. Group I (E70 and U1) samples have the lowest $\delta^{18}O$ and $\delta^{2}H$ values and lie on the GMWL indicating spring discharge from unevolved sources. $\delta^{13}C$ of DIC (DIC-$\delta^{13}C$) is only available for the MSS; its relationship with $\delta^{18}O$ is shown in Fig. 1.6b and show large differences in DIC-$\delta^{13}C$ between MSS sites. The data values for $\delta^{13}C$ ranged between -0,3 and -5,3‰ for P5, the results were slightly lower for P7 and U1, between -3,5 and -10,9 in P7 and between –9,3 and -12,2 in U1. $\delta^{13}C$ water was positively correlated with $\delta^{18}O_{VSMOW}$ (Fig. 1.6b).

3.2 Cyprideis torosa *life cycle and morphological and geochemical variables*

3.2.1 Population structure

The densities dynamics of adults and last juvenile instars of *C. torosa* in the 3 sites covered by the MSS (P5-P7-U1) can be seen in figure 1.7. The interest of these results lie on the potential of identifying main moulting periods that could allow establish relationships between valve traits and environmental variables at the precise time when shell calcification took place. However, for our results it is difficult to establish particular calcification periods, because these are very broad, taking place during several months and generations of adults overlap one another. As surrogates for adult recruitment periods, we took a combination of adult's densities peaks (but this can vary for other reasons) together with sex-ratios peaks (M:F) and occurrence of last juvenile instar peaks.

In the case of P5 (Fig. 1.7), one adult cohort increases densities (coming from A-1 juveniles) between June and July-01 and the second one, between October (where a sex ratio peak is also observed), November and January. Most adults are long-lived, but two main periods of decreasing adult populations (dying adults) appear to happen between August and September (where sex-ratio decreases) and between January and March. Main moulting periods to adulthood seem to happen at rising temperatures in spring and decreasing temperatures and photoperiod in fall. In addition, in late autumn-early winter the recruitment period coincide also with an increasing trophic level (Chl*a*) and pH and decreasing TDS (Appendix 1.2).

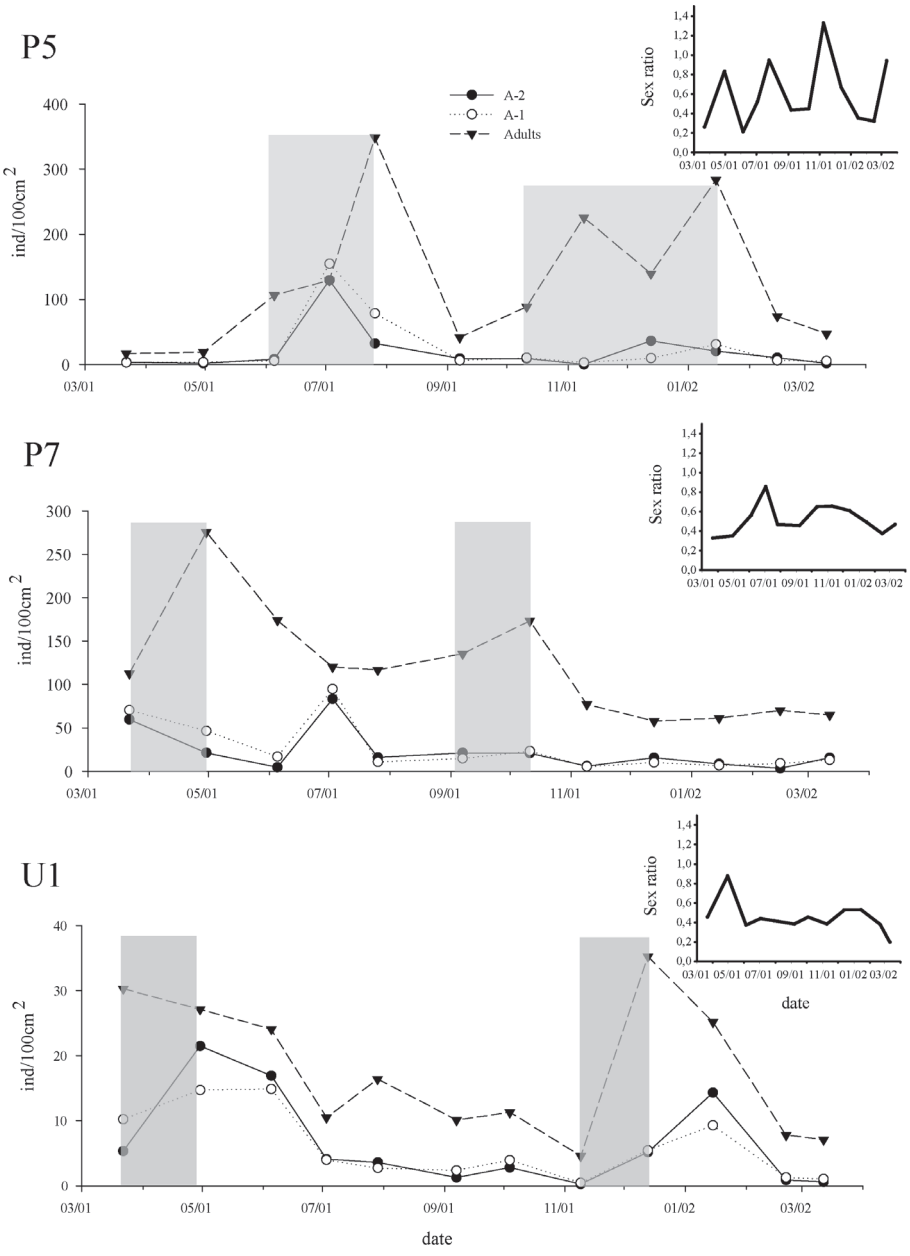

Figure 1.7: *C. torosa* densities and temporal variations of the late instars A-2, A-1 and adults for P5, P7 and U1 during the studied period, March-01 to March-02. Gray columns indicate the main moulting periods to adulthood and the graphics located on the right the monthly male:female sex ratio for each sampled site.

Figura 1.7*: Densidades poblacionales de* C. torosa *y variaciones mensuales para los últimos estadios A-2, A-1 y adultos en P5, P7 y U1 durante el periodo de estudio desde Marzo-01 hasta Marzo-02. Las columnas grises indican los principales periodos de muda a adulto y los gráficos colocados a la derecha la proporción sexual macho:hembra mensual para cada sitio de muestreo.*

In P7 (Fig. 1.7), *C. torosa* also seems to have two (overlapping) generations per year. One adult cohort increases between March and April. The second occur in September-October, when sex ratio increases too. An observed isolated peak in June for juvenile densities does not follow with increasing adult densities. However, this coincides with the highest increase in adults sex-ratios, suggesting this is a third moulting period to adulthood that is not reflected in increasing number of adults probably due to mortality of old animals. These periods would be coincident with the mains peaks of adults observed in P5.

In U1 (Fig. 1.7) two overlapping generations are also observed. One moulting period seems to happen between March and April (sex-ratio close to 1, high adult, A-2 and A-1 densities are also observed). At this time, increase both in temperature and Chl*a* and a decrease in pH and TDS is recorded. The second moulting period is more evident between November and December (high number of adults, increasing sex ratio and densities of A-1 and A-2). This period is also characterized by a decrease in temperatures and consistent showers.

In general, densities of *C .torosa* adults and juvenile individuals are variable through the year but clear adult recruitments period cannot be undoubtfully established due to the lack of synchrony between A-1 juveniles and adult peaks. However with the present data it seems that *C. torosa* can have two (even three) overlapping adult cohorts thought the year. Main moulting periods to adulthood take place in early summer, mid autumn and even late winter-early spring. Principal population declines occur in late summer and late winter at the period of most extreme temperatures.

3.2.2 Nodes

High correlations were found between arcsin($\sqrt{Pn}$) and $\log_{10}$TDS (mg/L) and water Ca (meq/L), Sr (meq/L) and they were statistically significant ($p<0.01$; r: -0.74, -0.74 and -0,83 respectively). When data from other published works were included (Vesper, 1972b and Van Harten, 1975), the arcsin$\sqrt{Pn}$ with the $\log_{10}$Salinity and $\log_{10}$Ca content of water presented normal distributions. Pearson bivariate correlation was calculated between arcsin($\sqrt{Pn}$) and $\log_{10}$Salinity and $\log_{10}Ca_{water}$; resulting in significant ($p<0.01$) values for both cases (r: -0.809 and -0.605; respectively). Linear regression analysis between $\log_{10}$salinity and arcsin$\sqrt{Pn}$ resulted in the equation shown in figure 1.8.

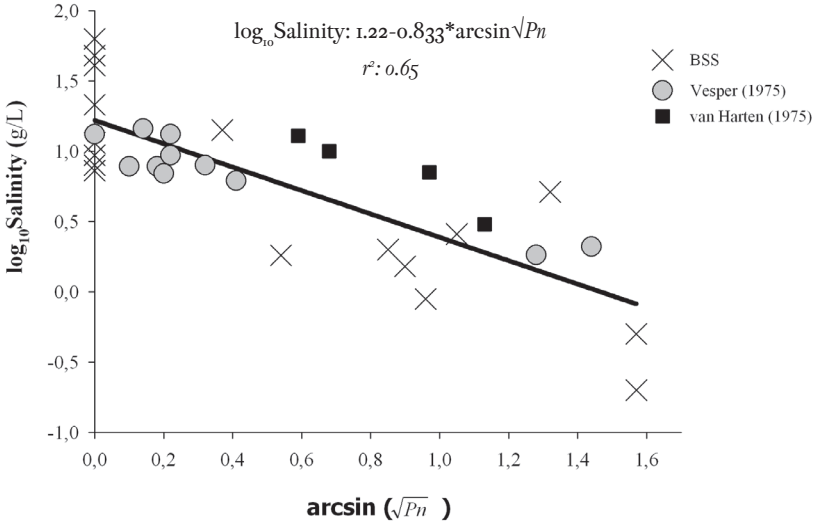

Figure 1.8: The figure shows the linear regression between $\log_{10}$Salinity and the arcsin√*Pn*, including data from Vesper (1975) and Van Harten (1975) and own data (BSS).

Figura 1.8*: La figura muestra la regresión linear entre $\log_{10}$Salinity y el arcsin√Pn, incluyendo los datos de Vesper (1975) y Van Harten (1975) y datos propios (BSS).*

3.2.3 Shell size and Ca content

Levene´s test of equality of variances for carapace lengths (CL) showed no homogeneity of variances among BSS sites ($p<0.01$; F: 2.816). Consequently, the Games-Howell non-parametric test was applied to these data, obtaining significant differences in adults CL between sites ($p<0.05$) for pairwise comparisons. Considering sexes separately, both females and males showed significant differences in CL for the 13 sites analyzed. The mean differences (based on estimated marginal means) between sexes (f-m) within samples, and applying Bonferroni adjustment, were significant ($p<0.05$) in all the places. Males were biggest regarding to CL (m>f) for all the places. Overall, CL measurements for females was CL= 969±76.6 μm (n=175) and for males CL= 1067.8 ±93.4 μm (n=147). Regarding intra-annual variability (MSS), animals were not measured, except for the two months mentioned above, and therefore it was not possible to compare the CL statistical differences between months.

CL data, showed normal distribution but we used Spearman correlation to compare with other variables because these did not show normal distributions. The only exception was the correlation with Ca_{SHELL} that also showed normal distribution, where Pearson correlation was applied. As we explained above female CL was different from Male CL (f≠m), so we considered both separately. Significant correlation values were found between CL (both females and males) and log_{10}salinity and between CL and water Ca.

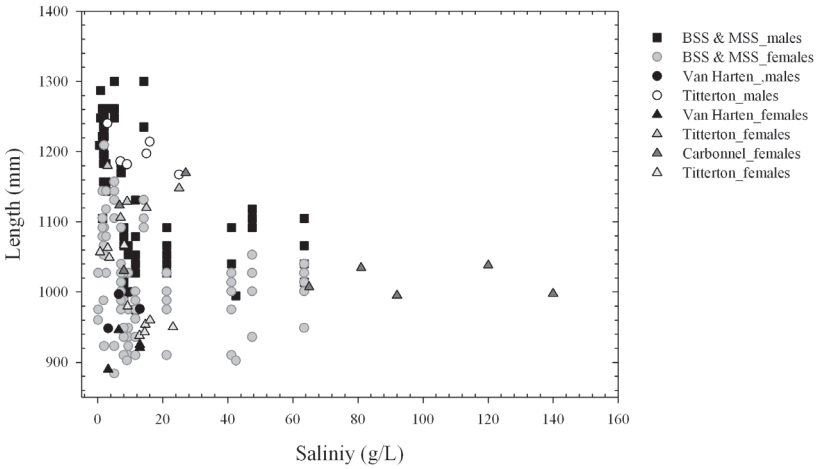

Figure 1.9: The graph shows *C .torosa* lengths with salinity (g/L) for our sampled places for both males and females. Moreover values coming from another works are also placed (Titterton 1978; Carbonnel, 1983; Van Harten 1996).

Figure 1.9*: El gráfico muestra las longitudes de* C .torosa, *para machos y hembras, en relación con la salinidad (g/L) para nuestros lugares de estudio. Los datos de otros autores encontrados en la bibliografía también fueron incluidos (Titterton 1978; Carbonnel, 1983; Van Harten 1996).*

To see if CL was related to environmental factors, we first used the data from the literature (Heip, 1976; Titterton, 1978; Carbonnel, 1983; Van Harten 1996; Mezquita *et al*., 2000) together with our information (Fig. 1.9). We tested again the normality of the data and the data showed normality for both variables (salinity and CL) in this case. Pearson correlation showed significant correlations for females ($p<0.001$; r:-0.34) and for males ($p<0.001$; r: -0.522) although the correlations were weak. CL decrease when salinity increases (Fig. 1.9), at salinities over 20g/L most animals are smaller than 1100 μm for males and 1060 μm in the case of females. Negative correlation between CL and salinity was significant for both females and males (Fig. 1.9). Other significant Pearson correlations ($p<0.01$) were found between females CL and Ca_{SHELL} and water Sr/Ca (r: 0.58; -0.49, respectively) and also for males (r: 0.64; -0.53, respectively).

As Ca_{SHELL} was positively correlated ($p<0.01$) with CL, both in females and males, linear regressions were carried out (see figure 1.10). Females showed slightly lower r^2 than males. Ca_{SHELL} for females and males, increased with CL. A few data were obtained in the case of juveniles and we did not apply any regression, but the few results indicated that juveniles followed the same trend than that found in adults.

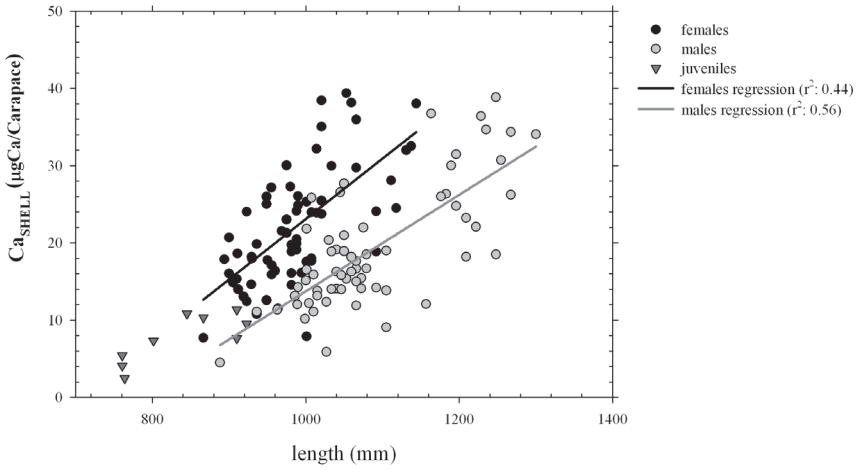

Figure 1.10: Relationship between Ca content per carapace (Ca_{SHELL}) and *C. torosa* carapace length for our 20 sampled places. Females are represented by black circles, males by gray circles, and juveniles by triangles. Outliers were excluded.

Figura 1.10*: El gráfico muestra la relación entre la concentración de Ca/caparazón (Ca_{SHELL}) y la longitud, para nuestros 20 puntos de estudio. Las hembras están representadas con círculos negros, los machos con círculos grises, y los juveniles con triángulos. Los* outliers *fueron excluidos.*

Comparing statistically Ca_{SHELL} between BSS sites showed no homogeneity of variances ($p<0.01$). So, an alternative non-parametric test (Games-Howell) was applied to these data, obtaining significant differences between sites for adults Ca_{SHELL}, where 13 of the 16 places analyzed, showed significant differences ($p<0.05$) with each other.

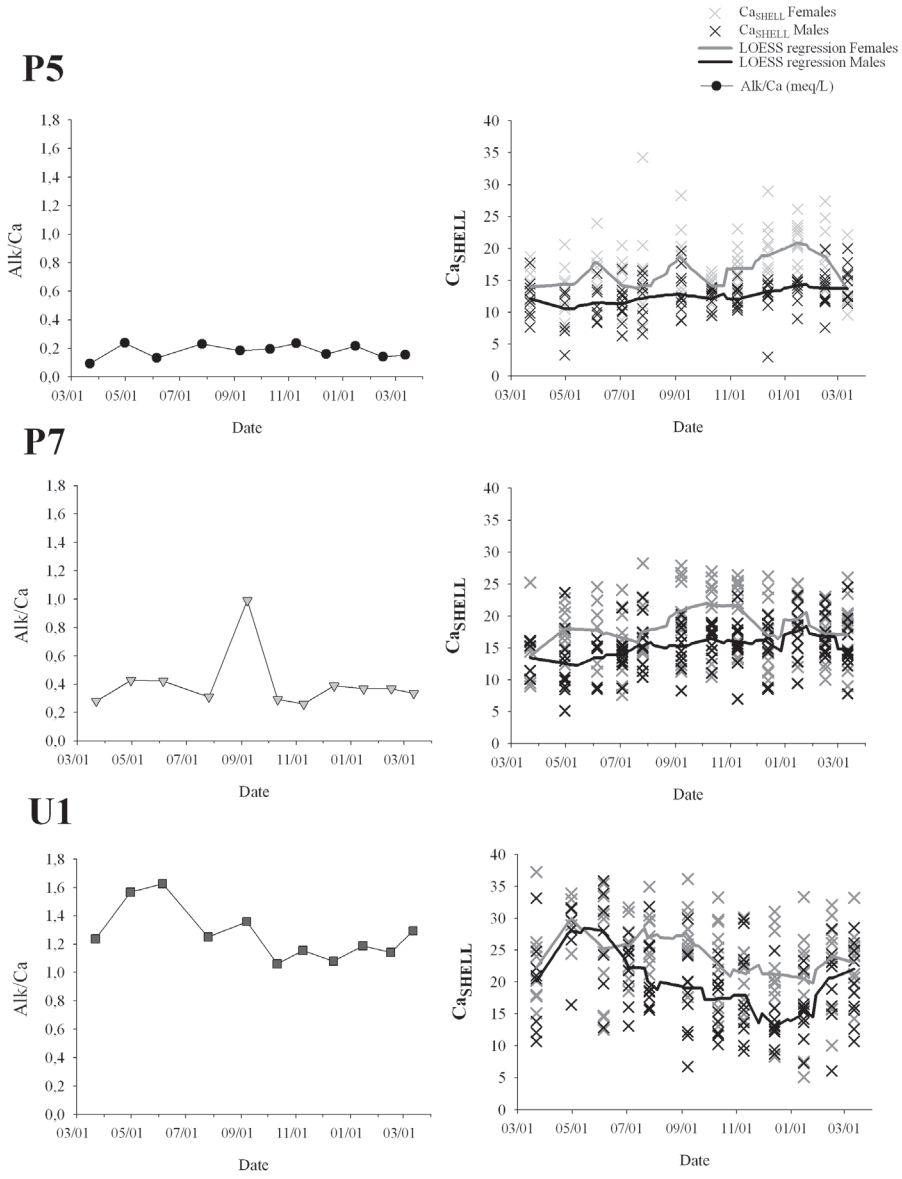

Figure 1.11: Water alkalinity/calcium water ratios and calcium content per carapace (Ca_{SHELL}; in μgCa/carapace) for P5-P7-U1 during the sampling period (March-01 to March-02). Lines were calculated as LOESS regression using 20 points.

Figura 1.11: *Evolución de la Alcalinidad/Ca y concentración de Ca por caparazón (Ca_{SHELL};μgCa/carapace) para P5-P7-U1 durante el periodo de estudio (Marzo-01 basta Marzo-02). Las líneas representan la regresi*ón LOESS aplicada a los datos *con un factor de 20.*

When we considered males and females separately, females showed significant Ca_{SHELL} differences in 15 places compared to others and males Ca_{SHELL} were different in 14 places. The mean differences (based on estimated marginal means) between sexes (f-m) within samples, applying Bonferroni adjustment, were significant ($p<0.05$) in seven places E06, E07, E21, E28, E53, P7 and U1. Generally, females (on average) were heaviest regarding to Ca_{SHELL} (f>m) for all the sites except in E21. Overall female Ca_{SHELL} varied between 5.1 and 37.2 μg, with the highest variance observed in U1. Male Ca_{SHELL} varied between 5.1 and 35.8 μg, with the widest range also seen in U1 (Fig. 1.11; Appendix 1.3 and 1.4).

Regarding to intra-annual variability during monthly monitoring in 3 sites (MSS), Levene's test showed no homogeneity of variances comparing Ca_{SHELL} months and instars. Consequently, multiple comparisons were carried out between months, applying Bonferroni adjustment. Males and juveniles did not show any statistical difference between months in the three cases, neither females from P7 and U1. Only females from P5-January-02 were statistically different to other months. Games-Howell post-hoc tests were applied to compare the differences between instars. The results showed statistical differences ($p<0.05$) between females, males and juveniles for P5, P7 and U1. Females were always heaviest regarding to Ca content (f>m>j)

BSS results show no clear relationship between water Alk/Ca and Ca_{SHELL} ($p>0.05$). Even with high divergences in water Alk/Ca among the 3 studied sites in the MSS (Fig. 1.11), ostracod Ca_{SHELL} did not show such strong differences. In general the three places showed statistical differences in Ca_{SHELL} between them although the temporal variability of the data does not present a clear pattern. In U1 the trend of Ca_{SHELL} seems to follow the changes in Alk/Ca of the host water for both females and males (Fig. 1.11). High Alk/Ca waters seem to be the optimal water for higher calcium content. On the other hand and taking into account all sampled sites, Ca_{SHELL} was on average higher at sites with low SO_4^{2-}/Cl^- and Sr/Ca ratios (Fig. 1.12).

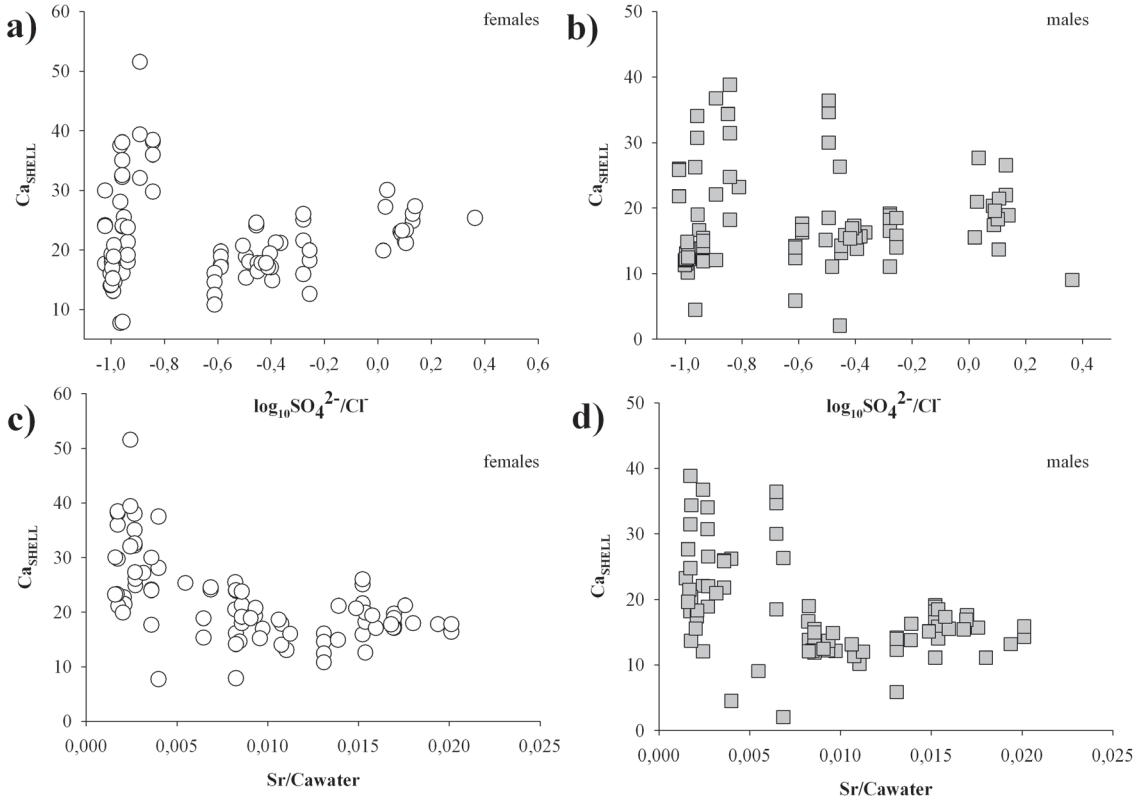

Figure 1.12: Micrograms of Calcium per shell (Ca_{SHELL};ugCa/carapace) for females (white circles) and males (gray squares) separately and compared with SO_4^{2-}/Cl^- and water Sr/Ca for BSS and MSS (monthly average values). a) Ca_{SHELL} of females vs. SO_4^{2-}/Cl^-; b) Ca_{SHELL} of males vs. SO_4^{2-}/Cl^- c) Ca_{SHELL} of females vs. water Sr/Ca; d) Ca_{SHELL} of males vs. water Sr/Ca.

Figura 1.12: *Micrograms de Calcio de la concha (Ca_{SHELL};ugCa/carapace) de BSS y MSS (valores medios mensuales), para hembras (círculos blancos) y machos (cuadrados grises) por separado y comparado con SO_4^{2-}/Cl^- y Sr/Ca del agua. a) Ca_{SHELL} de las hembras representado con SO_4^{2-}/Cl^- b) Ca_{SHELL} de los machos representado con SO_4^{2-}/Cl^- c) Ca_{SHELL} de las hembras representado con Sr/Ca del agua; d) Ca_{SHELL} de los machos representado con Sr/Ca del agua.*

3.2.4 *Mg/Ca and Sr/Ca ratios*

The Mg/Ca molar ratios of all analyzed shells fall within a relatively narrow range of values between 0.003 and 0.025, nearly independently of Mg/Ca or TDS of water, consistent with the mineralogy of the ostracode shells, low-Mg calcite (Fig. 1.13). No correlation of Mg/Ca with water temperature was seen in two of the MSS sites, P5 and P7, but there is a hint for such correlation in U1 for late-instar juveniles (Fig. 1.14). However, the monthly variation in water temperature and Mg/Ca has a similar pattern in U1. The Sr/Ca molar ratio fit in the range of values between <0.001 and 0.011 and is loosely correlated with Sr/Ca of water regardless of TDS (Figure 1.15). The Mg/Ca and Sr/Ca ratios of late-instar juveniles in dilute spring U1 showed good correlation with the Mg/Ca and Sr/Ca of water (Fig. 1.14 and 1.16).

Statistical analysis showed that Mg/Ca molar ratios of ostracod shell obtained in the BSS and MSS sites did not show homogeneity of variances ($p<0.01$). Games-Howell test showed that nine places (E06, E07, E08, E21, E45, E46, P5, P7 and U1) had significant differences ($p<0.01$) regarding to adult Mg/Ca content compared to some of the other 11 sites, but in all the cases they only differed in one or two pairwise comparisons. Three places presented significant differences ($p<0.05$) for females (E46, P5 and U1) and two for males (RA05 and U1) in a small number of comparisons. The mean differences (based on estimated marginal means) between sexes within samples, applying Bonferroni adjustment, were significant ($p<0.05$) in just two places: P7 and RA05, where males had higher Mg/Ca values than females in both sites. Mg/Ca ratio of ostracods sampled in the MSS, showed no homogeneity of variances ($p<0.05$) for the three places. Bonferroni adjustment was applied as described above. P5 showed significant differences ($p<0.05$) when we compared females, males or juveniles collected in Sepetember-01 with those collected in other months. P7 showed significant differences only among juveniles sampled in three different months, U1 showed statistical differences among juveniles from five different dates, and also between males of September-01 and those from January-02. Mg/Ca also showed no homogeneity of variances ($p<0.05$) for the three places comparing males with females and juveniles. Post-hoc Games-Howell test indicated that shell Mg/Ca in P5 was not significantly different between females, males and juveniles, so we accepted the equality of shell Mg/Ca among instars and adult sexes ($f=m=j$). In P7 significant differences were found comparing Mg/Ca of juveniles with males ($j\neq m$), whereas no differences were found in the other comparisons ($m=f$ and $j=f$).

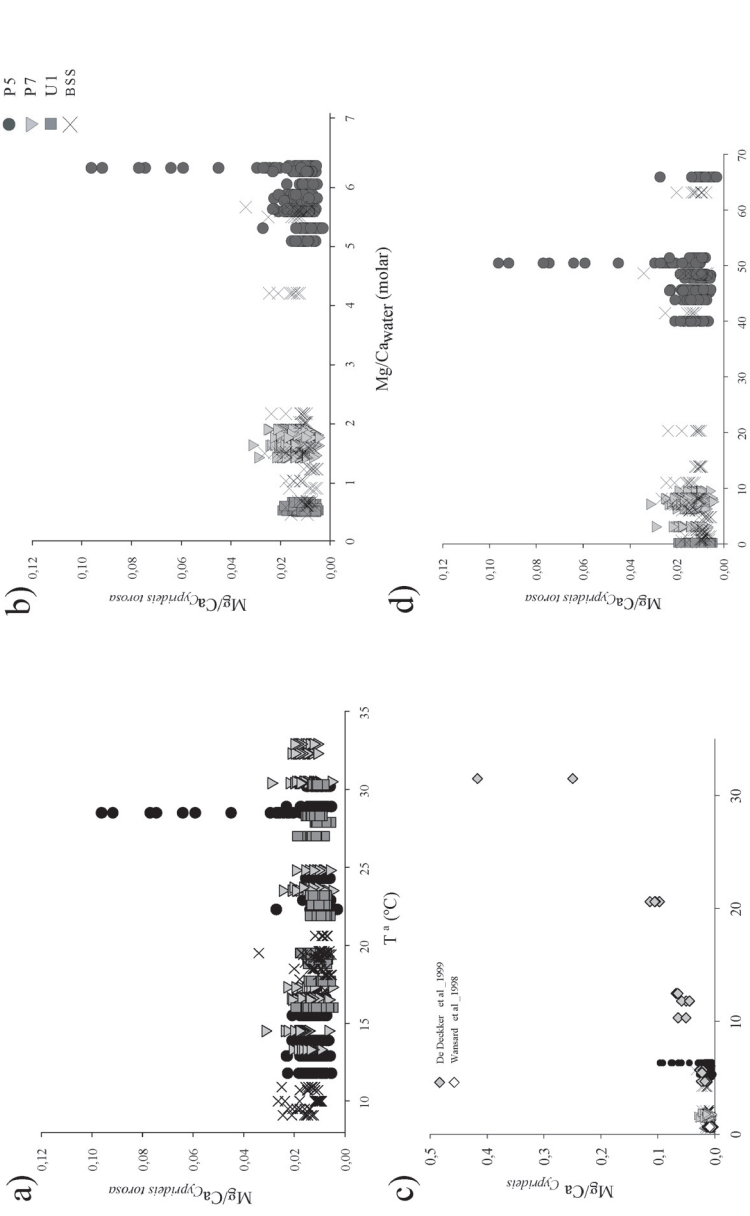

Figure 1.13: $Mg/Ca_{C.\ torosa}$ molar ratios compared with temperatures, water Mg/Ca and TDS. a) $Mg/Ca_{C.\ torosa}$ compared with the field measured temperatures from the 20 sampled places. b) $Mg/Ca_{C.\ torosa}$ vs water Mg/Ca for the 20 sampled places; c) Ostracod *Cyprideis* spp. Mg/Ca vs water Mg/Ca including data from other studies; d) $Mg/Ca_{C.\ torosa}$ vs TDS (g/l). Note that the values used in all the figures correspond to the 20 sampled places including all the results for P5-P7-U1 (MSS) and BSS+.

Figura 1.13: *$Mg/Ca_{C.\ torosa}$ comparado con las temperaturas de campo, Mg/Ca del agua y TDS. a) $Mg/Ca_{C.\ torosa}$ comparado con las temperaturas medias in situ de los 20 puntos muestreados. b) $Mg/Ca_{C.\ torosa}$ vs Mg/Ca agua para los 20 puntos muestreados; c) Mg/Ca de* Cyprideis *spp. vs Mg/Ca agua incluyendo datos de otros estudios; d) $Mg/Ca_{C.\ torosa}$ vs TDS (g/L). Los valores usados en todas las figuras incluyen todos los resultados de P5-P7-U1 (MSS) y BSS.*

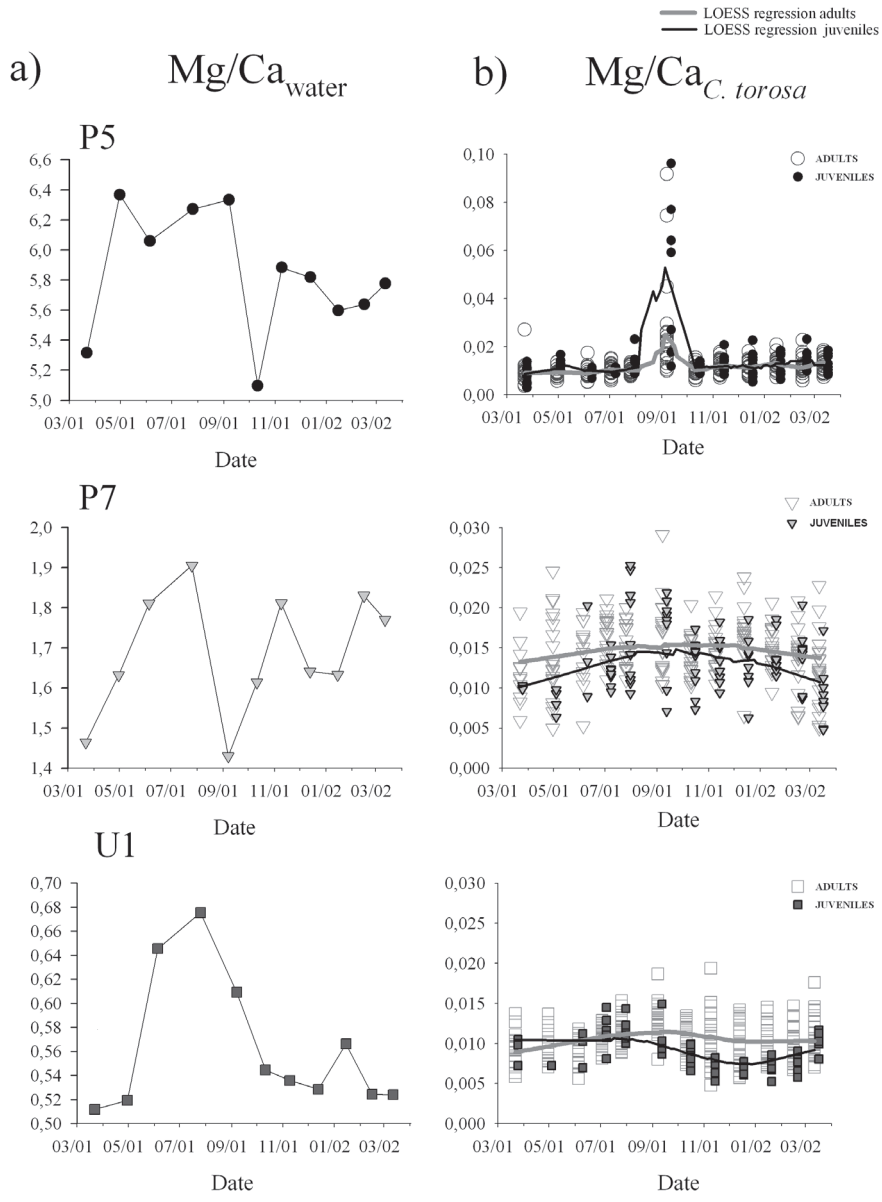

Figure 1.14: Water Mg/Ca molar ratios and *C. torosa* Mg/Ca molar ratios for MSS during the sampled period (March-01 to March-02). a) Water Mg/Ca along the year for the three sites; b) *C. torosa* Mg/Ca shows adults (empty symbols) and juveniles (filled symbols), lines were calculated as LOESS regression using 20 points.

Figure 1.14*: Mg/Ca del agua $Mg/Ca_{C.\ torosa}$ para MSS durante el periodo de estudio (Marzo-01 a Marzo-02). a) Mg/Ca agua a lo largo del año; b) $Mg/Ca_{C.\ torosa}$ mensual para P5-P7-U1, muestra adultos (símbolos vacíos) y juveniles (símbolos rellenos). Las líneas indican la regresión LOESS usando un factor de 20 puntos.*

In June and the end of July juveniles in P7 presented higher Mg/Ca values whereas in the other months males had higher Mg/Ca. In U1, we found just significant differences ($p<0.05$) only between males and females and between males and juveniles ($m \neq f$ and $m \neq j$), males always presented higher Mg/Ca values. In addition, U1 is the monitored site where ostracod Mg/Ca values, particularly in juveniles, seem to follow changes in water Mg/Ca.

Ostracod Sr/Ca molar ratios obtained in the BSS did not show homogeneity of variances among sites ($p<0.01$) according to a Levene´s test. Games-Howell tests showed that adults Sr/Ca presented significant differences ($p<0.05$) among almost all the sites. Taking sexes separately, both females and males presented significant differences ($p<0.05$) among almost all the places. In addition, the mean differences (based on estimated marginal means) between sexes within samples (applying Bonferroni adjustment), indicated that males and females were not different in Sr/Ca valves ($f=m$) except for two sites (E38BIS and E45) were males presented higher Sr/Ca molar ratios. In the case of the MSS, Sr/Ca variances where not homogeneous ($p<0.05$) for the different months, and therefore the same procedure was applied as explained above. Monthly comparisons showed only three isolated significant differences between months in the case of P5 for females and males. In the case of juveniles, those from July-01 showed significant differences with 7 months in P7. Similarly, in U1, Sr/Ca from March-01 showed significant differences with all the months for males and juveniles. We did not find any statistical difference between female Sr/Ca and male Sr/Ca for the three places neither with juveniles except for P5, were females and males were significantly different ($p<0.05$) for juveniles ($f \neq y$; $m \neq y$) with respect to Sr/Ca.

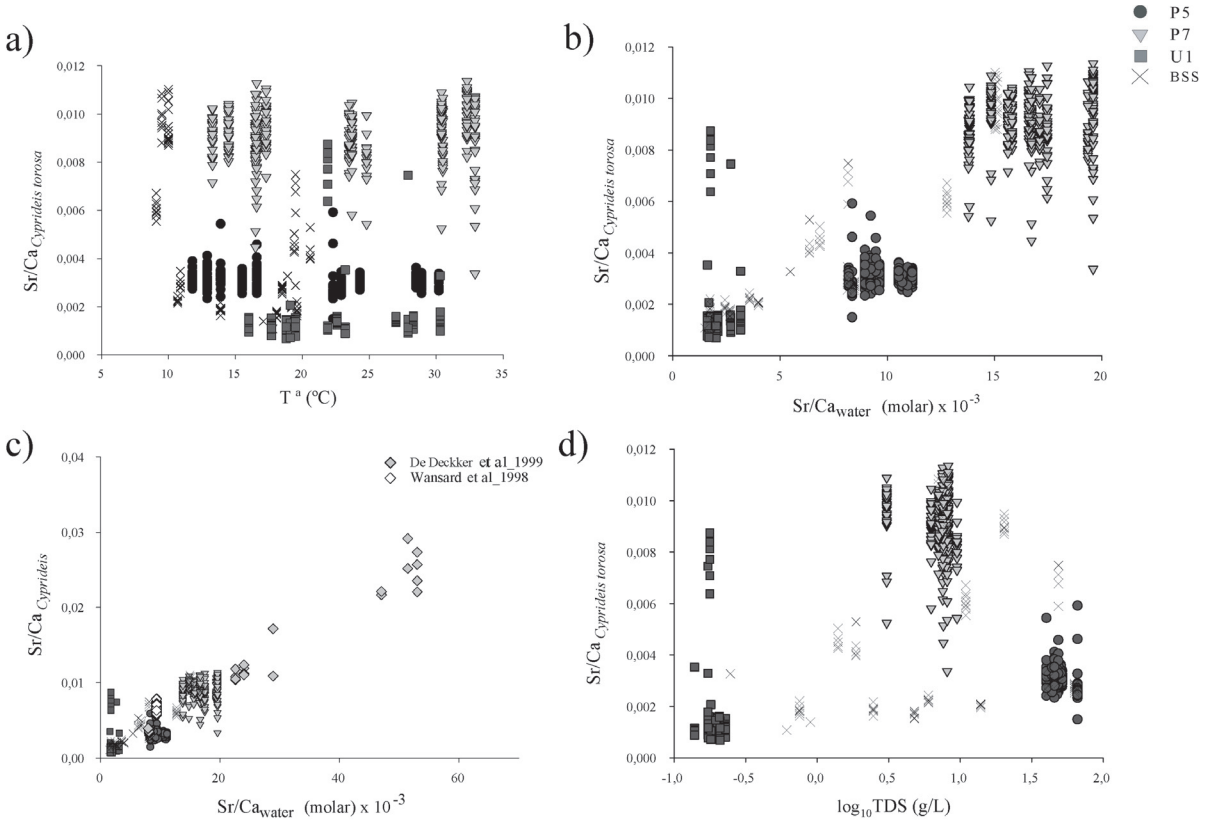

Figure 1.15: *Cyprideis torosa* Sr/Ca molar ratios compared with measured field temperatures, water Sr/Ca and TDS a) $Sr/Ca_{C.\ torosa}$ trend relationship with to water temperatures from the 20 sampled places; b) $Sr/Ca_{C.\ torosa}$ vs water Sr/Ca for the 20 sampled places; c) ostracod Sr/Ca vs water Sr/Ca, Note that data from other studies were included; d) $Sr/Ca_{C.\ torosa}$ vs $\log_{10}$(TDS, g/L). Note that the values used in all the figures, correspond to the 20 sampled places including all the results for P5-P7-U1 (MSS) and BSS.

Figura 1.15: $Sr/Ca_{C.\ torosa}$ *comparado con las temperaturas de campo, Sr/Ca agua y TDS. a)* $Sr/Ca_{C.\ torosa}$ *comparado con las temperaturas medidas* in situ *de los 20 puntos muestreados. b)* $Sr/Ca_{C.\ torosa}$ *vs Sr/Ca agua para los 20 puntos muestreados; c) Sr/Ca del ostrácodo vs Sr/Ca agua incluyendo datos de otros estudios; d)* $Sr/Ca_{C.\ torosa}$ *vs TDS (g/L). Los valores usados en todas las figuras incluyen todos los resultados de P5-P7-U1 (MSS) y BSS.*

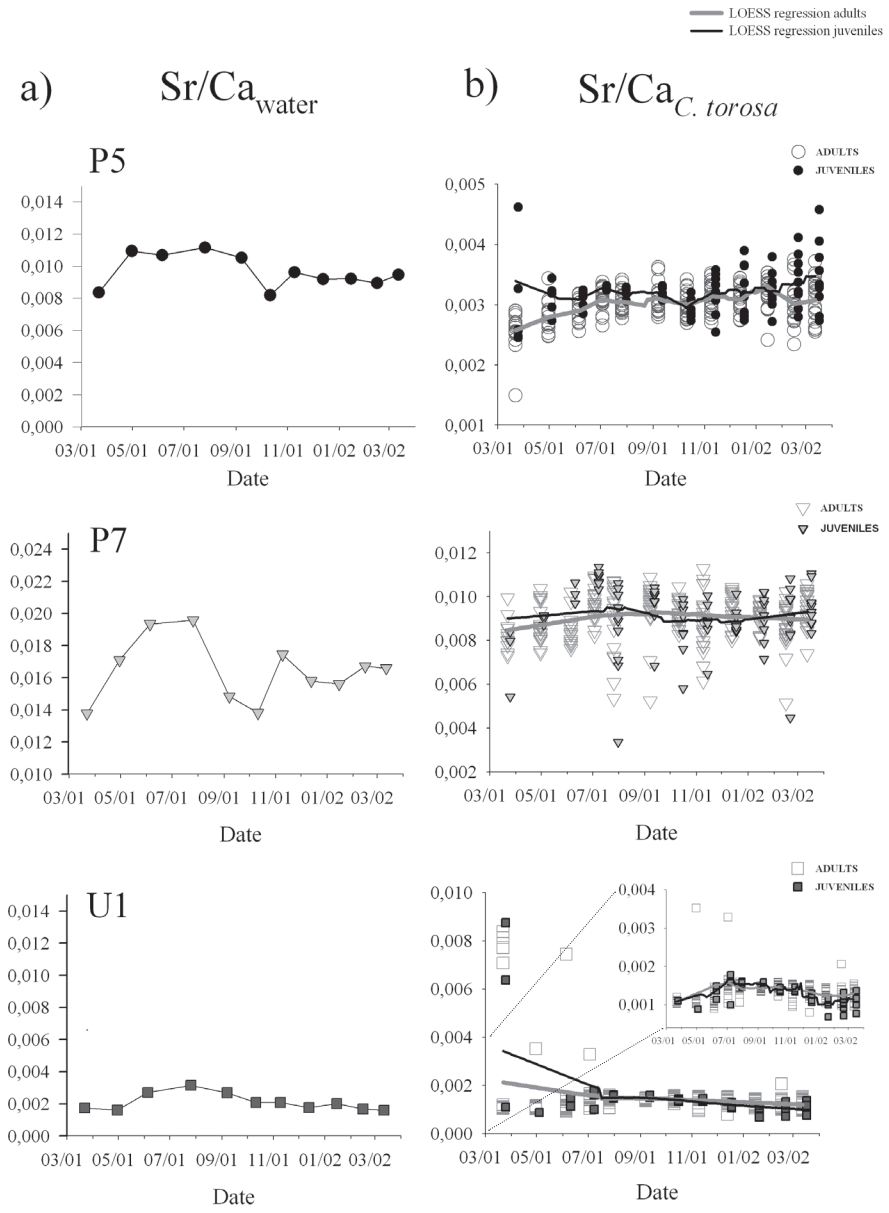

Figure 1.16: Water Sr/Ca molar ratios and *C. torosa* Sr/Ca molar ratios for MSS during the sampled period (March-01 to March-02). a) water Sr/Ca evolution along the year is indicated by different symbols (P5:black circles, P7: gray triangles and U1: gray squares); b) *C. torosa* Sr/Ca for adults (empty symbols) and juveniles (filled symbols), lines were calculated as LOESS regression using 20 points. Note In graphic U1 ostracod Sr/Ca Loess regression was calculated excluding outliers and the inset graph in the lowermost figure is the augmented graph for U1.

Figure 1.16*: Sr/Ca del agua y* $Sr/Ca_{C.\ torosa}$ *para MSS durante el periodo de estudio (Marzo-01 a Marzo-02). a) Sr/Ca agua a lo largo del año(P5:círculos negros, P7: triángulos grises and U1: cuadrados grises); b)* $Sr/Ca_{C.\ torosa}$ *mensual para P5-P7-U1, muestra adultos (símbolos vacíos) y juveniles (símbolos rellenos). Las líneas indican la regresión LOESS usando un factor de 20 puntos. Notar que en U1 la regresión LOESS se realizo excluyendo* outliers *y el gráfico insertado es el mismo aumentado.*

3.2.5 $\delta^{13}C_{VPDB}$ and $\delta^{18}O_{VPDB}$

$\delta^{13}C_{VPDB}$ and $\delta^{18}O_{VPDB}$ of *C. torosa* valves from all sites (Fig. 1.17a) are loosely correlated as might be expected for ostracods calcifying in water bodies dominated by evaporation process (Talbot, 1990). The differences between the valve-$\delta^{13}C$ and DIC-$\delta^{13}C$ for the MSS sites largely occupy the same range regardless of TDS (Fig 1.17b).

The time series for $\delta^{13}C$ values of DIC and ostracod valves for the three MSS sites are shown in Fig. 1.18 and $\delta^{18}O$ values of water and the valves are shown in Fig. 1.19. In broad sense, the DIC $\delta^{13}C$ and valve $\delta^{13}C$ values are similar, and the water $\delta^{18}O$ and valve $\delta^{18}O$ values are similar. The valve $\delta^{13}C$ and $\delta^{18}O$ values for any collection date shows a wide range likely because these animals had calcified some days before the sampling date. For adults, this could be weeks to months ago. Even for the juveniles, they may have calcified several weeks before they were harvested. The range of valve $\delta^{13}C$ values are small for U1 reflecting its hydrochemical environment (Appendix 1.4). The range is larger for P5 and P7 both of which showed a large seasonal change in DIC $\delta^{13}C$.

The $\delta^{18}O$ values of adults in U1 appears to show the effects of water temperature with higher than expected values in cooler winter months (November-December moult, sampled in January and February) and lower than expected values for those that moulted in March-April and harvested in summer through fall. The outliers seen for March 2001 valves were formed at some earlier time before the study started.

Regarding to statistical analyses, BSS data on $\delta^{13}C_{VPDB}$ did not show homogeneity of variances ($p<0.01$) according to Levene´s test. Games-Howell tests showed that adults from any site had significant differences ($p<0.05$) in $\delta^{13}C_{VPDB}$ with almost any other BSS site. Both females and males presented significant differences ($p<0.05$) between the majority of sites. Differences in $\delta^{13}C$ between sexes (based on estimated marginal means) within samples, applying Bonferroni adjustment, were significant ($p<0.05$) only for four places (E21, E38BIS, E39, RA05), were females showed high $\delta^{13}C$, except in RA05, where males had higher values. In the case of MSS, $\delta^{13}C_{VPDB}$ showed no homogeneity of variances among months and Games-Howell test was applied. In P7, females and males did not show significant differences between months. In P5, some significant differences were found in four months for females and six months for males. In U1, only June-01 males showed some significant differences with males

from other months. In the case of juvenile $\delta^{13}C$ we did not find any significant difference between months. In P5 and P7 juveniles from April-01 were different from those of July-01 Juveniles from March-01 were significantly different from those from other months. Females, males and juveniles did not show any significant difference among them in P5 and U1 (f=m=y). It was not the case of P7 were males and females were statistically different ($p<0.05$) between them (f≠m), but not from juveniles (j=m; j=f). In P7, female's $\delta^{13}C_{VPDB}$ values were higher than males. BSS $\delta^{18}O_{VPDB}$ did not show homogeneity of variances among sites ($p<0.01$; 3.136) according to Levene´s test. Games-Howell test showed that all adults, except those from E38BIS, had significant $\delta^{18}O$ differences ($p<0.05$) with adults from almost any other site.

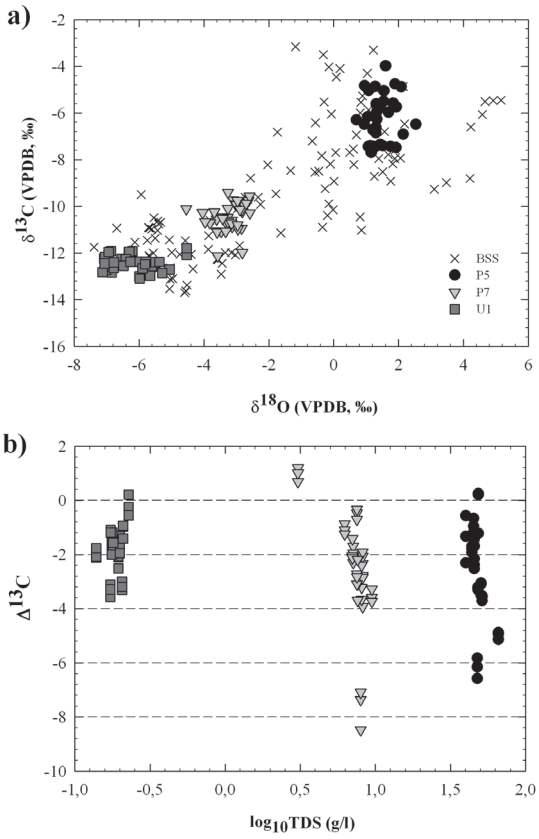

Figure 1.17: $\delta^{13}C_{VPDB}$ and $\delta^{18}O_{VPDB}$ values obtained for the BSS and MSS of females, males and juveniles are presented compared with environmental variables a) $\delta^{13}C_{VPDB}$ with $\delta^{18}O_{VPDB}$ of *C. torosa*; b) Increment of $\delta^{13}C_{VPDB}$ and $\delta^{13}C_{DIC}$ compared at different log_{10}TDS.

Figura 1.17*:* $\delta^{13}C_{VPDB}$ *y* $\delta^{18}O_{VPDB}$ *de hembras, machos y juveniles obtenido para BSS y MSS están representados con diferentes variables ambientales. a)* $\delta^{13}C_{VPDB}$ *con* $\delta^{18}O_{VPDB}$ *de* C. torosa*; b) Incremento de* $\delta^{13}C_{VPDB}$ *y* $\delta^{13}C_{DIC}$ *comparado a diferentes* log_{10}*TDS.*

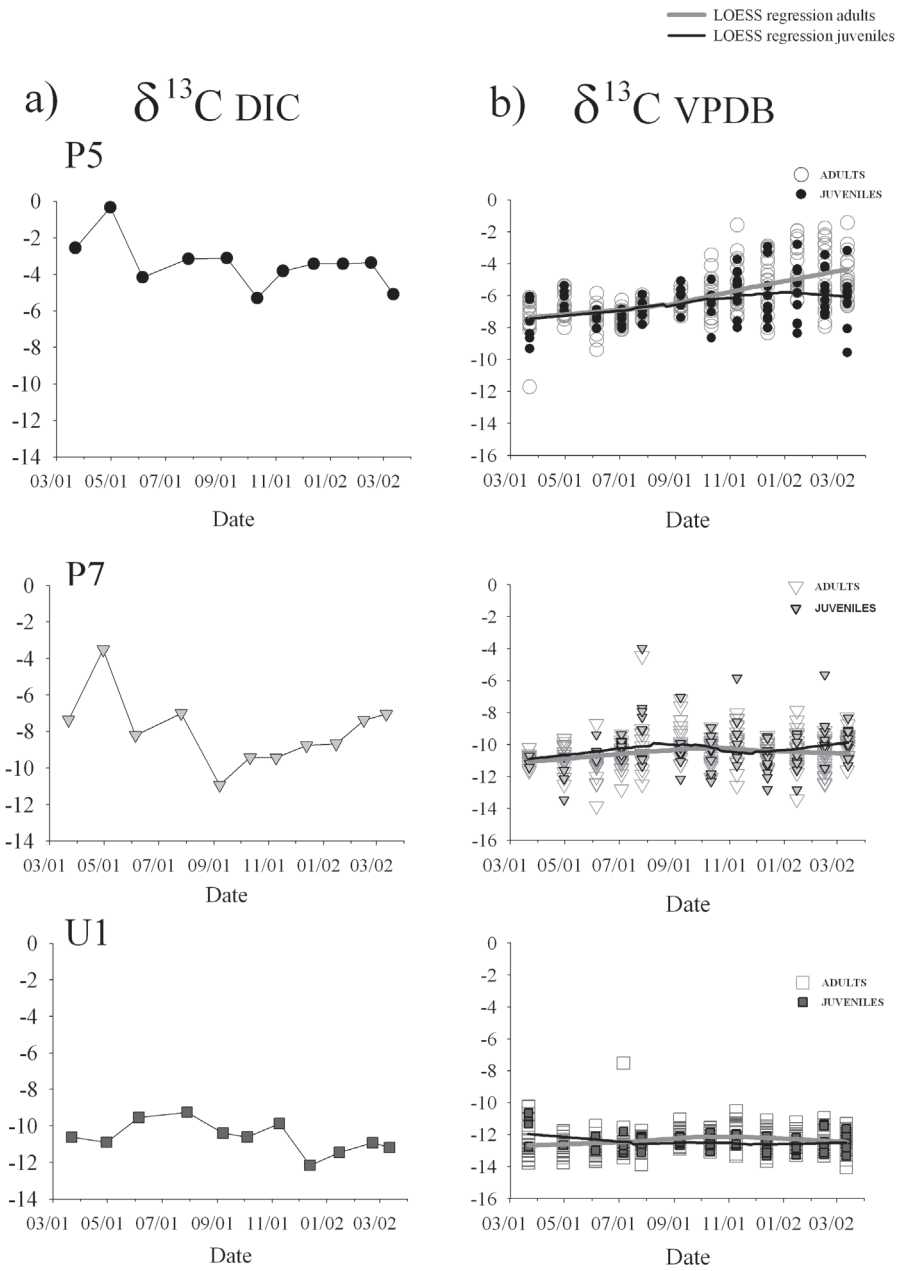

Figure 1.18: $\delta^{13}C$ calculated from DIC (Dissolved Inorganic Carbon) and $\delta^{13}C_{VPDB}$ from *C. torosa* either for adults or juveniles during the sampled period from March-01 to March-02. a) $\delta^{13}C_{DIC}$ along the year is indicated filled symbols; b) $\delta^{13}C_{VPDB}$ from *C. torosa* shows adults (empty symbols) and juveniles (filled symbols), lines were calculated as LOESS regression using 20 points.

Figure 1.18*: $\delta^{13}C$ del DIC (Carbono Inorgánico Disuelto) y $\delta^{13}C_{VPDB}$ de* C. torosa *tanto para adultos como juveniles durante el periodo de estudio, desde Marzo-01 a Marzo-02. a) $\delta^{13}C_{DIC}$ a lo largo del año para P5-P7-U1; b) $\delta^{13}C_{VPDB}$ de* C. torosa *muestra adultos (símbolos vacíos) y juveniles (símbolos rellenos). Las líneas indican la regresión LOESS calculada usando un factor de 20.*

Both females and males separately presented significant differences in $\delta^{18}O$ ($p<0.05$) between all sites in pair wise comparisons. The mean differences (based on estimated marginal means) between sexes (f-m) within samples, applying Bonferroni adjustment, were significant ($p<0.05$) for only two sites in the case of females (E38BIS vs U1) and only one in the case of males (RA05). In general, females and males showed similar values (f=m) at any site, but females showed higher $\delta^{18}O$ values in E38BIS and U1, whereas in RA05 males had higher values. The monthly comparisons (MSS) showed significant differences in $\delta^{18}O$ only in P5 (March-02 vs April-01 and March-02 either for males, females as juveniles). In P7 we found only two statistical differences with respect to juveniles between July-01 and February and March-02. In U1 no less than 2 significant differences either in male, female and juvenile $\delta^{18}O$ were found for any month, except in April-01 where only the juveniles were significantly different from juveniles from March-01. Post-hoc Games-Howell showed no significantly different from juveniles from March-01. Post-hoc Games-Howell showed no significant differences in $\delta^{18}O$ between females, males and juveniles (f=m=j=f) in P7 and U1. Only in P5, significant difference ($p<0.05$) between male and juvenile ($m\neq j$) was found, where males showed higher $\delta^{18}O_{VPDB}$ values.

We examined the apparent oxygen-isotope fractionation factor *vs.* water temperature from the previous month assuming those values are closer to when the valves calcified (Fig. 1.20). Due to the absence of clear moulting signal in our MSS study sites, it is impossible to know the actual water $\delta^{18}O$ and temperature at the time the analysed ostracods moulted. *C. torosa* in P5, P7 and U1 shows different apparent $^{18}O/^{16}O$ fractionation behaviour. P7 and U1 animals do not appear to show strong temperature dependence, showing a positive offset of 1-1.5‰ from the water $\delta^{18}O$. The offset of 1 to 1.5‰ has been reported for many Candonids and other benthic ostracods (Von Grafenstein *et al.*, 1999). P5, however, shows a trend similar to inorganic calcite (indicated by the line in Fig. 1.20a), indicating temperature dependent fractionation.

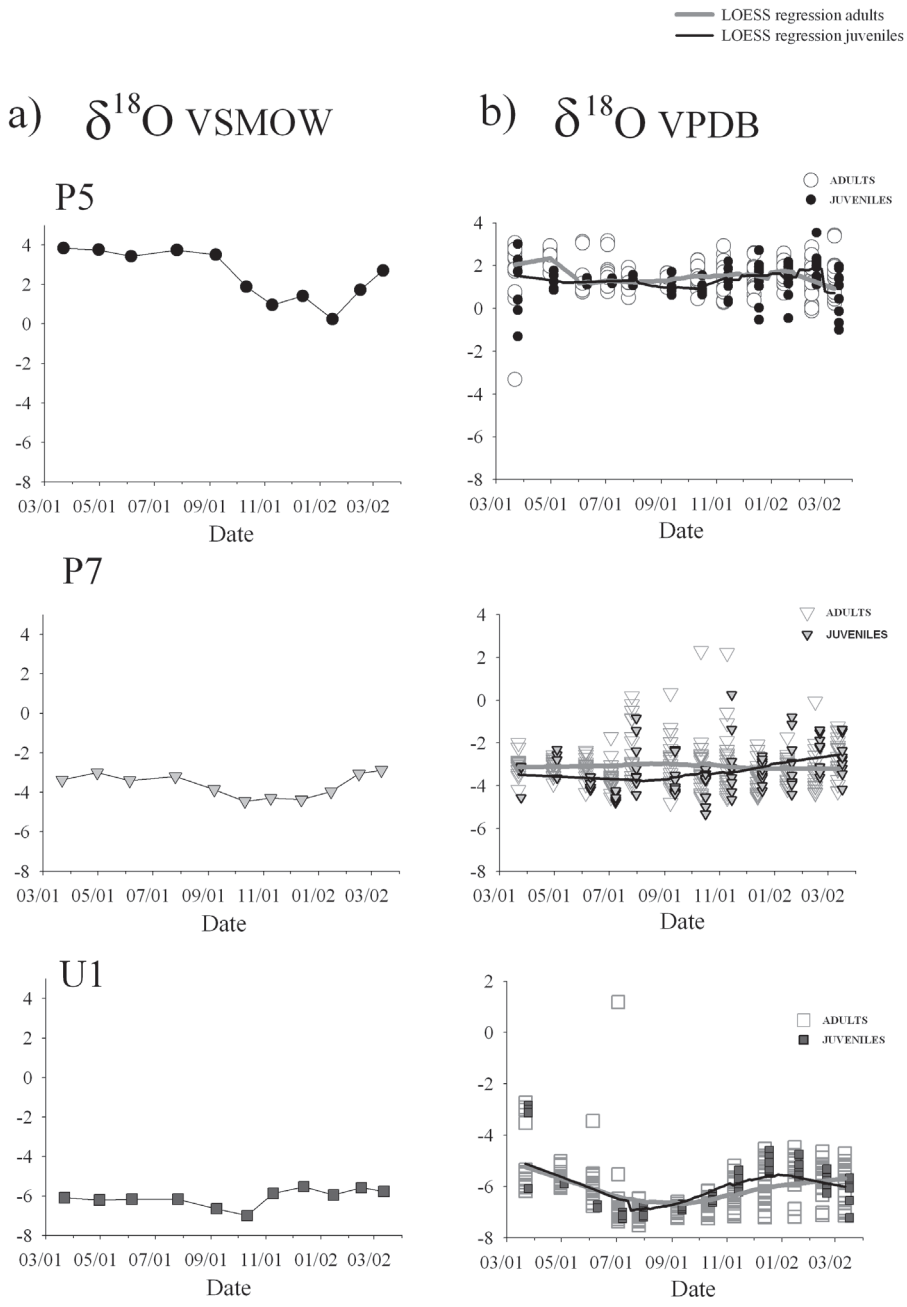

Figure 1.19: $\delta^{18}O_{VSMOW}$ and $\delta^{18}O_{VPDB}$ from *C. torosa* either for adults as juveniles during the sampled period from March-01 to March-02. a) $\delta^{18}O_{VSMOW}$ along the year; b) $\delta^{18}O_{VPDB}$ from *C. torosa* shows adults (empty symbols) and juveniles (filled symbols), lines were calculated as LOESS regression using a factor of 20.

Figure 1.18*:* $\delta^{18}O_{VSMOW}$ y *y* $\delta^{18}O_{VPDB}$ *de* C. torosa *tanto para adultos como juveniles durante el periodo de estudio, desde Marzo-01 a Marzo-02. a)* $\delta^{18}O_{VSMOW}$ *a lo largo del año para P5-P7-U1; b)* $\delta^{18}O_{VPDB}$ *de* C. torosa *muestra adultos (símbolos vacíos) y juveniles(símbolos rellenos), las líneas indican la regresión LOESS usando un factor de 20.*

3.3 Multiple regressions for hydrochemistry reconstruction

The response variable for species traits can be a function of a single environmental variable, or more frequently respond to more than one variable. Multiple regressions are commonly used in biology to understand biological species traits, but we applied the same procedure in the other way round, with the aim to reconstruct past water abiotical variables from ostracod shell data.

After application of AIC, we selected the most parsimonious subsets of ostracod variables with no more than three variables to reconstruct water hydrochemical variables. After this selection, we calculated linear multivariate regressions and and those equations with the high explanatory power were chosen (r^2> 0,7). Consequently, we show here only the results for the reconstruction of salinity and water Sr/Ca. We use salinity (g/L) instead TDS (g/L) because of the highest r^2 observed. We do not provide equations to reconstruct Mg/Ca, pH, Alkalinity, and SO_4^{2-} because of low r^2. However, we show the results for salinity reconstructions, despite its r^2>0,69, because of the general interest in this variable. Moreover, we carried out the multiple regressions between females and males and adults (females+males) separately. In any case, regressions with adults values were highly correlated especially in $\log_{10}$salinity models.

The table 1.1 shows the calculated equations for salinity and Sr/Ca derived from ostracod data, together with inferred minimum, maximum and mean values calculated from MSS data and compared with the observed data range of these variables in the field. All salinity regressions include the percentage of noded individuals (*Pn*), as the highest explanatory variable, and this can be combined with either trace elements or isotope ratios. Inferred values for MSS data are approximate to real values only in the case of P7, using either *Pn* alone or together with isotope ratios. The equations to infer water Sr/Ca have the highest r^2 and the inferred values are very close to real ones, especially for U1 and P7, but slightly low in the case of P5. As we saw, salinity is one of environmental factors that affects the ostracod morphology and geochemical composition of the shells. The percentage of noded animals (*Pn*) was chosen by AIC in all cases. It could be explained by the strong correlation that we found between this variable and salinity as it was discussed in many previous studies (Vesper, 1972b and Van Harten, 1975). These studies point to salinity as the main variable affecting node formation but none of them developed an exhaustive study to check it. Other variables, as isotopes, were included in the regressions, probably due to the good correlations between them and salinity separately. As we can see

the use of the first equation (Table 1.1) which only take into account the *Pn*, can be a good to tool to asses salinities below 20 g/L. P5 reconstructed salinity does not fit well, because probably *C. torosa* does not calcify well at high salinities, driving poor calcified shells with lighter isotopic composition. The anomalous high values obtained for P7 and U1 can be due to the fact that we only measured node formation in one month of P7 and neither in U1. If we assume 100% noding at U1 the inferred values fit well with the real ones. For that reason, we consider that at the time to apply these equations, the whole *C. torosa* node year frequency from each particular place should be take it into account to improve better and significant results of node proportion.

Table 1.1: This table shows the obtained environmental multiple regressions based on Akaike Information Criteria (AIC) results and the inferred values obtained from the average values of P5, P7 and U1. The real range of each environmental variable is also placed.

Tabla 1.1: *La tabla muestra las ecuaciones derivadas de las regresiones múltiples a partir de los resultados del test de Información de Akaike (AIC) y los valores ambientales inferidos a partir de los valores medios obtenidos de P5, P7 y U1. El valor real de cada variable ambiental se muestra en la tabla.*

Salinity	**p-valor**	**r^2**		**P5**			**P7**			**U1**		
(g/L)				*min*	MEAN	*max*	*min*	MEAN	*max*	*min*	MEAN	*max*
			REAL	**42,50**	**57,20**	**73,00**	**4,50**	**8,50**	***10,30***	**0,1**	**0,3**	**0,4**
(Eq. 1) $Log_{10}Sal=1,227-0,01464*Pn$	p<0.01	0,69	inferred	12,41	16,87	22,93	11,93*	16,09*	21,27*	12,41	16,87	22,93
										0,44**	0,58**	0,77**
(Eq. 2) $Log_{10}Sal=1,237-0,01292*Pn+0,02796*d^{18}O_{C.\ torosa}$	p<0.01	0,7	inferred	11,83	18,93	30,28	12,76*	13,13*	14,25*	16,35	11,63	23,74
										0,50**	0,59**	2,03**
Water Sr/Ca					**P5**			**P7**			**U1**	
molar $x10^{-3}$				*min*	MEAN	*max*	*min*	MEAN	*max*	*min*	MEAN	*max*
			REAL	**8,19**	**9,6**	**11,16**	**13,8**	**16,4**	**19,6**	**1,6**	**2,1**	**3,15**
(Eq. 3) $Sr/Caw=1,551*(Sr/Ca_{C.torosa})+0,00236$	p<0.01	0,79	inferred	6,92	7,14	7,36	16,04	16,41	16,77	2,21	2,25	2,28
(Eq. 4) $Sr/Caw=4,286+0,292*d^{18}O+0,228*d^{13}C+1,371*Sr/Ca_{C.torosa}$	p<0.01	0,95	inferred	6,47	7,51	8,54	13,24	13,36	13,48	0,00	1,64	3,44

Pn : frequency of nodes (%)

*Inferred values with real 1,39% of noding

**Inferred values assuming 100% of noding

4.-Discussion

The hydrochemical range and the type of water bodies in this study are very broad and are well suited to investigate possible effects of factors such as TDS, ionic compositions, and habitat. Our sites are similar in their hydrochemical characteristics to those reported for other coastal evaporative areas of the world (Bowling and Tyler, 1984; Geddes and Butler, 1984; Radke *et al*., 2002, 2003), and are typical of waters in the Spanish Mediterranean region (López and Tomás, 1989). Because *C. torosa* is widely distributed (e.g. Bronshtein, 1947; Mischke, 2001; Meisch, 2000), our findings that (1) TDS, (2) Alk/Ca (3) water Ca are the key habitat variables affecting its cation uptake, will have broad application in paleolimnological reconstructions.

4.1 Shell size and Ca uptake

Heip (1976), Van Harten (1975, 1996), and Mezquita, *et al.* (2000) studied *C. torosa* in different ecosystems and found that adults have smaller shells sizes in waters with high salinities. In agreement with those authors our data set shows that when solute concentration increases, the length of our specimens decrease (Fig. 1.9). Both males and females are smaller at high TDS waters (P5, E39, E38bis, and E38). Moreover, Mezquita *et al.* (2000) found that the adults that moulted in winter were longer than those that moulted in the summer period. They suggested that this may be due to low temperatures and/or by seasonal salinity variations during the year.

Our results show that the differences in size between males and females are statistically significant and differences between places comparing either males or females from different populations are also significant. Moreover these statistical differences can be found when we compare different systems, indicating that water chemistry has strong influence in the final length (Fig. 1.9). Combining our data on *C. torosa* CL, together with data from the literature, we observed that in water bodies with salt concentration over 20g/L, males were always smaller than 1100 μm in CL and females were always smaller than 1060 μm. TDS seems to have strong influence in the final CL of *C. torosa* adults shells, however no strong correlation was found when we compared the size of both females and males with salinity, as only male CL correlated weakly but significantly with salinity, showing that males are smaller with increasing solute

concentration. So, we suggest that other variables besides genetic constraints and salt content may be involved in adult CL, such as SO_4 concentration or Sr/Ca (see below). Importantly, we found that *C. torosa* CL is correlated with the amount of calcium of the shell (Fig. 1.10). The longest animals have higher Ca content indicating that the Ca concentrations of the carapace will depend of the final size or vice versa. Those parameters will be mostly controlled by the composition of the surrounding water and calcification time (Mezquita *et al.*, 1999; Wansard and Roca, 1997). Shell size has a clear relationship with TDS, but no just TDS is influencing sizes. For instance, temperatures (Mezquita *et al.*, 2000) and other possible factors such as food can be also involved. Hence size shell variations along a sedimentary sequence could be a good indicator that some environmental changes happened in the history of a lake (mainly solute composition) and supported by other proxies it could be a good tool for paleoenvironmental assessment. In particular, according to our data, if *C. torosa* individuals from a core are not longer than 1100 μm for males and 1060 μm for females, it probably could indicate that salinity at the time, where those specimens were living, was higher than 20 g/L.

The calcification process occurs by the reaction:

$$Ca^{2+}+HCO_3^-\rightarrow CaCO_3+H^+$$

in which bicarbonate is provided either directly from the external solution or by hydration of metabolic CO_2. Turpen and Angell (1971) demonstrated that the majority of calcium that forms the carapace is obtained directly from the surrounding water. In addition Keyser and Walter (2004) proved that ostracods prior to moult accumulate a huge amount of calcium phosphate together with chitin precursors in granules located at the outer epidermal cells, which are supposed to contribute significantly on the future composition of the carapace but not to be enough to build the whole ostracod shell. Crustaceans incorporate bicarbonate from the surroundings waters through a HCO_3/Cl^- antiport pump (Pequeux, 1995). Consequently, we should take into account that the final calcium concentration in the ostracod carapace must depend of Ca and HCO_3 content in the host water and the availability to capture those elements by ostracods. The availability of calcium depends on the composition of the water where ostracods live. Ca pumps in freshwater crustaceans work at the maximum rate when external calcium content surpasses 0.5-1mmol/l (Neufeld and Cameron, 1993). So, calcium concentration in our study sites does not seem to be limiting factor (Appendixes 1.1 and 1.2).

Cyprideis torosa has a preference for living (calcifying) in waters with Alk/Ca<1 (Mezquita *et al*., 2005). We saw that Alk/Ca ratio becomes lower with solute concentration in our systems (Fig. 1.4a) and *C. torosa* individuals living at high Alk/Ca waters are those with the highest Ca content (both males and females) and consequently also bigger regarding to CL (Fig. 1.10). The absence of correlation between ostracods Ca content and alk/Ca, indicates that neither is limiting directly the Ca uptake. So, the limitation factor may be HCO_3^- as it was mentioned by Mezquita *et al*. (1999), where they suggested that HCO_3^- could be the limiting factor for the calcification of *Herpetocypris intermedia* cultured in different water types. In this framework of interaction effects between ionic regulation and calcification processes in ostracods, *C. torosa* should be considered as a hyper-hyporegulator organism (see Pequeux, 1995). As an hyperosmotic organism in freshwater systems, *C. torosa* animals need to introduce more Cl^- inward their bodies to maintain the hyperosmosis with respect to the surrounding water, most probably through a HCO_3^-/Cl^- antiport pump. When HCO_3^- and Cl^- concentrations are high enough in freshwaters they do not represent a problem to calcify the shells. But if the ostracods live in a hypersaline environment they function as hyposmotic system, trying to keep the maximum amount of water inside the body. Under these stressful conditions, calcification might be *less efficient* because it results in a trade-off between Ca^{2+} uptake and H^+ exflow, giving an extra metabolic cost in calcification. Capturing Ca means losing H_2O (the proton that Ca^{2+}/H^+ antiporter use). So, less efficient calcifications could explain the lower Ca content at hypersaline environments.

We must also take into account the influence of other cations such as Mg and Sr (see below), and anions that can be involved in the calcification processes. For instance, in the case of SO_4^{2-} regulation, our results did not show a clear correlation between CL, Ca_{SHELL} and SO_4^{2-}/Cl (Fig 1.13a,b) although at high SO_4^{2-}/Cl^- waters animals seem to be smaller. SO_4^{2-} regulation has just been described in hepatopancreas epithelium for crustaceans, where the SO_4^{2-}/Cl- and $SO_4^{2-}/$ Oxalate antiporter plays a role (Ahearn *et al*., 1999). But the importance of both gills and antennal glands, or during moulting processes in sulfate regulation remain to be established in crustaceans and nothing has been studied about ostracods so far. Nevertheless, ecophysiological studies with *C. torosa* (Jahn *et al*, 1996) showed that *C. torosa* has high resistance to hypoxia and hydrogen sulphide concentrations. The ostracod is indeed able to oxidize the penetrating sulphide to non-toxic thiosulphate and to eliminate the oxidation products rather quickly (Jahn *et al*, 1996). These authors concluded that *C. torosa* can use

anaerobic pathways and can tolerate high sulphate concentrations but reducing the metabolism at places with high SO_4^{2-} concentrations. Consequently the capacity to moult and then to calcify must be negatively affected. Our water bodies suffer an increase in SO_4^{2-}/Ca with TDS (Appendix 1.1 and 1.2), and although we cannot conclude that increasing SO_4^{2-} drives smaller shells during calcification processes (Fig. 1.12a,b), it might reduce the metabolism of *C. torosa*. However, i*n vitro* experiments should be done to test if sulphate concentrations have influence on the final shell's size and Ca_{SHELL}.

4.2 Nodes

Variable noding in *C. torosa* is a phenomenon that has commonly been used in paleoecological studies as a salinity indicator. Different studies have been made about noding (see Sandberg, 1964; Kilenyi, 1972; Vesper; 1972b, 1975; Van Harten, 1975, 1996, 2000; Keyser, 2005). We did not find any animal that present nodes in salinities over 20 g/L (Fig. 1.8). Van Harten (2000) suggested that another factor (called factor X) could be involved in the noding process. He suggested that Ca concentration could be the main factor affecting node formation. A few years later, Keyser (2005) demonstrated that *C. torosa* needs Ca in the demosomas junctions to maintain the carapace structure at the time of moulting to avoid nodding, but they did not test what happens at different salinities in relation to the relative availability to uptake this Ca, or how much time the ostracods use to calcify at different salinities. So, focusing on these variables we found that the strongest correlation was between $\arcsin\sqrt{Pn}$ and salinity (Fig. 1.8). *C. torosa* probably needs more availability of Ca^{2+} available in the water when it is moulting. The low availability of this Ca^{2+} plus low salinities favour the possibility that nodes appear. We observed that animals living in waters with low Ca^{2+} content present nodes but are those with the highest Ca_{SHELL} per carapace. This apparently contradictory result could be explained by salinity limitation. We suggest that salinity might be one of the main factors affecting the calcification process. The osmoregulative cost to keep body water at high salinities and introduce HCO_3^- against a force to exclude it through HCO_3/Cl antiport drives the ostracod to calcify less efficiently (lower Ca_{SHELL}) and in addition to reduce the possibility of nodes formation as Ca content is high enough to moult (for demosomas junctions) in those waters (Appendixes 1.1 and 1.2). Therefore the cation an anion composition of the surrounding waters drives to calcify in a narrow window of time at higher salinities. In freshwater environments the availability of Ca could be lower at the time of moulting but

enough to built well calcified shells if the ostracods do not stop calcification process immediately and can incorporate more Ca into their shells along a longer period of time. Our results confirm the appropriated use of a morphological tool to reconstruct past salinities based on the percentage of noded valves (*Pn*) in *C. torosa*, and a more accurate equation is given in the present study to estimate salinities from sedimentary sequences.

4.3 Mg uptake

Mg incorporation into low-Mg calcite in water of constant Mg/Ca is strictly a function of temperature (Mucci and Morse, 1983; Morse and Bender, 1990). This has been used to reconstruct sea surface temperature from Mg/Ca of foraminifers assuming seawater Mg/Ca has remained constant over glacial-interglacial scales (e.g. Elderfield *et al*., 1996). Wansard (1996a,b) attempted to apply this idea to a lacustrine setting. However, as shown by De Deckker *et al.* (1999) in their culture study of *Cyprideis australiensis*, the effect of changing water Mg/Ca, for example, by evaporation, on valve Mg/Ca may be far larger than the temperature effect. Furthermore, in continental settings waters with similar Mg/Ca may have different TDS and ionic compositions and waters with similar TDS may have different Mg/Ca (Ito and Forester, 2009).

The TDS of our sites varied from <100mg/l to >70g/l and Mg/Ca co-varied with TDS increasing from 0.5 to 6.5 (Fig. 1.4c). The observed valve Mg/Ca ratios were between 0.05 and 0.3 seemingly independent of water temperature and Mg/Ca at the time of sampling, with the exception of adults and late-instar juveniles collected in September 2002 from P5, a seawater evaporation pond, that show ratios up to 0.1 (Fig. 1.14a, b). In general *C. torosa*, which was found in waters Mg/Ca < 6.5 in our study, seems to hold constant shell Mg/Ca along this chemical gradient, with high values (close to high-Mg calcite) observed only at the highest limit of water Mg/Ca. *C. torosa* seems to control the osmoregulative cost to built shells of low Mg calcite at waters with low Mg/Ca. However, particularly species from the same genus (De Deckker *et al*., 1999) could built shells with Mg/Ca up to 0,1 in waters with high Mg/Ca (Fig. 1.13c). Concretely, De Deckker *et al* (1999) showed a strong relationship between ostracods Mg/Ca and water Mg/Ca (Fig. 1.13c). As this author suggested, the ostracods that live in waters with high Mg/Ca (over 20) cannot exert a control in Mg incorporation to built low-Mg Calcite shells and the therefore values of ostracod Mg/Ca are relatively high. Our interpretation is that *C. torosa* exert a tight control of shell Mg/Ca, but Mg incorporation can be out of control at the extreme range of

living conditions, chiefly when Mg/Ca ratios and temperatures are very high.

At ambient temperature conditions, low-Mg calcite contains ≤ 6mol% $MgCO_3$ (Goldsmith and Newton, 1969), so the valve with Mg/Ca of 0.1 is not a low-Mg calcite. These high-Mg valves may contain especially high Mg concentration in the early calcified sections (Ito *et al*., 2003), or have some high-Mg calcite overgrowth that precipitated inorganically over the biogenically formed valve. *C. torosa* is too fragile to be analyzed by laser-ablation technique, but the possibility of high-Mg carbonate overgrowth should be tested by XRD. The possible metabolic cost of calcification in waters of high Mg/Ca has been discussed by several workers (Xia *et al*. 1997b; De Deckker *et al*. 1999). This is consistent with the known poisoning effect of Mg on calcite precipitation (Reddy and Wang, 1980).

4.4 Sr uptake

Low-Mg calcite has no solid solution with Sr carbonate mineral (Deer *et al*., 1996) so that Sr incorporation is assumed to be strictly a function of Sr/Ca of the solution from which it crystallizes and be independent of temperature. Some studies have focused on this and have used Sr/Ca of ostracod valves to reconstruct paleosalinity under the erroneous assumption that Sr/Ca of water will increase during solute evolution primarily driven by evaporation. However, in many waters, aragonite (with complete solid solution with $SrCO_3$, strontianite) becomes a stable phase as both the TDS and Mg/Ca increase (Müller *et al*., 1972; Eugster and Jones, 1979) and Sr/Ca decreases with increasing TDS or Sr/Ca can increase in low salinity waters because of water reverse back to calcite precipitation. Our data confirm that Sr uptake is independent of temperature (Fig. 1.15a). Most of our data show a correspondence between Sr/Ca of water and Sr/Ca of valves (Fig. 1.15b) and follow the general trend that was observed for *C. torosa* collected from other locations (Wansard *et al*. 1998) and in culture experiments with *C. auraliensis* (De Deckker *et al*. 1999; Fig. 1.15c). However, a good one-to-one relation is not observed for our samples. Animals harvested in March 2001 from U1 have valves with higher than expected Sr/Ca, and those from P5 show a large scatter. P7 animals show a lower than expected range of Sr/Ca ratios compared to all other samples (Fig. 1.14c). Xia *et al* (1997b) noted a possible relation between Mg and Sr incorporation into ostracode valves but the observed pattern for P5 is the opposite of what would be expected from the crystallographic argument they gave. The general correlation between the Sr/Ca of water and Sr/Ca of the valves of the genus *Cyprideis* can be quantified, but

because Sr is a minor to trace constituent of most waters and is not governed by aqueous mineral equilibrium, the knowledge of Sr/Ca of water will provide information on hydrochemical changes but not directly for TDS absolute values reconstruction (Fig. 1.4c). The positive correlation between ostracod Sr/Ca and water Sr/Ca holds at any conditions (e.g. at high TDS stressful conditions), suggesting that Sr uptake is not governed by ostracods in any instance. This can be also related to the fact that Sr concentration of the shell shows no variations, in spite of strong variability for other metals (Ito, 2003). This indicates that shell Sr concentration is independent of moulting time or stressful physiological conditions.

4.5 $\delta^{13}C_{VPDB}$

The $\delta^{13}C$ of carbonates is not highly influenced by temperature variations but is rather understood to respond to changes in the isotopic ratio of the total dissolved inorganic carbon (TDIC) from which the carbonates precipitated (Deines, 1974). Commonly, changes in water $\delta^{13}C$ are attributed to changes in carbon and productivity within the system (Schwalb, 2003; Leng and Marshall, 2004). Rates of exchange of CO_2 with the atmosphere, photosynthesis/respiration of aquatic organisms, organic decay, and bacterial processes are the main controlling factors for the $\delta^{13}C$ of TDIC (Von Grafenstein *et al.* 1999; Schwalb, 2003; Leng and Marshall, 2004). We only analyzed ostracod $\delta^{13}C$ in MSS, see figures 1.17 and 1.18 (not BSS), and observed a slight correlation with $\delta^{13}C$ water (Fig. 1.6b) indicating that $\delta^{13}C_{ostracod}$ can reflect $\delta^{13}C$ from the host water. Host water has different origins, as U1 is a spring (groundwater $\delta^{13}C$), P7 water is coming from runoff from a wetland inland with high macrophyte coverage and eutrophic waters and P5 water originate from the seawater evaporation pathway. In general, *C. torosa* $\delta^{13}C$ is -2‰ lower than water $\delta^{13}C$, suggesting that animals are moulting under pore water $\delta^{13}C$ of the DIC in the interstitial environments, where $\delta^{13}C$ is expected to be lower than our measured water $\delta^{13}C$ values, because of the decay of organic matter (Ito, 2003).

In addition the pattern drew by *Cyprideis* $\delta^{13}C$ at different MSS sites shows seasonal changes, suggesting that the intrannual variations in the $\delta^{13}C$ TDIC might have a strong influence (Fig. 1.18). The juvenile population shows more clear seasonality of $\delta^{13}C_{VPDB}$ because of their shorter life duration.

Changes in water $\delta^{13}C$ in the three sites don't show a common pattern because of independent hydrology and productivity. High values are generally observed in spring summer most probably because of increasing photosynthetic activity (either by macrophytes U1 and P5 or phytoplankton in P7) and low rain, drops in September for P5-P7 seem to be related to quick response to heavy rains (Fig. 1.2) and in the spring-fed U1 the response to rains is delayed about one month. However, recovery of high values in P5 after the rain event is getting $\delta^{13}C$ to constant values because of inflow of water of sea origin controlled by humans. In P7, after the rainy period the recovery of phytoplankton production probably promotes a gradual increase in $\delta^{13}C$. In U1, even changes are not as wide as in P5 or P7, there is a marked decline in early winter that can be caused by the delayed effect of previous rains through increase of low $\delta^{13}C$ CO_2 coming from groundwaters.

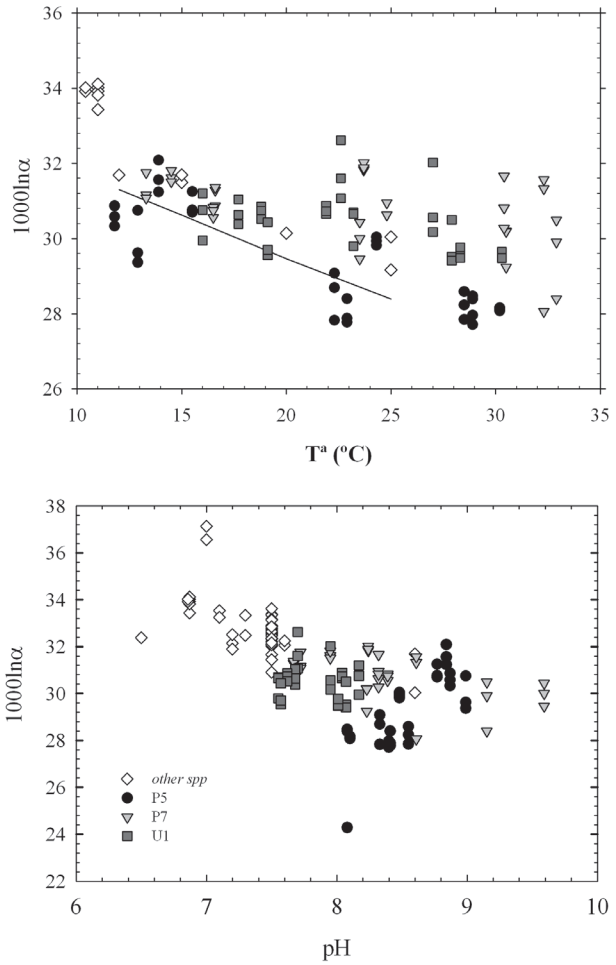

Figure 1.20: 1000lnα represented with temperatures and pH. a) 1000lnα vs temperatures; b) 1000lnα vs pH. Note that temperatures, pH and the $\delta^{18}O_{VSMOW}$ used on the calculus correspond to water values from the month before. In both cases data from other studies was included (Xia *et al*., 1997a, b; Keatings *et al*., 2002; Von Grafenstein *et al*., 1999; Wetterich *et al*., 2008). Other spp: other especies.

Figura 1.20*: 1000lnα representado con las temperaturas y el pH. a) 1000lnα vs temperaturas; b) 1000lnα vs pH. Temperaturas, pH y el* $\delta^{18}O_{VSMOW}$ *usado en los cálculos corresponde con los valores del agua del mes anterior. En ambos casos datos de otros estudios fueron incluidos (Xia* et al., *1997a, b; Keatings* et al., *2002; Von Grafenstein* et al., *1999; Wetterich* et al., *2008). Other spp: otras especies.*

4.6 $\delta^{18}O_{VPDB}$

In contrast to the results of precipitation of synthetic calcite by Kim and O'Neil (1997), several studies published during the last ten years show that the ostracod oxygen isotopic fractionation differ from thermodynamic equilibrium with water, ostracods take up more ^{18}O compared with inorganic calcite (Xia *et al*., 1997a, b; Von Grafenstein *et al*., 1999a; Keatings *et al*., 2002; Wetterich *et al*., 2008). In the present study we show that the euryhaline *Cyprideis torosa* has different vital offsets in different hydrochemical habitats. Similarly, Chivas *et al*. (2002) found high variability of vital offsets under variable experimental conditions of temperature and salinity for *A. robusta*.

Animals in P5 have poorly calcified shells, and vital offsets of 0 to 0.5‰ (Fig. 1.20). Animals in P5 calcify under suboptimal conditions (high salinity), consequently they may accomplish *less effective* calcifications; animals at higher salinities are poorly calcified and they show temperature dependence close to inorganic calcite precipitation without almost any vital offset. This may be related to fast calcification under stressful environmental conditions (*e.g.* ionic regulation, extreme temperatures), as it was observed at the present study for the other studied variables (e.g. high Mg/Ca values and high temperatures in P5) and the wide range of temperatures when they moulted (Fig. 1.2 and 1.7).

The highest α values in P7 and U1 (Fig. 1.20), together with the apparent absence of thermodependence can be explained by the low range of temperatures at the time of moulting (spring-autumn) (Fig. 1.2 and 1.7). On the other site, apparent thermodependence of $\delta^{18}O$ in P5 is explained by the wider range of water temperature between the two periods where adults calcified (summer-winter) (Fig. 1.2 and 1.7). In addition populations in U1 at a particular sampling occasion are composed of various animals overlapping generations of adults that moulted under different water $\delta^{18}O$ conditions (Fig. 1.2 and 1.7). In P5 the differences between juveniles and adults $\delta^{18}O$ is not as long as in U1 (Fig. 1.19) suggesting shorter life time for adults. In P7 the pattern of ostracod $\delta^{18}O$ is not clear where more near constant values both in water and ostracod $\delta^{18}O$, and in particular some extreme high values cannot be explained. It is possible that human regulation at particular short time periods provoked strong $\delta^{18}O$ changes (e.g. throw evaporation) that are not seen in snapshot water samples but are reflected by long-lived adult shell geochemistry.

In our study the $\delta^{18}O_{VPDB}$ is correlated with the increase of $\delta^{18}O_{water}$ and TDS, especially until values of $\delta^{18}O_{water}$ 0‰ (approximately 20g/L of salinity). Evaporation removes ^{16}O and therefore more concentrate waters (high TDS) through evaporation in Mediterranean or semi-arid conditions also present high $\delta^{18}O$ (Craig and Gordon, 1965). Therefore, $\delta^{18}O_{water}$ is indirectly related to TDS changes, and then, *C. torosa* $\delta^{18}O$ can reflect those changes. However, in some cases, the vital offsets of $\delta^{18}O_{VPDB}$ are highly negative with respect to water $\delta^{18}O_{SMOW}$ especially at high TDS sites (P5, E38bis and E39). Chivas *et al* 2002 suggested that poorly calcified shells result in low $\delta^{18}O$ while good calcified shells show high $\delta^{18}O$. In agreement with those assumptions and due to worse environmental conditions at high salinity sites, the ostracods cannot built their shells discriminating well between ^{18}O and ^{16}O and they incorporate more ^{16}O into their shells, which also present the lowest values in Ca_{SHELL} and smallest sizes (Fig. 1.20d) (*less effective calcifications*). Also Xia *et al.* (1997a) suggested, thermodynamically ^{18}O is preferred by calcite over ^{16}O. This is may be because ^{18}O provides higher calcite stability to calcite (Ito *et al.* 2003), and ostracods at optimal conditions increase the discrimination against ^{16}O (higher $\delta^{18}O$). If the conditions are not favourable (*less effective* calcification) the discrimination between ^{18}O and ^{16}O decrease and more ^{16}O is fixed into the shell (lower $\delta^{18}O$).

Zeebe (1999) proposed that calcite-water fractionations could be influenced by the response of carbonate water equilibrium variability in relation to changes in pH, being the isotopic $\delta^{18}O$ content of HCO_3^- higher than in CO_3^{-2}. If we compare our results with other studies (Fig. 1.20b) the ostracod isotope fractionation decrease with increasing pH at a pH range below 7 when the concentration of HCO_3^- decreases (as discussed by Zeebe). However under the range of pH values in our study (7,2-9,8), HCO_3^- is highly dominant and the variability of α values (Fig. 1.20b) with pH is so wide that no clear pattern emerges only from our results with *C. torosa* except that this variability is lower at low pH (below 8). As Chivas *et al.* (2000) suggested, and our results confirm, it is not just the temperature that is affecting isotopic fractionation, more variables can be involved: the pH of the surrounding water at the time of calcification, the possibility that ostracod regulate the surrounding pH microhabitat and the speed of calcification or even evaporation. Faster calcifications under suboptimal conditions (either low temperatures or high salinities) that are close to the species' tolerance limits, may provoke *less effective calcifications*, resulting in poorly calcified shells and oxygen-isotope fractionations lower than expected (small vital effects).

The assumption of the possibility to reconstruct water $\delta^{18}O$ from the $\delta^{18}O$ostracod has not a straightforward applicability in coastal environments; even taking into account that *C. torosa* $\delta^{18}O$ is well correlated with water $\delta^{18}O$ until water values of 0‰. Water $\delta^{18}O_{VSMOW}$ increases with TDS through oxygen isotope fractionation accompanying evaporation (except in very high TDS). However, this relationship between water $\delta^{18}O$ and TDS is not unique and cannot be applied in a general context (Ito and Forester, 2009).

4.7 Hydrochemistry reconstruction

According to our multiple regressions analyses, TDS cannot be reconstructed from ostracod shell geochemical data alone. A combination of shell morphology (noding) and isotope data provide a rough quantitative estimation of salinity (TDS) but reconstructed values deviate more at high salinity (Table 1.1). This occurs because i) the model is built on a logarithm scale; ii) noding is restricted to the low salinity range and iii) because ostracod $\delta^{18}O$ fractionation at high salinities shown a deviation from the general pattern due to stressful calcification. Further studies including more data on noding percentage and isotope data from a similar hydrochemical environment setting may improve the model performance. In addition, if ostracod samples are not representative in terms of time averaging and number of individuals studied, reconstructions based on nodes may incorporate a wide error component.

Reconstruction of water Sr/Ca from *C. torosa* shells Sr/Ca has a high statistical fit which improves when isotope information is added. The use of equations where ostracod Sr/Ca and either $\delta^{18}O$ or $\delta^{13}C$ are combined referred because these are the most fitted and simplest models (Table 1.1). The resulting model for waters Sr/Ca reconstruction from ostracod Sr/Ca provides the best of the tested models for quantitative reconstruction of a hydrochemical variable from ostracod shell geochemistry. Further research is needed to check if the relationship holds for other species and waters of different hydrochemical trends.

Reconstruction of water $\delta^{18}O$ from ostracod $\delta^{18}O$ is possible with certain error but at high salinities the error becomes bigger, probably because of stressful condition during calcification.

We consider that the obtained regression equations, together with other paleolimnological proxies can help paleolimnologists to quantify and reconstruct past salinities and water Sr/Ca along sedimentary sequences when *C. torosa* (or

other *Cyprideis* species with similar hydrochemical requirements) is present. However, when studying fossils shells, these equations should not be applied before study shell size, morphology, Ca_{SHELL} or other indicators of possible stressful conditions.

5. Conclusions

C. torosa populations show overlapping adult generations through the year in the studied sites. Because of this, it is not possible to know with enough confidence the right time and environmental conditions when moulting and calcification occurred. Juveniles shell traits, however, might reflect better water changes, due to their shorter life span.

Animals with the longest shells are also the heaviest regarding to shell Ca content. In addition, shell size is correlated with water chemistry; both males and females are smaller at higher salinities. *C. torosa* U1 shells show higher Ca_{SHELL} in their shells than those for P7 and P5 (U1>P7>P5), although, statistically (U1=P7) ≠ P5. The low salinities and water Alk/Ca between 1 and 2 in our studied waters ratio seems the optimal to build more calcified shells.

As discussed in previous studies, the proportion of noded individuals of *C. torosa* may be one of the best proxies for salinity reconstruction. This can be combined with geochemical data (particularly isotope ratios) to better estimate past salinities using *C. torosa* shells. According to our results salinity reconstruction cannot be done by geochemistry alone and needs information from shell morphology (noding).

In general for the isotopic and trace metal ratios analyzed in *C. torosa* shells there are no differences between males and females. Consequently in paleoecological studies there is no need to analyze separately sexes when using these geochemical variables. However, the use of size and Ca_{SHELL} as paleoenvironmental proxies should take into account sex differences.

No effects of either temperature or water Mg/Ca is observed on Mg/Ca assimilation in the ostracod *C. torosa*, in waters within a Mg/Ca ratio below 6. *C. torosa* makes shells with low Mg/Ca in a wide gradient of salinity. In other studies that involve higher water Mg/Ca ratios a direct relationship between these and ostracod Mg/Ca are observed for other particular species De Deckker

et al (1999), Wansard (1996a).

Ostracod shell Sr/Ca in *C. torosa* is strongly and significantly related to water Sr/Ca. In fact, regression analyses show that reconstruction of water Sr/Ca from ostracod Sr/Ca is the most accurate (in statistical terms) paleoenvironmental proxy using *C. torosa* shells.

$\delta^{13}C$ in *C. torosa* shells are 2‰ lower than expected from $\delta^{13}C_{DIC}$ reflecting that calcification taking place in the infaunal environment.

In *C. torosa* there is a significant positive relationship between ostracod $\delta^{18}O$ and water $\delta^{18}O$. However, at high salinities (> 20 g/L) more ^{16}O is incorporate into the shell as observed in previous works for other stressful conditions (Chivas *et al.*, 2002; Xia *et al.*, 1997a).

Multiple regressions help us to reconstruct past hydrochemistry from ostracod shells, supported by other proxies. The given equations can assess salinities and other water variables (Sr/Ca) in a quantitative manner

PART II

The mid Holocene history of Albufera de Valencia

CHAPTER II

Paleolimnology of the Albufera de Valencia based on ostracod assemblages and geochemical analyses: sea level changes and climatic influences during the mid Holocene

1. Introduction

Reconstructing the evolution of Mediterranean coastal systems using palaeoenvironmental methods is complicated and a difficult task. The mix of waters of diverse origins produces complex ecosystems. Several attempts have been made in the past 20 years to reconstruct variables such as temperature using sedimentological, geochemical, palaeoecological and isotopic techniques (Hazel, 1988; Barbieri *et al*., 1999). However, the complexity of the system and the lack of good proxies to reconstruct temperature in such of habitats has limited their success. Nevertheless, other climatic and environmental variables such as sea-level changes, effective moisture, and salinity can be reconstructed using multiproxy studies, combining indicators such as sedimentology, mineralogy, diatoms, pollen and ostracods. In this study, we combine ostracod palaeoecology, shell morphology and geochemistry in order to reconstruct the paleoenvironmental evolution of Lake Albufera.

The Albufera de Valencia is the largest coastal oligohaline lake in the Iberian Peninsula. It is located 17 km to the South of the town of Valencia in the Albufera Natural Park., has an area of 2320 ha and it is separated from the sea by a sand bar of 30 km long and between 500 and 1200 m wide and with dune systems of 3-5 m a.s.l. nowadays (Sanjaume, 1985). The Albufera is located on Quaternary silt deposits (Fig. 2.1). Sediments deposited from North to South, formed the different sand bars, which contributed to the closing of the present lake (Roselló, 1995; Carmona and Ruiz, 1999, Santiesteban *et al*., in press). Two rivers "surround" the Albufera of Valencia, the Túria River and the Júcar River. Túria River is located to the North of the lake and is the main influence on the formation of the sandy bar that currently separates the lake from the sea. Júcar River is located in the Southern end of the ancient lagoon and probably had a big influence on the closing of the sand bar at the southernmost part and on the final isolation of the lake from the sea over the last 500 years (Ruiz and Carmona, 2005; Santiesteban *et al*., in press). In addition, the same sea level and climatic changes in the Mediterranean Spanish coasts suggested by several authors (Somoza *et al*., 1998, Zazo *et al*., 2008) will also have influenced the Holocene history of the Albufera and the formation of the sand bar. These changes during the transgressive phase are well recorded in the sedimentary infilling of the nearby estuaries (Somoza *et al*., 1998), whereas during the phase of high standing sea waters (HST) they are best recorded in beach–barrier environments (Zazo

et al., 2008). The Holocene sea level rise in the western Mediterranean took place in two phases: a rapid rise until 6500 cal yrs BP, and a second phase of relative stability with minor oscillations of metre-scale magnitude during the late Holocene. During these two phases different authors identified different highstand events (HST; *h1*, *h2*, *h3*, *h4*, *h5*) of maximum sea level, composed by aggrading units and prograding units (H1 to H6 or d1 to d5, repectively) (Somoza *et al*., 1998; Zazo *et al*., 2008) throughout the Holocene. There are no temperature reconstructions for the coastal zones of southern Spain, although it is thought that after 7–5 cal kyrs BP, the general climatic trend towards aridity was punctuated by several centennial-scale episodes of increased aridity that occurred with millennial intervals, often coincident with cooling events and in some cases accompanied by reduced sea surface temperatures (Zazo *et al*., 2008). There were minimal anthropogenic effects on vegetation composition of the area until 2000 cal yrs BP (Zazo *et al*., 2008) suggesting that the observed coastal shifts were largely natural.

Previous studies of Lake Albufera are mainly concerned with its ecology (Arévalo, 1916; Pardo, 1942; Blanco, 1973; Boira, 1987; Miracle *et al*., 1984, 1987; Alfonso and Miracle, 1990 Vicente and Miracle, 1992; Romo and Miracle, 1994; Soria, 2006; Blanco and Romo, 2006; Romo *et al*., 2008) and the recent Holocene evolution of the surrounding alluvial areas and coastal zones (Sanjaume *et al*., 1996; Chapría, 1999, Ruiz and Carmona, 2005): paleoecological information is very scarce (Margalef and Mir, 1973; Robles *et al*., 1985).

The aim of this study is to reconstruct the Holocene evolution of Albufera of Valencia, including salinity changes and possible climatic influences within the framework of a multidisciplinary project (VARECOMED) focused on Holocene salinity changes, sea level influences, hydrological changes and human influences in the Spanish Mediterranean area. We combine information from ostracod paleoecology, shell morphology, shell preservation and shell geochemistry in order to reconstruct Holocene history and evolution of Lake Albufera.

We focus on ostracod remains as the main source of paleoenvironmental information. First, the ecological interpretation of fossil ostracod assemblages may help to decipher past changes in salinity or water chemistry, and their seasonal variability (Boomer and Eisenhauer, 2002; Griffiths and Holmes, 2000; Anadón, 2005). Moreover, the ecological preferences of the modern ostracods of Lake Albufera and other nearby wetlands are well known (Mezquita *et al*., 2005; Rueda *et al*, 2006; Poquet *et al*., 2008). Secondly, we use a detailed morphological

study of the shells of *Cyprideis torosa*, a euryhaline ostracod that is very common in coastal systems. Owing to its abundance and its tolerance of high salinity variation, it has been the subject of many studies into the morphological variations of its shells and their relationships with salinity (Vesper 1972a,b; Harten, 1975). In addition, Marco-Barba *et al.* (Chapter I) carried out a calibration of variations in size and morphology of *C. torosa* shells across a wide salinity gradient.

Third, we will pay also attention to shell preservation, since this is a good taphonomical indicator. The state of preservation (SP), either as the grade of broken valves or the fragments ratio are good indicators, especially as a means of assessing the presence of reworked material. Finally, we will use ostracod shell geochemistry (trace elements and stable isotopes) as a proxy for water composition (De Deckker and Forester 1988; Holmes and Chivas, 2002; Schwalb, 2003; Leng and Marshall, 2004).

2. Material and Methods

An 18.5 meters long core (Palmar core) was recovered in July 2000 using a 15 cm diameter corer from a location on the shore of the channel "Carrera de la Reina Nova" near to El Palmar village (UTM: 30S 07310/43548) in the marshland of Albufera Natural Park (Fig. 2.1). The composition of the sediment matrix was described and subsampled down to 8.5 m; below this, the presence of red-coloured carbonate sediments suggested the existence of Pleistocene terrestrial conditions and so was not relevant to this study.

2.1 Core subdivision

The core was subdivided into 17 units based on lithology (Fig. 2.2; Santiesteban *et al.*, in press). In most cases, three samples were taken from each unit for subsequent analysis, one each from the top, middle and bottom, although only one or two samples were taken for very thin units (<13 cm). In total, sixty-five samples were obtained for different analysis (geochemistry, mineralogy, phosphorus content, and micropalaeontological studies), resulting in an average sampling interval of 10 cm. An aliquot subsample was taken to determine dry weight per sample. The water content of each subsample was determined by drying a subsample at 105˚C for one hour. The organic carbon and carbonate contents were then determined by heating the dried sediment at 460˚C for 7.5 hours and 950˚C for 8 hours, respectively.

Ostracod subsamples were processed following the method of Griffiths and Holmes (2000); 10-15 g of wet sediment were weighed, air dried and then wet-sieved through 400 and 250 μm mesh sieves for several minutes and then, air dried once again. After each sieving, the sieve was cleaned with water and introduced in a solution of methylene blue (to control the contamination of possible left over remains from one sample to another) and washed again. We avoid the treatment with acids or peroxides to prevent the influence of these substances on the preservation of biogenic remains and their geochemical composition. Therefore, only mechanical treatments were used to disaggregate the sediment; in the case that washing with water was not enough to disaggregate all the sediment, we applied a mechanical protocol that consisted in one or several cycles of drying-wetting-drying-sieving until all the sediment was totally disaggregated. If this protocol did not work, we applied the freeze-unfreeze-sieve procedure following Griffiths and Holmes (2000).

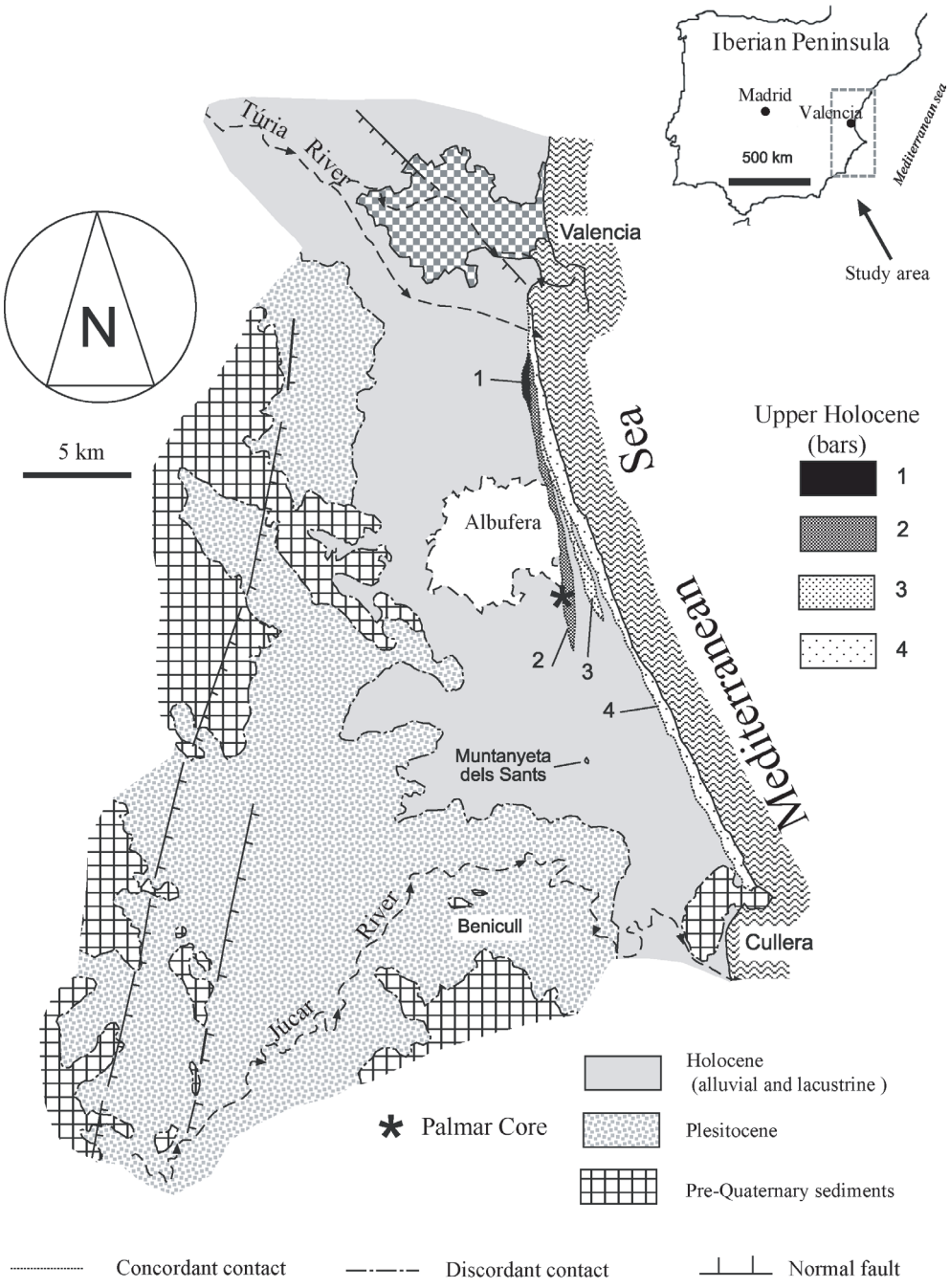

Figure 2.1: This figure shows the Palmar core location and the geological composition of the studied area. Figure adapted from Santiesteban *et al.* (in press).

Figura 2.1: *La figura muestra la localización del sondeo Palmar y la composición geológica del área de estudio. Figura adaptada de Santiesteban* et al. *(in press).*

Microfossils were picked from the coarse, dried residues with a 'oo' paint brush under low power magnification using an Olympus SZX 12 stereoscope microscope and stored in micropalaeontological slides. The total number of ostracod valves was counted per sample, and the abundance expressed as number of valves per 10 g dry weight (10g dw^{-1}). Species identifications followed Athersuch *et al.* (1989), Meisch (2000) and Poquet *et al.* (2008).

2.2 Preservation state

We assigned each ostracod shell to one of three preservation classes: **A**: well preserved remains with no holes or other mechanical damage; **B**: partially broken (no more than half) and/or presence of some holes; **C**: totally re-mineralised valves or broken in pieces smaller than one half of a valve. Only valves falling into preservation classes A and B were considered well enough preserved for inclusion into the multivariate statistical analyses (cluster and ordination analysis, see below).

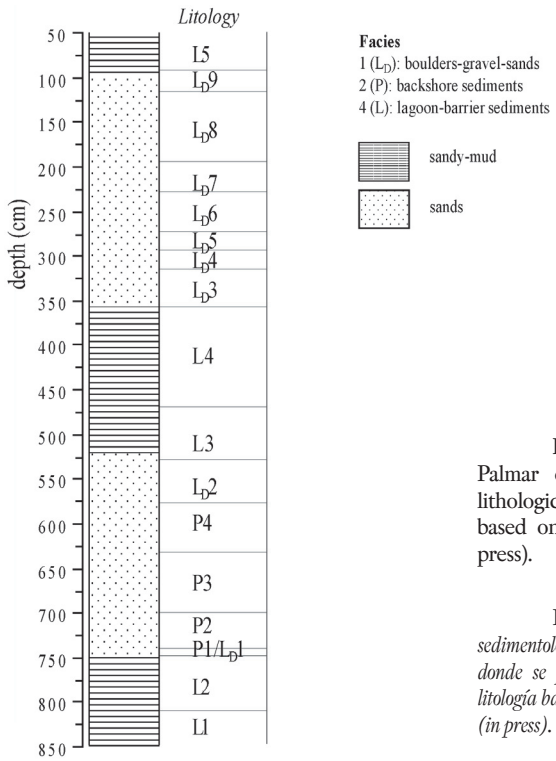

Figure 2.2: Sedimentary Palmar core column, showing lithological and facies descriptions based on Santiesteban *et al.* (in press).

Figura 2.2*: Columna sedimentológica del sondeo Palmar, donde se pueden ver las facies y la litología basadas en Santiesteban* et al. *(in press).*

For geochemical analysis, each ostracod valve that was previously classified as A+B was further separated in a gradient from 1 to 7 based on valve transparency state of preservation (VPI), under the binocular microscope (Griffiths and Holmes, 2000). However, for the other analyses and graphics we simplified the assigned codes in two classes: valves that ranged from 1 to 4 (both included) were considered as transparent and valves that ranged from 5 to 7 were considered as opaque. Valves in pristine conditions are transparent, whereas valves that have undergone some alteration become opaque (Keatings *et al.*, 2007). This state of preservation was applied because this method is more accurate than A-B-C (classification explained above), to choose the best preserved material for geochemical analysis. Ostracod fragments were defined as parts of shells that could not be identified: the total number of fragments was counted in each sample and expressed as per 10 gdw^{-1} sediment. The fragment ratio (FR), used to assess the energy at the time of deposition, is defined as follows: FR = (number of fragments + number of valves in SP type C)/(total valves + fragments).

2.3 Morphology of C. torosa *shells*

Particular attention was paid to the shells of *Cyprideis torosa*. Lengths of female and male *C. torosa* valves were measured, and the proportion of noded valves per sample was calculated, in order to apply the known association between salinity and the different morphotypes: i.e. the tendency of noded forms to occur in freshwater and smooth valves in saline and hypersaline water (Van Harten, 1975; Chapter I). Sieve-pores morphology in *C. torosa* was used as a further salinity indicator (Rosenfeld and Vesper, 1976). The shells of *C. torosa* are punctured by filtering pores, through which pass the sensory bristles (setae), that are assumed to transfer information about the external environment to the animal (Bronshtein, 1947). The size and shape of sieve pores appears to vary with salinity. Here, sieve-pore morphology was determined using images produced by a scanning electron microscope and image analysis software (Image pro-plus) was used to measure them. We measured the size, shape and area of pores (between 2 and 52 nodes/per valve) from a total of 115 ostracod valves picked from 13 selected samples. The selection of those samples was based on downcore variations in ostracod assemblages and shell chemistry. Around 179 valves with good preservation (transparent) were picked up from the different samples but only 115 were used, because the remaining valves, in spite of being transparent (regarding to preservation state-VPI- Griffiths and Holmes, 2000), presented some alterations, mainly calcareous deposits over the shells, or in some cases

the calcite was corroded. The results were expressed as percentage of rounded, elongated and irregular pores.

2.4 Geochemical analysis

Fifteen ostracod shells of *Cyprideis torosa* were initially selected from each sub sample placed into a preservation class and then cleaned with distilled water and a 00 paintbrush. Between eight and ten valves from each level were taken to determine Ca, Mg and Sr using ICP-AES. Analysis were generally performed on single valves, although bulked samples of 2-3 shells were used for some samples of juveniles (A-1 and A-2 and in a few cases A-3) were pooled in groups of two or three. The subfosils which had the two valves stuck were subject to ultrasounds to separate the valves, in some cases the two shells were broken and then the fragments were recovered and cleaned carefully, and then, used for the analytical process. Cleaned valve material was placed into sterile 5ml polypropylene transport tubes and dissolved in 5ml 6 M HCl. Aristar™ HCl and 18mΩ water from an Elgastat™ RO deioniser were used to produce the solvent acid. The Ca, Mg, Sr content of ostracod valves was determined using a Horiba JY Ultima 2C ICP-AES at Kingston University, UK, calibrated using multi-element (Ca, Mg, Sr) standards. The data were corrected for instrumental drift using an external drift monitor run after every ten samples, and blank-corrected for any contamination from the solvent acid. An 'in-house' standard (UCL-calcite) was also analyzed to assess instrument precision and to normalize the results of samples run on different occasions. Based on the relative standard deviation (RSD) of this standard, the analytical precision was estimated as ±1.1% for Ca, ±2.2% for Mg and ±2.5% for Sr.

For isotope analysis ($^{18}O/^{16}O$ and $^{13}C/^{12}C$), we used between 2-3 adult valves and 4-5 juveniles A-1 and A-2 late instars and at least 5 analyses (3-4 adults analysis and 2-3 juveniles analyses) were performed at each statigraphic level. Adults and juveniles were never mixed together for the analysis. Ostracods were analyzed at University College London (UCL) or University of Michigan using a Finnigan MAT 253 (UCL) or MAT251 (Michigan) mass spectrometer, both connected to a Kiel carbonate preparation device. The $^{18}O/^{16}O$ and $^{13}C/^{12}C$ ratios were converted to $\delta^{18}O$ and $\delta\,^{13}C$ versus VPDB, based on calibration of the laboratory standard against NBS-18 and NBS-19. Analytical precision was typically <0.1‰ for both $\delta^{13}C$ and $\delta^{18}O$. Ostracods analyzed at University of Michigan were previously cleaned following Ito's (2001) protocol. We run samples from the same statigraphical levels in the two different labs and therefore

we can ensure that the different cleaning and analytical protocols did not affect the results. The cleaning protocol (Ito, 2001) consists of two parts: bleaching and cleaning. Bleaching consists in sinking the 2-3 ostracod shells in sodium hypochlorite 2.5% for 24 hours. After that, these valves are cleaned with 0.5L of distilled water (Cleaning), dried with 100% pure ethanol and stored in ultra-clean vials (cleaned in advance with HNO_3 10%).

2.5 Diversity indices, Cluster analysis and Statistical methods

The Shannon-Wiener index ('H-value': Shannon and Weaver, 1963) was used to calculated the diversity of ostracods assemblages. It is given by

$$H = -\sum_{i=1}^{S} p_i \log_2 p_i \qquad \text{(Eq. 5)}$$

Where p_i = proportions of species i; and S is the number of species present. Evenness E (Margalef, 1974) was also calculated as

$$E=H/Hmax \qquad \text{(Eq. 6)}$$

In addition we used the index of fluctuation D_o formulated by Dubois (1973) as Taylor's expansion of the diversity index H around the reference state:

$$D_o = \sum_{i=1}^{S} p_i \log_2 (p_i/\overline{p}_i) \qquad \text{(Eq. 7)}$$

Where $\overline{p}_i$ = mean p_i. D_o is a function of time representing the deviation of the species proportions through time from an average state.

A data matrix was constructed (Appendix 2.1), consisting of the $\log_{10}$(number of valves+1) transformation of the original ostracod concentration data: adults and juveniles were not separated in this exercise. To analyze the changes in composition of ostracod assemblages through the core sequence, a constrained cluster analysis was performed applying the CONISS method and the Edwards and Cavalli-Sforza distance (Grimm, 1993). In addition, we used unconstrained cluster analysis for the study of ostracod species association excluding minority species (*L. rhomboidea*, *D. stevensoni*, and *Hemicypris* sp.) and with two samples with only the most common species (per variables) and per samples, because 14 samples with fewer than 12 of the most common species, were excluded from the analysis. In this classification analysis, we used the single UPGMA (Unweighted Pair Group Method Average) method and the Pearson correlation coefficient distance index. The transformed data matrix, as used in CONISS, was also analysed by means of Detrented Correspondence Analysis (DCA) (Hill and Gauch, 1980) in order to obtain an ordination of samples for a better evaluation of ecological similarities among them.

Correlations between *C. torosa* valve lengths, Mg/Ca, Sr/Ca molar ratios, and isotope values ratios ($\delta^{18}O_{VPDB}$ and $\delta^{13}C_{VPDB}$) were analysed using either Pearson (for normally distributed data) or Spearman (for non-normally distributed data) correlation techniques.

The equations obtained in the *C. torosa* calibration study by Marco-Barba *et al.*, (Chapter I) were used to reconstruct salinity changes and water Sr/Ca. We used the following equation:

$$Sr/Ca_{water} = 4.29 + 0.292 * \delta^{18}O_{C.torosa} + 0.228 * \delta^{13}C_{C.torosa} + 1.371 * Sr/Ca_{C.torosa} \quad \text{(Eq. 4)}$$

to reconstruct past water Sr/Ca in all the samples for which all three variables were analyzed. However, for the samples without isotopic information (112, 233, 245, 274, 288, 355, 360, 385, 420, 436, 451, 503, 643, 655, 666, 709, 717, 726, and 745 cm), an equation that uses only ostracod Sr/Ca was applied:

$$Sr/Ca_{water} = 1.5513 * (Sr/Ca_{C.torosa}) + 0.00236 \quad \text{(Eq. 3)}$$

We used the following equation to reconstruct past salinities:

$$\log_{10}\text{salinity} = 1.237 - 0.0129 * (Pn * 100) + 0.0279 * \delta^{18}O_{C.\,torosa} \quad \text{(Eq. 2)}$$

Where *Pn*: percentage of noded valves, in all the samples for which the both variables were analyzed. For the samples lacking isotope data, we reconstructed past salinities with the following equation:

$$\text{Log}_{10}\text{Salinity} = 1.227 - 0.01464 * Pn \quad \text{(Eq. 1)}$$

In both reconstructions the mean and the respective standard error values were estimated.

2.6 Radiometric dating

Due to the lack of dateable organic material in this core, radiocarbon dating was undertaken on pollen concentrates. Five sediment samples were selected to obtain pollen concentrates for radiocarbon measurements. These samples were concentrated at the Palynology laboratory of Prehistoric area at *Universidad Rovira i Virigili* (Tarragona-Spain). They were checked to confirm the absence of other remains in order to avoid hard-water error (Fontes and Gasse, 1991). Four of the obtained samples (88, 319, 398, 503 cm) were processed by the AMS ^{14}C Facility in Florida, Miami, USA by Beta Analytic Radiocarbon. One sample (118 cm depth) was dated in Pozna´n Radiocarbon Laboratory, Poland. The radiocarbon measurements (BP) were converted to calendar years (cal yrs BP), using Cal.5.0 program and linear depth age interpolations were made using the INTCAL 98 Radiocarbon age calibration (Stuiver *et al*., 1998) and corrected subtracting 390 years to the calibrated date in accordance to the Mediterranean reservoir effect (Siani *et al*., 2000).

3.-Results

3.1. Radiocarbon dates

Low organic content precluded any dating whatsoever below 600 cm in the core. Of the five dates obtained from the upper part of the core, three were used to construct an age model (Table 2.1): the other two dates, which were believed to contain reworked material, were excluded.

Table 2.1: Radiocarbometric dates for Palmar core, indicating the material used and the laboratory that carried out the analysis.

Tabla 2.1*: Dataciones radiocarbométricas del sondeo Palmar, el material usado para datar y el laboratorio están indicados.*

Core	Depth (cm)	years BP	cal. yr BP (2σ)	Correcting factor (-390 yr)	Material	Laboratory	lab. Code
PALMAR	88	**3220** *±40*	3425±65	3035±65	pollen concentr.	Beta Analytic	Beta-215488
	118	7660 *±50*	8464±85	8074±85	pollen concentr.	Poznań Radiocarbon	Poz-18289
	319	10960 *±60*	12695±25	12305±25	pollen concentr.	Beta Analytic	Beta - 208372
	398	**6250** *±40*	7140±120	6750±120	pollen concentr.	Beta Analytic	Beta - 208373
	503	**6600** *±50*	7505±75	7115±75	pollen concentr.	Beta Analytic	Beta - 204241

3.2 Ostracod analysis of core Palmar: relationships with lithological facies

Ostracods were absent from two of the 65 samples examined from the Palmar sequence, and 9 samples had only one species present. Almost half of the samples, mainly located in the lower part of the core and with high concentrations of valves (up to 3383 x10g dw^{-1}) contained the 2 or 3 most frequently occurring species. In contrast, the highest numbers of species (up to 9) were found in the samples at the top of the core. Approximately 17500 ostracod valves, representing 12 species from 11 genera, were identified (Appendix 2.1). Two of these taxa were only identified to genus level, mainly due to the low number of valves found. SEM images of the 12 taxa are presented in plates 1.1,1.2 and 1.3.

The states of valve preservation (SP) varied along the core and between species (Fig. 2.3). We only took into account the valves with states of preservation A+B (13364 valves) for the calculation of diversity indexes and for carrying out cluster and ordination analyses. *Cyprideis torosa* and *Loxoconcha elliptica* were the two most abundant species along the core (Fig. 2.3). In addition, *Aurila arborescens* and *Candona angulata* were also abundant, especially in the upper part, followed

by *Cypridopsis vidua* and *Xestoleberis nitida*. *Loxoconcha rhomboidea*, *Pontocythere* sp., *Hemicypris* sp., *Darwinula stevensoni* and *Ilyocypris gibba* appeared in very low abundances.

Three lithofacies (1, 2 and 4; Fig. 2.2) were clearly distinguished by Santiesteban *et al.* (2009). Facies 1 (depositional lobes=L_D) was characterized by a mix of inland water, brackish and euryhaline ostracod species, where *C. torosa* dominated, followed by *L. elliptica* and *X. nitida*. In facies 2 (backshore-swamp sediments=P) ostracods were very rare or absent (Fig. 2.2); when present, the species found were *C. torosa*, with occasional *L. elliptica* and some marine species (mainly *Aurila arborescens*). Freshwater species were very rare. In facies 4 (lagoon sediments=L; Fig. 2.2) ostracods assemblages varied between units. Ostracods were very scarce or absent at L3 and L4. However L1 and L2 were dominated by *C. torosa* accompanied with the brackish species mentioned for facies 1, whereas L5 is the richest level, including all the species indicated for facies 1, but with a higher proportion of freshwater species compared to both facies 1 and 2. For more detailed lithological descriptions see Santiesteban *et al.* (2009).

3.2.1 Cluster analysis and DCA

Application of stratigraphically-constrained cluster analysis to the ostracod assemblages (Fig. 2.3) showed the differentiation of 3 main biostratigraphical zones that could be further subdivided onto 6 further zones or subzones. Zone **1** (844 to 511 cm) is subdivided into subzones **1a** and **1b**. Subzone **1b** is further subdivided into $1b_1$ and $1b_2$. Subzone **1a** (844 to 713 cm) corresponds to facies type 4, was mainly dominated by *C. torosa* and *Loxoconcha elliptica* at the bottom, with a very few samples with low abundances of *Aurila arborescens* and scattered presence of *L. rhomboidea*, *Cypridopsis vidua* and *Candona angulata*. Valve numbers at the base of the subzone are at a maximum for the core as a whole, although abundances decrease towards the top.

The lower part of subzone **1b** (713 to 577cm; $1b_1$) corresponds to facies type 2. It is characterized by an increase of *C. torosa* valves in the lower part. Peaks in abundance of *L. elliptica* and *A. arborescens* coincide with those of *C. torosa*. The upper part of subzone 1b (577 to 511 cm; $1b_2$) corresponds to a facies type 1 and 4. It is characterized by an increase of *C. torosa* valves in the lower half, together with *L. elliptica* and *A. arborescens*. A few valves of the freshwater species *C. angulata*, *C. vidua*, *I. gibba* and of species with marine affinities (*Pontocythere* sp.), were also found.

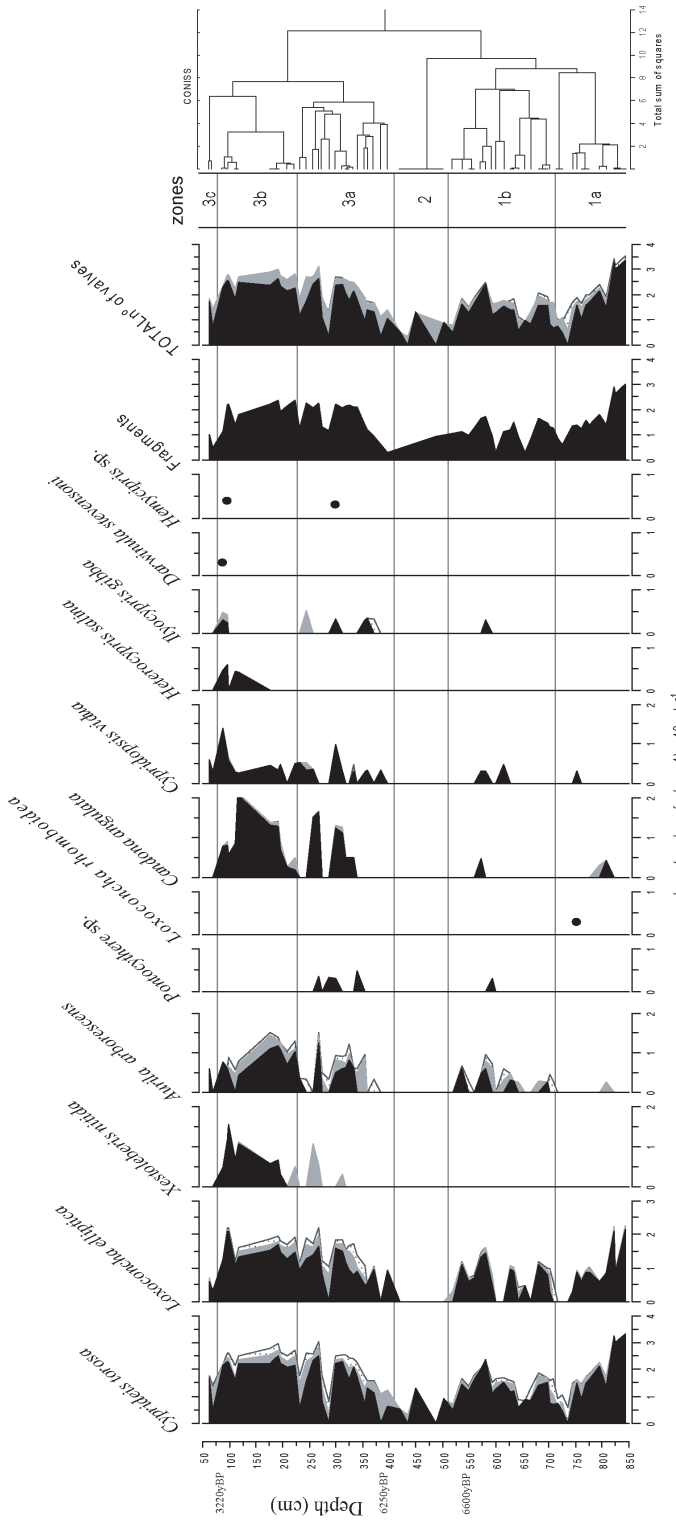

Figure 2.3: Diagram of ostracod abundances as a function of depth in core Palmar. The diagram shows all the preservation states: **A** black color; **B** gray color and **C** dotted area. The total number of valves (states A+B+C), as well, the numbers of valve fragments (all data in valves per 10 gram of dry sediment in log scale) are shown in the right-hand columns. The dots indicate the presence of these species. The established zones by the constrained cluster analysis (CONISS) are represented in the adjacent dendogram.

Figura **2.3**: *Diagrama de las abundancias de ostrácodos en función de la profundidad en el sondeo Palmar. El diagrama muestra los estados de preservación:* A: *negro,* B *gris y* C *área punteada. El número total de valvas (estados A+B+C), como el número de fragmentos de valvas (todos los datos expresados por 10g de sedimento seco en escala logarítmica), se muestran en las columnas de la derecha. Los puntos indican la presencia de dichas especies. Las zonas establecidas por el análisis de agrupación constreñido por profundidad (CONISS) están representadas en el dendograma adyacente.*

Zone **2** (511 to 409 cm) is strongly depleted of ostracod valves; it presented the lowest densities along the core and *C. torosa* was the only species found. The states of preservations were dominated by B forms. It corresponds to facies type D4.

Zone **3** was subdivided in three subzones. Subzone **3a** (409 to 228 cm) is characterized by a large number of species. The base of this subzone was marked by the presence of *Cypridopsis vidua*, changing to a mixed assemblage of *C. torosa*, *L. elliptica* and *A. arborescens* towards the centre, with increasing numbers of *Candona angulata*. There is a drastic reduction in the number of valves of almost all the species at 274 cm, followed by a recovery in the upper part, involving the aforementioned dominant species as well as the appearance of the brackish species, *Xestoleberis nitida*. The repeated appearance of the freshwater species such as *I. gibba*, *C. vidua* and *Hemicypris* sp., as well as the marine taxon *Pontocythere* sp., is also noted.

In subzone **3b** (228 to 78 cm) high abundances of *C. torosa* and *L. elliptica* are recorded, together with C. *vidua*, *X. nitida*, *C. angulata* and *A. arborescens*. The number of valves of *A. arborescens* was reduced towards the top of the zone, whereas *X. nitida* increases along with freshwater species such as *C. angulata* and *C. vidua*. In the top of this subzone, *Heterocypris salina* appears for the first time along with other freshwater species (*D. stevensoni* and *Hemicypris* sp.). At 112 cm all the species decreased and then immediately recovered their abundances: *C. vidua* reached its highest abundance for this species along the core. *X. nitida* and *H. salina* reached their highest abundances at 88cm and 100 cm respectively. Subzone **3c**, was composed of two samples characterised again by a smaller number of species, all of which are amongst the most commonly-occurring in the whole profile, namely *C. torosa*, *L. elliptica* and *A. arborescens*.

Unconstrained cluster analysis of the ostracod abundance data (Fig. 2.4) resulted in two main assemblage groups (A and B). Group A included the most typical coastal euryhaline species and species with marine affinities, namely *C. torosa*, *L. elliptica*, *X. nitida* and *Aurila arborescens* as well as the inland water species *C. angulata* which can tolerate slight salinity variations (Meisch, 2000). However, the marine *A. arborescens* was separated from the other species suggesting that it may have differing environmental preferences, or alternatively that its valves were reworked from the coast. Group B included strictly continental species; it was composed of *C. vidua* (the most common in the subgroup) plus *I. gibba* and *H. salina*, although the last mentioned is quite tolerant of high salinity and was

further separated from the other two. The marine species *Pontocythere* sp. was separated from the two main groups.

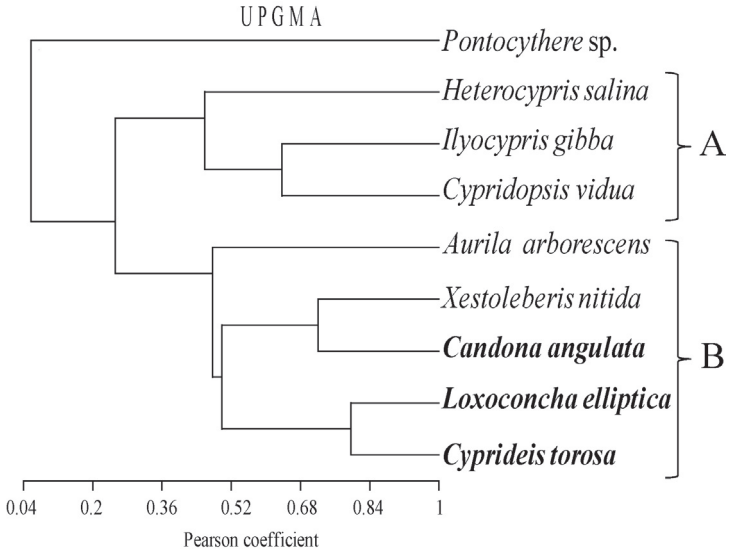

Figure 2.4: Unconstrained cluster analysis applied to transformed data ($log_{10}(x+1)$), using UPGMA method and Pearson correlation coefficient. The most frequent species are typed in bold italic; the main groups are also indicated.

Figura 2.4*: Análisis de agrupación sin constreñir por profundidad aplicado sobre los datos transformados ($log_{10}(x+1)$), usando el método UPGMA y el coeficiente de correlación de Pearson. Las especies más frecuentes están subrayadas en negro, y los principales grupos están indicados.*

The results of DCA are shown in figure 2.6. Factor 1 (F1) accounted for 40.5% of the total variance and the Factor 2 (F2) for 17.7%. The species with higher axis 1 weights are *C. angulata* and *X. nitida* (negative) and *C. torosa* (positive). *I. gibba* and *C. vidua* were the most important species for axis 2 (negative) and *Pontocythere* sp. (positive) (Fig. 2.6). The samples were grouped on the DCA graph according to the zones obtained with the constrained cluster analysis. Zone 1 is located at higher end of the DCA factor 1. This zone is composed of samples dominated by brackish species such as *C. torosa* and *L. elliptica*. The second main subzone (Zone 3b), at the higher end of factor 2, was characterized by samples with the presence of *C. torosa* and *L. elliptica* but altogether with high abundances of *A. arborescens* and *X. nitida* and the presence of inland water species *C. angulata* and *C. vidua* and occasionally other species. Zone 3a seems to be a transitional zone located between the zone 1 and zones 3c and 3b. It shows large scatter: moreover, some samples were included in the other two groups in the ordination diagram, but mainly it has higher affinities with the assemblages of Zone 1.

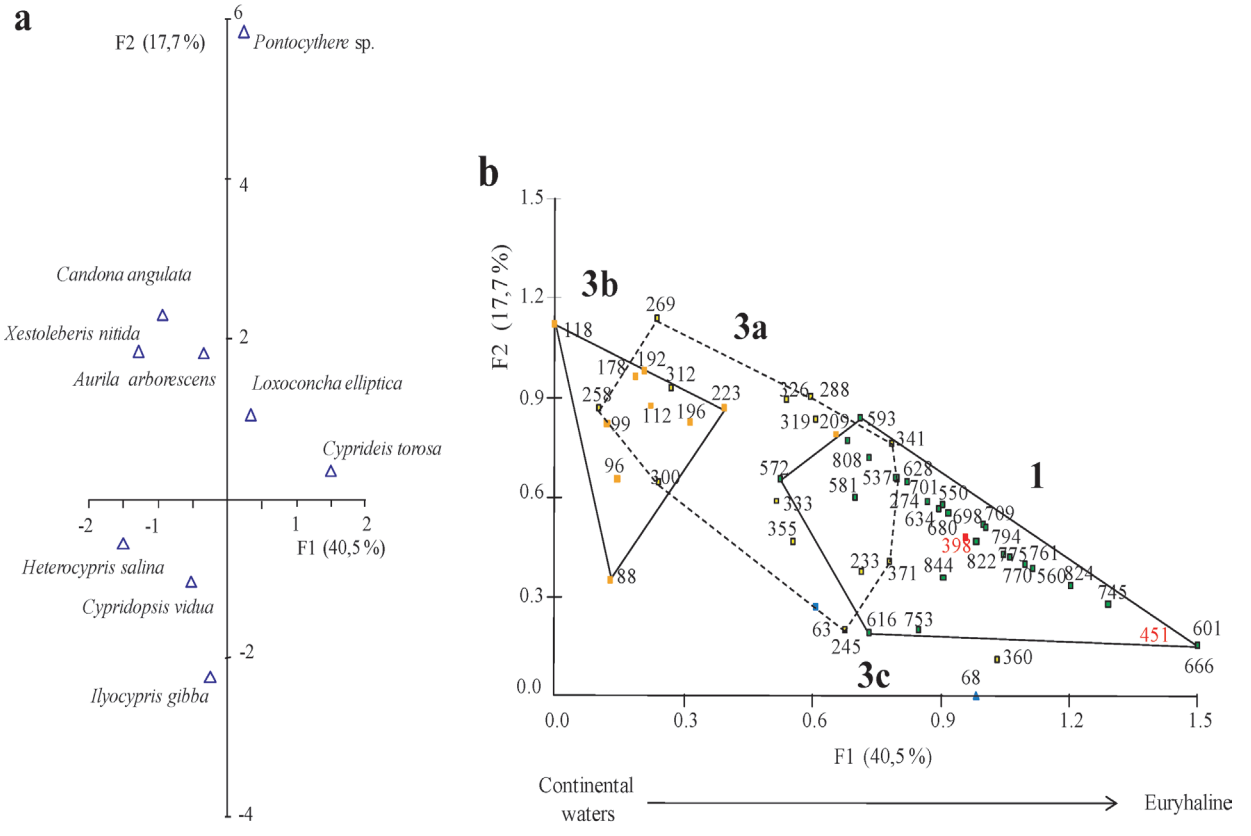

Figure 2.5: Detrented correspondence analysis (DCA). **a**) DCA for ostracod species. **b**) Samples represented by their depth (cm) in the core. The CONISS established groups that are marked with polygons. Note that the samples that were excluded from the analysis are also.

Figure 2.5: *Análisis de correspondencias sin tendencia (DCA).* a*) DCA para las especies de ostrácodos.* b*) DCA para las muestras representadas por su profundidad (cm). Los grupos establecidos en el CONISS están marcados con polígonos. Notar que las muestras excluidas del análisis están situadas en el gráfico.*

3.2.2 Ostracod Abundances and Diversity indices

Ostracod abundance changes show some relationships with the zones established by the constrained cluster analysis (Fig. 2.6). The basal part of zone 1a shows the highest abundances for the whole core, but values decrease upwards. Zone $1b_1$ presented reduced but variable abundances in the lower part that corresponded with facies type B, described above. Subzone $1b_2$ had higher abundances. Zone 2 presented the lowest abundances of the core, with samples containing only *C. torosa*: some levels were barren. Zones 3a, 3b and 3c, presented generally high abundances, with the exception of the base and top of zone 3a.

Diversity indices (Fig. 2.6) are generally low and most samples were dominated by two or three species. However, minimum values clearly correspond to zones of changing conditions. Two distinct patterns are clearly differentiated. First, in the lower half of the core (from zone 2 downward) diversity values are low with recurrent minimum values related to a low number of valves and the absence of most species*:* i.e. a clear inverse relationship between diversity and absolute abundances and the intervals of lowest diversity marked by monospecific occurrence of *C. torosa*. Second, higher and more stable diversities occur in the upper parts of the core (zone 3). Maximum diversity values occur at 355 and 112 cm (1.58 and 1.63 bits/ind respectively).

The D_o index indicates deviation of the community from a reference state, defined as the average species proportions in the whole sequence. The zones that showed D_o closer to zero were zones 3a and 3b. D_o reaches maximum values at depths where *C. torosa* dominance was reduced, such as at 288cm (at the top of zone 3a) and 118cm (top of zone 3b), the latter coinciding with the maximum evenness value reached in zone 3b. The sample at 288cm has the highest values of *L. elliptica* and low number of valves, and the peak at 118cm (zone 3b) corresponds to the sample in which *C. angulata* reached the maximum abundance. D_o show the third highest peak at 355 cm, also corresponding with a diversity peak (1.63). This peak also coincides with the maximum abundance of *C. vidua*. The changing values of H and D_o within zones 1a and 1b ($1b_1$ and $1b_2$) indicates instability in the ostracod assemblage during these periods. In contrast, the zones 3a, b, c showed higher and more stable H and E values. Zones with D_o values close to zero indicated periods closest to average state with shared dominance of the most abundant species, *C. torosa* and *L. elliptica* altogether with the marine *A. arborescens* and some freshwater species. Where *C. torosa* is the only species, D_o show intermediate values.

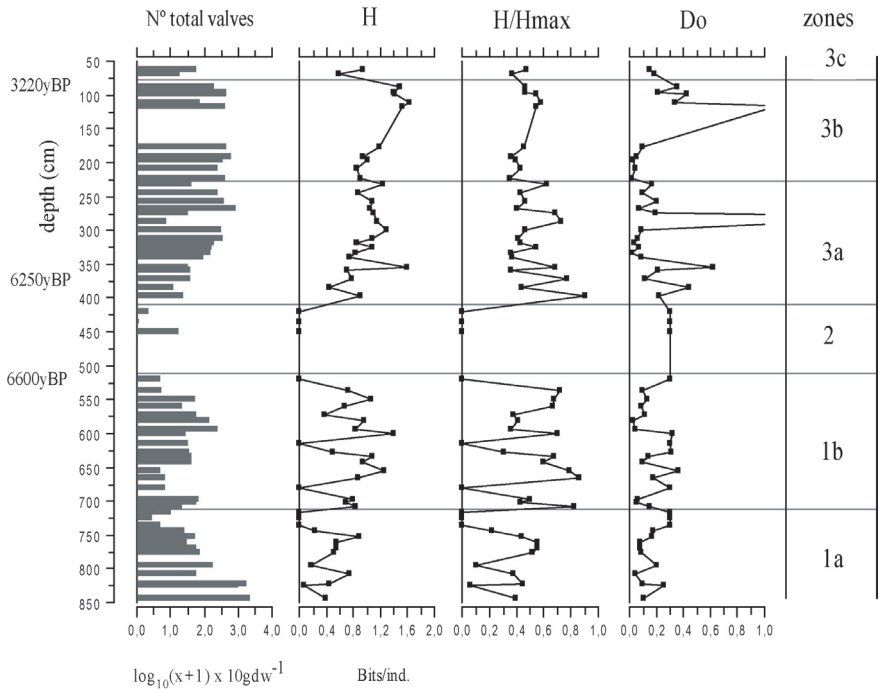

Figure 2.6: Diagram of total abundances of ostracods for Palmar core per 10g dry weight sediment, together with community indices: Shannon diversity index *H*, evenness index H/Hmax, Dubois fluctuation index D_o. The total number of valves is expressed as $\log_{10}$ (total number of valves+1).

Figura 2.6: *Diagrama de abundancias totales de los ostrácodos del sondeo Palmar (expresados en 10g de sedimento seco), junto con los índices de las comunidades: índice de diversidad de Shannon H, índice de equitabilidad H/Hmax, índice de fluctuación de Dubois* D_o. *El número total de valvas esta expresado como* $\log_{10}$ *(número de valvas+1).*

3.2.3 Ecophenotypic responses of C. torosa

A total of 922 ostracods (707 females and 215 males) were measured in the 65 subsamples, (Fig. 2.7; Appendix 2.2). LOESS regression was applied to female and male specimens separately and showed that both followed the same stratigraphical pattern of variations in the biozones 1a and 1b where the number of measured valves was similar. Valve lengths exhibited a negative correlation with shell chemistry (Mg/Ca) for the whole sequence (r: 0.11; $p<0.05$; and r: 0.19; $p<0.05$; for females and males respectively), more markedly so near the base of the core, in zone 1a (females: r: 0.33; $p<0.01$ for Mg/Ca; and r: 0.23; $p<0.05$ for Sr/Ca; males: r: 0.76; $p<0.01$ for Mg/Ca). The lengths of female and male shells were positively correlated with calcium content per carapace (Ca_{SHELL}) for the whole sequence (r: 0.38; $p<0.01$ and r: 0.5; $p<0.01$ respectively) and individually

in each zone. Moreover female valve lengths were positively correlated with $\delta^{13}C$ in subzone 1a (r: 0.55; $p<0.05$) and male valve lengths with Sr/Ca in subzone 3b (r: 0.47; $p<0.05$;).

Noded valves. The pattern of occurrence of noded valves (Fig. 2.7) falls into two parts: the valves found at the lower parts of the core (zones 1 and 2) were smooth, with the percentage of noded forms increasing at the top of zone 1b ($1b_2$). The upper part of the core, zone 3, showed alternating phases of noded and smooth forms, but with a higher proportion of noded valves overall, reaching a maximum in those samples in which *C. torosa* was found together with freshwater ostracods.

Sieve pores. 3403 pores were counted and measured from 115 well preserved valves (Fig. 2.7). Rounded pores dominate in almost all the samples, with just a few samples dominated by shells with elongate and irregular pores, mainly at the base of zone 1a and the top of subzone 3b, suggesting that conditions, especially salinity, changed at those points. Two samples selected in each of the subzones 1a and 1b showed similar frequencies of rounded, elongate and irregular pores presented quite for each pair of samples (Fig. 2.7). The percentages of rounded pores in subzone 1b were higher than in subzone 1a. In zone 3a there is an increase in the frequency of irregular pores with respect to zone 1. This increase is generally associated to a decrease in the frequency of round pores as in the top of subzone 3b and a sample in zone 3a.

3.3 Trace elements

Mg/Ca ratio for *C. torosa* (Fig. 2.8) ranged from 0.007 to 0.048 (mean 0.018) whereas Sr/Ca ratios ranged from 2.52 $x10^{-3}$ to 12.14 $x10^{-3}$ (mean 4.39 $x10^{-3}$). Mg/Ca showed low variability at the bottom of zone 1a (Table 2.2). Shell Sr/Ca and Mg/Ca values were positively correlated (r: 0.15; $p<0.01$) along the whole sequence, but especially within zones 1a and 1b that followed the same trend, suggesting that probably they were controlled by the same factor. Mg/Ca was negatively correlated with $\delta^{13}C_{VPDB}$ (r:0.23; $p<0.01$) and with Ca_{SHELL} (r:0.21; $p<0.01$). The mean and the variability between samples of both ratios was low at the base of the zone 1a, increasing to the middle of zone 1b and then decreasing in subzone 1c.

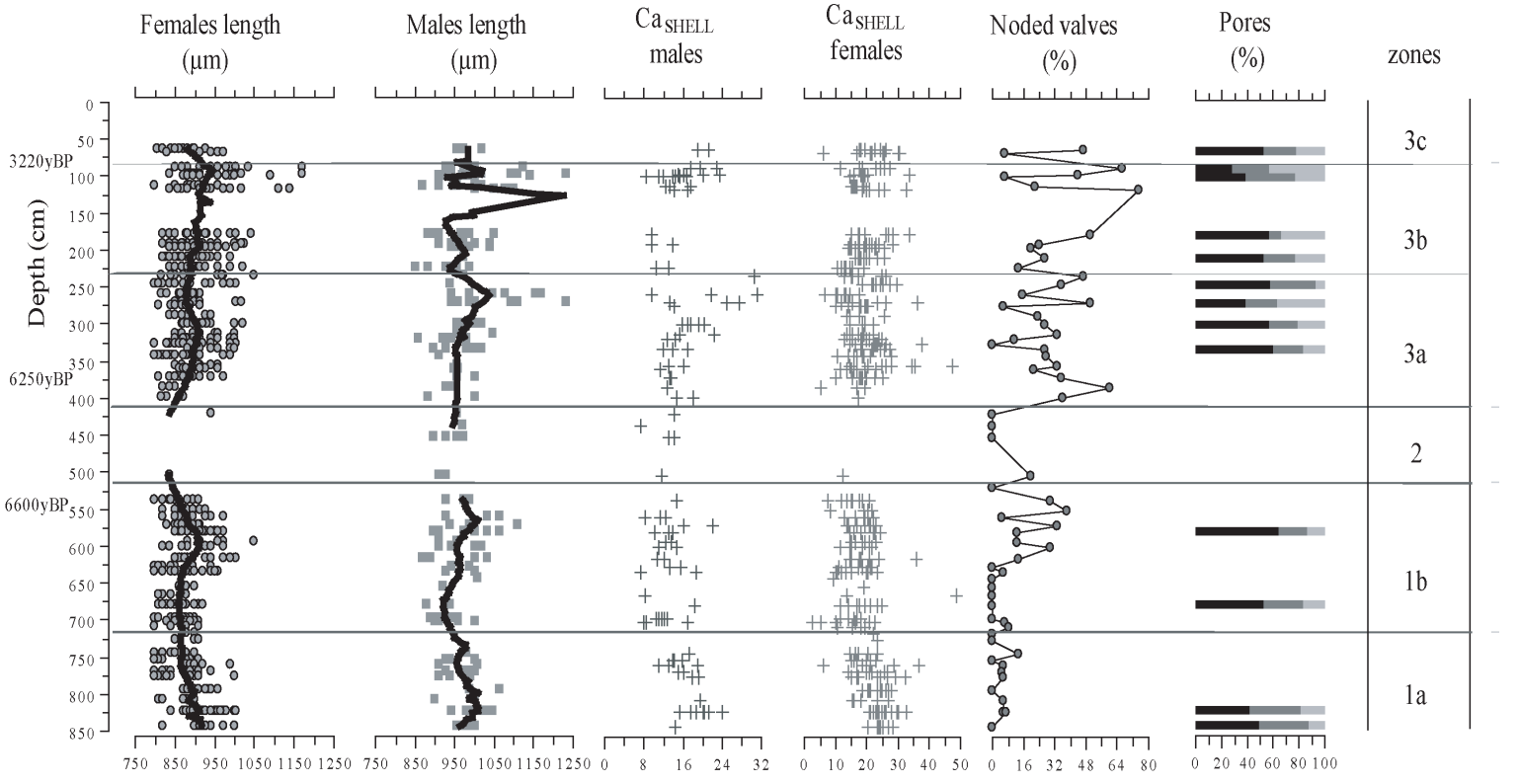

Figure 2.7: *C. torosa* shell length of females and males, Ca_{SHELL} of females and males, the percentage of noded valves and the *Cyprideis torosa* sieve pores types are expressed as percentages (black bar: rounded; dark gray: elongate; gray: irregular). LOESS regression was applied for length data, using average scale of 20.

Figura 2.7: *Variables morfológicas y geoquímicas de* C. torosa. *Longitud de las valvas de hembras y machos, Ca_{CONCHA} de hembras y machos, el porcentaje de valvas nodadas y de poros filtradores (barra negra: redondeados; gris oscuro: elongados; gris: irregulares). La regresión LOESS se aplico sobre los datos de longitudes usando un factor de escala de 20.*

Few analyses were performed for zone 2, owing to scarcity of ostracods. The results were similar to those for the top of zone 1b.

In subzone 3a, Mg/Ca and Sr/Ca were not correlated ($p<0.05$; r: 0.01), suggesting that they were controlled by different factors. Mg/Ca shows slightly higher values than in the other zones and peaks around 350 cm. The Sr/Ca ratio shows low variability.

In subzone 3b, as in zone 3a, Mg/Ca and Sr/Ca were not correlated ($p<0.05$; r: 0.01). Mg/Ca displayed lower variability than zones 1b and 3a: Sr/Ca showed low variability at the base, increasing towards the top reaching values close to those for zone 1b. Zone 3c was composed only of two samples. Mg/Ca presented a low variability, but Sr/Ca was highly variable.

Table 2.2: Mean, maximum and minimum values of Mg/Ca and Sr/Ca molar ratios from *C. torosa* valves in the different established bio-zones along the Palmar core.

Tabla 2.2*: Valores mínimos, máximos y medios de los ratios molares de elementos traza (Mg/Ca y Sr/Ca) de* C. torosa *en relación con las biozonas de ostrácodos.*

	Mg/Ca			Sr/Ca		
ZONES	min	media±*SD*	max	min	media±*SD*	max
4	0,009628	0,013704 ± *0,0025*	0,020838	0,002615	0,004715 ± *0,0014*	0,007003
3b	0,007118	0,016601 ± *0,0047*	0,027487	0,002679	0,004568 ± *0,0015*	0,009203
3a	0,006863	0,019349 ± *0,0067*	0,048290	0,002517	0,003984 ± *0,0010*	0,006861
2	0,012590	0,016457 ± *0,0018*	0,018198	0,003127	0,003446 ± *0,0002*	0,003633
1b	0,009406	0,019152 ± *0,0062*	0,036837	0,002744	0,004929 ± *0,0014*	0,012140
1a	0,006933	0,016234 ± *0,0050*	0,033676	0,002964	0,004427 ± *0,0009*	0,007720

3.3 Stable Isotopes

The isotope values for *C. torosa* shells ranged from -10.2‰ to -0.3‰ (mean -5.46‰ ± 1.81) for $\delta^{13}C$ and -6.36‰ to 4.39‰ for $\delta^{18}O$ (mean value of -0,15±1,79‰) for the core as a whole (Fig. 2.8, Table 2.3). Both $\delta^{13}C$ and $\delta^{18}O$ showed low variability, between samples, in the lower part of zone 1a and high variation at the top of this zone. $\delta^{13}C$ and $\delta^{18}O$values were positively correlated throughout the core as a whole (r: 0.2; $p<0.01$) but especially so in zone 1a (r: 0.64; $p<0.01$). The variability of the isotopic values was greater in subzone 1b and the

correlation between oxygen and carbon much weaker (r: 0.01; p>0.01): moreover, variability increased towards the top of the zone. There are no isotope values for zone 2 owing to low abundance and poor preservation of *C. torosa*.

Very low $\delta^{13}C$ and $\delta^{18}O$ values (-8.86‰ and -6.36‰ respectively) are found at the base of zone 3a, but values increase upwards within the zone to values similar to those in zone 1b. $\delta^{13}C$ and $\delta^{18}O$ values are positively correlated ($p<0.05$; r: 0.31). In zone 3b, $\delta^{13}C$ values are quite similar results to those reported for the previous zone, whereas $\delta^{18}O$ values showed decreased variability and limited statigraphic change leading to weak correlation between the two isotopes ($p>0.05$; 0.28). Few analyses (4) were performed for the zone 3c and the results were not very different to those reported for the zone 3b, but with slightly lower mean values.

Table 2.3: Minimum, maximum and mean values for isotopical variables ($\delta^{13}C_{VPDB}$ and $\delta^{18}O_{VPDB}$) according to ostracod bio-zones.

Tabla 2.3*: Valores mínimos, máximos y medios de las variables isotópicas ($\delta^{13}C_{VPDB}$ and $\delta^{18}O_{VPDB}$) en relación con las biozonas de ostrácodos.*

	$\delta^{13}C_{VPDB}$			$\delta^{18}O_{VPDB}$		
ZONES	min	mean± *SD*	max	min	mean± *SD*	max
3c	-9,19	-6,08 ± *2,18*	-4,22	-2,12	-0,02 ± *1,48*	1,27
3b	-8,07	-4,81 ± *1,68*	-0,30	-1,94	0,76 ± *0,98*	2,76
3a	-8,86	-5,41 ± *1,42*	-0,64	-6,36	0,17 ± *1,96*	4,39
1b	-10,18	-7,07 ± *1,89*	-4,25	-5,24	-0,24 ± *1,75*	3,60
1a	-8,18	-4,72 ± *1,22*	-2,81	-5,27	-1,25 ± *1,75*	2,07

We compared Palmar core isotope values with the data obtained by Marco-Barba *et al*., (in prep), in *C. torosa* from different biozones (see figure 2.9). Some of the results inform the Palmar core follow the same trend as that in the data of Marco-Barba *et al.* (Chapter I), but many values from subzones 1a, 1b and 3 are displaced from the trend, with higher $\delta^{13}C$ values.

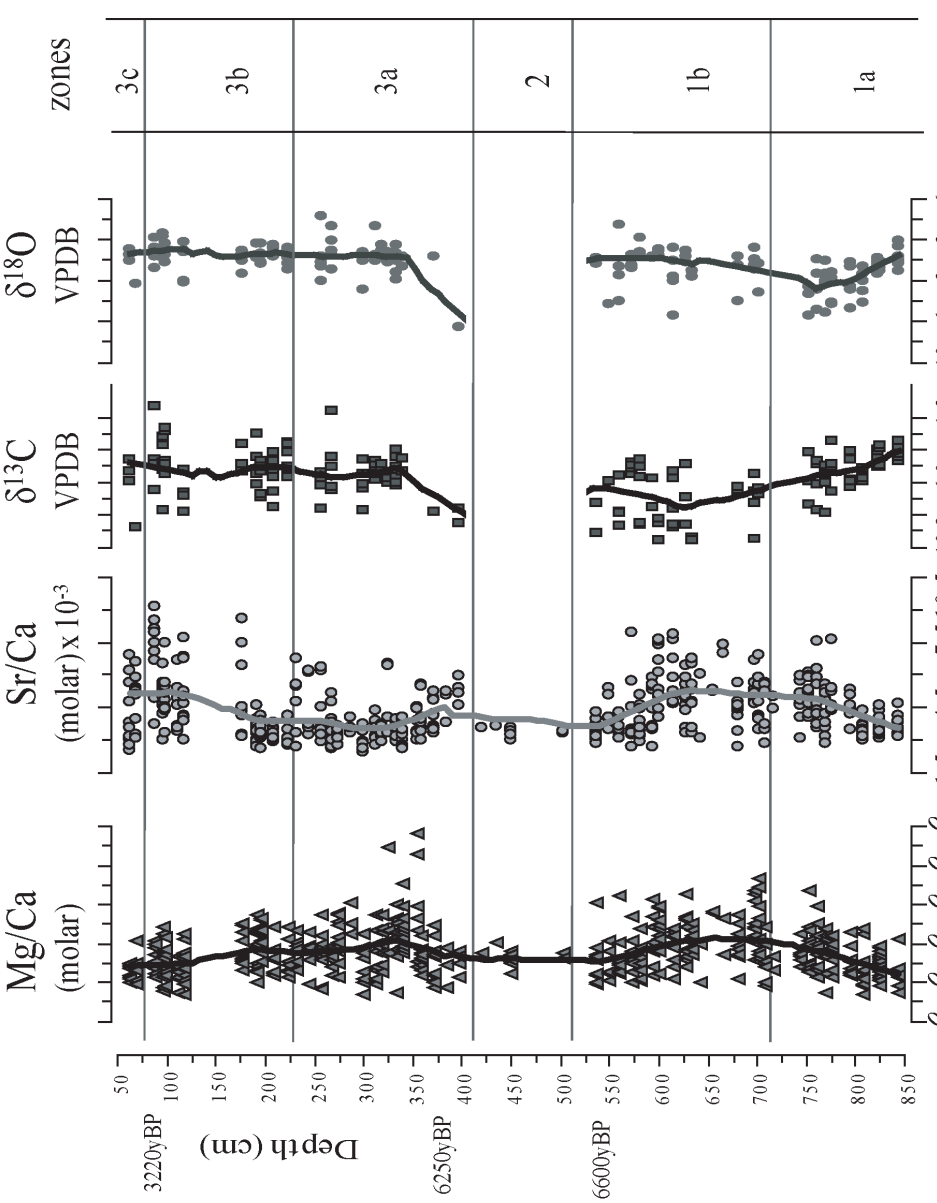

Figure 2.8: Mg/Ca and Sr/Ca molar ratios and isotopic ratios ($^{13}C/^{12}C$ and $^{18}O/^{16}O$) along the sedimentary sequence, for the geochemical analysis performed on the ostracod species *C. torosa*. Loess regression was performed for all the variables using average scale of 20 points. The established ostracod biozones are also placed on the right column.

Figura **2.8**: *Mg/Ca y Sr/Ca ratios molares y ratios isotópicos ($^{13}C/^{12}C$ and $^{18}O/^{16}O$) a lo largo de la secuencia sedimentaria, correspondientes a los análisis geoquímicos realizados en al especie de ostrácodo* Cyprideis torosa. *La regresión LOESS se aplico a todas las variables usando un factor de escala de 20. Las biozonas de ostrácodos se muestran en la columna de la derecha.*

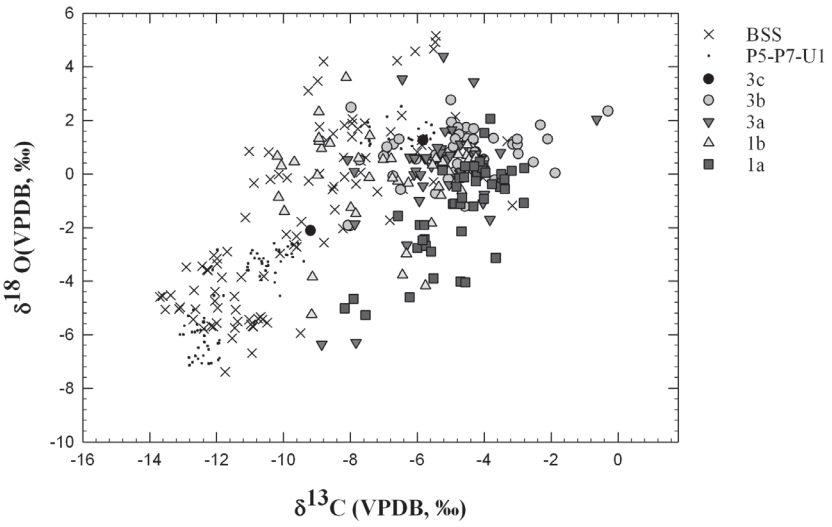

Figure 2.9: Stable isotopic composition ($\delta^{13}C$ and $\delta^{18}O$; VPDB notation) of *C. torosa* calcite valves. The established ostracods biozones are plotted above Marco-Barba *et al*., (Chapter I) *C. torosa* actual data (Broad survey: BSS and Monthly survey: P5-P7 and U1).

Figura 2.9*: Composición isotópica de la calcita de las valvas de* C. torosa *(*$\delta^{13}C$ *and* $\delta^{18}O$*; VPDB notación). Las muestras de las biozonas establecidas para los ostrácodos están dibujadas sobre los datos actuales de* C. torosa *(Capitulo I) (Estudio extensivo: BSS y estudio mensual: P5-P7 y U1).*

3.4 Sr/Ca_{water} and salinity reconstructions

Both past water Sr/Ca and past salinity were inferred from *C. torosa* morphological and geochemical results applying the equations of Marco-Barba *et al*. (Chapter I) shown in methods. Past water Sr/Ca was reconstructed based in ostracod Sr/Ca and isotopic results, and salinity reconstruction was based in the percentage of *C. torosa* noded forms and $\delta^{18}O_{VPDB}$. The past water chemistry reconstructions are shown in figure 2.10. Water Sr/Ca was negatively correlated with salinity at subzones 3a (r: 0.57; $p<0.05$) and 3b (r: 0.79; $p<0.01$). Although in some depths there is a positive relationship such as in the bottom and top of subzone 1a and some peaks of 3a and 3b.

.

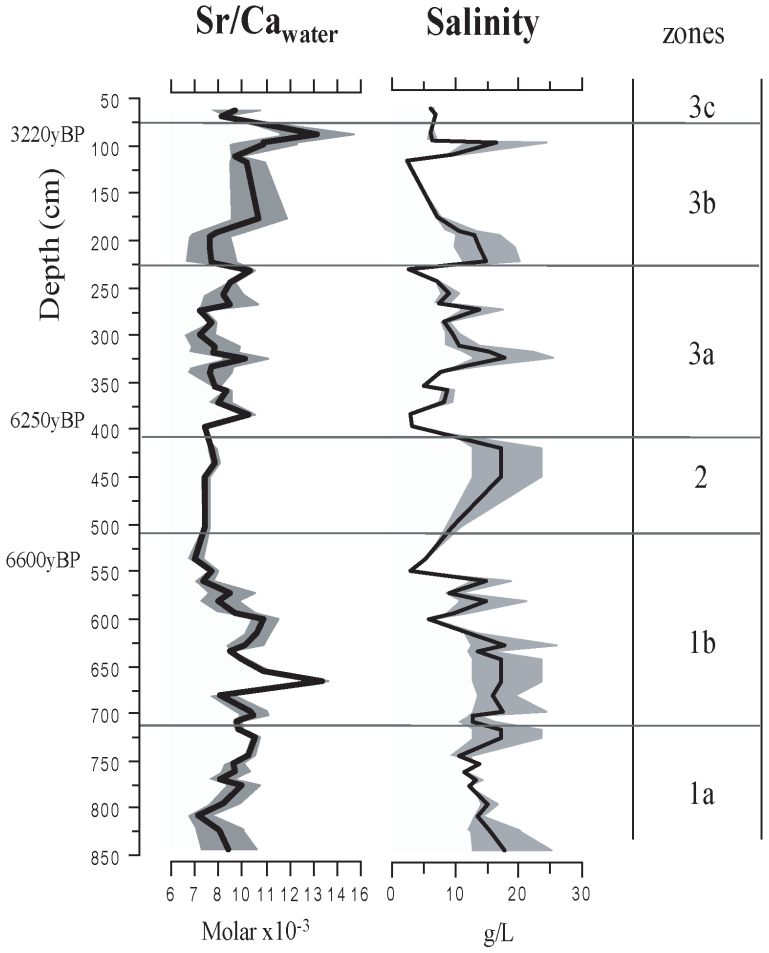

Figure 2.10: Inferred water Sr/Ca and salinity from multiple regressions (equations in methods). The line indicates the mean estimated variable and the shadow parts the minimum and maximum errors. The ostracod established biozones are show in the right column.

Figura 2.10*: Sr/Ca y salinidad del agua inferidas a partir de las regresiones múltiples (ecuaciones de los métodos). La línea indica la media estimada y las zonas sombreadas los errores mínimos y máximos. Las zonas de ostrácodos establecidas se muestran en la columna de la derecha.*

4.-Discussion

There is good agreement between the Palmar core ostracod assemblage zones and the sediment facies. As we discuss below, the distribution of ostracods assemblages in the different bio-zones are mainly due to changes in solute composition of the ancient lake, sea level changes, storms events and freshwater inputs from rivers, gullies or springs.

The sand bar, from where the core was extracted, has probably suffered movements and transformations due to sea level changes, storm events and changing patterns of sediment deposition. For that reason, the study of ostracod remains has been carried out carefully using the taphonomical indicators to help us to elucidate the energy of the environment where the assemblage was formed and the possibility of reworking.

In this section, we first discuss the paleoenvironmental interpretation for each bio-zone based on our multi-proxy data, and then place the Holocene evolution of the lake in the general context of environmental change in the Western Mediterranean region.

4.1 Core interpretation

4.1.1 Zone 1

The ostracod paleoassembalges and geochemical analyses throughout zone 1 (850- 511cm) represent a widely fluctuating environment, varying between an open Albufera influenced by marine waters during times of Holocene marine transgressions, to a mixture of waters derived from freshwater inputs related to wetter periods.

Subzone 1a

Subzone 1a (850-713 cm) is clearly dominated by a brackish ostracod assemblage. *C. torosa* and *L. elliptica* are dominant in this level appearing in high abundances and with high SP. These species are usually found establishing assemblages that tolerate high salinity fluctuations (transitional environments), mainly in estuaries and coastal lakes with muddy sediments enriched in sands (Ruiz *et al.* 2000a,b, 2006). Slight changes in *L. elliptica* abundances can be noted

with respect to *C. torosa*. *C. torosa* is a species that prefers low-energy environments, whereas L. elliptica is more adapted to higher energy levels (Carbonel, 1980; Ruiz *et al*., 2000b), suggesting more fluctuating and higher energy events at the start of the subzone 1a. The sporadic occurrence of species such as C. angulata and *A. arborescens*, *C. vidua* and *L. rhomboidea* also indicates widely-varying conditions, although the shells these species are probably reworked, as suggested by their low abundance and poor preservation (EP mostly type B). The reduced numbers and poorer preservation of shells of *C. torosa* towards the top of the subzone point to the onset of a higher-energy environment (Fig. 2.11).

Diversity indices (Fig. 2.6) indicated wide environmental fluctuations along the zone, with events where only *C. torosa* with low abundance was found. Slight variations can be seen in the percentage of noded forms of *C. torosa* and only a little increase could be seen at the top of the zone indicating possible freshwater influence (Fig. 2.7). However, the decrease in shell weight and *C. torosa* valve lengths to the top suggested increasing salinities (Fig. 2.7), although the upper part of this subzone shows a discontinuity.

Covariance of carbonates $\delta^{18}O$ and $\delta^{13}C$ usually occurs in lake sediments under the condition of hydrological closure for time periods of the order of 5000 y or longer (Li and Ku, 1997). We found a weak but significant correlation between these variables within subzone 1a (r^2: 0.47); the $\delta^{18}O$ values at the bottom of subzone indicate brackish to hypersaline waters similar to those reported at the Santa Pola salt pans (Marco-Barba *et al*., Chapter I) and $\delta^{18}O$ values similar to those of ostracods living in freshwater conditions at the top. The correlation can be explained by a relatively closed lake; probably a coastal lagoon system influenced by marine waters and evaporation processes that were getting gradually isolated from the sea and progressively fresher the lake, due to inland water inputs increase to the top of the subzone. These assumptions correlated with the sedimentology of the deposits that suggests a subaerial floodplain and the ostracod assemblages that point to brackish-water marshes with seasonal drying.

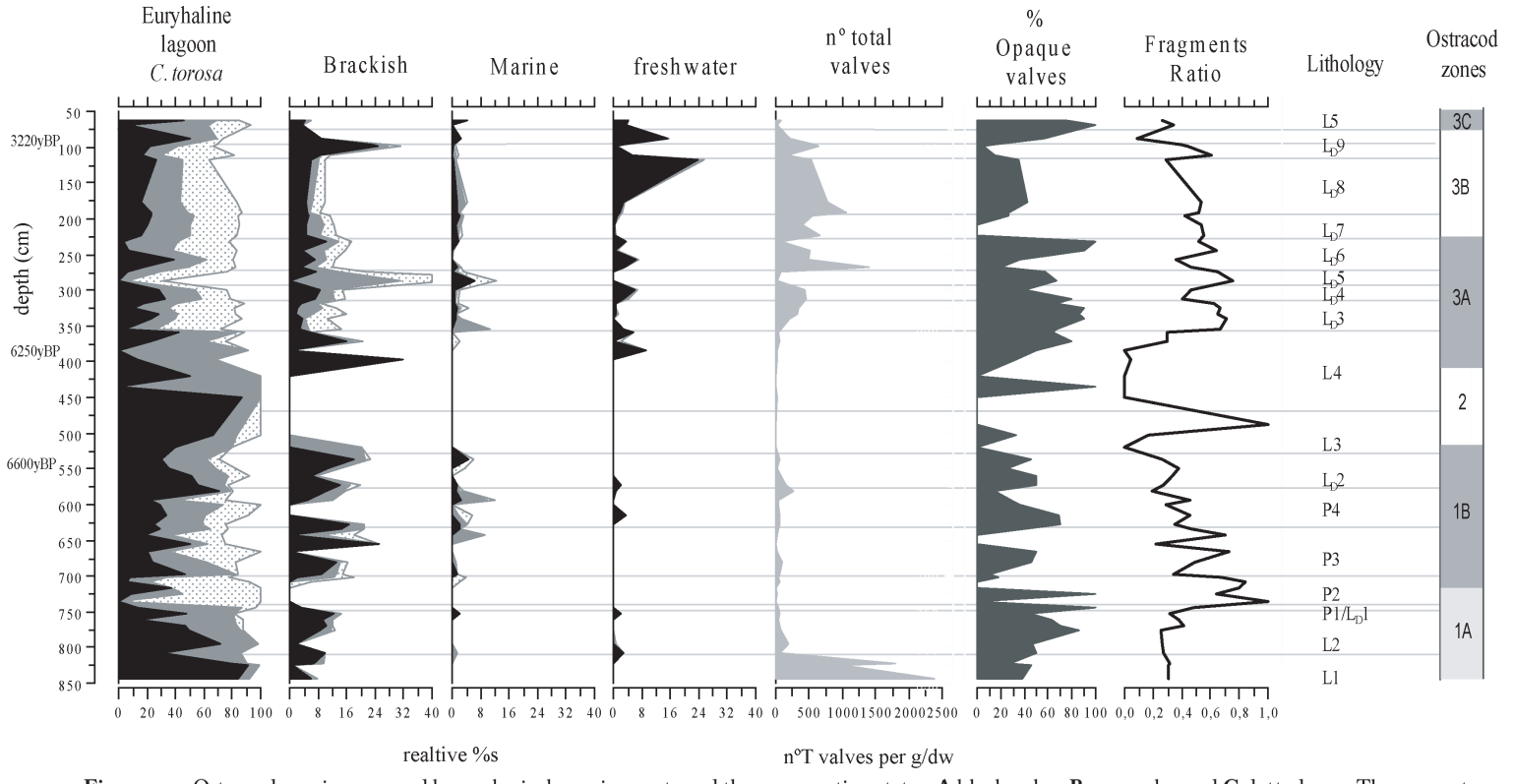

Figure 2.11: Ostracod species grouped by ecological requirements and the preservation states: **A** black color; **B** gray color and **C** dotted area. The percentage of *C. torosa* opaque valves and the ostracod calculated fragment ratio are also placed. Lithological facies and ostracod established zones are placed on the last two columns. Euryhaline: *C. torosa*; Brackish: *L. elliptica*, *X. nitida*; Marine: *A. arborescens*, *L. rhomboidea*, *Pontocythere* sp.; Freshwater: *C. angulata*, *C. vidua*, *D. stevensoni*, *I gibba*, *H. salina*, *Hemicypris* sp.

Figura 2.11: *Especies de ostrácodos agrupadas según sus requisitos ecológicos y con sus estados de preservación:* A *negro;* B *gris y* C *área punteada. El porcentaje de valvas opacas de* C. torosa *y el ratio de fragmentos también se muestran. Las facies litológicas y las zonas establecidas para ostrácodos se sitúan en las dos últimas columnas. Euribalinos*: C. torosa; *Salobres*: L. elliptica, X. nitida; *Marinas*: A. arborescens, L. rhomboidea, Pontocythere *sp.*; *Agua dulce*: C. angulata, C. vidua, D. stevensoni, I gibba, H. salina, Hemicypris *sp.*

The application of different transfer functions to reconstruct past salinities and past Sr/Ca waters based on *C. torosa* (Marco-Barba *et al*., in prep.) suggest brackish waters along the zone (between 10 to 18 g/l) with a decrease in salinity in the middle part and an increase in the very top (17 g/l), whereas reconstructed water Sr/Ca values are quite similar for those reported of sea water (Renard, 1985; Weinbauer and Velimirov, 1995; de Villiers., 1999) at the bottom of the subzone. However, the increase of water Sr/Ca and the decrease of $\delta^{18}O$ values to the top indicate a mixed source of water due possibly to freshwater inputs. The Sr/Ca ratios and $\delta^{18}O$ values indicate high salinities (estimated 15 g/l; brackish water) towards the middle of the zone and a coincident trend from the bottom of the zone 1a (possibly due to freshwater inputs) and in the upper part salinity increase again. The Sr/Ca_{water} increase may be explained by anomalously high Sr content in the freshwater sources. The Júcar River, located at the southern end of Albufera, cross zones dominated by Keuper (Triassic) materials. One of the typical rocks from this Triassic formation is gypsum, which usually has high Sr content (Anadón and Juliá, 1990). Moreover, high Sr contents/anomalies have already been reported by Müller in lake Constance (Müller 1968, 1969), by Anadón and Juliá (1990) at the locality of Baza (SE Spain), and by Marco-Barba *et al*. (Chapter I) at the nearby zones of the region of Valencia. Particularly, Marco-Barba *et al*. (Chapter I) studied localities with salinities below sea water, which presented Sr/Ca values higher than those reported for the sea.

Subzone 1b

The lower part of subzone 1b (713-577cm; $1b_1$) shows a low number of valves but is characterized by an increase in brackish and marine species with the occasional occurrence of the freshwater species *C. angulata*. Low diversity indices and large fluctuations in D_o mark events of change only in *C. torosa*, suggesting a peculiar environment with less dominance of this species. Brackish and marine species are well preserved (Fig. 2.11) whereas *C. torosa* valves showed poor preservation, with types A, B and C in equal same proportions. Marine species are mainly represented by *A. arborescens*; this phytal ostracod is commonly found in shallow marine and estuarine environments (Athersuch *et al*., 1989) and its presence suggests marine influence. The percentage of opaque valves and the fragment ratio of *C. torosa* fluctuate along the zone (Fig. 2.11), but in general both decrease to the top, suggesting a shift to a low-energy environment. The sedimentology of the deposits suggests three backshore events (indicated by Facies 2) and inferred salinity points to a brackish environment. Overall, the various proxies indicate that the lower part of subzone 1b ($1b_1$) represents a period

with relatively high salinity and limited fluctuations, especially in the lower half.

At the upper part of subzone 1b (577-511 cm; $1b_2$), two inferred storms events coincide with the rises of the preservation type C, the percentage of opaque valves, and the fall of diversity indices and D_o values. Inferred salinity values fluctuate suggesting that there were more freshwater periods than the lower part of subzone 1b. Sr/Ca is not related with marine influence in this section of the core but contrarily it seems more related to fluvial inputs, due to the same causes mentioned above. However minor increases in Sr/Ca_{water} values coupled with stable or rising salinity can be explained by arid periods where the temperature increase could favor calcium carbonate precipitation and then, Sr/Ca increases due to Ca depletion.

Most of the *C. torosa* morphological variables increased, including the percentage of noded forms, the dominance of rounded pores and the increase in shell length and weight also suggest fresher-water environments. Overall this period had lower and more variable salinity than the lower part of subzone. D_o values were low in this subzone, indicating that this community is similar to the theoretical average assemblage characteristic of the depositional lobes.

4.1.2 Zone 2

This zone (511 to 409 cm) marks a clear regressive period between zones 1 and 3, with the sedimentology of the deposits suggesting a predominantly subaerial environment. The zone is characterized by few ostracods valves and very low diversity with reworking of pre-existing sediments to form a prograding bar.

4.1.3 Zone 3

Zone 3 shows a return to lacustrine conditions as well as important changes in ostracod assemblages. Diversity increased with species other than the two dominant brackish-water taxa. *Xestoleberis nitida* is restricted to this zone. Valve numbers are much higher in this zone than in the rest of the core except for the bottom of subzone 1a. D_o values were low in this subzone (as in most of the top half of zone 1), suggesting that this community is similar to the theoretical average assemblage characteristic of the depositional lobes.

Subzone 3a

In Subzone 3a (409 to 228 cm), *C. torosa* and *L. elliptica* remain the most common species but there is an increase in *A. arborescens* and appearance of *Pontocythere* sp. Marine influence is seen in some samples, whereas the freshwater species *C. angulata* and *C. vidua* appear in a few levels. *C. vidua* is a cosmopolitan freshwater species that can tolerate a wide type of habitats; while *C. angulata* prefers permanent freshwater water bodies but can tolerate some salinity variations (Meisch, 2000). H shows an increasing trend to the middle of the zone whereas evenness showed higher and more fluctuating values at the start of the zone, with changes in the composition of the species reflecting varying habitats in this complex wetland ecosystem. Both the percentage of opaque valves and the fragment ratio are coincident with high relative abundances of brackish and marine species with SP type B and C, suggesting that they are reworked. The freshwater species present, however, are better preserved and show a negative correlation both with marine species and the aforementioned ratios. The percentage of *C. torosa* with noded valves and rounded pores, together with carapace lengths and weights were more or less correlated, and we infer that lower-salinity water was associated with the samples with higher values. Inferred salinity values were generally below 10g/l, with occasional maxima as high as 15g/l. Water Sr/Ca was relatively low and constant suggesting more stable water, however the main peaks coincide with drops in salinity (negatively correlated), indicating that Sr/Ca increases could have resulted from freshwater inputs. Moreover, lithology and the SP of marine and brackish species plus taphonomical indices indicate that most of this material was reworked and deposited at this zone probably by the storms events, but an autochthonous community of freshwater species was able to thrive for short periods of more stable conditions.

Subzones 3b and 3c

Subzone 3b (228 to 78 cm) differs from subzone 3a by the increase of the number of valves, the decrease of marine species and the increase of freshwater species towards to the top. *C. angulata* is the most common species. The brackish *Xestoleberis nitida* usually linked to macrophytes (Athersuch *et al.*, 1989) appears almost exclusively in this zone and following a similar profile as *C. torosa* and *L. elliptica*. On the other hand, *C. angulata* is negatively correlated to *C. vidua* as in subzone 3a. *C. vidua* is associated in the upper part of this subzone with the presence of *H. salina*, which is a typical association of temporary ponds on

the back of dunes (Rueda *et al*., 2006). In the uppermost part of this subzone, a peak of *C. vidua* and other freshwater species common in temporary waters coincides with a peak of *A. arborescens*. This event coincides with L_D9, where a storm event suggests the possibility of a mixture of waters and reworked material (see the increase of fragments ratio). With the exception of this upper part, the percentage of opaque valves and the fragment ratio remain fairly constant along this zone. *C. torosa* carapace lengths tend to increase, but the SP seems to be in the same proportions of the three types suggesting possible reworking events for the SP type B and C. Nevertheless, the freshwater species show very good preservation, with SP type A the most abundant.

The percentage of noded valves of *C. torosa* as well as the length of shells of this species, increased towards the top of the subzone. There is an increase in valve weight and in the percentage of rounded pores, but with variability in both, suggesting periods of mixed-source water interrupting the freshwater environment. Inferred salinity and Sr/Ca values suggest elevated salinity (10-12g/l) at the start of the subzone followed by a decrease and then a sharp increase during the aforementioned storm event in the upper part of the zone.

Subzone 3c consists of only two samples, both with low diversity and strong dominance of *C. torosa* as in zone 1. The percentage of noded specimens of *C. torosa*, as well as the presence of other morphological features suggestive of low salinity, point to a relatively fresh environment, an inference supported by the occurrence of some freshwater species.

4.2 The mid Holocene history of the Albufera Lake

The lower half of the Palmar core is characterized by sediments typical of a lagoon-barrier system, which suggests that the main Holocene transgression reached the maximum below the eastern limit of the present Albufera of Valencia (Santiesteban *et al*., in press) at that time. The initial part of this transgression was described as a prograding beach-barrier system that grew above Pleistocene sediments in most of the studied Mediterranean coastal systems (Goy *et al*., 1987). Goy *et al*. (1996) described the existence of early Holocene surface above the Pleistocene that lies at the marine platform and it is characterized by overlapping beach systems. According to Vita-Finzi's (1972) curve of sea level changes, the early Holocene transgressive sequence should be dated before 13000 cal yrs BP and the maximum regression should have occurred between 13000 and 11000 cal yrs BP.

We estimate that in our core the contact between the Pleistocene and the first Holocene deposits in this locality are represented at 8.5 m depth by a discontinuity, in which there is evidence of exposure, including paleosols and root traces. If our age model is correct, we hypothesize that at this depth corresponds to the period before of the maximum transgression that should have occurred before 6600 yrs BP (7115 ±75 cal yrs BP) that we found about 7 m (Fig 2.12).

Our inferred salinity changes correlate with sea level changes (eustatic fluctuations), indicated in other Holocene Mediterranean coastal studies. For example, Somoza *et al.* (1998) described how high frequency global sea-level fluctuations have affected the Ebro River Delta over the last 8000 yrs BP. Zazo and Goy (2000) have interpreted high stands as warm events and intervals of high mean sea level (MSL) (see figure 2.12). These events were followed by cold periods, with lower MSL, which allowed progradation of the main delta complexes ('d-episodes' and H1, H2, H3). If these assumptions are true, we can establish a concordance with other studies along the Spanish coast, and hypothesize that we registered the *h1*, *h2* and *h3* high stand events relative to the maximum flooding stages of Ebro peat developments and the progradational events d_0, d_1 and d_2 of the Ebro Delta and H1, H2 and H3 of Goy *et al.* (2003).

Part of event d_0 can be identified at the bottom of Palmar core (Fig. 2.12), covering an episode represented within the core between 850-750 cm that coincides with our ostracod zone 1a. The high ostracod abundances, the well preserved shells of *C. torosa* and *L. elliptic*a and the lithology descriptions of the lower part of subzone 1a suggest a more stable environment, permanent waters and moderate salinities. However, evidence of more unstable environments is found at the end of this zone, indicating that the lake was shallower, hydrologically open and subject to alternating periods of desiccation and flooding.

Figure 2.12: Tentative Holocene Palmar highstand events (*h-h3*) and prograding units (d and H) based on ostracod zones, inferred water Sr/Ca and inferred salinity compared with the reconstructed high-frequency climatic eustatic swings based on delta del Ebro (gray bumps: sea level rising, black bumps: regressive phases) and other paleoclimatic reconstructions over the last 8000 years. BP*: age scale in cal yrs BP for the events located in the box and yrs BP for the remaining figures.

Figura 2.12: *Reconstrucción tentativa de los niveles altos del nivel del mar (hr-h3) y unidades de progradación (d, H) basados en las biocanas de ostrácodos, Sr/Ca del agua y salinidad inferida todo ello comparado con las oscilaciones eustáticas reconstruidas los eventos altos del nivel del mar basados en el delta del Ebro (gris: subida nivel del mar; negro: fase regresiva) y otras reconstrucciones paleoclimáticas durante los últimos 8000 años. BP*: escala de edad en cal yrs BP para los eventos localizados en la caja y yrs BP para el resto de gráficos.*

The marine highstand *h1* was described by Zazo *et al*. (2008) on the basis of progradational deposits that postdate the Holocene maximum mean sea level, and is associated with high rates of sedimentations. An analysis of sedimentation rates during the Holocene in estuaries in the southwestern coast of the Iberian Peninsula (Dabrio *et al*., 1999; Lario *et al*., 2002) demonstrated that these rates varied from the first phase between 10000 and 6500 cal yrs BP, with rates of sedimentation of 5 mm a^{-1} to a second during highstand (6500 cal yrs BP to present) with rates of sedimentation of 1.5-2 mm a^{-1}. This episode coincides with the thick sediment unit from 750-325 cm in the Palmar core. This period was also characterized by high rates of sedimentation in our core, encompassing part of our zone 1b, zone 2 and the bottom part of the zone 3a. Based on the lithological descriptions, we suggest backshore sediments (Facies 2/P) and storm events (Facies L_D) (Fig. 2.2; Santiesteban *et al*., in press) throughout zones 1b and zone 2, whereas the first part of zone 3a is interpreted as lagoon barrier sediments (Facies 4/L). The brackish-marine ostracod assemblages and the peaks in inferred Sr/Ca that occur throughout these zones suggest a mixture of fresh and marine waters. The changes in SP, in the fragment ratio and the large oscillations of diversity indices indicate high energy (low stability) and fluctuating environments. We can recognize three maximum levels of salinity that are coincident with the highstands peaks of *h1* during this period (Fig. 2.12) and the drops in salinity (within *h1*) that would coincide with progradation intervals (d intervals). The progradation events (d) can be interpreted as cold events that occurred due to the oscillations during marine high stands (HST). The progradation event associated with the Maringoun regression (Fig. 2.12) can be identified between the first increase in salinity and the second; the Bayou Têche regression occurs between the second and third peak.

Events *h2* and *h3* are represented by a thinner accumulation of sediment due to reduced sedimentation rates. They correspond with the top of zone 3a and zone 3b. Between *h1* and *h2* we can identify an interval of several salinity maxima but a mean value that is lower compared with *h1* event. The presence of well-preserved shells of freshwater species coincident with Sr/Ca peaks and inferred salinity minima suggest freshwater influences. This Sr/Ca anomaly could be explained by fluvial inputs in a period of erosion and dissolution of evaporite-rich soils (Keuper) (Anadón and Julia, 1990). This interval correlates well with the regressive phase corresponding to d_1 that further correlates with the Maringouin complex (between 6150-5350 yrs BP).

The d_2 phase corresponds with the decrease in salinity between 200-100 cm in the Palmar core and correlates with the Têche delta complex (4400-3600 yrs BP). It is located between *h2* and *h3* and is where we estimated the lowest salinities along the core, where the freshwater species reach the highest abundances and the MSL is the lowest for the study period. The *h3* event can be recognized because (3220 yrs BP≈ 3035±65 cal yrs BP) fits well with sediments type (lagoon-marsh), the inferred salinity peak, the increase in well-preserved brackish species and a fragment ratio that is consistent with a high energy environment and our datation at 88 cm.

5.- Conclusions

According to earliest historical records (from the middle ages and more reliably from 17th century), the Albufera of Valencia was an ancient enclosed bay that was connected to the sea (Sanchís Ibor, 2001), probably by a wide channel located at the south of the present coastal plain. The morphological and sedimentary study (Santiesteban *et al*., in press) shows the formation of four individual bars that were progressively separating the lake from the sea. These bars developed from the North to the South, starting at the mouth of Túria river, as a consequence of the sediments deposited by this and other rivers (e.g. the Palancia) due to high frequency sea level oscillations since the maximum flooding surface of the Flandrian transgression (Ruiz and Carmona, 2005). The study of the Palmar core is supported by three radiocarbon dates, lithological descriptions, paleoecological indices, fossil assemblages and geochemical analyses that helps to understand the Holocene evolution of the Albufera de Valencia, as well as the influence of sea level changes that could be correlated to Ebro Delta depositional sequence.

The global Holocene rise in sea level is particularly well recorded in Atlantic estuaries (Zazo *et al*., 2008). Nevertheless, small fluctuations during the Holocene are best recorded in beach, barrier systems, and sometimes in deltas such as the case of the Ebro Delta (Somoza *et al*., 1998). Two steps can be seen in these kinds of sedimentary records, a first rapid rise in sea level between ≈13000 and 7000-6500 cal yrs BP that resulted in rapid vertical aggradations, and a second phase of deceleration dominated by lateral progradation (Zazo *et al*., 2008). These two steps can be well recognized on the Palmar sequence. The first set of backshore sediments is of almost 3 meters thickness, where an unstable

environment can be recognized by the increase in the Albufera salinity (brackish waters with some freshwater oscillating periods) and high energy environments. Second, two sedimentary sets that correspond to the progradation phase that include two Holocene periods (H2 and H3) are intercalated with more humid events that introduced more freshwater into the lake, as shown by the ostracod assemblages and ostracod geochemistry.

The Palmar sequence can be interpreted as a sediment sequence over the main marine transgression and the immediately prograding phase that occurred along the Mediterranean Spanish Holocene, in concordance with other studies on coastal Holocene evolution. However, other cores should be extracted to the eastern part of the sandy bar and in the middle of the lake to corroborated our interpretations on the upper part of the Holocene, the bar evolution and to know how the last marine transgressions affected the coastal lagoon/marshlands.

PART III

The late Holocene evolution of Albufera de Valencia

1.-General introduction and study site of chapters III and IV

Lagoons, estuaries and coastal wetlands ecosystems are ecotones located at the transitional zones between continental and marginal marine environments. These environments can be natural, seminatural or human dominated ecological systems, which altogether cover an average of 6% of the Earth's land surface (Gönenc and Wolflin, 2004). These systems play important biogeochemical roles such as nutrient cycling, nutrient production, decomposition of organic matter, and fluxes of material (e.g. nutrients, water, particles and organisms) between the land, the sea and the atmosphere (Levin *et al*., 2001; Viaroli *et al*., 2007). Coastal lagoons are dynamic and open systems with particular features such as shallowness and the presence of characteristic physical and ecological boundaries. Shallowness provides usually lighted bottom and facilitates wind effects over the entire water column, promoting resuspension of materials, nutrients, and small organisms from the sediment to the surface layer (Gönenc and Wolflin, 2004). Furthermore, seawater mixes with fluvial or groundwater sources produce subsaline or brackish water bodies, although some of these systems may be more saline than sea water as a result of evaporation processes (Cohen, 2003).

Coastal lakes are sensitive indicators of sea level and human influences, mainly changes in hydrology, water chemistry, and eutrophication processes. Hence, paleolimnological studies can help to understand lake evolution through time, climatic and anthropogenic impacts on it, and also to detect important historical events that remain not clear on historical archives. The different processes that can be involved on the limnological characteristics of these systems are usually linked to climatic and dynamic factors such as sea level rising, evaporation/precipitation cycles, floods and storms events before man's influence. Most of the coastal lagoons were formed during the Holocene or Pleistocene as a consequence of rising sea levels. During the late Holocene (last 4000 years), sea-level fluctuations (HST= high stand sea level; *h* events) were relatively minor, compared with the HST that occurred during the early Holocene (between 12000 and 4000 years BP), fluctuating by less than 1 m (Zazo *et al*., 2008). However, different authors identified different high stands (*h*3, *h*4, *h*5 even *h*6) recorded in estuaries or beach barrier systems at Spanish Mediterranean coasts during the last 4000 years (Somoza *et al* 1998; Zazo *et al*., 2008).

The first paleolimnological study carried out by Margalef and Mir (1973) based on a study of diatom remains from three short cores extracted in the Albufera de Valencia Lake (two of them of 35 cm depth and another of 42.5 cm depth) showed the previous brackish stage of Albufera de Valencia. The same stage was observed by Robles *et al.* (1985) in his study about the gastropod fauna of three cores (maximum length 80 cm) located at the littoral zone of the lake, close to the sandy bar. In both studies, these authors concluded that Albufera (presently oligohaline) presented an earlier brackish stage that changed to a freshwater one. Nevertheless, in any of these studies the sediments were dated, and only Robles *et al.* (1985) suggested the possibility that the change from brackish to freshwater probably took place during the XV century. This deduction was based on one radiocarbon date carried out in a previous work. However, large uncertainity about how historical human activities affected the hydrology and solute composition of this lake remain unanswered. Later on, Sanjaume *et al.* (1992) carried out another palaeolimnological study focused on the rates of sedimentation of Albufera de Valencia. These authors analysed 7 short cores (maximum length 215 cm), but they focused only on the lithological and granulometric exploration of these sequences. They calculated different rates of sedimentation based on two radiocarbon dates (on mollusks) and one cesium analysis. Despite this was one of the firsts approximations to the sedimentological evolution of Albufera de Valencia supported by radiocarbon dates, they did not take into account the reservoir effect that the dated material (frequently older) usually shows (Stuiver *et al.*, 1986; Stuiver and Becker 1993; Siani *et al.*, 2000).

In the following chapters we study the recent evolution of Albufera with another approach based on Ostracoda. Their usefulness, as has been said from its shell morphology, shell geochemical composition and species assemblages, provides important clues for paleoenvironmental reconstructions (De Deckker and Forester, 1988). Geochemical shell composition has been used in different paleolimnological studies to reconstruct past salinities (Anadón and Juliá 1990), water Sr/Ca (see Chapter II of this Thesis), temperatures, precipitation/evaporation processes (Anadón and Juliá 1990; Holmes *et al.*, 1998; Von Grafenstein *et al.*, 1999a,b) and water total dissolved inorganic carbon (TDIC) (von Grafenstein *et al.*, 1999; Leng and Marshall, 2004). The aim of our studies on the sedimentary sequences of the Albufera de Valencia is to reconstruct the ecological evolution of the lake during the past 3500 years, based on the knowledge and open questions resulting from the oldest sequence analysed in this thesis

(see Chapter II). Our objective is to analyse how the last marine transgressions affected the solute composition of the lake, how the Albufera de Valencia became progressively more isolated from the sea and how rice fields expansion and human hydrological management affected the lake salinity evolution. This work was carried out in the framework of a multidisciplinary project (VARECOMED) focused on Holocene sea level rise, hydrological changes and human influences in the Spanish Mediterranean area. In addition, we want to see how the increasing use of fertilizers and the change of rice cultivation practices which drove the lake to a eutrophic stage, affecting the ostracod fauna of the lake. We combine information from ostracod paleoecology, shell morphology, preservation and geochemistry using updated ostracod calibrated data in order to reconstruct the late Holocene history of Lake Albufera.

In the next two chapters, we focus on ostracods paleoecology and geochemistry. As a first proxy, we will use the paleoecological application of ostracod assemblages to approximate salinity changes and water chemistry (Griffiths and Holmes, 2000; Boomer and Eisenhauer, 2002; Anadón *et al*., 2002) taking into account previous knowledge of ostracod assemblages from Spanish Mediterranean wetlands (Mezquita *et al*., 2005; Rueda *et al*, 2006; Poquet *et al*., 2008). Secondly, we will pay also attention to ostracods preservation, sex ratio, valve/carapace ratio and juveniles/adults ratio since they are good taphonomical indicators. The state of preservation (SP), either as the grade of broken valves or the fragments ratio (FR) are good indicators to assess the proportion of reworked material (Whatley, 1988; De Deckker, 2002 and Chapter II). Third, we will apply the known association between morphology of the target species *C. torosa* and habitat salinity (Vesper, 1972b, Van Harten 1975; Chapter I) to infer past salinities and water chemistry variations. Fourth, we will use ostracod shell geochemistry (trace elements and isotope composition) and multiple regressions (Chapter I) as a proxy for paleoenvironmental lake reconstructions (De Deckker and Forester, 1988; Griffiths and Holmes, 2000; Ito, 2001; chapter I). Finally, we will use instrumental data of lake salinity, lake chemistry and chemical composition of the surrounding rivers, arid and wet periods obtained from WEMOI index (Martin-Vide and Lopez-Bustins, 2006), plus historical data of river floods obtained from the bibliography and databases to discuss our salinity approximations and historical human management of the Albufera Lake.

Study area and historical setting

The Albufera de Valencia is a shallow polimictic and hypereutrophic Lake. As it was described on the previous chapter the lake is enclosed in the Albufera Natural Park that comprises an area of 21000 ha, most of them dedicated to rice farming. The morphology and dimensions of the lake were described at the previous chapter (see chapter II for further details). Júcar and Túria rivers (and perhaps also R. Palancia) contributed to the formation of the different sand bars and probably to the formation of the last sand bar over the last 500 years (Roselló, 1995; Ruiz and Carmona, 2005; Santiesteban *et al*., in press and Chapter II). Santiesteban *et al*. (2009) postulated that the last sand bar was formed during the last marine regression that took place over the last 500 years and probably and triggered the lake closing. But the real lake closing and the consequent fresher of the lake remain unknown.

The Albufera de Valencia concession to the Spanish central government by the queen Isabel II (1865AD) allowed the progressive expansion of rice farming, which started at the 2nd half of the XIX century (from 1865 to 1927) and provoked a reduction of the Lake surface (5000 Ha) (Sanchis Ibor, 2001). It is well known that the Lake was covered by a dense submerged macrophyte meadow in the 1950-60s (Docavo, 1979). Due to the use of fertilizers and pesticides and sewage increases, the macrophytes disappeared and the Lake arrived to an eutrophic stage in the 1970s (Romo *et al*., 2008). The hydrological Lake level is currently controlled by the hydrological cycle of the rice and by three lockgates that connect the Lake to the sea through three channels. In addition to the intensive rice agriculture development, the Albufera de Valencia is currently surrounded by small villages, an important town and several industries. Currently, the Albufera de Valencia is dominated by dense phytoplankton populations, mainly cyanobacteria (Romo and Miracle, 1993, 1994; Villena and Romo, 2003), the macrophytes are absent or very rare at present and the Lake conductivity vary between 1 and 3 mS cm^{-1} (Villena and Romo, 2003).

CHAPTER III

The late Holocene evolution of Albufera de Valencia based on ostracod assemblages and geochemical analyses: sea level changes and anthropogenic influences

2. Material and Methods

2.1 Core extraction and whole core examination (imaging and XRF)

A 240 centimetres core (core Center) was taken in July 2006 from a point in the middle of Albufera Lake (UTM: 30S728065/4357504, Fig 3.1). The core was extracted using a Livingstone corer with 8 cm liner inner diameter and kept in a polyethylene tube. The core was analyzed every 0.5 cm for density and magnetic susceptibility (MS) with a GEOTEK core logger at the Limnological Research Center (LRC), and then, the core was subdivided in two halves. One halve was used for imaging (DMT core scanner) color, grain-size descriptions and ITRAX XRF core scanner, the other one was sample for fossil content, geochemical and Nitrogen/Phosphorous analyses.

The main geochemical elements Al, Si, P, S, Cl, Ar, K, Ca, Ti, V, Cr, Mn, Fe, Co, Ni, Cu, Zn, As, Rb, Sr, Y, Zr, Ba and Pb were analyzed every 5 mm from the bottom to 66 cm depth and every 2 mm from 66 cm to the top of the core by using the ITRAX XRF core scanner in the Large Lakes Observatory of the University of Minnesota (Duluth, USA) using 30 seconds count time, 30 kV X-ray voltage and an X-ray current of 20 mA. The obtained values are given as relative concentrations, however, high correlations have been found between ICP-OES and XRF-scanner data for some elements in different studies, such as Boyle (2000). The stratigraphy of the core was described and then, subsamples were collected (see below).

2.2 Core subdivision and analysis of subsamples

The core subdivision was carried out at approximately 2 cm intervals at the bottom meter and every 1 cm (high resolution) at the upper meter. In total, 72 samples were obtained for different analysis (geochemistry, mineralogy and micropalaeontological studies). An aliquot subsample weighting between 0.3 and 0.7 g was taken to determine dry weight per sample. These aliquots were weighed, dried at 105°C during 1 hour and weighed again to determine water content and dry weight per gram of fresh sample.

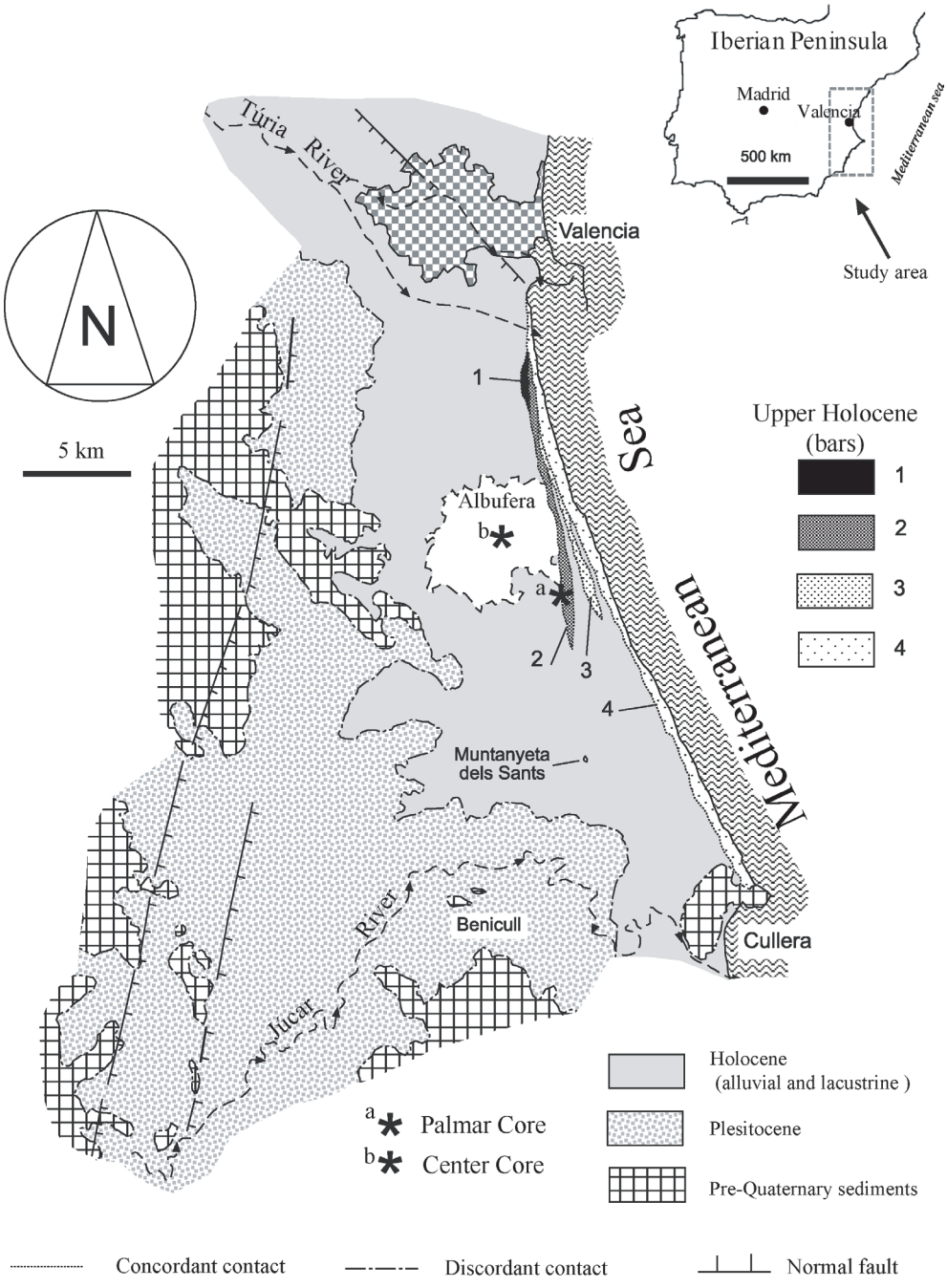

Figure 3.1: This figure shows the core Center location and the geological composition of the studied area. Figure adapted from Santiesteban *et al.* (in press).

Figura 3.1: *La figura muestra la localización del sondeo Centro y la composición geológica del área de estudio. Figura adaptada de* Santiesteban *et al. (in press).*

The remaining sediment was dried at 460ºC during 7.5 hours to determine organic matter content (LOI) and later on at 950ºC during 8 hours to obtain the concentration of carbonates per sample. Subsamples were also taken to measure total nitrogen (TN) and phosphorus (TP) content. To follow a simultaneous oxidation of both compounds, samples were digested according to Valderrama (1981) modified for sediments. Given that reaction starts at pH 9.7 and ends at pH 5-6, this method results appropriate for a combined digestion. This is because nitrogen oxidation requires alkaline conditions to yield suitable results, whereas oxidation of phosphorus compounds must be performed in acidic medium. However, to check a possible disagreement between methodologies, samples were also submitted to a conventional digestion procedure with sulphuric acid and potassium persulphate for phosphorus analysis. Once oxidized, the nitrogen and phosphorous content in all samples was determined spectrophotometrically; orthophosphate concentrations were quantified by the ascorbic acid method (APHA 1992; method 4500E), and nitrogen amounts were measured as nitrate applying the second derivative UV/visible spectroscopy technique (Ferree and Shannon, 2001).

The ostracod subsamples were processed following the method suggested by Griffiths and Holmes (2000) and explained in detail in Chapter II of this Thesis; 10-15g of wet sediment were weighted, air dried and then wet-sieved through 400 and 250 μm pore size using a water flux during 30 minutes. For further descriptions of the method see chapter II.

Biogenic remains were picked from the sieved sediment with a `00´ paintbrush under a low power Olympus SZX 12 stereo microscope and stored in micropalaeontological slides. Ostracod valves were counted for each sampled depth and the abundance expressed as number of valves per 10 g dry weight (10g dw^{-1}). The different species were identified following Athersuch *et al.* (1989), Meisch (2000) and Poquet *et al.* (2008).

2.3 Ostracoda preservation states

The preservation states for ostracod remains were analyzed in the same way as in chapter II, to have an indication of the proportion of reworked valves. Different studies (*e.g.* Danielopol and Handl, 1990) showed the differences between valves that were deposited in quiet environments and valves that suffered strong flows and turbulences previously to deposition. In quiet sites the number of well preserved shells was significantly higher than in the high energy

environment. For that reason, the application of a preservation index could be a good taphonomical tool to assess the grade of reworking.

We used the states of preservation (SP, see chapter II) A-B-C plus the ostracod fragments and the fragments ratio (FR= (fragments+PE type C)/nºTotal valves+fragments) to assess the energy of the environment at the time of deposition (see chapter II for further details). Once more, valves falling into preservation states A and B were considered well enough preserved and consequently these were the valves included into the multivariate analysis (cluster and ordination analysis, see below). For geochemical analyses each ostracod valve that was previously classified as A or B was further assigned to a category in a gradient from 1 to 7 based on valve transparency state of preservation (Griffiths and Holmes, 2000) and only valves that ranged between 1 and 4 were used for geochemical analyses. For further details of these indices see chapter II.

2.4 Morphology and preservation of C. torosa *shells*

Particular attention was paid to *Cyprideis torosa* remains. Between 1 and 137 *C. torosa* adults per sample (adult females and males) were measured for carapace length. The percentage of noded animals per sample (Van Harten, 1975; this thesis, Chapters 1, 2, 3) was also calculated. In addition, *C. torosa* male:female (M:F) sex ratio, single/double valves ratio (VCR) and juveniles/adults (J/A) ratio were taken into account in order to assess *C. torosa* autocthonous or alocthonous populations origin and the energy at the time of deposition of these populations (Kilenyi, 1969).

The taphonomical processes taking part during deposition after an animal die affect the number and type of valves that are preserved in the sediment. Thus, the study of the sex ratio, Juveniles/adults ratio or valve/carapace ratio of each *C. torosa* assemblage can give us relevant information about the conditions at the time of deposition (Van Harten, 1975; Whatley, 1983a), and indirectly these data may be of great value in interpreting the recent evolution of the lake.

Sex ratio (M:F). Sex ratio is the unique variable that is recorded in the fossil record to assess the reproductive strategy of the species at that time (Boomer and Eisenhauer, 2002). Additionally, the study of the living populations gives us information about the type of reproduction and the theoretical sex ratios of each species, consequently, variations from the theoretical value on dead populations could give an indication on the degree of stability of the environment at the

time of deposition. Different studies have been performed about the life cycle and population structure of *C. torosa* (Heip 1976; Mezquita *et al*., 2000; this Thesis Chapter I). In that way, the use of a species such as *Cyprideis torosa* that present living populations with sex ratio very close to 1:1 can be very helpful, because variations from this theoretical value in dead populations could inform on the stability of the environment where paleoassemblages were formed.

Juveniles/adults ratio (J/A). Whatley (1983a,b, 1988) developed this very useful tool for paleoenvironmental reconstructions. The observation of the age structure of valves and carapaces that accumulate in habitats where living populations exist can provide good tools to assess the energy where the assemblage was formed (Whatley, 1988; De Deckker, 2002). In high energy environments, such as shallow costal lakes, where bottom currents, wind effect, floods and storms play an important role, the small juvenile valves can more easily be transported away from the place where they died. Thus, J/A ratio vary between 1:1 and 1:4 at high energy environments (Danielopol *et al*., 2002), because the population structure is mainly represented by adults and a few juveniles of the late instars. Note that we calculated the J/A ratio only for samples where adults were present.

Valve/carapace ratio (VCR ratio). Ostracod valves become disarticulated very rapidly after death. In a slow sedimentation process and with optimal conditions after the animal die, the putrefaction processes and bacteria activity facilitates that valves become disarticulated (De Decker, 2002). Once the valves are open, other small organisms can eat the soft body parts and the valves become separated. But, if we found complete carapaces, we can assume that other possible processes happened. These processes can be summarized in three possibilities (modified from De Deckker, 2002). First, if the animal dies due to rapid sedimentation rates and is trapped in the sediment, the process mentioned above cannot be completed, then, complete carapaces can be found. Second, if the animal dies in anoxic sediment conditions, those conditions prevent further activities of bacteria disarticulating the valves after death. Third, if a dead animal is exposed to a high energy post-mortem environment valves became disarticulated. Thus, depending on the amount of single valves or complete carapaces that we found in the sediment and combined with other paleoecological indices we can estimate if these valves have suffered post-mortem transportation, rapid burial or slow deposition over the sediment (Kilenyi, 1969).

2.5 C. torosa *geochemical analysis*

Between four and twenty *Cyprideis torosa* valves were analysed per sample of core Center. Analyses were usually performed on single adult valve, or at least 3 adult valves; however, sometimes juveniles of late growth instars (A-1 and A-2) were pooled in groups of 4 or 5 valves. Adults and juveniles were never analyzed together and males and females were always analyzed separately.

Between 2 and 10 analyses per sample were carried out to determine isotopical ratios $^{18}O/^{16}O$ and $^{13}C/^{12}C$. Ostracod valves were cleaned for geochemical analysis using the method described in Ito (2001) and in the previous chapters of this thesis (2 and 3). Cleaned valves were analyzed mostly using a Kiel-II online carbonate preparation device coupled to a Finnigan MAT 252 stable isotope ratio mass spectrometer (University of Minnesota) and a few samples (60 samples≈159 valves) using a MAT 251 (Michigan) mass spectrometer, both connected to a Kiel carbonate preparation device. Analytical precision was typically <0.1‰ for both $\delta^{13}C$ and $\delta^{18}O$. For further details see chapter II where the same procedure was applied. We run samples from the same levels in the two different labs and therefore we can ensure that the different analytical protocol did not affect the results.

2.6 Diversity indices and statistical methods

Several diversity indices were used to calculate diversity of ostracod assemblages; we employed the Shannon-Wiener index (Shannon and Weaver, 1963) to estimate diversity (H; equation 1) and Evenness (E; equation 2), in order to know how the species were distributed per sample (Margalef, 1974). In addition, we used the index of fluctuation (D_o; equation 3) formulated by Dubois (1973) to assess ostracod community fluctuations with respect to the average state calculated for the whole sequence. High values indicated major fluctuations of the community and maximum deviations from the state to which the structure of the community is approaching (Miracle, 1978). For more detailed explanations of the Diversity indices and D_o see chapter II.

The XRF results for each element were transformed to sample percentages with respect to the whole sequence and the transformed (arcsine of the square root of proportions) data matrix was analysed by means of PCA (Principal Component Analyses) in order to obtain an ordination of elements (Jongman *et al.*, 1995) for a better evaluation of geochemical similarities among them. Calcium

was excluded from the PCA analysis due to the high amount of calcareous shells that were found along the sequence

A data matrix was constructed (Appendix V), with the number of valves per 10 grams of dry weight of each ostracod species for each core sample (N= 70). Number of valves was log transformed ($\log_{10}$(number of valves+1)) for statigraphical analysis. Adults and juveniles were not considered as separated variables in the matrix. To analyze the changes in composition of ostracod assemblages through the core sequence, a constrained cluster analysis was performed applying the CONISS method and the Edwards Cavalli-Sforza distance (Grimm, 1987).

In addition, we used unconstrained cluster analysis for the study of ostracod species association with the number of valves expressed sample proportions and arco sine square root transformed (arcsin$\sqrt{p}$; *p*: proportion). Two samples with no ostracod remains (at 3 cm and 19.6 cm depth) and six occasional species (*Leptocythere* sp., *Cypria ophtalmica*, *Ilyocypris gibba*, *Herpetocypris* sp., *Limnocythere stationis*, *Potamocypris* sp.) were excluded from the analysis. In this classification analysis, we used the UPGMA (Unweighted Pair Group Method Average) method and the Pearson correlation coefficient distance. The whole transformed data matrix (same as used in CONISS) was analysed by means of Principal Component Analysis (PCA) (Jongman *et al*., 1995) in order to obtain an ordination of samples for a better evaluation of ecological similarities among them.

Correlations between *C. torosa* shell lengths and isotopes ratios ($\delta^{18}O_{VPDB}$ and $\delta^{13}C_{VPDB}$) were analysed using either Pearson (when data was normally distributed) or Spearman (not normally distributed data) correlation techniques.

The equation obtained in the *C. torosa* calibration study by Marco-Barba *et al*., (Chapter I) was used to reconstruct salinity changes. We used the following equation:

$$\log_{10}sal=1.237-0.0129*(Pn*100)+0.0279*\delta^{18}O_{C.torosa}; \quad \text{(Eq. 2)}$$

(where *Pn*: proportion of noded valves), in all the samples were both variables (*Pn* and $\delta^{18}O_{C.torosa}$) were analyzed. The mean and the corresponding standard error values were estimated.

2.7 Radiometric dating

^{210}Pb and ^{137}Cs analyses were performed at St. Croix Watershed Research Station (Minnesota), by D. Engstrom on a twin core that was extracted at the same place only exclusively to carry out these analyses. ^{210}Pb activity was measured for 1-6 x 10^5 s with ion-implanted surface barrier detectors and an Ortec alpha spectroscopy system. Unsupported ^{210}Pb is calculated by subtracting supported activity from the total activity measured at each level; supported ^{210}Pb is estimated from the asymptotic activity at maximum depth (the mean of the lowermost samples in a core). Dates and sedimentation rates are determined according to the c.r.s. (constant rate of supply) model (Appleby and Oldfield, 1978) with confidence intervals calculated by first-order error analysis of counting uncertainty (Binford, 1990). Cesium-137 activity was measured for 1-2 x 10^5 seconds using an EG and G Ortec high-resolution germanium well detector and multichannel analyzer (same instrumentation used for ^{210}Pb above).

Three sediment samples were selected at the mid and the bottom of the core (135, 229 and 233 cm) for the concentration of pollen remains to be used to obtain radiocarbon measurements. These samples were processed at the Palinology laboratory of the Prehistoric Area at the *Universitat Rovira i Virgili* (Tarragona-Spain). Although these samples were checked to ascertain the absence of aquatic remains to avoid hard–water error, they contain organic carbon from aquatic plants, which is not possible to eliminate completely with chemical treatments (Fontes and Gasse, 1991). These samples were dated in Poznan Radiocarbon Laboratory. The radiocarbon measurement (´BP´) was calibrated to calendar years (´cal.BP´) using OxCal v3.10 software (Reimer *et al*., 2004; Bronk Ramsey, 2005) and corrected subtracting 390 years to the calibrated date in accordance to the Mediterranean reservoir effect (Siani *et al*., 2000).

3.-Results

3.1. Radiometric dates

Three radiocarbometric dates were obtained from different pollen concentrates, selected from lacustrine phases with high organic matter content, although one of them, which gave an anomalous result was excluded (Table 3.1). However the other two datations, even being on the corresponding age range gave apparently older ages than those expected when fitting the hydrological and historical events to sediment facies. The reason of that can be explained because pollen concentrates contain left over organic carbon from aquatic plants that give older ages, due to hard-water error. Consequently, we applied the mollusc correcting factor of 390 years for Mediterranean reservoir effect (Siani *et al.*, 2000) to fit these results (Table 3.1), althought we think that for the coastal lagoon conditions the correcting factor should be higher to avoid the influence of hard-water error.

Table 3.1: Radiocarbometric dates for Center core, indicating the material used and the laboratory that carried out the analysis.

Tabla 3.1*: Dataciones radiocarbométricas del sondeo Centro, el material usado para datar y el laboratorio están indicados.*

Core	Depth (cm)	years BP	cal. yr BP (2σ)	Correcting factor (390±85)	Material	Laboratory	lab. Code
C-CENTRO	135	**2655** *±30*	2794±55	2404±55	pollen concentr.	Poznań Radiocarbon Lab.	Poz-19788
	229	**3520** *±35*	3789±100	3399±100	pollen concentr.	Poznań Radiocarbon Lab.	Poz-18865
	233	22260 *±140*	22265±285	21875±285	pollen concentr.	Poznań Radiocarbon Lab.	Poz-18288

Two different models were applied to the ^{210}Pb data (c.r.s and cf:cs models) and we decided to choose the c.r.s. (constant rate of supply) model, which assumes a constant flux of ^{210}Pb to the core site (Figure 3.2, Appendix 3.1) and calculates dates based on the inventory of excess ^{210}Pb in the core. This model was chosen because it fits better with the ^{137}Cs results and yields a good age model until 30 cm, fitting well with historical data on Túria and Júcar floods. However we observed an unreasonably old date of 1838 AD at 41 cm, probably due to the observed additional excess of ^{210}Pb below 41 cm, but it cannot be discerned because dilution processes and high rates of sedimentation diluted Pb concentration.

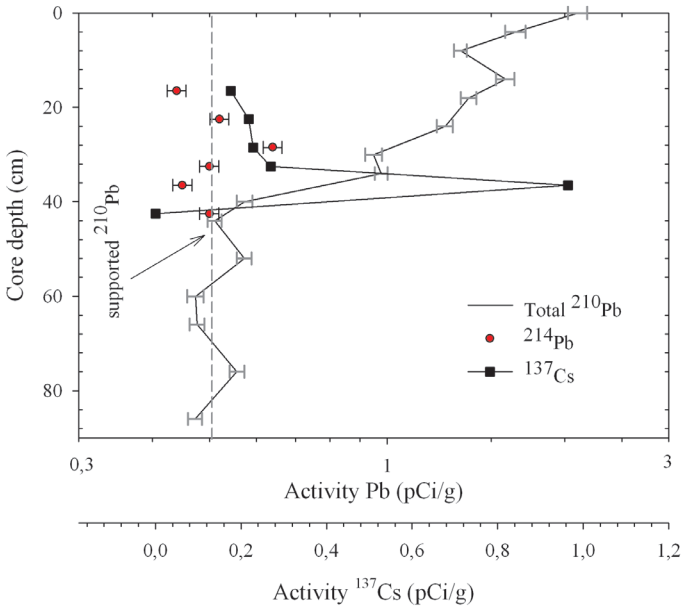

Figure 3.2: Radionuclide activities (pCi/g) of ^{210}Pb (gray straight line), ^{214}Pb (red circles) and ^{137}Cs (black squares) from core Center. Note that supported activity is also placed.

Figura 3.2*: Actividades radionucleótidas de ^{210}Pb (línea gris), ^{214}Pb (círculos rojos) y ^{137}Cs (cuadrados negros) del sondeo Centro. Notar que la* supported activity *se muestra también en el gráfico.*

3.2 Lithological facies, magnetic susceptibility (MS), LOI, carbonates, N:P ratio and XRF results

Two sedimentary units and five lithological facies (A, B, C, D, and E) were identified at the Albufera core Center, after visual inspection (Fig. 3.3); the integration of data on magnetic susceptibility (MS), LOI, percentage of carbonates and X-ray fluorescence (XRF) analysis helps to better define these facies. Unit 1 was identified between the bottom part of the core and 72 cm and unit 2 between 72 cm and the top of the core. Facies A is made up by levels with different thickness varying between 3 cm and 18.5 cm (A1 to A6). This facies is formed by gray sandy silt sediments, carbonate grains and plant fragments. Bioclasts of gastropods and bivalves, mainly *Cerastoderma glaucum* valves, and also foraminifers could be found. Facies B is formed by homogeneous fine silt sediments with gray coloration (Fig. 3.3). It is characterized by very low sand content, plant fibre remains of variable length and microscopic carbon particles. Bioclasts of molluscs and articulated valves were usually absent (facies B2, B5, B6 and B7) or scarce. Seven levels were described at this lithofacies (B1 to B7) with different thickness (between 4 cm and 30 cm). Facies C is formed by homogeneous ochre fine silt sediments, highly enriched on plants remains. Three levels were identified at this lithofacies (C1, C2 and C3) with different thickness, usually narrow layers (between 3 cm and 12 cm). Facies C1 and C3 (between 186 and 189 cm and between 76,5 cm and 85 cm core depth respectively) were composed by plant remains of different lengths, bioclasts of molluscs and articulated valves of *Cerastoderma glaucum*. Facies A5/C2 showed the typical sediment composition of facies C although highly enriched in sands. Facies D is formed by heterogeneous dark gray silt sediments, without plant and mollusc remains. Five levels were identified as lithofacies D1 to D5, always consisting of very thin layers (between 0.5 cm and 3 cm thick). The majority of these levels coincide with MS increases (Fig. 3.4), mainly at D4 and D5, suggesting that this material was reworked, transported into the lake, probably due to flood events. The basis of this assumption comes from to the high content of detritic elements as titanium, potassium or aluminum (Cohen, 2003; Lopez-Buendía *et al*., 1999). D2 and D3 were located immediately above facies C1 and C2; but it was not the case for D4 that was located below facies C3. Facies D5 (between 30 cm and 33 cm core depth) correlated with the highest MS peak accounting for the entire core, suggesting an important flood event. Facies E was characteristic of unit 2, located at the top of the core and composed by fine silts and without or with a very low amount of plant or mollusc remains. Three levels were identified at this

lithofacies (E1, E2 and E3) with different thickness (between 7 cm and 36 cm). The bottom of facies E1 (between 39 and 73 cm depth) marks a big discontinuity in sediments composition between the bottom part of the core (unit 1) and the upper part (unit 2).This facies E1 is composed by soft pink mud sediments with carbonate grains.

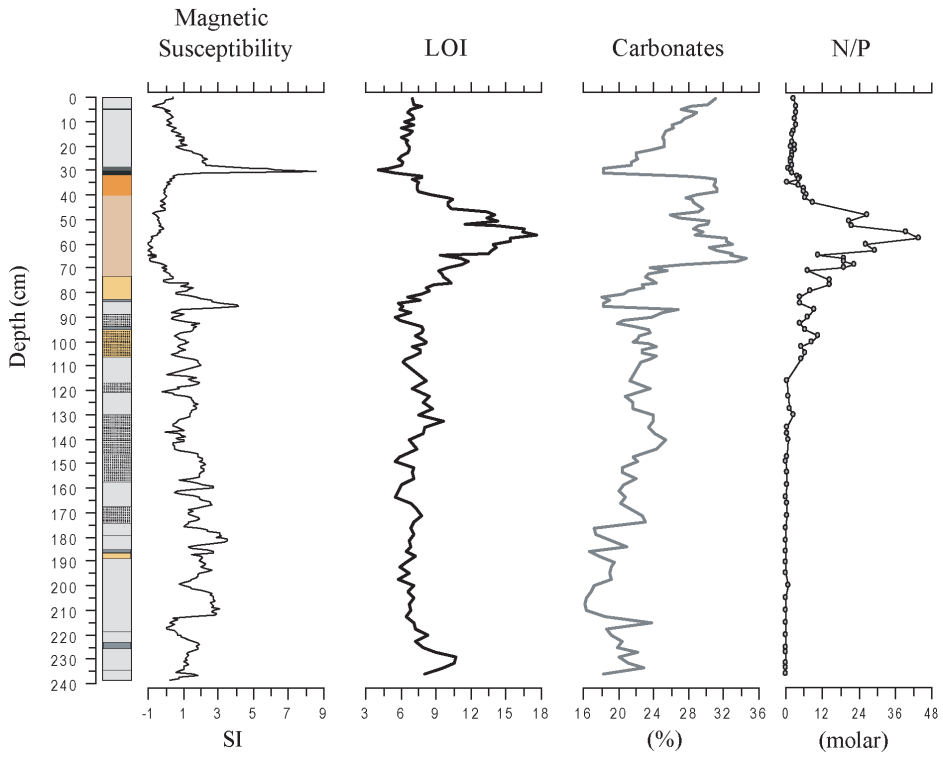

Figure 3.4: Sedimentary Core Center column, showing lithological facies descriptions, MS, LOI (460ºC) , % carbonates (950ºC) and Total Nitrogen/Total Phosphorus ratio.

Figura 3.4*: Columna sedimentaria del sondeo Centro, mostrando las descripciones litológicas de las facies, MS, LOI, % carbonatos y el ratio Nitrógeno total/Fósforo total.*

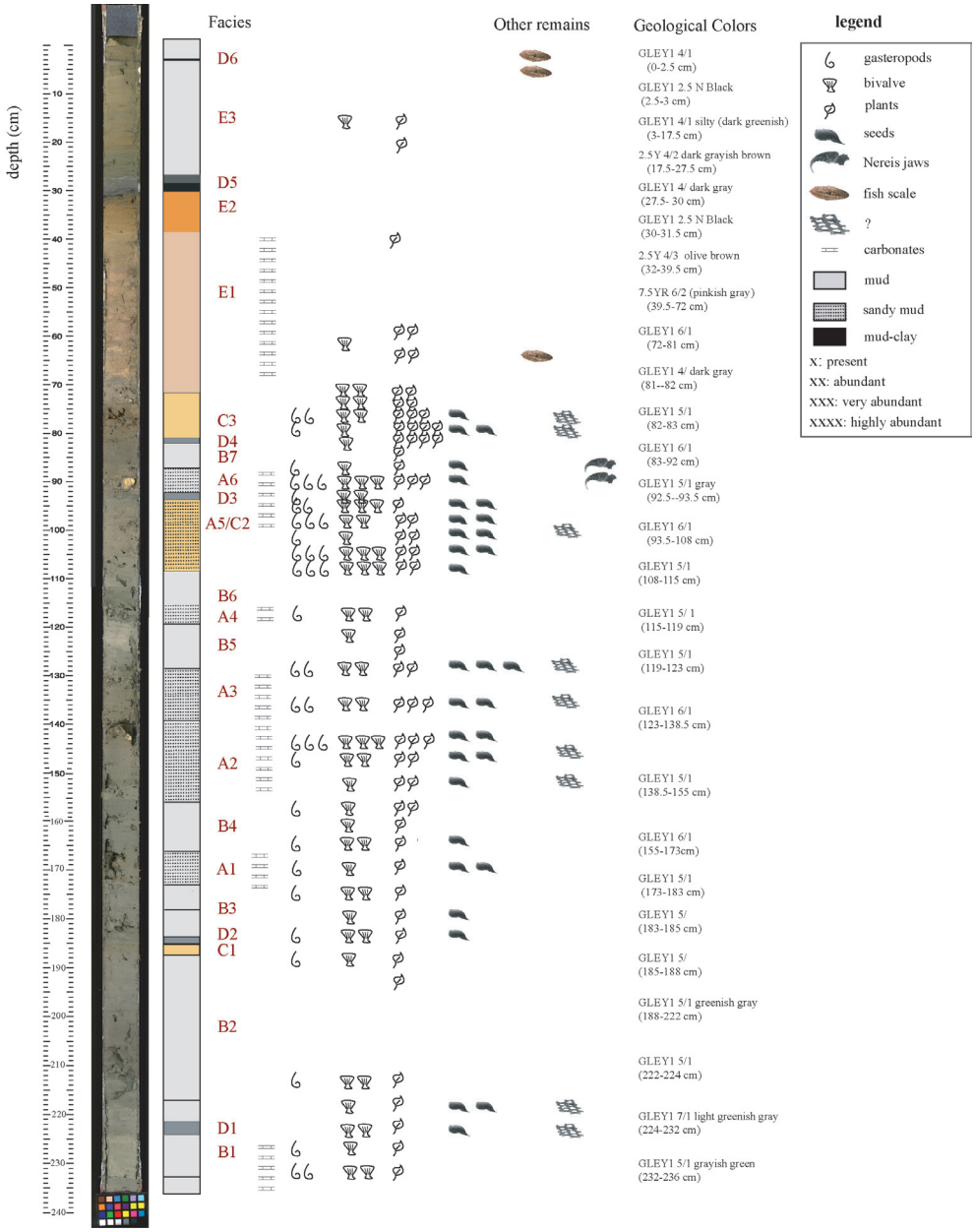

Figure 3.3: Lithological descriptions and visual remains of Core Center. The symbols are shown in different frequencies regarding to the next code: **x**: presence; **xx**: abundant; **xxx**: very abundant; **xxxx**: highly abundant. Interrogation symbol means no identified remains. Munsell soil colors are also indicated with Munsell's codes on the right.

Figura 3.3*: Descripciones litológicas y restos visuales del sondeo Centro. Los simbolos están representados en distintas frecuencias según el siguiente código:* x*: presente;* xx*: abundante;* xxx*: muy abundante;* xxxx*: altamente abundante).El símbolo de interrogación se refiere a restos no identificados. Los códigos de colores establecidos en la tabla de colores geologicos de Munsell se sitúan a la derecha.*

We describe hereafter the main features of each of the two main sedimentary units.Unit 1 is located at the bottom part of the core sequence (between 240 and 73 cm) and comprised most of the previously described facies (A, B, C and D). MS showed variable peaks along this unit, following a possible cyclic pattern being the highest peak observed at 85 cm (Fig. 3.4), which coincides with the lithological facies D4, and with a decrease in LOI and carbonates content. LOI showed small changes with a mean value of 7% along the unit and generally correlated with the percentage of carbonates. Carbonate content showed wider variations, increasing towards the top of this unit, except between 215 cm and 200 cm depth where a marked decrease was observed. N:P ratio (Fig. 3.4) and TN and TP separately (Fig. 3.16) showed relatively low values and small changes along the unit, except at the top (between 105 cm and 75 cm) where a slight increase was observed for TN.

Unit 2 encompasses the upper part of Albufera lake sequence (between 73 cm and 0 cm). This unit is composed by facies D and E. The coincidence of low values of MS, high percentage of carbonates and the highest LOI and N:P peaks at the mid part of facies E1 is remarkable. The observed high percentage of carbonates was relatively constant until the very top of facies E2 where it decreased markedly, coinciding with the highest MS peak observed along the core. LOI and N:P ratio decreased following the same pattern from the mid part of facies E1 to E2. TN followed the same trend as observed for the N:P ratio, however TP increased from 50 cm towards the top of the sequence. Facies E3 and D6 are located at the very top of the core sequence coinciding with a MS decrease, a carbonates increase and slightly increasing LOI.

The high-resolution record of the most significant geochemical elements obtained by the XRF analysis is plotted in figure 3.5. A marked pattern was observed for Cl, an element that remained above its mean core value from the bottom to 118 cm, suggesting sea water influence; since 118 cm to the top of the core showed values below the general core mean. Ti, Fe and K were highly positively correlated with MS ($r>0.7$; $p<0.01$) along the core, and negatively correlated with LOI and the proportion of carbonates ($r>-0.4$; $p<0.01$ and $r>-0.7$; $p<0.01$ respectively) suggesting that these elements, due to its detritic character, could be considered as allocthonous and probably were mostly deposited into the lake by flood events. A reverse pattern in Sr is detected along the whole record (Fig. 3.5). Sr was positively (but weekly) correlated with LOI and carbonates ($r=0.3$; $p<0.01$ and $r=0.38$; $p<0.01$ respectively) and negatively with the Ti, Fe and K ($p<0.01$).

Figure 3.5: Diagram of geochemical XRF Fluorescence data from core Center as a function of depth. The samples scores 1, 2 and 3 from PCA sample results are also plotted.

Figura 3.5: *Diagrama de los elementos geoquímicos obtenidos a partir de la técnica de fluorescencia-XRF del sondeo Centro en función de la profundidad. Las puntuaciones para las muestras obtenidas de los resultados del PCA para las muestras están situadas en el gráfico.*

Principal Component Analysis (PCA) was performed on the transformed (%) XRF geochemical data. The results (Fig. 3.6) confirm the above mentioned opposite trends of two groups of elements, one comprising those of detrital origin and characteristic of high erosive periods and the other more characteristic of autogenic stable periods. The analysis confirms as well the salinity variation along the sequence. The species with higher weight on Axis 1 are Ti, Fe and K (group 1: Ti, Fe, K, Co, Rb, Si, S and Al) on the positive part and Sr (group 2: Sr, Zr, Ni, Cr, Pb, Ba and Ar) on the negative one (Fig. 3.6). Axes 2 did not contribute highly to the total amount of variance (3.3 %) but an interesting pattern was observed. The species with higher weight on Axis 2 were Zn and Cu (group 3) on the positive part and Cl and As (group 4) on the negative one (Fig. 3.6). Due to the proximity of the lake to the sea, Cl and As variations indicate salinity variations and sea water influence along the core. Cl was positively correlated with MS ($r=0.59$; $p<0.01$) and negatively with the proportion of carbonates ($r=-0.69$; $p<0.01$), suggesting that sea water played an important role on the geochemical composition of the lake sediments at the bottom half of the core, due to sea water inputs. In addition, carbonates precipitation probably took place when sea water had less influence on the lake water composition (at the top of the core).

Copper (Cu) (and other members of group 3), positively correlated with elements of group 2, mostly with Pb and Cr ($r\geq0.6$; $p<0.01$). Zn was negatively correlated with LOI ($r=-0.7$; $p<0.01$). These elements (usually related to chemical industrial activities) are more important at the very top of the core. The weak correlation between Sr and Cu and Zn probably indicates that these elements came from different sources as for example direct spills into the Lake (see discussion below). Lead showed constant values along the bottom part of the core until 73 cm where we noted a sharp increase coinciding and correlating with increasing carbonates content ($r=0.48$; $p<0.01$).

The amount of Ca could be related to many factors beside the bioclasts content, such as the amount of calcium carbonates accumulated in the sediments, either coming from surrounding limestone, or from endogenic processes in the lake, mainly due to high photosynthetic rates. Only at the very top of the core, the variation of the proportion of calcium carbonates could be related with endogenic processes in the lake, due to the scarce number of carbonate shells that were found at this part. At the top 50 cm, the increase in Ca could be associated to a high primary production period. However, the presence of many layers with high amounts of carbonated shells prevents any further detailed analysis at the bottom of the core.

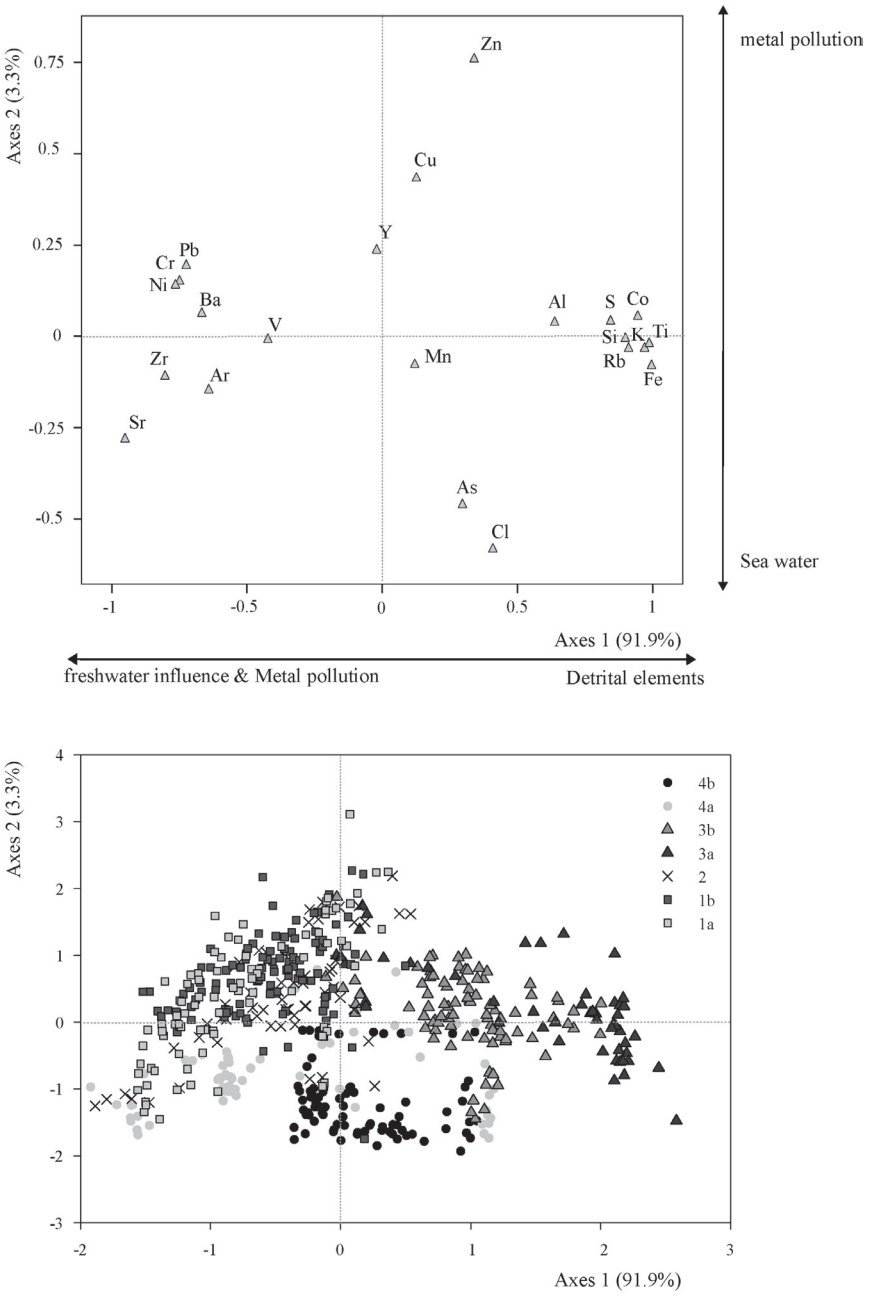

Figure 3.6: Principal component analysis (PCA) of XRF-Ray Fluorescence transformed data (%s) and excluding Ca for core Center. **A**) Elements species are positioned on the first two PCA factors. **B**) Samples labeled by their depth in the core are ordered in the first two PCA factors space.

Figura 3.6*: Análisis de Componentes Principales (PCA) de los datos transformados (%) del análisis XRF y excluyendo Ca para el sondeo Centro. a) Elementos geoquímicos posicionados en los dos primeros ejes del PCA. b) Las muestras ordenadas por profundidad ordenadas en los dos primeros ejes del PCA.*

3.3 Ostracod analysis and relationships with lithological facies

We identified 100952 ostracod valves, representing 18 species of ostracods from 15 genera (Appendix 1). SEM images of the 18 taxa are presented in plates 3.1, 3.2, 3.3. Due to the low number of valves found from four of these genera they have been only identified to genus level. The states of valve preservation (SP) varied along the core and between species.

We only took into account the valves with states of preservation A+B (albeit valves with SP type C were very scarce) for the calculation of diversity indexes and for carrying out multivariate statistical analyses. In the Albufera core Center sequence, ostracods were absent from two of the 70 samples (at the top of the core), and 6 samples had only one species present. The highest number of valves (up to 9631 per 10gdw^{-1}) was found at 88.6 cm depth with five species. The highest number of species (up to 9) was found in samples located at the half top of the core. However, almost half of the samples, mainly those located at the bottom and the uppermost zone of the core, contained only 2 or 3 species. In spite of the low species richness, the samples located at the bottom of the core had higher number of valves than those at the top.

Cyprideis torosa together with *Loxoconcha elliptica* and *Xestoleberis nitida* were the most abundant species along the core (Fig. 3.7). In addition, *Aurila arborescens*, *Candona angulata* and *Darwinula stevensoni* were also abundant, especially the first one in the lower part of the sequence. *C. angulata* and *D. stevensoni* were abundant in the upper part and *Paralimnocythere psammophila*, *Cypridopsis vidua* and *Limnocythere innopinata* appeared with lower abundances. On the other hand, *Leptocythere* sp., *Cytherois* cf *stephanidesi*, *Limnocythere stationis*, *Potamocypris* sp., *Ilyocypris gibba*,

Herpetocypris sp. and *Cypria ophtalmica* were very scarce.

The previously described lithofacies (A, B, C, D and E) were clearly distinguished in this sequence (Fig. 3.3). The associated ostracod fauna in each facies are described below. Facies A: The ostracod fauna at facies A1 (between 167 cm and 174 cm) presented high abundances, mainly composed by the euryhaline ostracod *Cyprideis torosa*, the brackish species *Loxoconcha elliptica* and the marine species *Aurila arborescens* and *Loxoconcha rhomboidea*. The presence of the brackish-water ostracod *Xestoleberis nitida* is also remarkable.

The highest ostracod abundances were found at facies A2 and A3 (between 156 and 139 cm and 139 cm and 127 cm respectively), at the bottom half of the core. These facies A2 and A3, as well as facies A5/C2 (between 98 cm and 109 cm) showed the same ostracod species mentioned at facies A1. However, A3 presented the highest abundances for the marine species through the entire core. At facies A4 (between 114 cm and 118 cm) a rapid decrease of all ostracod abundances is observed. At Facies A6 (between 91 cm and 96 cm), very high abundances of mollusc bioclasts and plant remains were found as well as a high number of articulated bivalves and entire gastropods. We observed in this facies the highest abundances for the brackish ostracods *L. elliptica* and *X. nitida* through the entire core. *C. torosa* and *A. arborescens* also presented high abundances and a small proportion of the brackish *Cytherois* cf. *stephanidesi* was found.

Facies B. B1, located at the bottom of the core, was composed and dominated by *C. torosa* and *L. elliptica* remains. Facies B2 presented very low ostracod abundances and was dominated by the last mentioned species, however in some samples only *C. torosa* was present. Facies B3, B4, B5, B6 and B7 were located alternately between facies A1 and A6. *C. torosa* and *L. elliptica* were also the dominant species at facies B, and the marine species that were highly abundant at facies A were present in very low abundances too.

At facies C, *C. torosa* and *X. nitida*, followed by *L. elliptica*, dominated the ostracods association, together with the scattered presence of *A. arborescens*. At facies D, the ostracod fauna found was mainly the same as the observed in nearby facies

Facies E was characterized by freshwater species such as *Candona angulata*, *Darwinula stevensoni*, *Paralimnocythere psammophila*, *Cypridopsis vidua* and *Limnocythere inopinata*, which dominated in the middle part of this facies. It should also be noticed the presence of other freshwater species such as *Limnocythere stationis*, *Potamocypris* sp. *Ilyocypris gibba*, *Cypria ophtalmica* and *Herpetocypris* sp. Nevertheless, *C. torosa* dominated at the top and bottom of this facies.

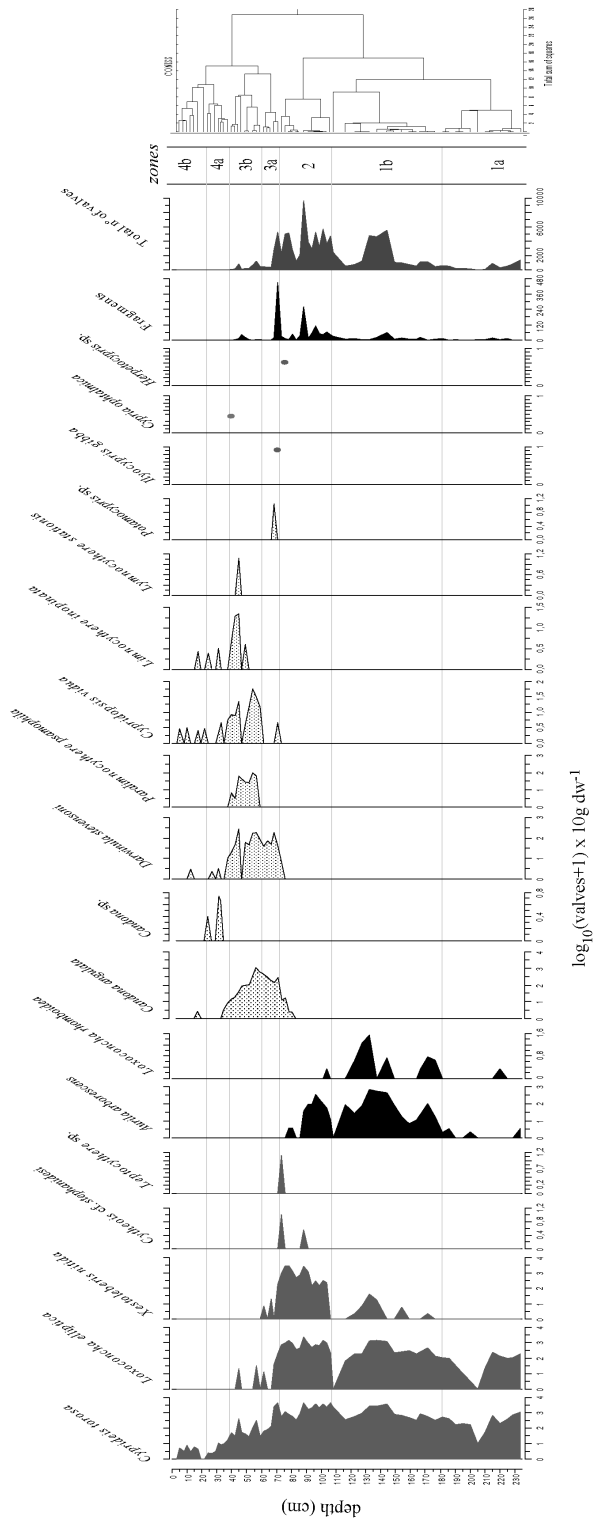

Figure 3.7: Diagram of ostracod abundances as a function of depth in core Center. The total number of valves (states A+B) as well the number of valve fragments are shown in the right-hand columns, all data expressed in valves per 10g dry weight in log scale. The established zones by the constrained cluster analysis (CONISS) are shown in the adjacent dendogram.

Figura 3.7: *Diagrama de las abundancias de ostrácodos en función de la profundidad en el sondeo Centro. El número total de valvas (EP A+B) y el número de fragmentos se muestran en las columnas de la derecha, todos los datos se expresan por 10g/dw en escala logarítmica. Las zonas establecidas por el análisis de agrupación constreñido por profundidad (CONISS) están representadas en el dendograma adyacente.*

3.3.1 Cluster analysis and PCA

Application of a statigraphically-constrained cluster analysis to the ostracod assemblages (Fig. 3.7) allowed the differentiation of 4 main statigraphical zones that could be further subdivided onto 7 different subzones. The first zone (zone 1) covered from 234 to 181 cm depth and could be further subdivided in two more subzones: subzone 1a and subzone 1b. Subzone 1a (from 234 to 181 cm) corresponds mainly to facies type B, although very thin layers of facies C and D were also present. This subzone was mostly dominated by the euryhaline *C. torosa* and the brackish species *L. elliptica*. It should be remarked the scattered, scarce, and not coincident presence of *Aurila arborescens* and *Loxoconcha rhomboidea*. The abundances of ostracods remains (total number of valves) decreased drastically at the mid part of this subzone.

Subzone 1b covered from 176 to 108 cm depth. This subzone presented higher ostracod abundances and higher number of ostracod species than the previous subzone. We recorded a rapid increase of the marine ostracods *A. arborescens* and *L. rhomboidea* at the bottom half of this subzone, which immediately diminished drastically their abundances towards the mid part and disappeared completely in the case of *L. rhomboidea*. Afterwards, both species increased again in the upper half of the subzone and reached the highest abundances for the entire core. The scattered presence of some valves of *X. nitida* in this subzone should also be noticed, and *C. torosa* and *L. elliptica* were also very abundant. Moreover, it is remarkable that the total number of ostracod valves followed the same trend as it was observed for the most abundant species *C. torosa*, *L. elliptica* and *A. arborescens*. The last two species decreased drastically towards the top of the subzone until they disappeared. It should also be noted that *A. arborescens* had a peak prior to disappearance at the top of this subzone and that at the top limit of the subzone (108 cm) there is a discontinuity where *C. torosa* was the only species present, which showed an slight increase, altogether with the total number of ostracod remains, both entire valves and fragments.

The second zone (zone 2) covered from 106 to 74 cm depth. It is characterized by the increase of abundance of *X. nitida*, which showed several peaks following the same profile than *L. elliptica* and *C. torosa* abundances. *A. arborescens* abundances were high at the bottom half, but decreased drastically from the mid part, disappearing at the top sequence. A few valves of two species, with affinity for marine waters, rarely occurring in Albufera cores, appeareing at the top of this subzone: *Cytherois* cf *stephanidesi*, and *Leptocythere* sp. The total

number of ostracod valves and fragments followed similar trends until the mid part of this zone, reaching at this depth (89 cm) the highest number of ostracod valves in the entire core.

Zone 3 (71-40 cm) was subdivided in two subzones. Subzone 3a (from 71 to 61 cm) was characterized by the dominance of species most typical of freshwaters, particularly *Candona angulata*, *Darwinula stevensoni* and *Paralimnocythere psammophila* whereas the brackish waters species *C. torosa*, *L. elliptica* and *X. nitida* showed a rapid fall. Another unidentified *Candona* species occurred in much lower numbers. Other inland water species such as *Cypridopsis vidua*, *Potamocypris* sp. and *Ilyocypris gibba* were also present in lower numbers. The total number of ostracod valves and fragments followed the same trend and the ostracod fragments reached the highest number for the whole sequence in this subzone. At subzone 3b (from 59 to 40 cm), *C. angulata* showed the highest peak at the bottom half of this subzone accounting for the whole sequence, but decreased towards the top. *D. stevensoni* was also very abundant and its pattern of change was similar to *C. angulata* but delaying the last reduction in number of remains with respect to *C. angulata*. *Paralimnocythere psammophila*, *Cypridopsis vidua*, *Limnocythere inopinata* and *Limnocythere stationis* were characteristic of this subzone, especially the first one which was very abundant and exclusive of this part of the core. We want to indicate also the presence of the freshwater species *Cypria ophtalmica* at the top of this subzone that corresponded to the only occurrence along the core.

Subzone 4 covered from 37 to 0 cm. In this subzone ostracod valves were very scarce and no fragments were found. It was subdivided in two subzones (4a and 4b). Subzone 4a (from 37 to 24 cm) and presented very low ostracod abundances that decreased towards the top of the subzone. *C. torosa*, suffered a drastic decrease in abundance, but it still was the most abundant species and followed the same trend as the total number of ostracod valves at this subzone. *Candona angulata*, *D. stevensoni*, and *C. vidua* also decreased and even disappeared in the case of the first one, showing some isolated peaks at the very top of this subzone for the other two species. *L. inopinata* presented some isolated peaks at the bottom half and at the top of this subzone. Subzone 4b (from 22 cm to the top) was strongly depleted of ostracod valves and presented the lowest densities of ostracod valves and fragments along the core. However, *C. torosa* was still being present in most of the samples. A few valves of *Candona* sp. *C. vidua*, *D. stevensoni*, and *L. inopinata* were detected in this subzone.

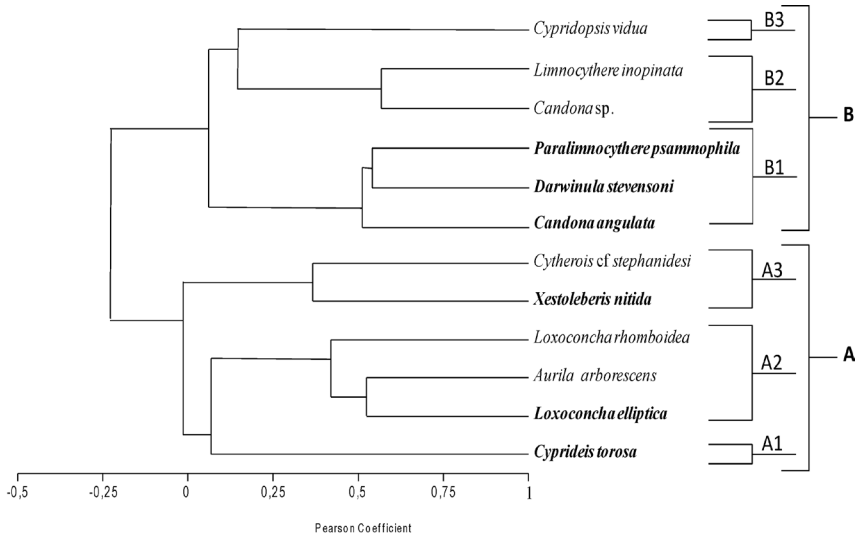

Figure 3.8: Unconstrained cluster analysis of species found in core Center, applied for transformed data (arcsin√*p*) using UPGMA method and Pearson coefficient distance. The most frequent species are typed in bold italic; the main groups are also indicated.

Figure 3.8*: Análisis de agrupación sin constreñir por profundidad, aplicado sobre los datos transformados (*arcsin√*p), usando el método UPGMA y el coeficiente de correlación de Pearson. Las especies más frecuentes están subrayadas en negro, y los principales grupos están indicados.*

Unconstrained cluster analysis applied to the ostracod abundances (Fig. 3.8), resulted in two main assemblages, A and B, which could be divided in three further groups each. Group A1 included the euryhaline species *C. torosa*, separated from the other two groups of brackish water species (A2 and A3) probably due to its wider salinity tolerance (see discussion below). A2 was composed by the phytophylous brackish-marine species *L. elliptica* and the littoral and shallow sublittoral marine species *A. arborescens* and *L. rhomboidea*. A3 included the brackish and phytophylous species *Xestoleberis nitida* and *Cytherois* cf. *stephanidesi*.

Assemblage B included the freshwater species and was subdivided in three groups (B1, B2 and B3). B1 was composed by *C. angulata*, *D. stevensoni* and *P. psammophila*. B2 included the freshwater species *Candona* sp. and *L. inopinata*. These species were probably more separated from this subgroup because its low occurrence along the core, suggesting that probably this material was reworking. On the other hand, subgroup B3 included only the freshwater species *C. vidua*, probably due to its wide tolerance limits to many environmental variables that give to this species its condition of eurioic species.

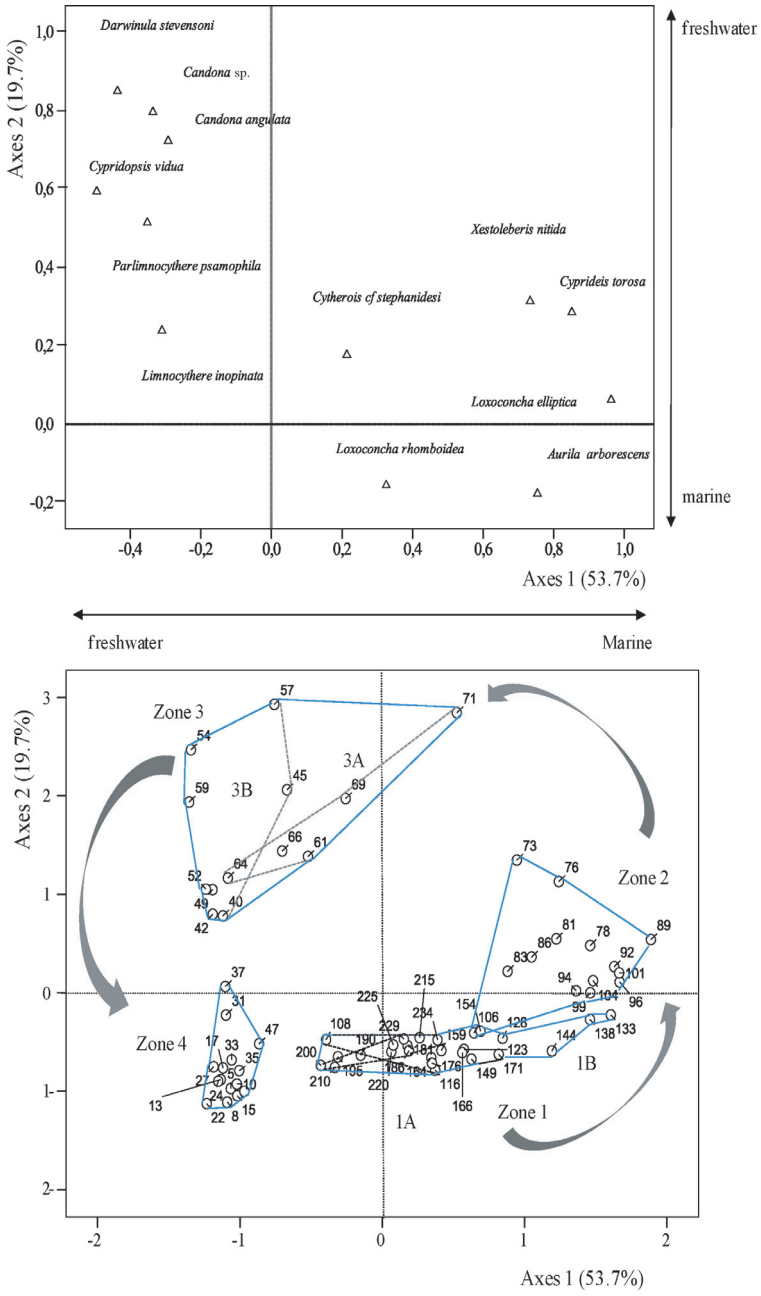

Figure 3.9: Principal component analysis (PCA) of ostracod samples and species for core Center. **a**) Ostracod species are positioned on the first two PCA factors. **b**) Samples labeled by their depth in the core are ordered on the first two PCA factors space and the CONISS established zones and subzones are marked with polygons. The arrows indicate the chronological zone evolution along the core.

Figure 3.9*: Análisis de componentes principales (PCA).* a*) PCA para las especies de ostrácodos.* b*) PCA para las muestras representadas por su profundidad (cm). Los grupos establecidos en el CONISS están marcados con polígonos. Las flechas indican la evolución cronológica de las zonas a lo largo del sondeo.*

The PCA results are shown in figure 3.9. The first factor (F1) accounted for 53.7% of the total variance and the second (F2) for 19.7%. The first axis can be regarded as a salinity gradient. The second axis separates mainly the samples rich in freshwater species of zone 3 from the rest of the core. The species with higher weight on Axis 1 are *L. elliptica*, *C. torosa*, *A. arborescens* and *X. nitida* on the positive part and *C. vidua* and *D. stevensoni* on the negative one. *D. stevensoni* and *C. angulata* are the most important species for Axis 2 on the positive part and *A. arborescens* and *L. rhomboidea* on the negative one (Fig. 3.9).

Samples were grouped on the PCA graph according to the zones obtained with the constrained cluster analysis. Axis 1 separated zones 1 and 2 on the positive part, which corresponded to the brackish and brackish-marine assemblages, from zones 3 and 4 on the negative one, which corresponded to the freshwater assemblages. Zone 2 is ordered on the positive part of Axis 1 and mostly on the positive part of Axis 2. Axis 2 separated mainly zone 3 from the other zones and especially from zone 4. The main reason of the different ordination of these two zones (3 and 4) fall on the reduced number of ostracod remains and species richness found at zone 4. However, we observed one isolated sample from zone 4 located at the positive part of axis 2 (37 cm) which correspond with the sample with the highest abundances of ostracods remains accounting for all the samples of this zone.

3.3.2 Ostracod abundances and diversity indices

The total amount of ostracod valves varied along the core and between zones (Fig. 3.10). Subzone 1a presented high abundances at the bottom of the subzone, decreasing to the mid part and increasing upwards. Ostracod abundances increased towards the mid part of subzone 1b showing higher values than those observed at the previous subzone. Subzone 2 showed the highest ostracod abundances for the whole core. At the mid part of subzone 3a ostracod abundances showed a marked fall that would continue steadily with this trend until the top of the core. Thus, subzones 4a and 4b presented the lowest abundances, but only two samples (located at the bottom and the top of subzone 4b) were barren.

Diversity indices (Fig. 3.10) were generally low; the minimum values corresponded to zones of changing conditions where only one or two species were present. We should emphasize that the highest diversities (2.28 bits/ind was the maximum value) were not located where the highest number of valves were counted, but in subzone 3b, where the species richness was highest.

Diversity (H) and evenness (E) were moderately high at the bottom of subzone 1a; but showed a drastic fall at the mid part of this subzone where the number of ostracod valves decreased too. These values recovered until similar or slightly higher values in subzone 1b. Diversity did not varied along subzone 1b, however a drastic fall was observed at the last sample of this subzone, because only one species (*C. torosa*) was found at this particular sample. The D_o index was close to 0 and did not varied along subzones 1a and 1b suggesting that there were not ostracod assemblages fluctuations with respect to the average core state in these subzones. H and E showed two steps of change along zone 2. The samples located at the bottom of this zone showed similar values to those reported at subzone 1b,and D_o was close to 0, suggesting that they presented ostracod assemblages close to the average state. However, the top half of zone 2 was characterized by higher values of H, E, and D_o, indicating that the ostracod community changed from the average state to a more complex community. A drop of the values of these indexes indicated changing conditions between zone 2 and subzone 3a. Even though the number of species increased, diversity indices showed a drastic fall at the very bottom of subzone 3a, probably because *C. torosa* valves increased significantly. At subzone 3b, diversity indices showed the highest values of the entire core. However, abrupt diversity changes and high D_o displacement from the average stage was observed at the mid part of

the subzone, suggesting changing environmental conditions. Abrupt shifts in diversity indices indicated fluctuating conditions along subzones 4a and 4b. However, D_o presented generally values close to 0, due to the impoverished ostracod community in recent years, dominated by *C. torosa* remains.

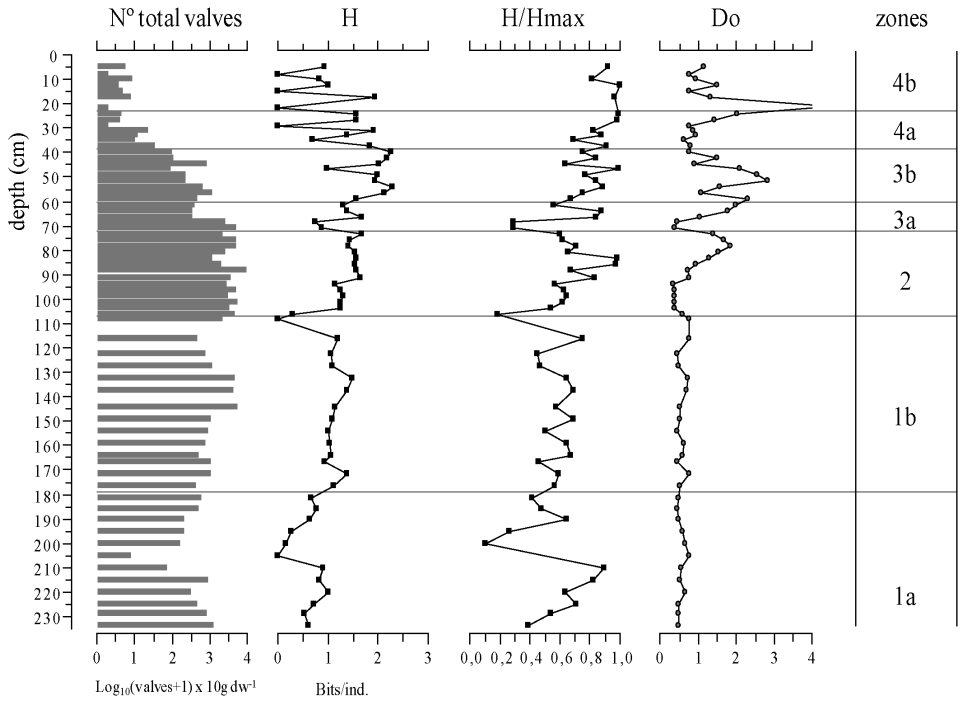

Figure 3.10: Diagram of total abundances of ostracod valves (log(x+1)) for core Center, together with community indices: Shannon diversity index *H*, evenness index E=H/Hmax, Dubois fluctuation index D_o.

Figura 3.10: *Diagrama de abundancias totales de los ostrácodos del sondeo Centro (expresados en 10g de sedimento seco), junto con los índices de las comunidades: índice de diversidad de Shannon H, índice de equitabilidad H/Hmax, índice de fluctuación de Dubois D_o. El número total de valvas esta expresado como log_{10} (número de valvas+1).*

3.3.3 C. torosa ecophenotypic responses

A total of 2110 *C. torosa* valves (994 females and 1116 males) were measured from 57 subsamples (Fig. 3.11; Appendix 3.3). LOESS regression was applied separately to female and male size changes through the core and showed that both followed the same variations of carapace length with depth in all the biozones; the greater length was observed for zone 3.

All counted valves of *C. torosa* were checked for the presence of nodes (Fig. 3.11). The valves found at the bottom of the core, subzone 1a and 1b were smooth. Zone 2 showed smooth valves in all the samples except in one sample near the top of this subzone where a low proportion of noded valves was observed. At Subzone 3a the percentages of noded valves increased rapidly towards the top of this subzone; however, these percentages decreased at the boundary with the next subzone. At Subzone 3b the percentage of noded valves increased again towards the center of the subzone and decreased at its top, following a similar trend as in the previous subzone and reaching the highest percentages of *C. torosa* noded individuals for the entire core. At Zone 4 the percentage of noded *C. torosa* was never higher than 20%, but these values should be interpreted cautiously due to the low values of ostracod abundances. As a general trend, the percentages of *C. torosa* noded forms increased at subzone 3a and 3b, suggesting an important salinity decrease; furthermore, smooth valves of some samples in zone 3 and most samples of zone 4 should be interpreted as transported and reworked remains.

3.3.4. C. torosa population structure

Sex-ratio (M:F) of *C. torosa* in the samples of subzone 1a showed values below one, (Fig. 3.12), but at the mid part of subzone 1b some samples presented values displaced to males dominance. Zone 2 was highly variable with respect to M:F sex-ratio , which was highly displaced in favor to males in most of the zone, except at the bottom and top, where it was closer to one. These variations were probably affected by the possible reworked events which affected the number of *C. torosa* valves (see below juvenile/adults ratio). Subzone 3a, 3b, 4a and 4b (Fig. 3.12) showed highly variable sex ratios, probably due to the low number of ostracod valves (Fig. 3.7). Sex ratio was positively correlated with the total number of *C. torosa* valves ($r=0.8$; $p<0.01$), with juveniles/adults ratio ($r=0.69$; $p<0.01$), valve/carapace ratio ($r=0.65$; $p<0.01$) and FR ($r=0.27$; $p<0.05$) when the entire core was considered. However, when these data was analyzed separately by biozones, no significant correlations were found.

Juveniles/adults ratio (J/A ratio). The J/A ratio at core Center (Fig. 3.12) showed low values at subzone 1a and still low but higher at 1b suggesting only slightly higher proportions of juveniles with respect to adults. Zone 2 showed high values of this ratio, although very variable. Subzone 3a showed high values in its mid part but in subzone 3b the ratio was low at the bottom and increased towards the top. At subzones 4a and 4b no adult valves were found. J/A ratio was

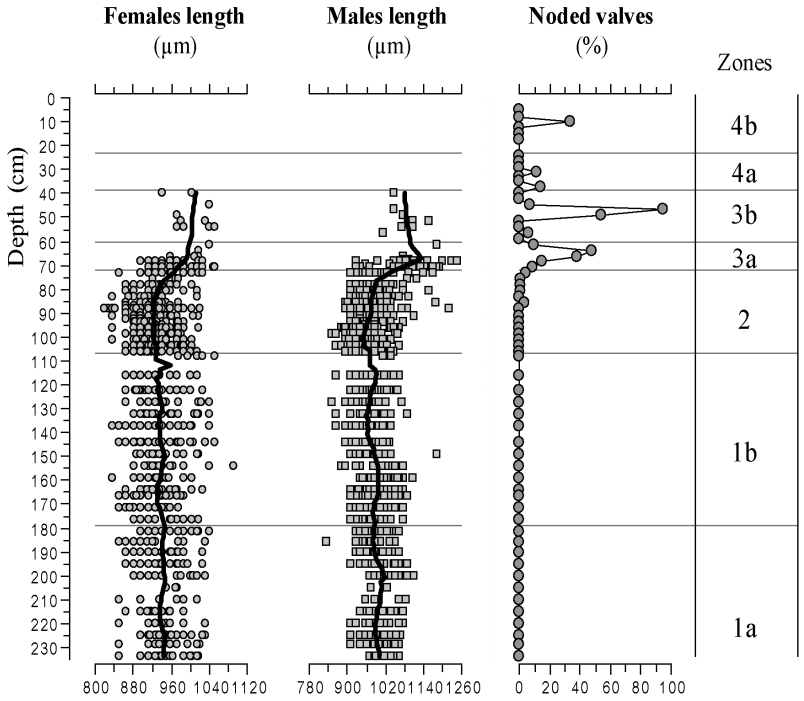

Figure 3.11: *C. torosa* measured lengths for females and males and percentages of noded *C. torosa* valves. LOESS regressions were applied for length values (using average scale of 10 for females and for males).

Figura 3.11*: Medidas de longitudes de* C. torosa *hembras y machos y el porcentaje de valvas nodadas de* C. torosa. *La regresión LOESS se aplico a los datos de longitudes (usando un factor de escala de 10 para ambos sexos).*

positively correlated with total number of valves ($r=0.69$; $p<0.01$), FR ($r=0.69$; $p<0.01$) and valve/carapace ratio ($r=0.67$; $p<0.01$) taking into account the entire core. When the analysis was applied separately for each biozone, we found a strong positive correlation with valves/carapace ratio ($r=0.78$; $p<0.01$) at zone 2.

Valve/carapace ratio (VCR ratio). Variations in VCR ratio are shown in Fig. 3.12. We observed a peak of VRC ratio about the middle of subzone 1a, thus suggesting possible rework events. Nevertheless, the ratio decreased at the very top of this subzone. Subzone 1b showed very low values, except for two peaks, one at the bottom half and the other at the limit with zone 2. The later was

the highest peak for this ratio in the entire core. Zone 2 showed relatively low ratios with some variations. We observed very few samples with carapaces at subzones 3a and 3b and the samples from the zone 4 did not presented carapaces, suggesting changing depositional conditions along these subzones. VCR ratio was positively correlated with sex ratio ($r=0.65$; $p<0.01$) and juvenile/adult ratio ($r=0.67$; $p<0.01$) accounting for the entire sequence. Moreover this variable was positively correlated with juveniles/adults ratio ($r=0.78$; $p<0.01$) at zone 2 and negatively with total number of valves ($r=-0.7$; $p<0.05$) at subzone 1a.

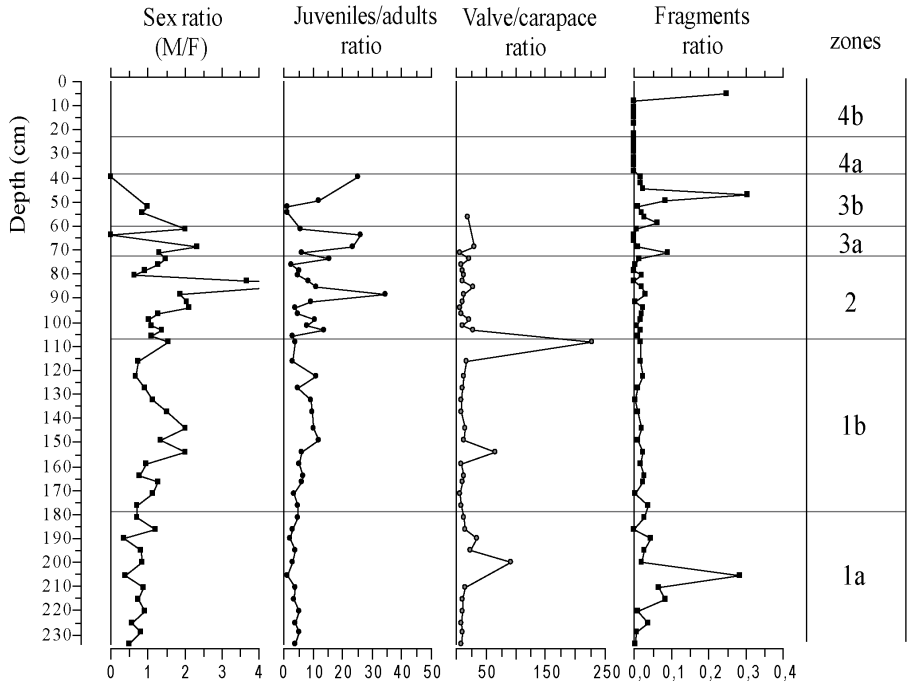

Figure 3.12: Fossil population structure of the ostracod *C. torosa*, and FR (fragments ratio) for the whole ostracod paleoassemblage. Ostracod grouped zones are located on the right column. There were not found adults valves or carapaces in zone 4, for that reason the relevant ratios were not calculated at this zone.

Figura 3.12*: Estructura de la población fósil de* C. torosa *y el FR (ratio de fragmentos) para todo el paleoensamblaje de ostrácodos. Las zonas agrupadas por CONISS para los ostrácodos se sitúan en la columna de la derecha. No se encontraron valvas de adultos o caparazones de adultos en la zona 4, consecuentemente no se calcularon los ratios relevantes.*

Fragment ratio (FR= (fragments+EPtypeC)/nºTotal valves+fragments). FR at subzone 1a increased towards the mid part and immediately decreased to the top of this subzone. Subzone 1b, zone 2 and subzone 3a showed very low ratio values, except one isolated low peak at the bottom of subzone 3a. Subzone 3b presented also low values; however, we observed the highest peak at the mid part of this subzone accounting for the entire sequence. FR remained low at subzone 4a and 4b except in the top sample. FR was correlated with sex ratio ($r=0.27$; $p<0.05$) and juvenile/adults ratio ($r=0.39$; $p<0.01$), taken into account the entire core, as was mentioned above. When subzones were separately analyzed, FR was negatively correlated with total number of valves ($r=-0.59$; $p<0.01$) for subzone 1b and positively ($r=0.97$; $p<0.01$) for subzone 3a.

3.4 Isotope results

The isotope values for *C. torosa* shells ranged between -10.06‰ and 2.33‰ (mean value -5.45‰±1.61) for $\delta^{13}C$ and between -4.98‰ and 3.29‰ (mean value of -0.18‰±1.71) for $\delta^{18}O$ along the core (Fig. 3.13; Table 3.2). For the entire sequence, these two variables were not correlated, however, $\delta^{13}C$ exhibited a weak positive correlation with valve lengths of *C. torosa* females ($r=0.28$; $p<0.01$) and $\delta^{18}O$ was negatively correlated with valve lengths for both sexes ($r=-0.2$; $p<0.05$ for females and $r=-0.33$; $p<0.01$ for males).

Table 3.2: Minimum, maximum and mean values for isotopical variables ($\delta^{13}C_{VPDB}$ and $\delta^{18}O_{VPDB}$) according to ostracod bio-zones.

Tabla 3.2*: Valores mínimos, máximos y medios de las variables isotópicas ($\delta^{13}C_{VPDB}$ and $\delta^{18}O_{VPDB}$) en relación con las biozonas de ostrácodos.*

	$\delta^{13}C$ (‰)			$\delta^{18}O$ (‰)		
biozones	**min**	MEAN±*SD*	**max**	**min**	MEAN±*SD*	**max**
4a	-7,18	-6,71±*0,67*	-6,23	-2,92	-2,75±*0,24*	-2,58
3b	-9,17	-4,72±*1,72*	-0,06	-4,98	-2,63±*0,91*	0,31
3a	-10,06	-4,88±*2,67*	2,33	-4,68	-1,41±*1,84*	2,21
2	-8,12	-5,28±*1,54*	0,53	-3,24	1,06±*1,16*	3,19
1b	-8,65	-5,85±*1,18*	-2,57	-1,98	0,82±*0,92*	3,16
1a	-9,04	-5,85±*1,25*	-3,22	-1,26	0,63±*0,95*	3,29

Both $\delta^{13}C$ and $\delta^{18}O$ showed high variability among individual valves at the bottom and at the top of subzone 1a and low variability at the mid part of this subzone. Both variables were positively correlated at this subzone ($r=0.34$; $p<0.01$). A high variability, as that observed at the bottom of the previous subzone, was again observed for $\delta^{18}O$ at the bottom of subzone 1b, however, $\delta^{18}O$ and its standard deviation (SD) decreased upwards within the subzone. On the other hand, $\delta^{13}C$ showed a slight increase at the bottom but then (contrarily to $\delta^{18}O$) decreased softly to the mid part of this subzone and increased again from there towards the top. There was no correlation between these two variables at this subzone. However, $\delta^{13}C$ exhibited a positive correlation with *C. torosa* valve lengths ($r=0.527$; $p<0.01$) in the case of females.

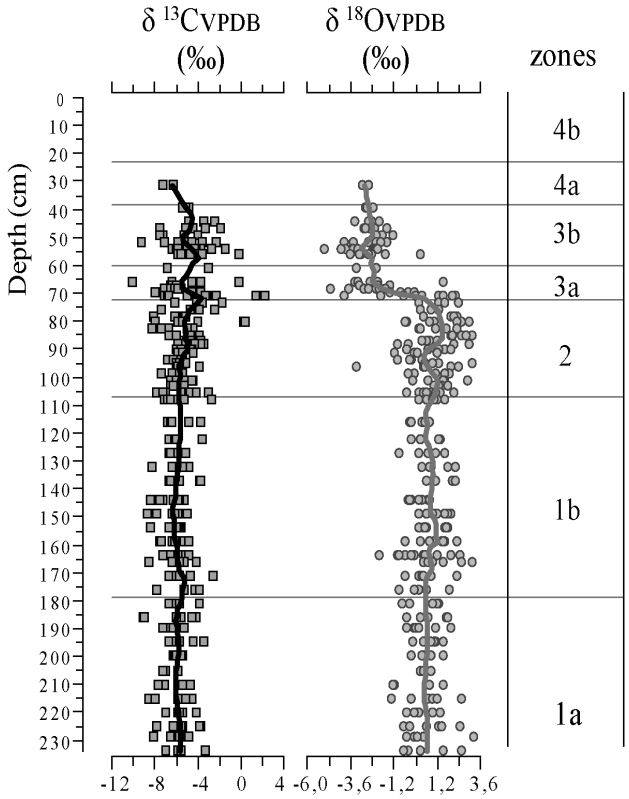

Figure 3.13: Isotopic change ratios ($^{13}C/^{12}C$ and $^{18}O/^{16}O$) along the sedimentary sequence of core Center, geochemical analysis performed on *C. torosa* valves. Loess regression was performed for both ratios using average scale of 10.

Figure 3.13*: Cambios en los ratios isotópicos ($^{13}C/^{12}C$ and $^{18}O/^{16}O$) a lo largo de la secuencia sedimentaria del sondeo Centro realizados sobre las valvas de* C. torosa*. La regresión LOESS se aplico para ambos ratios usando un factor de escala de 10.*

We observed important variations for $\delta^{18}O$ at zone 2. Two marked increases were observed at the bottom and the top of this subzone with a decrease in the middle, but values did not differ too much from those in the previous zone 1. $\delta^{13}C$ increased towards the mid part of this zone (decreasing significantly its SD) and increased again at the top end of this subzone. Despite both variables seemed to have opposite trends at this subzone, no significant correlations were found.

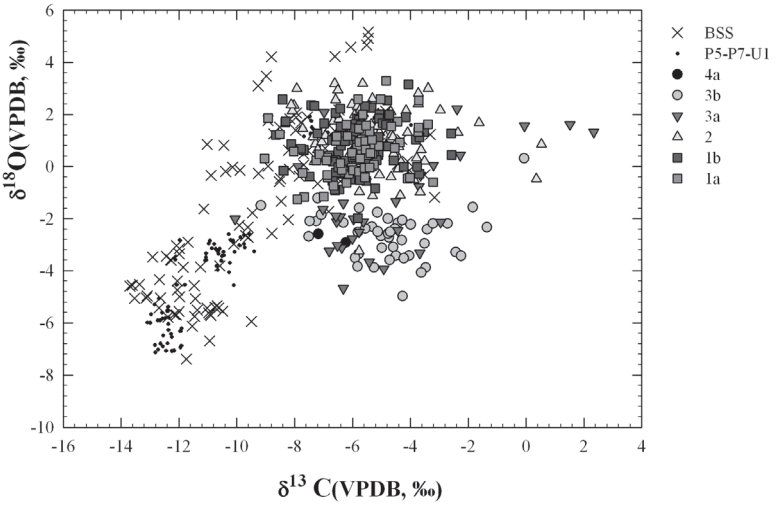

Figure 3.14: Stable isotopic composition ($\delta^{13}C$ and $\delta^{18}O$; VPDB notation) of *C. torosa* calcite valves. The established ostracods biozones samples (1a, 1b, 2a, 2b, 3a, 3b, 4a) are plotted over *C. torosa* actual data (Chapter I) recent data (Broad survey: BSS and Monthly survey: P5-P7-U1).

Figure 3.14: *Composición isotópica de la calcita de las valvas de* C. torosa *($\delta^{13}C$ and $\delta^{18}O$; VPDB notación). Las muestras de las biozonas establecidas para los ostrácodos (1a, 1b, 2a, 2b, 3a, 3b, 4a) están dibujadas sobre los datos actuales de* C. torosa *(Capitulo I) (Estudio extensivo: BSS y estudio mensual: P5-P7 y U1).*

Important changes were observed for both variables at subzone 3a (Fig. 3.13). $\delta^{18}O$ decreased fast and markedly towards the mid part of the subzone, reaching very low values for $\delta^{18}O$. $\delta^{13}C$ was also decreased upwards but not so drastically. No correlation was found between both variables at this subzone. At subzone 3b, $\delta^{18}O$ values were kept as low as at the top of zone 3a and showed little variation. $\delta^{13}C$ was highly variable at subzone 3b, ant the few isotopic shell analyses (2) performed for zone 4a gave values that were somehow lower (but still in the range) than those reported at subzone 3b. No correlations were found between both variables.

Figure 3.14 shows the isotopic results together with data on *C. torosa* recent shells isotopes analyzed in chapter I for comparison. Our established ostracod zones 1 and 2 fitted well with the typical brackish and hypersaline sites studied in the mentioned chapter. On the other site, results on $\delta^{18}O$ for zones 3 and 4 correspond to low salinity environments as compared with previous data on recent ostracods (Fig. 3.14, Chapter I). However, points in the graph are displaced from the expected trend because their $\delta^{13}C$ values are higher (than expected for their $\delta^{18}O$ values) in comparison with recent data.

3.5 Salinity reconstructions

Past salinity was inferred from *C. torosa* morphological and geochemical results applying Marco-Barba *et al.* equation (Chapter I), presented in the methods section of this chapter. Salinity reconstruction was based on the percentage of *C. torosa* noded forms and $\delta^{18}O$ shell values.

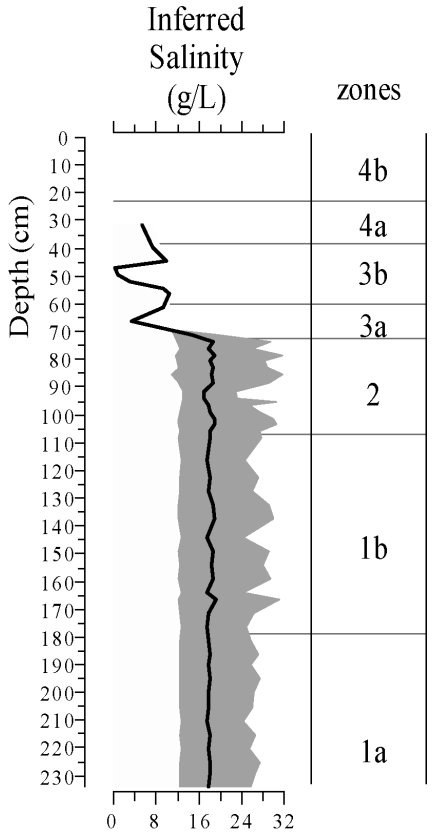

Figure 3.15: Inferred salinity from calculated multivariate regressions (methods equations). The line indicates the mean estimated value and the shadow parts the minimum and maximum standard errors.

Figura 3.15*: Salinidad del agua inferida a partir de las regresiones múltiples (ecuaciones de los métodos). La línea indica la media estimada y las zonas sombreadas los errores mínimos y máximos. Las zonas de ostrácodos establecidas se muestran en la columna de la derecha.*

The past water salinity reconstructions are show in figure 3.15. In general, salinity did not vary highly along zones 1 and 2 (brackish waters around 17 to 19 g/L were estimated), although the maximum error value was highly variable. However, a rapid salinity decrease was observed at the bottom of subzone 3a (average 3.5 g/L) and a low salinity was maintained until the top. Two secondary salinity peaks were observed at the very bottom of subzone 3b (10.4 g/L) and at the top (9.8 g/L), although we inferred the lowest salinity values (0.2 g/L) at the mid part of this subzone.

4.-Discussion

The previous chapters showed that Albufera was an ancient bay highly influenced by sea level changes, storms events, floods and humid and warm periods during the mid Holocene (between c. 8000 and 3000 cal yrs BP). However, these studies did not cover the events that occurred along the time frame of the last millenniums. The two meters length of Core Center helped us to resolve some of the questions remaining from the previous chapter (Chapter II). Two radiocarbometric dates with pollen concentrates at the bottom of the core showed that the sediment of core Center covered the last 3400 cal yrs BP (corrected). However, the ^{210}Pb age model at the top indicates that this sediment must be more recent. Dating sediments with ^{14}C in these kinds of lakes can be problematic due to the presence of organic matter other than terrestrial remains (e.g. aquatic plants), which can be included in the pollen concentrates. In addition, many factors that can affect the sediments structure, such as bioturbation, floods, storm events, dissolving processes and high sedimentation rates, make historical and paleoclimatic reconstructions very difficult and these should be carried out with great caution.

In this section, we first discuss the interpretation of the different paleoenvironmental events that took place on the lake at each bio-zone, based on our multi-proxy data. Afterwards, we place the Holocene evolution of the lake in the general context of sea level changes and human management.

4.1 Core interpretation

4.1.1. Zone 1

As we discuss below, the ostracod paleoassembalges and geochemical data throughout zone 1 (234 cm to 108 cm) represent the changes that took place at Albufera de Valencia, from a brackish environment at subzone 1a, influenced by precipitation/evaporation processes and storm events, to an open brackish-marine environment derived from a mix of waters at the mid and the top half of subzone 1b, related to sea level rising.

Subzone 1a

The sedimentary composition of subzone 1a (234-181 cm) corresponds mainly to facies type B, a homogeneous silt with low amounts of bivalve fragments and fibre plant remains. The ostracod fauna, dominated by a brackish ostracod assemblage composed by *C. torosa* and *L. elliptica* indicates that sediments came from transitional marine environments such as a brackish coastal shallow lake. This association, characterized by low species richness with high densities, has also been described as typical from sandy silt substrates at other localities (*e.g.* Ruiz *et al*., 2000a,b; Smith and Horne, 2002; Ruiz *et al*., 2006). *Cyprideis torosa* is a highly halotolerant ostracod species (salinity range=0.2-59 g/L) (Heip, 1976; Mezquita *et al*., 2000, 2005; this Thesis, Chapter I) that is usually found in sandy substrates and forming assemblages with *L. elliptica*. *Loxoconcha elliptica* is a brackish (salinity range=8-25 g/L; Mezquita *et al*., 2005) and leaf-dwelling ostracod species with oval cross-sections and legs with hooked claws which aid them in climbing (Smith and Horne, 2002). These species can stand living in sandy substrates and places where the hydrodynamic processes (waves, wind effects) and daily salinity variations, play an important role (Carbonel, 1980; Ruiz *et al*., 2000b; Smith and Horne, 2002).

The scattered occurrence of species more typical of marine environments such as *A. arborescens* and *L. rhomboidea* (Athersuch *et al*., 1989) at the bottom and the top of subzone 1a, suggests that the lake was in some way connected to the sea in some periods. The low abundances of these species and the high taphonomical ratios (valve/carapace ratio and FR) at these levels may indicate high energy at the time of deposition, probably due to storms events that reworked this marine material onto the lake. Nevertheless, *C. torosa* sex ratio values close to one and J/A ratio with values between 1.5 and 9.0 are good indicators that the

assemblages represent a natural living population (Kilenyi, 1969; Heip, 1976). Thus, ostracods species and taphonomical indicators suggest stable conditions for the most common species and the majority of the zone, except at the interval located between 200 and 212 cm. Especial attentions should be done for this particular event, because no mollusc fragments or entire shells were found and the substrate was not the typical sandy sediment coming from marine influence. Additionally, MS and the geochemical elements from group 1 (Ti, K...) at this depth increased and carbonates and Sr were relatively low compared with the previous centimetres. Altogether, the type of sediments, the absence of mollusks remains, the ostracod taphonomical ratios, the high MS, the increase of detritic elements from group 1 (e.g. Ti) and the Sr reduction suggest external deposition in this interval (200-220cm); thus, we can suggest that probably this corresponds to an important flood event that brought different water and sediment composition into the lake.

Regarding to diversity indices (Fig. 3.10), these indicated constant environmental conditions along this subzone except for the slight variations observed at the bottom half, probably due to the last mentioned flood event. Constant D_o values close to 0, suggest no ostracod assemblages fluctuations with respect to the average stage. These transitional environments (coastal lagoons) with high fluctuations and gradients (salinity, high hydrodynamic effects...) do not favour ostracod species survival, for that reason, only a few tolerant species can survive in these habitats (Dorgelo, 1976). This explains the low number of species, the high ostracod abundances and the constant D_o at this zone, coming from the special features of this kind of systems.

C. torosa valve lengths exhibit a slight increase at the bottom and at about 200 cm depth, mainly observed in males' size, and not so much in females. This slight increase in valve lengths could indicate some water chemistry changes, probably a mix of waters with freshwater input, but not important and not trespassing threshold points since the % of noded valves did not varied along the zone. Possibly the 200-212 cm depth event discussed above was related to increased precipitation and therefore more freshwater input allowed *C. torosa* individuals to grow slightly bigger carapaces (see Chapter I).

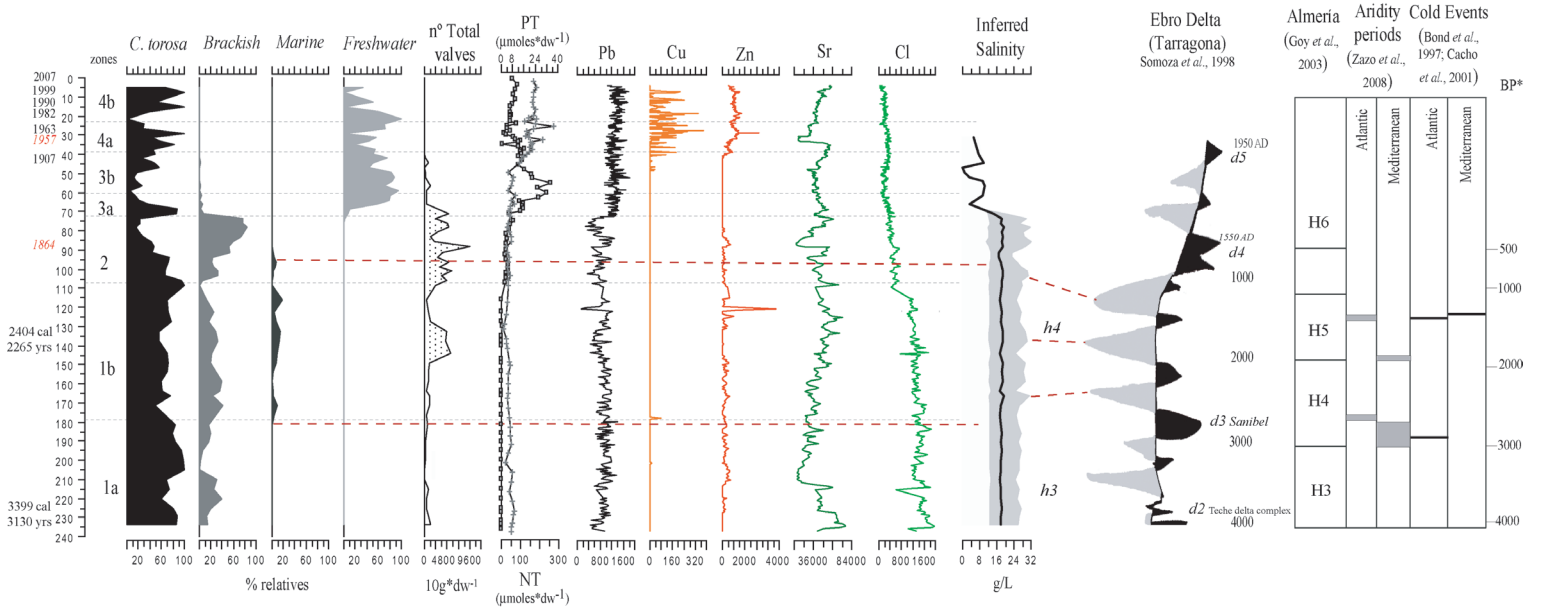

Figure 3.16: Tentative late Holocene core Center highstand events (*h*), delta (d, H) units based on ostracod zones, geochemical data and inferred salinity and compared with the reconstructed high-frequency climatic eustatic swings based on delta del Ebro and other paleoclimatic reconstructions over the last 4000 years. BP*; age scale in cal yrs BP for the events located in the box and yrs BP for the remaining figures.

Figure 3.16*: Reconstrucción tentativa de los niveles altos del nivel del mar (h1-h3) y unidades de progradación (d, H) basados en las biozonas de ostrácodos, datos geoquímicos y salinidad inferida. Todo ello comparado con las oscilaciones eustáticas reconstruidas los eventos altos del nivel del mar basados en el delta del Ebro y otras reconstrucciones paleoclimáticas durante los últimos 4000 años. BP*: esacala de edad en cal yrs BP para los eventos localizados en la caja y yrs BP para esl resto de gráficos.*

Despite a somehow wide scatter for $\delta^{18}O$ until the mid of this subzone, suggesting mix of waters, the reduced variability of $\delta^{18}O$ and $\delta^{13}C$ from the mid to the top, together with a slow increase of Sr and Cl in the sediment of this subzone indicates minor salinity increase probably due to sea level rising (Fig. 3.16). $\delta^{13}C$ and $\delta^{18}O$ isotopic ratios were positively correlated at this subzone, albeit the correlation was weak (r: 0.34). As it is well known carbonates from hydrologically open lakes typically show poor correlations between precipitated carbon and oxygen isotopes (Talbot, 1990), as observed here. The Albufera de Valencia was an open coastal lake connected to the sea as it is shown by the ostracod isotopic composition at this time. However, the high $\delta^{18}O$ variability, the inferred salinity (17-19 g/L) and the absence of an established marine species assemblage indicate that this subzone was most probably a shallow lagoon under the effects of seasonal processes, including high evaporation and freshwater inputs. On the other side, the reduced $\delta^{18}O$ variability and the increasing marine species abundances at the top limit of subzone 1a and at the bottom of the next subzone indicates salinity increasing most probably due to marine influence (see below). Moreover, the isotopical results at subzone 1a correspond to brackish waters influenced by high evaporation processes and/or by mixing of continental and marine waters compared with the results shown in chapter I (Fig. 3.14 of this chapter).

Subzone 1b

The lithological composition of subzone 1b (176-108 cm) was mainly represented by facies type A, *i.e.* with an important component of sands. The ostracod fauna showed a marked increase of species richness and abundance, compared with the previous subzone. This subzone was characterized by a typical brackish-marine ostracod assemblage. The dominant brackish species *C. torosa* and *L. elliptica* were maintained, but accompanied by high abundances of the marine species *A. arborescens* and *L. rhomboidea* (salinity tolerance: 20-30 g/l and >5 to 30 g/l respectively; Wagner 1957; Neale, 1964; Athersuch *et al.*, 1989), suggesting an important marine influence. In addition, another brackish species *X. nitida* (salinity tolerance: 8-29 g/l; Athersuch *et al.*, 1989; Mezquita *et al.*, 2005) appeared periodically. Nevertheless, the two previously mentioned marine species and the brackish *L. elliptica* and *X. nitida* decreased and disappeared at the top of the subzone, and the total number of valves was highly reduced, suggesting a drastic environmental change.

The increase in the number of ostracod species and ostracod abundances coincides with lithological facies A, where a typical sandy substrate was found. Marine ostracod valves abundances, especially for *A. arborescens*, were particularly high in facies type A. Marine species such as *A. arborescens* and *L. rhomboidea* are adapted to inter-mareal environments where sandy substrates are found. Species from the same genus were found at the artificial outlets and marine channels of Melah Lagoon and the Tunisia platform (Ruiz *et al*., 2006). The association of *C. torosa* and *L. elliptica* is common in sites with high salinity variations and sandy silt substrates (Ruiz *et al*., 2000a). *L. elliptica* and *Xestoleberis* species are more adapted to high hydrodynamic gradients such as estuarine places, where a high algae concentrations such as macroalgae (*Ulva* sp.) could be present and be an important food supply for these phytophylous species (Ruiz *et al*., 2000a). Finally, the decrease in ostracod species richness and abundances at the top of the subzone coincides with a lithological change from sandy silt to fine mud sediments (between facies B6 and A4).

MS, LOI, Cl and Sr did not show wide variations at subzone 1b, suggesting constant sea water supply along the subzone. However the maximum peak of carbonates (at *c.* 140 cm depth) and a sudden change in Cl content coincide with the maximum ostracod abundances. Below this depth, the content of detrital elements (group 1; Ti, K, etc.) was generally higher than at the top half of this subzone. Aluminum (Al) is usually related with rainfall events, but the interpretation of Al profiles is complicated due to its increased solubility under acidic (pH<4.5) conditions (Cohen, 2003) and the lesser solubility under alkaline conditions (found as hydroxide in soils). **Acid rain dissolves salts in soils, and transports these to water sources, this may cause an increase of aluminum concentrations in rivers and lakes**. In addition, Al was well correlated with elements from group 1 of Ti, suggesting an association with detrital components. The high proportions of these elements could be probably related to more humid periods or increase of precipitation patterns. Furthermore, previous works based on the study of the geochemical components in organic rich coastal peat marshes at nearby zones of Valencia (Castellón, Valencia) also demonstrated the relationship of Al, K and other elements with a detrital origin of the sediments (López-Buendía *et al*., 1999).

If we take into account that FR was in general low and negatively correlated with the total number of ostracod valves at subzone 1b, J/A and M:F ratios were relatively high, and the VCR ratio only presented two anomalous values, then, the ostracod fauna could be considered as autocthonous along this subzone.

In addition, diversity indices (Fig. 3.10) indicated constant environmental conditions along the subzone, being in agreement with the last approximations except at the top sample of the subzone (at the transitional zone between Facies B6 and A4).

In this subzone *C. torosa* valve lengths (particularly males) seem to be good indicators of minor salinity changes. These increased when the proportion of marine species decreased, and vice versa. Moreover, valve lengths exhibited a negative correlation with $\delta^{18}O$ and the slight valve length increase at the bottom of the subzone coincides with the wide scatter observed for $\delta^{18}O$, suggesting salinity decrease at the middle of the bottom half and at the top of the subzone. However, the percentage of noded forms did not show any clear change along the subzone, therefore salinity values were kept in the brackish range, as indicated by our salinity reconstruction.

Isotopic variables showed similar values to those reported at the previous subzone (1a), suggesting similar hydrology, salinity and trophic state. $\delta^{18}O$ increased, suggesting salinity increases probably due to sea level rising (see below; Fig. 3.16). Both isotopic variables were not correlated at this subzone suggesting an open lake (Talbot, 1990). Reconstructed salinity also indicated low variation maintaining the mesohaline conditions (17-19 g/L) of the last subzone. Nevertheless, the maximum salinity variation (maximum error) indicates that at this period the salinity of the lake attained values probably close to seawater, higher than in the previous subzone.

The different taphonomical indices suggest constant environmental conditions along the subzone. However, ostracod species assemblages, lithological composition and isotopic signatures indicate possible mix of waters at the bottom and the top and a salinity increase at the mid part of this subzone, possibly related to sea level rising (see below).

4.1.2. Zone 2

The ostracod species composition, the increase in submerged plants remains, the isotopical values of ostracod shells and the sedimentary composition, all suggest important changes with respect to zone 1, as well as salinity variations and important floods events along this zone.

Salinity changes are clearly indicated by a marked Cl decrease with respect to the previous zone, suggesting a salinity decrease related to sea level

variations (see below). On the other hand, Sr showed a important variations suggesting different water supply or at least mixing of waters of different origin. The plant remains increase (Fig. 3.3) and the positive correlation between LOI and N:P ratio, suggest that the mixing of waters favored macrophyte meadow development towards the top of this zone.

This zone is characterized by the high abundance of *Xestoleberis nitida* and high concentration of plant remains. *C. torosa*, *L. elliptica* and *X. nitida* (a typical brackish water ostracod assemblage) increased their abundances following parallel trends and reaching the highest abundances for *X. nitida*, which is almost exclusive of this zone. *X. nitida* is a mixohaline species commonly found in estuaries and lagoons at places rich in vegetation (Athersuch *et al*., 1989; Smith and Horne, 2002). The presence of some valves of the brackish *Cytherois* cf. *stephanidesi* and *Leptocythere* sp., the marine *A. arborescens* and inland water species such as *C. angulata*, *Candona* sp., *D. stevensoni*, *C. vidua* and *Herpetocypris* sp. at the top of the subzone should be remarked. The presence of these species should be interpreted carefully due to the low abundances, perhaps originating from the channel that connected the lake to the sea or from the nearby springs, rivers or gullies in the case of the inland water species. However, sex-ratio, J/A ratio, and VRC ratio suggest no reworking material for the *C. torosa* population. Furthermore, diversity indices (Fig. 3.10) H and E showed that ostracod assemblages at the bottom samples were similar to those reported at the previous zone. However, the assemblages changed (D_o increase) throughout the mid part (due to rise in *X. nitida* abundances) and to the top of this zone (increase of freshwater species) suggesting changing environmental conditions (salinity reduction).

Two flood events (facies D3 and D4) occurred in this zone, as indicated by a sharp decrease in the number of valves of the marine species *A. arborescens* and a slight decrease on *C. torosa*, *L. elliptica* and *X. nitida* abundances. In addition, MS and the XRF elements from group 1 (Ti, Fe, K, and Al; detritic elements) increased markedly and Sr decreased at facies D4 suggesting possible flood events and different water supply (similar patterns were observed at all D facies). Sex ratio and J/A ratio in general suggest low energy depositional environments in this zone, but the extreme high peaks at the mid part of the zone may suggest reworking (Kilenyi, 1969) perhaps in relation to the flood event.

Regarding marine species, these reached the maximum number of valves at Facies A6, after the D3 facies event, where we also observed high number of marine gastropods and bivalves and plant remains. Mediterranean storms

can produce violent precipitation extremes at the end of the summer season (Trigo *et al*., 2002). These storms could provoke important floods and transport of reworked material both from the continent and from the coast (e.g. sea water, sand, gastropods, ostracods...), introducing this material into an adjacent coastal lagoon, such as the Albufera de Valencia.

C. torosa valve lengths increased towards the top of this subzone although with a big scatter, suggesting mixing waters and decreasing salinities. $\delta^{18}O$ varied along this subzone correlating with the presence of marine species, suggesting salinity decrease to the mid part of the zone, followed by an increase to the top half and again a reduction at the top limit of this zone. At the D3, $\delta^{18}O$ values decreased suggesting freshwater input, which is in agreement with the increase in the total number of ostracod valves and the decrease of *A. arborescens* abundances. $\delta^{13}C$ increases from the bottom to the mid part and again at the top of the zone. This slight increase coincides with carbonates and N/P increases, suggesting enhanced productivity.

At this zone, shell isotopic values were positioned generally at the same range as in the previous zones for the wide *C. torosa* isotopic scatter (Fig. 3.14), suggesting similar salinity conditions. Nevertheless, we observed some samples with $\delta^{13}C$ higher than for the studied living populations, suggesting a period of enhanced productivity (Leng and Marshall, 2004). Inferred salinity was similar to the values calculated for the previous subzones; however a slight decrease was estimated at the middle of this subzone (≈17 g/L).

4.1.3. Zone 3

The most important changes along the core were observed at this zone. The ostracod species composition, isotopic values and sedimentary composition suggest a sudden and drastic salinity reduction with important chemical changes, probably related to human hydrological management and pollution.

Subzone 3a

The constant low values of Cl indicate constant low salinity, independently it was corroborated by our salinity reconstruction (see below). LOI and N:P increased, and mainly N (see Fig. 3.15) suggesting macrophyte proliferation, which increased dead organic matter on the sediments (high LOI). The high correlation between LOI and nitrogen indicates that most of this organic

material corresponds to macrophyte remains; this is also supported by the observed high concentration of plant remains and high values of N and LOI. The mixing of waters favored macrophyte proliferation, which in turn facilitated high carbonate precipitation and consequently an increase of carbonates in the sediment of this zone. It should also be emphasized the increase of Pb values (Fig. 3.15), probably due to pollution of atmospheric origin and also to the increase of hunting practices at this time in the Albufera (discussed below).

The dominance by a brackish ostracod assemblage observed at previous zones, changed to a freshwater assemblage at this subzone. *L. elliptica* and *X. nitida* decreased rapidly at the bottom of this subzone. *C. torosa* increased at the interfase layer, at the lower limit of this subzone, reaching the highest abundances but immediately after decreased constantly towards the top. On the other hand, the increasing number of inland water species (mainly, *C. angulata*, *Candona* sp. and *D. stevensoni*) confirmed the salinity decrease throughout the subzone.

C. torosa valve lengths increased importantly to the top of this subzone, as well the percentage of noded forms also suggesting a change from a brackish to a more diverse freshwater environment.. The salinity reduction is also in agreement with the sharp decrease of $\delta^{18}O$. However, $\delta^{13}C$ increased and showed a wide scatter from the mid part of the previous zone to the bottom of this one, however, immediately decreased towards the top. This $\delta^{13}C$ increase can be related the high density of plants and enhanced photosynthesis (that preferentially utilize ^{12}C). However, the sudden decrease could be explained by different factors, such as the respiration of the sinking organic matter or by carbonates precipitation (Leng and Marshall, 2004). Both processes take CO_2 from the water and produce the inverse process (leading to a low $\delta^{13}C$ in the T-DIC). Most of the samples showed oxygen ostracod shell isotopic values which corresponded to mesohaline water bodies (10g/L), compared with the samples studied in Chapter I (Fig. 3.14). However, these samples were displaced outside of the *C. torosa* scatter due to the observed high $\delta^{13}C$ values, which could be explained by the different processes that can be involved on the $\delta^{13}C$ of T-DIC water content, as explained above.

Inferred salinity showed a marked decrease from the bottom to the top, with salinities that ranged from 9 to 3 g/L which coincided with the important historical transformations taking place during this period in Albufera de Valencia. The Spanish crisis (by the beginning of XXth century) and the changes on the property of the surrounding land leaded to an intensive agriculture expansion and to a strong hydrological control of the Albufera de Valencia.

Subzone 3b

The most important changes along this subzone relate to the increase in nutrient load, indicated by a rise in phosphorous, and the drastic reduction of the macrophyte cover indicated by a decrease in LOI and N and the absence of mollusks and plants remains (Fig. 3.16). On the other hand Sr, Cl and Pb remained constant along the subzone suggesting similar water supply and constant lead pollution by hunting or industrial activities.

The number of ostracod valves decreased considerably with respect to the previous subzone. This subzone is dominated also by freshwater species, such as *C. angulata*, *Candona* sp., *P. psammophila* and *D. stevensoni* (salinity tolerance: 0.2 to 15 g/L for the Candoninae species, 0.2-1.7 g/L for *P. psammophila* and 0.3 to 2.1 g/L, even up to 15 g/L for *D. stevensoni*; Meisch, 2000; Mezquita *et al*., 2005). At the top of this subzone, other freshwater species appeared such as the cosmopolitan species *Limnocythere inopinata*. *L. inopinata* can tolerate either permanent or temporary water bodies and is usually found in muddy to sandy substrates with a wide salinity tolerance (0.8 to 3.7 g/L up to 18 g/L) (Meisch, 2000; Mezquita, *et al*., 2005). The high relative abundance of cosmopolitan, eurytopic and phytophilous species *C. vidua* (salinity tolerance: 0.3 to 2.3, up to 8 g/l; Meisch, 2000; Mezquita *et al*., 2005), may indicate high vegetation cover but also fluctuating trophic conditions.

Taphonomical indices in this subzone are highly variable and sometimes contradictory because high proportions of juveniles indicate low energy depositional conditions, but this coincides with low sex-ratios and varying FR values. Diversity of ostracods, particularly the Shannon index, show the highest mean values for the whole sequence, suggesting the presence of a rich community in a relatively stable, not stressful environment. D_o varied considerable at the bottom half and at the top half due to the increase of freshwater ostracods, a community far from the *C. torosa* dominated assemblage common through most of the sequence.

A few *C. torosa* adult valves were measured and the lengths were quite similar to those reported at the last samples of subzone 3a, suggesting similar mesohaline conditions. The percentage of noded valves showed a slight increase at the bottom and high percentages at the mid part, suggesting salinity still was decreasing towards the mid part of this subzone.

$\delta^{18}O$ showed similar values to those reported at the top of the previous subzone, suggesting similar freshwater conditions. $\delta^{13}C$ showed also a scatter of values similar to subzone 3a (and with maximum values higher than in zones 1 and 2), in suggesting also high variability of photosynthetic and respiration activities, as discussed above. The pattern of inferred salinity is similar to the previous zone, with average values in agreement with the known salinity tolerance of the species found.

4.1.4. Zone 4

Again PT increased throughout the zone, suggesting important nutrient inputs to the lake in this recent period (Fig. 3.16). The decrease of TN and LOI and the increase of TP is most probably related to the loss of macrophytes meadows and the eutrophication of the lake in the last 50 years (Fig. 3.16) (Miracle *et al.*, 1987). Cu, Zn and Cr content was very high along this zone, suggesting a growing industrial contamination. On the other hand, MS did not varied markedly except for one isolated high peak (facies D5), accounting for the highest peak along the core, which may correspond to the extreme Túria river flood event that took place in 1957 (Carmona and Ruiz, 2000).

The sediment of this zone and also of subzone 3b, was characterized by fine mud sediments, absence of mollusks and plant remains and a very low number of ostracods valves. Subzone 4a was characterized by a poor mesohaline ostracod assemblage, dominated by *C. torosa*, but this species decreased its abundances towards the top of the subzone. Other species such as *C. vidua*, *Candona* sp., *D. stevensoni* or *L. inopinata* showed a scattered presence along this subzone. No *C. torosa* adults or entire carapaces were found, and most of the taphonomical ratios could not be calculated. The low number of remains also prevents a strong inference of paleoenvironmental conditions from ostracod valves. Only two isotopical analyses were performed at this subzone, resulting in $\delta^{18}O$ and $\delta^{13}C$ values similar to those reported at the previous subzone, suggesting similar salinity and T-DIC isotopic composition. Inferred salinity gave salinity values slightly lower than those obtained at the top of subzone 3b.

At subzone 4b very few ostracod valves were found. *C. torosa* was present in almost all the samples, and when other species were present they were composed by the cosmopolitan *C. vidua* and *L. inopinata* and Candoninae species.

The ostracod disappearance and the absence of plant and mollusk remains could be explained by human impact on the Lake. The uncontrolled watersheds, agricultural residues and industrial spills into the lake modified the natural conditions of the system driving it to an hypereutrophication state, added to pollution by heavy metals, and consequently to the loss of biodiversity (particularly of ostracods; Poquet *et al.*, 2008) and to the currently low water quality (Romo *et al.* 2008).

4.2 The late Holocene history of the Albufera de Valencia

The study of the Palmar core in the Chapter II accounted for the environmental changes of the Albufera lake for most of the mid part of the Holocene; however, the late Holocene was lost from that sequence and it is here studied in detail. The two radiocarbometric dates, calibrated and corrected for the reservoir effect, provide an indication of the period interval studied in this sediment sequence of Albufera de Valencia. In addition, the ^{210}Pb age model and the main Túria and Júcar rivers floods allowed us to approximate a useful age model for the last 200 years.

Based on ostracod paleoassemblages and geochemistry, sedimentology, MS and geochemical XRF results, we were able to infer salinity changes for the Albufera system and correlate these variations with sea level changes (eustatic fluctuations) proposed for other Mediterranean coastal areas during the late Holocene. In the preceding chapter we discussed Zazo and Goy (2000), Goy *et al.* (2003) and Zazo *et al.* (2008) description of sea level fluctuations with prograding periods (H_1-H_6) on the Spanish Mediterranean coasts that were interpreted as cold events. Furthermore, the study of Somoza *et al.* (1998) at the Ebro river delta described prograding events (*d* episodes), interpreted as cold periods corresponding to reducing mean sea level (MSL), and agrading events (*a* episodes) of increasing sea level, attaining maximum values of sea level rise at highstands (*h1*-*h5*). We discuss the links between our results and these sea-level changes that could have shaped the history of coastal Lake Albufera.

Part of Zazo *et al.* (2008) H_3 prograding period may be identified at the bottom of Albufera core Center, encompassing an episode of approximately 28 cm (between 238 and 210 cm) that coincides with the bottom of our ostracod subzone 1a. The high ostracod abundances, the typical brackish assemblage (inferred salinity≈17 g/l), the good preservation and the lithological descriptions suggest a relatively stable environment. The small variation of Sr and Cl suggested

a constant supply to the lake from the same water source. Even so, the lake was poorly connected to the sea at this time, since the marine ostracod assemblage was not established. Storm events and evaporation processes likely played an important role in the salinity of the lake. At subzone 1b, important changes in the ostracod paleocommunity that become enriched in marine species suggest higher sea water influence, probably related to a marine transgression, that could attain the maximum influence at Somoza *et al.* (1998) *h3* or *h4* highstand at around 3000 yrs BP, or the transition between H_3 and H_4 prograding events (Zazo *et al.* 2008). Cl content and the inferred salinity did not show wide variations, suggesting a brackish environment with higher marine influence. In summary: (1) the sandy silt sediments (facies A; marine influenced), (2) the Sr increase (suggesting different water supply), (3) the $\delta^{18}O$ increase (salinity increase) and the (4) typical brackish-marine assemblages indicates that the lake was open to the sea, probably due to a sea level rising that might have taken place from the top of our ostracod subzone 1a to the top of subzone 1b (between around 3400 and 2400 cal yrs BP). This event correlates with the high stand period *h4* described by Somoza *et al.* (1998) and with the time between H_3 and H_4 prograding periods described by Goy *et al.* (2003) at Almería coasts.

We hypothesize that the *d4* regressive phase at the Ebro delta (dated between 1110 AD and 1550 AD) may probably correspond with the decrease of salinity and reduced dominance of marine species assemblages between 90 and 100 cm at the top of ostracod zone 2 when the ostracod assemblage change from brackish-marine to brackish, and Sr and Cl decrease. In addition, the facies D3 may correspond with the Túria flood event that took place in 1589 (Carmona and Ruiz, 2000). However, this event should be interpreted carefully due to the relatively low MS compared with the other flood events (facies D4 and D5) and the poor reliability of dating at this level.

The inferred flood event at facies D4 coincides with the second highest peak of MS, and could be correlated with the main Júcar flooding that took place in 1864 (Carmona and Ruiz, 2000). From this flood event (D4) towards the top, we observed a salinity increase that correlates with the last marine transgression that occurred during the last 500 years (*h5* in Somoza *et al.*, 1998). But most importantly, different authors suggest that the subsequent marine regression *d5* (Somoza *et al.*, 1998) was one of the main factors involved in the development of a sand bar that drove the isolation of lake Albufera de Valencia from the sea (Santiesteban *et al.*, in press). Ostracod marine species disappeared and *C. torosa* significantly decreased in abundance; however, the brackish species

(mainly *X. nitida*) and plants remains increased notably, suggesting brackish waters and vegetation growth. In addition, Total Nitrogen and LOI increased with parallel trends throughout the zone (Fig 3.4 and 3.16), suggesting that most of the deposited organic matter corresponded to macrophyte meadows. It is well known that Albufera de Valencia was highly influenced by human activities especially since medieval times. Historical archives demonstrated that humans undertook important hydrological management since the beginning of the XV century (Sanchís Ibor, 2001). For instance, the lake was used for intensive fishermen activities since 1600. Especially from 1600 to 1680 fishermen used to build an artificial dam (called *Parada Fija*) in the channel located at the southern part of the lake that closed and isolated the lake from the sea. The reason for this particular activity during those years came from the idea of using the lake for extensive fish culturing.

At zone 3 inferred salinity and Cl decreased markedly, the brackish species decreased almost disappearing, and freshwater species increased steadily. If we take into account the historical archives of the history of Albufera de Valencia we estimate that the age at the bottom of this zone could be around 1888 AD (correlating with the increasing hunt use of Pb at this date, see below). Different authors (Robles *et al*., 1985; Santiesteban *et al*., in press) suggested that the main salinity reduction occurred around 500 years ago, which drove the Albufera from a brackish stage to the present freshwater conditions due to the regressive phase occurred at this time that closed and isolated the lake from the sea. However, despite the Albufera suffered important hydrological changes (explained above) since medieval times, we observed that the phenomena of desalination did not occur until most probably later than the end of the XVIII or the beginning of the XIX century. Between 1864 AD and 1927 AD, humans undertook a strong control of the Albufera resulting in numerous modifications. In 1865, Spain was under a drastic economic crisis. This crisis and the high economic expenses involved in the management of the Albufera de Valencia was the reason why the queen Isabel II decided to transfer the property of Albufera of Valencia to the Spanish government (Sanchís Ibor, 2001). This facilitated the agricultural expansion of the region, specifically the expansion of rice fields. The rice fields' capacity for water retention resulted in increased hydrological control of the area. Between 1865 an 1927, the open lake surface was strongly reduced, and waters coming from rivers Júcar and Túria were diverted for irrigation of the surrounding areas of the lake. The increasing water input from irrigation surpluses draining into the lake modified its water chemistry, most notably its salinity, Sr, and T-DIC

concentrations. Furthermore, salinity reduction allowed the development of macrophyte meadows that drove the colonization of these new habitats by freshwater ostracod species. Proxies such as LOI, N and carbonates increased in this subzone and reached the highest peaks at 59 cm where we also recorded the maximum freshwater ostracod species abundance and the highest $\delta^{13}C$ values. Macrophytes increase habitat diversification and provide food and protection to freshwater ostracods. As a result, the increase in macrophyte coverage correlated well with freshwater ostracods, which exhibited a high diversity in the ostracod subzone 3a. Following this, the increase of macrophytes could also lead to very high $\delta^{13}C$ T-DIC values, mainly due to preferential uptake of ^{12}C by aquatic plants during photosynthesis (Leng and Marshall, 2004), and high carbonate precipitation. Moreover, TN concentration increase could also be related to organic matter enrichment due to macrophyte detritus.

The abundant macrophyte meadows became depleted due to intense urbanization of the lake surroundings, its coupled untreated sewage diversion to the lake, and the increased use of fertilizers, herbicides, and pesticides since 1950s (Vicente and Miracle, 1992). Urban development followed by the use of fertilizers increased the phosphorous load to the lake, which consequently favored the phytoplankton development and started the eutrophication processes. On the other hand, N and LOI decreased progressively probably related to the macrophyte meadows' degeneration. Untreated domestic sewage waters and agricultural pollution brought the lake to an hypereutrophic state, which has switched to a complete dominance of phytoplankton, and macrophytes were wiped out from the lake since the last years of the 1960 decade.

The most recent sediments (mainly last century) showed an increase of heavy metals similar to many lakes around the world, mainly at our ostracods zone 4. One of the main metals was Pb. The Pb concentration increased markedly after 1864. One of the main traditional activities at Albufera de Valencia since medieval times is hunting. The local council allowed the hunting expansion at Albufera in 1888 due to the great demand of this activity in the area. The use of lead in ammunition is one of the main problems at wetlands around the world, due to lead toxicity and has been registered in Albufera sediments and local hunters continue to use lead ammunition with the local government permission. Furthermore, important quantities of lead might have been deposited into the lake through atmospheric deposition, as registered in other Iberian areas (Martínez-Cortizas *et al.*, 1997). Other metals such as Cr, Cu and Zn also increased (Fig. 3.5) since the beginning of the XX century and

more intensely since the middle of it. The presence of industries around the lake suggest that the lake and catchment soils were increasingly contaminated by aerial transport of emissions or direct water spills of Cr, Cu and Zn into the lake as a result of industrial activity. Albufera de Valencia represents since the last years of the 1970's decade a hypereutrophic state (Vicente and Miracle, 1992) with a consequent loss of ostracod communities (Poquet *et al.*, 2008). Several studies have been carried out during the last years about hydrology (Soria and Vicente, 2002; Soria, 2006), nutrient loads and eutrophication processes (Soria *et al.*, 1987), and phytoplankton tendencies (Romo *et al.*, 2008) which demonstrated the negative effects of humans in the lake, thus, calling for effective water management and the reduction of the inflow of polluted waters.

5.-Conclusions

According to the previous studies (Santiesteban *et al.*, in press and chapter II of this Thesis) the Albufera de Valencia was strongly influenced by sea level changes along the Holocene and these changes are well recorded on the Albufera lake sediments. Core center sediment sequence spans a period accounting for approximately the last 3400 years. Sedimentological composition, ostracod assemblages and geochemical analyses interpretations are in concordance with other studies on Spanish coastal Holocene evolution. We recognized the marine transgressions *h3* and *h4* (Somoza *et al.*, 1998) occurred during the late Holocene because these were recorded by the ostracod fauna and the salinity proxies. However, the last marine transgression that occurred during the last 500 years (*h5*) is not clear in this record because the lake was highly controlled and exploited by humans during these years. During the last 200 years, the Albufera de Valencia show the typical patterns observed for this kind of systems around the world (Halpern *et al.*, 2008). The high human pressure mainly based on the hydrological control of the lake, rice field expansion and hunting affected the whole system droving the lake to a highly deteriorated system. The untreated sewage from Valencia city and the surrounding towns increased the nutrients load onto the lake favoring a drastic eutrophication process. Additionally the uncontrolled spills from the nearby industries increased the heavy metals charge.

We call for a better water management of the lake, industrial control of spills and for a better cooperation of all the organisms that are involved on the management of Albufera Natural Park, from hunters, fishermen, farmers and

other user associations to the government in charge (Conselleria de Medio Ambiente), because, if we all are not aware of the problem, it will not be easily solved.

CHAPTER IV

Reconstruction of the XXth century ecological evolution of Albufera de Valencia (Spain), salinity changes and anthropogenic influences, based on ostracod remains

2.-Material and Methods

2.1 Core extraction and treatment

A 63 centimetres core (L'Antina core) was taken in June 2004 from a point in the western of Albufera Lake (Fig. 4.1) close to reed beds called L'Antina (UTM: 30S 0726941/4357037). The core was extracted using a 1 meter manual Uwitec corer (usually for ^{210}Pb cores) with 8.6 cm liner inside diameter and it was kept in a polyethylene tube. The stratigraphy of the core was described and then, subsamples were collected.

Core subdivision

The core subdivision was made based on the observed lithological statigraphic layers carried out at approximately 1 cm intervals (high resolution). In total, fifty-nine sub-samples were obtained for different analysis (geochemistry, mineralogy, and micropalaeontological studies).

An aliquot subsample was taken to determine dry weight per sample. These aliquots were weighted, dried at 105^{o}C during 1 hour to determine water content and dry weight per gram of fresh sample. The remaining sediment was dried at 460^{o}C during 7.5 hours to determine organic matter content (LOI) and later on at 950^{o}C, during 8 hours to obtain the concentration of carbonates per sample.

The ostracod subsamples were processed following the method of Griffiths and Holmes (2000) and by Marco-Barba *et al.* (Chapters II and III); 10-15g of wet sediment were weighted, air dried and then wet-sieved through 400 and 250 μm pore size using a water flux during 30 minutes. For further descriptions of the method see chapters II and III.

Biogenic remains were picked from the coarse with a `00´ paintbrush under low power Olympus SZX 12 stereoscope microscope and stored in micropalaeontological slides. Ostracod valves were counted per sample and the abundance expressed as number of valves per 10 g dry weight (10g dw^{-1}). The different species were identified following Athersuch (1989), Meisch (2000) and Poquet *et al.* (2008).

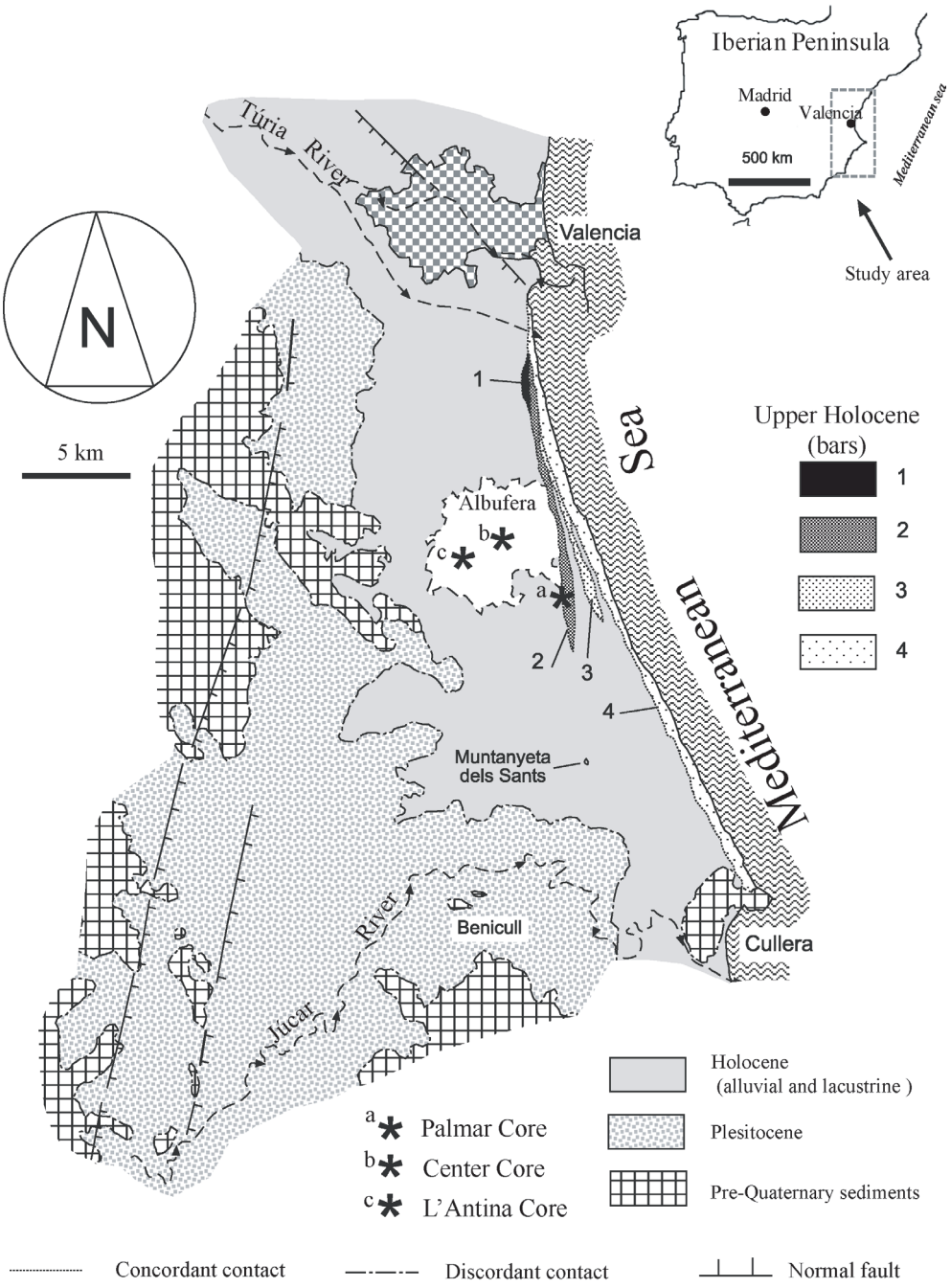

Figure 4.1: This figure shows the L'Antina core location and the geological composition of the studied area. Figure adapted from Santiesteban *et al.* (in press).

Figura 4.1: *La figura muestra la localización del sondeo de l'Antina y la composición geológica del área de estudio. Figura adaptada de* Santiesteban *et al. (in press).*

2.2 Preservation states

The preservation states for ostracod remains were analyzed, as it was done in the last chapters, to have an indication of the proportion of reworked valves. The states of preservation **A-B-C**, the ostracod fragments and the fragments ratio (FR) were applied to assess the energy of the environment at the time of deposition (see chapter II and III for further details). Once more, valves falling into preservation states A and B were considered well enough preserved and consequently these were the valves included into the multivariate analysis (cluster and ordination analysis, see below). For geochemical analysis each ostracod valve that was previously classified as A or B was further separated in a gradient from 1 to 7 based on valve transparency state of preservation (Griffiths and Holmes, 2000) and valves that ranged from 1 to 4 were used on the analysis. For further details of these indices see chapter II and III.

Ostracods fragments (Chapter III) and fragments ratio (FR= (fragments+PE type C)/nºTotal valves+fragments) can give us an estimation of the possible physical rework events at the depositional time for the entire ostracod assemblages. If the fragments ratio is high it suggests high energy of the environment at the time of deposition, whereas if it is low it can indicate low energy depositional environment (Chapter II).

2.3 Morphology and preservation of C. torosa *shells*

Particular attention was paid to *Cyprideis torosa* remains. Lengths of female and male *C. torosa* valves were measured, as well the percentage of noded animals per sample (Van Harten, 1975; Chapter I, II, III). In addition, *C. torosa* sex ratio, single/double vales ratio and juveniles/adults ratio were taken into account in order to assess *C. torosa* autocthonous or alocthonous populations and the energy at the time of deposition of these populations (Kilenyi, 1969)

The taphonomical processes at the time of deposition after an animal dye affect the number and type of valve that are preserved in the sediment. Thus, the study of the sex ratio, juveniles/adults ratio or valve/carapace ratio of each *C. torosa* assemblage can give us relevant information about the conditions that happened at the time of deposition (Van Harten, 1975; Whatley, 1983a) and indirectly this data may be of some value in interpreting the recent evolution of the lake.

Sex ratio. Different studies have been performed about the life cycle and population structure of *C. torosa* (Heip, 1976; Mezquita, 2000; Chapter I). In this way, we can estimate if the sex-ratio of our ostracod population can suggest possible reworked processes, mix populations or stable communities that were established at the time of deposition.

Juveniles/adults ratio (J/A). The study of ontogenetic series of ostracod populations could be good tools to assess the energy where the assemblage was formed (Whatley, 1988; De Deckker, 2002). Noted that only samples where adults present, the J/A ratio was calculated

Valve/carapace ratio (VCR ratio). Depending of amount of single valves or complete carapaces that we can found on the sediment we can estimate if these valves have been suffered post-mortem transportation or slow deposition over the sediment (Kilenyi, 1969).

2.4 C. torosa *geochemical analysis*

Between five and fifteen shells of *Cyprideis torosa* (when there was enough material) were initially selected from each subsample into a preservation class. Analyses were performed for each single carapace (2 valves), however, sometimes juveniles of first growth instars (A-1 and A-2 and in a few cases A-3) were pooled in groups of 4 or 5 valves. Males and females were analysed separately and we used between 2 and 3 valves per analysis. Only in a few cases when material was not enough to carry out one analysis, males and females were pooled together.

Between 1 to 5 analyses per sample were made to determine isotopical analyses $^{18}O/^{16}O$ and $^{13}C/^{12}C$ and trace elements Ca, Mg and Sr. Ostracod valves were cleaned for geochemical analysis using the method described in Ito (2001) and in the last Chapters (I, II and III). Cleaned valves were analyzed using a Kiel-II online carbonate preparation device coupled to a Finnigan MAT 252 stable isotope ratio mass spectrometer at the University of Minnesota and the residue of this analysis was used for trace elements. For further details see chapters I, II and III, where the same procedure was applied.

2.5 Diversity indices, Cluster analysis and Statistical methods

Several diversity indices were used to calculate diversity of ostracod assemblages, we employed Shannon-Wiener index (Shannon and Weaver, 1963) as diversity (equation 5), and Evenness (E; equation 6) to known how the species were distributed per sample (Margalef, 1974). In addition, we used the index of fluctuation D_o (equation 7) formulated by Dubois (1973) to assess ostracod community fluctuations with respect to the average state calculated for the whole sequence. High values indicated major fluctuations of the community and maximum deviations from the state to which the structure of the community is approaching (Miracle, 1978). For more detailed explanations of the Diversity indices and D_o see chapters II and III.

A data matrix was constructed (Appendix 4.1), with the number of valves per 10 grams of dry weight of each ostracod species for each core sample (N= 59). Number of valves was log transformed ($\log_{10}$(number of valves+1)) for statigraphical analysis. Adults and juveniles were not considered as separated variables in the matrix. To analyze the changes in composition of ostracod assemblages through the core sequence, a constrained cluster analysis was performed applying the CONISS method and the Edwards Cavalli-Sforza distance (Grimm, 1993).

In addition, we used unconstrained cluster analysis for the study of ostracod species association with all the species and two samples with no ostracods remains were excluded from the analysis (6,5 cm and 17,5 cm). In this classification analysis, we used the single LINKAGE similarity method and the Euclidean coefficient distance index. The whole transformed data matrix (same as used in CONISS) was analysed by means of Principal Component Analysis (PCA) (Jongman *et al*., 1995) in order to obtain an ordination of samples for a better evaluation of ecological similarities among them.

Correlations between *C. torosa* valve lengths, Mg/Ca, Sr/Ca molar ratios, and isotopes ratios ($\delta^{18}O_{VPDB}$ and $\delta^{13}C_{VPDB}$) were analysed using either Pearson (when data was normally distributed) or Spearman (no-normally distributed data) correlation techniques.

The equations obtained in the *C. torosa* calibration study in Chapter I, were used to reconstruct salinity changes and water Sr/Ca. We used the following equation:

$$Sr/Ca_{water}=4{,}29+0{,}292*\delta^{18}O_{C.torosa}+0{,}228*\delta^{13}C_{C.torosa}+1{,}371*Sr/Ca_{C.torosa}; \quad \text{(Eq. 4)}$$

to reconstruct past water Sr/Ca in all the samples were the three variables were analyzed.

We used the following equation to reconstruct past salinities:

$$\log_{10}sal=1{,}237-0{,}0129*(Pn)+0{,}0279*\delta^{18}O_{C.torosa}; \quad \text{(Eq. 2)}$$

Where *Pn*: proportion of noded valves, in all the samples were the both variables were analyzed. In both reconstructions the mean and the respective standard error values were estimated.

2.6 Radiometric dating

^{210}Pb and ^{137}Cs analysis were performed on a twin core that was extracted at the same place only exclusively to carry out these analysis. ^{210}Pb activity was measured for 1-6 x 10^5 s with ion-implanted surface barrier detectors and an Ortec alpha spectroscopy system at University of Barcelona. Unsupported ^{210}Pb is calculated by subtracting supported activity from the total activity measured at each level; supported ^{210}Pb is estimated from the asymptotic activity at depth (the mean of the lower most samples in a core). Dates and sedimentation rates are determined according to the c.r.s. (constant rate of supply) model (Appleby and Oldfield, 1978) with confidence intervals calculated by first-order error analysis of counting uncertainty (Binford, 1990). Cesium-137 activity was measured for 1-2 x 10^5 seconds using an EG and G Ortec high-resolution germanium well detector and multichannel analyzer (same instrumentation used for ^{210}Pb above).

One sediment sample was selected at the bottom of the core (53-54 cm) to concentrate pollen to obtain radiocarbon measurements. This sample was processed at the Palinology laboratory of Prehistoric area at *Universidad Rovira i Virigili* (Tarragona-Spain). These samples were checked to ascertain the absence of aquatic remains or algae to avoid hard–water error (Fontes and Gasse, 1991). The sample was dated in Pozna´n Radiocarbon Laboratory. The radiocarbon measurement (´BP´) was calibrated to calendar years (´cal. BP´) using OxCal v3.10 software.

3.-Results

3.1 ^{210}Pb and ^{137}Cs and ^{14}C age model

The chronology of this core (based on the c.r.s model) is very similar to that from the previously dated Core Center. The ^{137}Cs peak in this core was located at about 30cm. The 5 cm of difference is due to the sediment accumulation in 4 years time period elapsed between the two core extractions. Both cores show very similar LOI profiles with clearly identified mid-core section with high organic matter (OM) between about 30 and 50 cm in this core and 5 cm below in core Center. As noted above, the two cores also show similar ^{210}Pb profiles. However, the radiocarbon date performed on pollen concentration located between 53 and 54 cm and corrected for reservoir effect (chapter III) give an anomalous older age of 1314 AD (see below for further discussion).

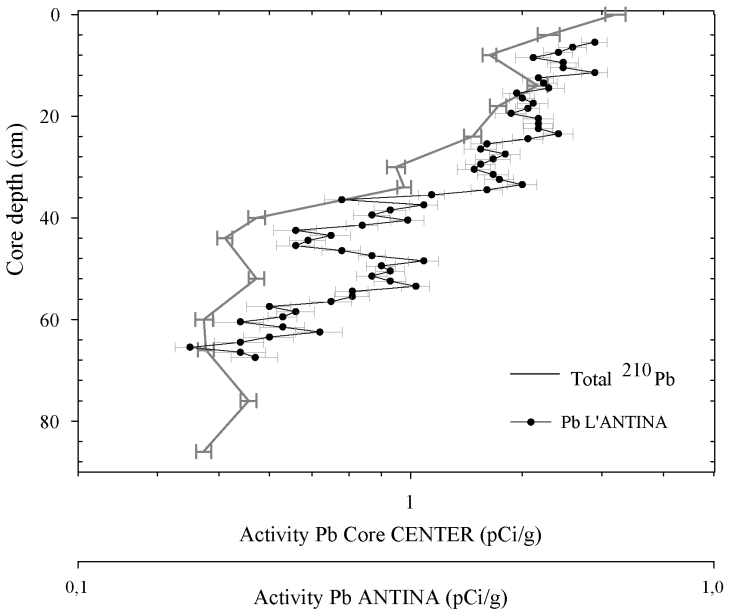

Figure 4.2: Correlation between ^{210}Pb of L'Antina core and Center core as a function of depth and moving down 5 cm L'Antina core.

Figura 4.2*: Correlacione entre los sondeo de L'Antina y sonde centro. Notar que el sondeo de L'Antina se ha desplazado 5 cm hacia abajo.*

LOI, ^{137}Cs, and facies descriptions, allowed the possibility to correlated the present core with the previous one (Center core). As we employed two different corers to take the sediments cores, first, we estimated the compressive factors that influenced the real length of these sedimentary sequences, and then, we displaced 5 cm down L'Antina core ^{210}Pb profile to compare both cores, because Center core was extracted 4 years before L'Antina core (Fig. 4.2). Despite of the difficulties to date this kind of systems and in particularly the Albufera de Valencia, those approximations allowed us to reduce possible dating errors and to reduce the heterospatial variability in the lake at the time to give reliable interpretations.

3.2 Ostracod analyses of core L'Antina: relationships with lithological facies

Approximately 15000 ostracod valves, representing 18 species of ostracods from 17 genera were identified (Appendix 4.1). Three of these taxa were only identified to genus level, mainly due to the low number of valves. SEM images of the taxa are presented in plates 4.1, 4.2 and 4.3. L'Antina sequence was represented by 59 samples (with ostracod remains). Ostracods were absent in only two samples and 16 samples only presented one species. Twenty samples presented between 2-3 species. The highest number of species (9 species) was found in three samples at the bottom of the core, which were as well the samples with the highest ostracod abundances observed along the core; these samples corresponded to the depths: 61; 53; and 54 (between 2217 and 3970 valves*10gdw^{-1}). On the other hand, in the samples located at the top of the core, from surface to 22 cm of depth (Fig. 4.5) the ostracod abundances were very scarce, less than 4 valves*10gdw^{-1}.

The states of valve preservation (SP) were very similar along the sedimentary sequence and between species. Moreover, the poorest preserved valves (type C) were rarely found, being the well preserved ones (types A+B) the most commonly found *C. torosa* was the most frequent species followed by *L. elliptica* and *X. nitida*, at the bottom of the core, and by *C. angulata*, especially at the middle part (Fig. 4.5).

Four sedimentary facies were clearly distinguished: facies A, B, C and E (Fig. 4.3). The facies and associated ostracod fauna are described below.

Facies A: Facies made up by levels with different thickness varying between 3 cm and 12 cm (A1, A2 and A3). This facies is formed by ochre-colored sandy silt sediments, carbonates nodules, coal particles and plant fragments. Bioclasts of mollusks, *Cerastoderma glaucum* valves and foraminifers could be found.

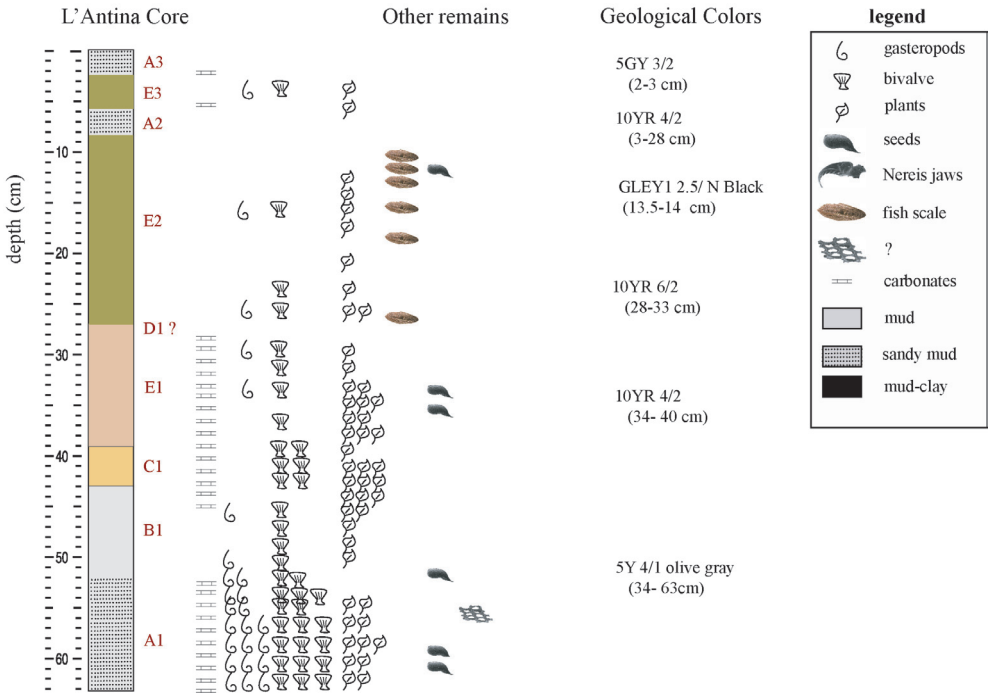

Figure 4.3: Lithological Facies and visual remains of L'Antina Core. Munsell soil colors are also indicated with Munsell's codes on the right.

Figura 4.3*: Facies litológicas y restos visuales del sondeo de L'Antina. Los códigos de colores establecidos en la tabla de colores geologicos de Munsell se sitúan a la derecha.*

Ostracod fauna is different depending on the levels. At the bottom of level A1 (between 62cm and 52cm) presented high abundances mainly composed by the euryhaline *Cyprideis torosa* and the brackish *Loxoconcha elliptica* and *Xestoleberis nitida* at the bottom. On the other hand at the top off level A1 beside brackish water species there are increasing abundances of freshwater ostracods such *Candona angulata* and *Darwinula stevensoni* (Fig. 4.5). This Facies will be equivalent to Facies A6-A5 at core Center. The ostracod fauna at Facies A2 and A3 (between 6 cm and 8 cm and between 3 cm and 0 cm respectively) ostracods were very scarce or absent; when present, the species found were *C. torosa*, *Limnocythere innopinata*, *Sarcypridopsis aculeata* and *Ilyocypris gibba*.

Facies B: This Facies is formed by very fine homogeneous silt with gray coloration. It contained carbon particles (Fig. 4.3) and fibre plants remains of variable length. Bioclasts of molluscs or articulated valves were scarce or absent. In the sequence there is only one level of this lithofacies (B1) between 43 and 52 cm. The ostracod fauna presented low abundances dominated by *C. torosa* remains accompanied by the freshwater species *Candona angulata*, *Darwinula stevensoni* and *Iliocryptus* (Anomopoda, Branchiopoda) at the top of this lithofacies. This Facies will be equivalent to Facies B7 at core Center.

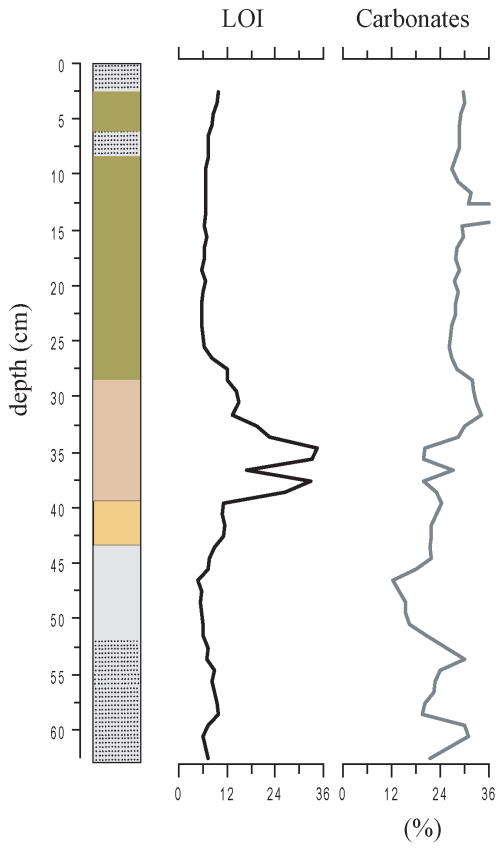

Figure 4.4: Sedimentary L'Antina core column, showing lithological facies, LOI and % carbonates.

Figura 4.4*: Columna sedimentaria del sondeo de L'Antina mostrando las facies litológicas, LOI y carbonatos*

Facies C: Facies made up by homogeneous ochre silt sediments with a moderate proportion of sand, highly enriched on plants remains. One level was identified at this lithofacies (C1=between 39 cm and 43 cm). Facies C1 was composed by short and long fiber plant remains, carbonate particles, bioclasts of molluscs and articulated valves. *C. torosa*, *C. angulata*, *Cypridopsis vidua* and *Ilyocypris gibba* dominated this zone. This Facies will be equivalent to Facies C3 at core Center.

Facies E: Facies formed by homogeneous silt with pink or dark olive coloration and carbon particles (Fig. 4.3) with different thickness (between 3 and 18 cm). Facies E1 (between 27 cm and 39 cm) showed a big discontinuity in sediment composition, between the bottom part of the core and the upper part. Facies composed by soft pink mud sediments, carbonate nodules, carbonate particles and very scarce on plants and mollusks remains. The ostracod fauna at this facies presented low ostracod

abundances, mainly dominated by *C. torosa* and the freshwater species *Candona angulata*, *Darwinula stevensoni*, *Bradleystrandensia* cf *reticulata*, *Paralimnocythere psammophila*, *Limnocythere innopinata*, *Cypridopsis vidua*, *Cypria* sp. among others. This Facies will be equivalent to Facies E1 at core Center. At Facies E2 (between 9 cm and 27 cm) and E3 (between 3 and 6 cm) ostracod fauna was scarce and also very low molluscs or plants remains were found.

3.2.1 Cluster analysis and DCA

Application of statigraphically-constrained cluster analysis (Fig. 4.5) allowed the differentiation of 3 main statigraphical zones, which could be further subdivided onto 6 different subzones. The first zone (zone **1**) covered from 63 to 51 cm depth and it could be further subdivided in two subzones: **1a** and **1b.** Subzone **1a** corresponds to facies type A (from 63 to 55 cm) was dominated by the euryhaline *Cyprideis torosa* and the brackish species *Loxoconcha elliptica* and *Xestoleberis nitida*. The very high abundances of ostracods remains (Fig. 4.5; Appendix 4.1) that were found at the bottom of the subzone are remarkable, especially for *X. nitida*. However, the abundances of these brackish species decreased to the top of this subzone and just at the very top of it, *C. angulata* and *Herpetocypris chevreuxi* appeared but with a very low presence

Subzone **1b** corresponds to a narrow layer from 55 to 51cm depth, involving the top of facies A1 and the bottom of facies B1. This subzone presented the highest ostracod abundances along the core. The number of the abundant *L. elliptica* and *X. nitida* decreased to be drastically reduced at the top of the zone and practically disappeared from the sedimentary sequence above 51 cm. In this subzone, we recorded a rapid increase of *C. torosa* that reached the highest valve abundances along the core and the same was recorded for the freshwater species *C. angulata* and *D. stevensoni* at the middle part of the subzone. However, there is a drastic fall of the number of valves at the top of the subzone. The total number of ostracod valves and the number of ostracod fragments followed the same tendency of these last three mentioned species. Moreover, it is remarkable the repeated appearance of minoritary freshwater species such as *Bradleystrandensia* cf *reticulata*, *P. psammophila*, *L. inopinata*, *H. chevreuxi* and *Limnocythere* cf *stationis* and punctually some valves of *Heterocypris* sp.

The second zone (zone **2**) covered from 51 to 26 cm depth could be further subdivided in two more subzones: 2a and 2b. This zone corresponded to facies B1, C1 and E1. Subzone 2a covered from 51 to 32 cm (most of the last mentioned

facies). The number of ostracod valves was lower than in zone 1 and ostracod fragments showed some peaks at the top of subzone. *C. torosa* maintained more or less constant relatively low levels in this subzone, and *C. angulata* showed abundances similar to those of *C. torosa*. It should be noticed the presence of some valves of *D. stevensoni*, *L. inopinata* and *I. gibba* in the lower half of this subzone. However, in the top half, we observed a rapid fall on *C. angulata* abundances at 38.5 cm, but followed by a recovery and an important presence of the cosmopolitan freshwater species *Cypridopsis vidua*, as well as of *Bradleystrandensia* cf *reticulata* in the top of this subzone, being the main and almost exclusive occurrences of these species along the core. *Cypria* sp. appeared also with low abundances at the top part of the subzone. Most of the *Cypria* sp. individuals presented the morphology of *Cypria subsalsa*; however, the wide variability between *Cypria subsalsa* and *Cypria ophtalmica* (Meisch, 2000) and the lack of sufficient remains, made the identification of these species very difficult. At subzone 2b (from 32 to 26 cm, top of facies E1) the number of valves increased being the most abundant species *C. torosa*, *C. angulata* and *D. stevensoni*. *D. stevensoni*, *P. psammophila* and *L. inopinata* presented two big peaks in this subzone, accounting for the highest abundances for *P. psammophila* and *L. inopinata* along the core. In addition, we also observed some small peaks of *Bradleystrandensia* cf *reticulata*, *C. vidua* and *Cypria* sp. at the bottom of this subzone.

Zone **3** was subdivided in two subzones. Subzone **3a** covered from 26 to 22 cm (facies E2). *C. torosa* and *C. angulata* recovered their previous abundances and immediately decreased to the top almost disappearing. We observed the presence of a few valves of *Bradleystrandensia* cf *reticulata*, *P. psammophila* and *L. inopinata* at the bottom half of this subzone and a few valves of *Sarcypridopsis aculeata* at the top of the subzone.

The last subzone, subzone **3b,** covered from 22 to 0 cm (facies E2, E3, A2 and A3). This subzone presented very low abundances of ostracod valves and ostracod fragments. However, *C. torosa* was still present in most samples. *C. angulata* presented two small peaks at the bottom. Minoritary species as *S. aculeata* appeared at the mid part of the subzone, reaching the highest abundances along the core and *L. inopinata* and *I. gibba* presented some small peaks at the top half part of the subzone.

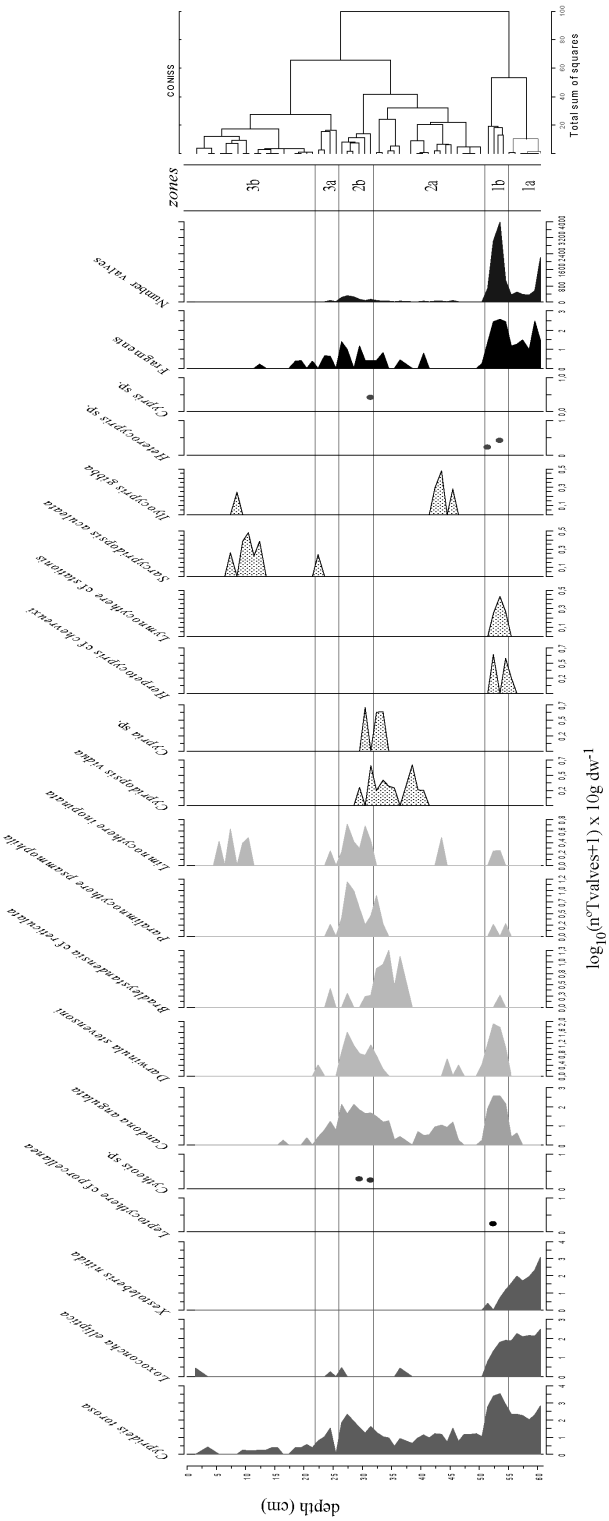

Figure 4.5: Diagram of ostracod abundances as a function of depth in L'Antina core. The total number of valves (states A+B) as well the number of valve fragments are shown in the right-hand columns, all data expressed in valves per 10g dry weight in $\log_{10}$ scale. The established zones by the constrained cluster analysis (CONISS) are shown in the adjacent dendogram. Dots indicates species presence or with very low abundances.

Figura 4.5: *Diagrama de las abundancias de ostrácodos en función de la profundidad en el sondeo de L'Antina. El número total de valvas (SP A+B) y el número de fragmentos se muestran en las columnas de la derecha, todos los datos se expresan por 10g/dw en escala logarítmica. Las zonas establecidas por el análisis de agrupación constreñido por profundidad (CONISS) están representadas en el dendograma adyacente. Los puntos indican la presencia o abundancias muy bajas de dichas especies*

Unconstrained cluster analysis of ostracod abundances (Fig. 4.6), resulted in three main species groups (A, B and C). Group A included only the euryhaline species *C. torosa*, separated from the other two groups probably because of its wide salinity tolerance. Group B included freshwater species; this group can be further subdivided in three more subgroups (B1, B2 and B3). B1 was composed only by *C. angulata*. *C. angulata* is a permanent freshwater species that can tolerate some salinity variations (Meisch, 2000). B2 included only the permanent freshwater species *D. stevensoni* and probably was separated from the subgroup B1 by its reduced salinity tolerance and from group B3 by its permanent ecological recruitments. On the other hand, subgroup B3 included the remaining freshwater species: *P. psammophila*, *L. innopinata*, *S. aculeata*, *I gibba*, *H. chevreuxi*, *Cypris* sp. *Heterocypris* sp., *Limnocythere* cf *stationis*, *C. vidua*, *Cypria* sp., and *Bradleystrandensia* cf *reticulata*. The brackish species *Leptocythere* cf *porcellanea* and *Cytherois* sp. were probably included in this group because their low abundances, suggesting that this material was reworked from other parts of the lake. Group C included the brackish and phytofagus species *L. elliptica* and *X. nitida*.

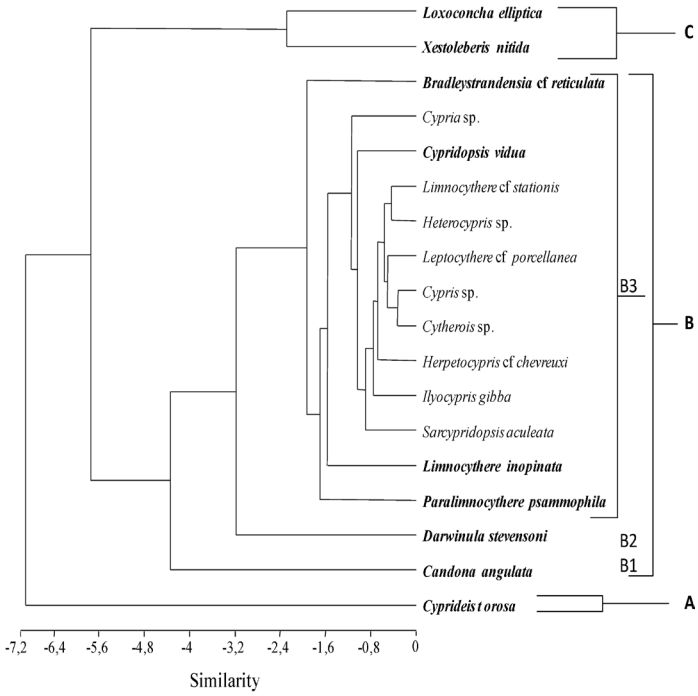

Figure 4.6: Unconstrained cluster analysis of species found in Core L'Antina. The most abundant species ($log_{10}(x+1)$ transformed) are typed in bold italic; the main groups are also indicated.

Figura 4.6*: Análisis de agrupación sin constreñir por profundidad en el sondeo de L'Antina. Las especies más frecuentes transformadas ($log_{10}(x+1)$ están subrayadas en negro, y los principales grupos están indicados.*

The results of PCA are shown in figure 4.7. The main factor (F1) accounted for 57.9% of the total variance and the second (F2) for 30.3%. The species with higher weights on Axis 1 were *C. torosa*, *L. elliptica* and *X. nitida* on the positive part and *S. aculeata* on the negative one. *X. nitida* and *L. elliptica* were again the most important species for Axis 2 in the positive part and *C. angulata* and *D. stevensoni* in the negative one (Fig. 4.7). The samples were grouped on the PCA graph confirming the subzones obtained with the constrained cluster analysis. It clearly separates the three zones and subzones 1a, 1b and 2b. Subzone 1a located in the positive part of both Axis (F1 and F2) was composed by samples dominated by the euryhaline species *C. torosa* and the brackish species *L. elliptica* and *X. nitida*. Subzone 1b, located at the positive part of Axis 1, and at the negative part of the Axis 2, was characterized by samples with main presence of *C. torosa*, accompanied with *L. elliptica*, *X. nitida* but with a co-occurrence at the same level of the latter two species of the freshwater species *C. angulata* and *D. stevensoni*. It is a narrow layer indicating changes and the same is true for subzone 2b, located at the positive part of Axis 1 and at the negative part of the Axis 2. In this subzone the euryhaline *C. torosa*, co-dominates at the same level with the freshwater species *C. angulata* and *D. stevensoni*, but also other species were present, some quite importantly, such as *P. psammophila*, *L. inopinata* and punctually such as *L. elliptica*, *Cytherois* sp., *Bradleystrandensia* cf *reticulata*, *C. vidua*, *Cypria* sp. and *Cypris* sp. Subzone 2a is located between the positive part and the negative part of Axis 1, although most of the samples are located at the negative one. This subzone was characterized by reduced abundances of the euryhaline species *C. torosa* and higher diversity and abundances of freshwater species typical of permanent/semipermanent water bodies such as *C. angulata*, *D. stevensoni* and *Cypria* sp. It is noteworthy, the high abundance of the cosmopolitan freshwater species of semipermanent habitats *C. vidua*, together with other freshwater species (*I. gibba*, *L. inopinata* and *P. psammophila*) and more interestingly the high abundances of the temporary species *B.* cf *reticulata*. Subzone 3a is also a narrow zone of changes, made up by a low number of samples ordered by PCA in the middle of subzone 2a. These samples were composed by *C. torosa* and *C. angulata* and the punctual presence of *L. elliptica*, *D. stevensoni*, *Bradleystrandensia* cf *reticulata*, *P. psammophila*, *L. inopinata*, and *S. aculeata*. Subzone 3b was located at the negative part of Axis 1 and at the positive part of Axis 2. This subzone was characterized by very low abundances of ostracods.

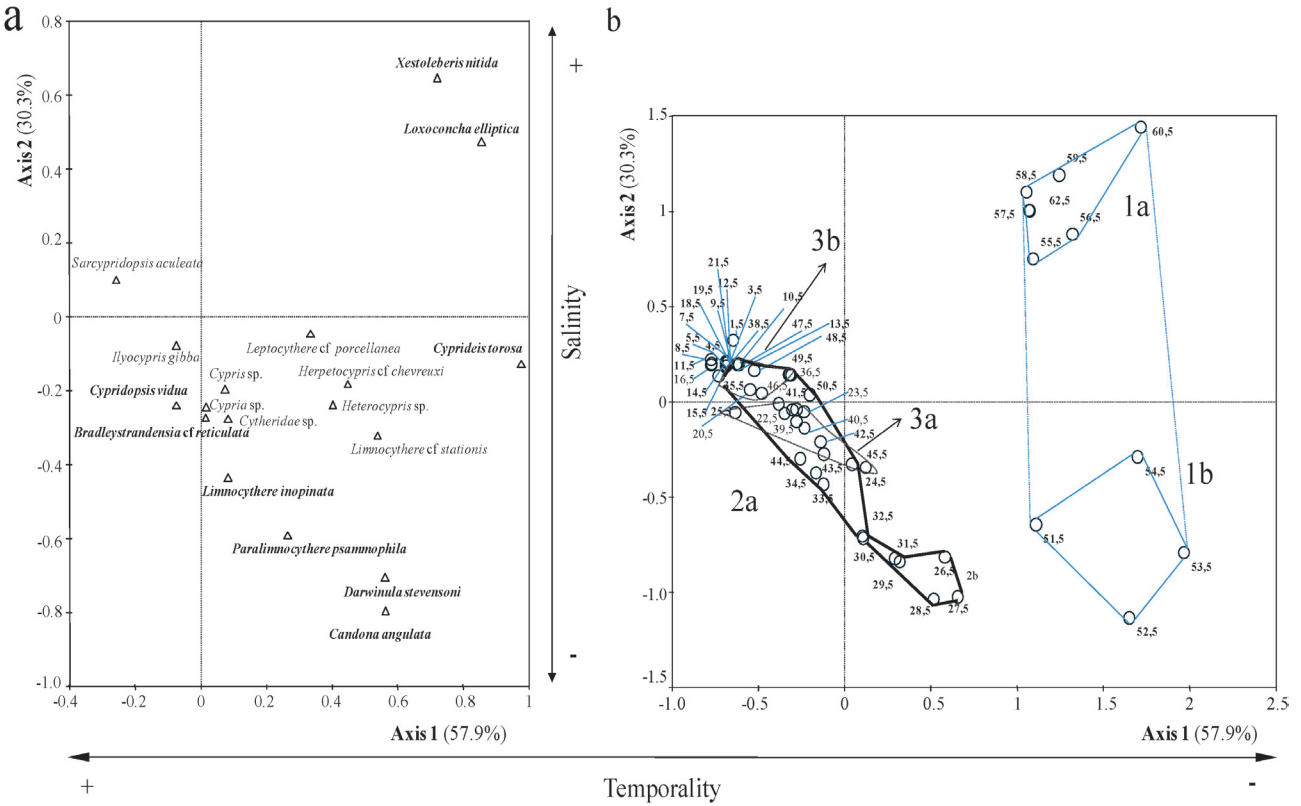

Figure 4.7: Principal component analysis (PCA) of ostracod samples and species for L'Antina core. **a)** Ostracod species are positioned on the first two PCA factors. **b)** Samples labeled by their depth in the core are ordered on the first two PCA factors space and the CONISS established zones and subzones are marked with polygons.

Figure 4.7: *Análisis de componentes principales (PCA).* a*) PCA para las especies de ostrácodos.* b*) PCA para las muestras representadas por su profundidad (cm). Los grupos establecidos en el CONISS están marcados con polígonos.*

3.2.2 Diversity indices

The total amount of ostracod valves varied along the core and between zones (Fig. 4.8). Subzones 1a and subzone 1b showed the highest abundance values observed along the core. Subzone 2a showed intermediate number of ostracod valves and maintained constant levels along the zone. The total number of valves was again high at subzone 2b. Subzone 3a and especially subzone 3b presented a very low number of valves.

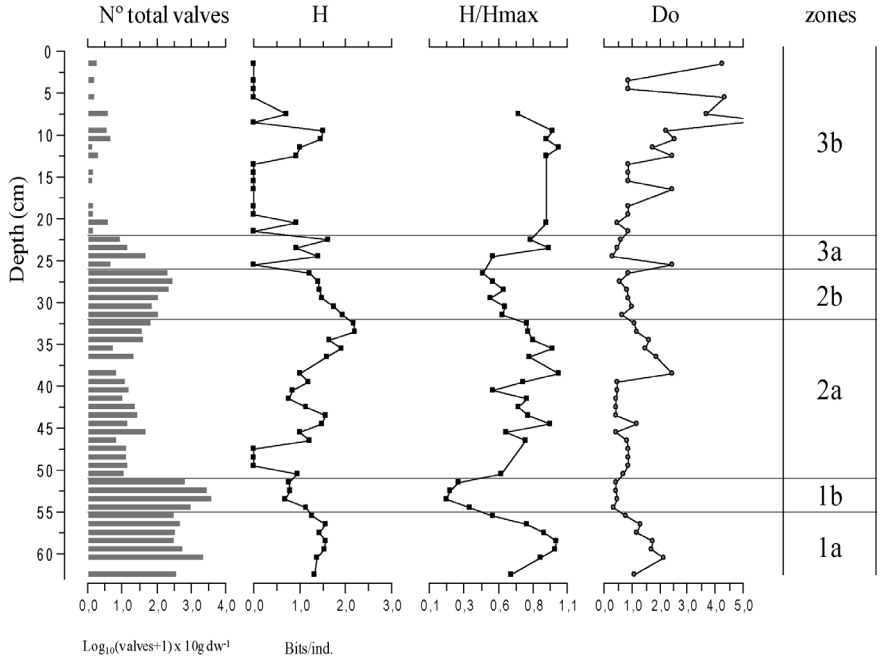

Figure 4.8: Diagram of total abundances of ostracod valves (log(x+1)) for L'Antina core, together with community indices: Shannon diversity index H, evenness index E=H/Hmax, and Dubois fluctuation index D_o.

Figura 4.8: *Diagrama de abundancias totales de los ostrácodos del sondeo de L'Antina (expresados en log de sedimento seco), junto con los índices de las comunidades: índice de diversidad de Shannon H, índice de equitabilidad H/Hmax, índice de fluctuación de Dubois* D_o. *El número total de valvas esta expresado como* log_{10} *(número de valvas+1).*

Regarding to diversity indices (Fig. 4.9), the minimum values corresponded to subzone 3b and samples corresponding to changing conditions (e.g. between zones 1-2 and 2-3). H showed the highest peaks at 32.5 cm and 33.5 cm, where the highest number of freshwater ostracod species was recorded. At subzone 1a and at the top of subzone 2a maximum diversity values were registered (between 1,6

and 2,2 bits/ind). Diversity indices remained high at subzone 1a, and decreased at subzone 1b. At Subzone 2a abrupt diversity changes were registered but it showed a tendency to increase with decreasing depth. On the other hand, diversity indices decreased constantly at subzone 2b. Subzone 3a seems to be a changing period were abrupt changes in diversity indices were registered. Subzone 3b showed the lowest diversity index and its fluctuations are not good indicators due to the low number of valves found.

The changing values of H and E along subzone 2a and subzone 3a showed changes on ostracod assemblages at the top of these subzones. Zones with Do close to cero (1b, 2a bottom half, 2b and 3a) indicated periods closest to average state (dominated by *C. torosa*), although changes were evident due to the fluctuations of biotic indices. In contrast, subzones 1a and 3b and punctual samples at the other subzones showed higher Do values indicating ostracods assemblage's fluctuations with respect to that average state.

3.2.3 C. torosa *ecophenotypic responses*

Between 1 and 104 *C. torosa* adult individuals per sample (females and males) were measured for carapace length (Fig. 4.9; Appendix 4.2). A total of 753 ostracods were measured in the 22 subsamples where adults were present, 371 corresponded to females and 382 to males. LOESS regression was applied for females and males separately and both followed the same trend at all biozones. Valve lengths exhibited significant correlations with the following shell chemistry variables along the core: positively with Ca_{SHELL} (r: 0.347; $p<0.05$) and Sr/Ca (r: 0.53; $p<0.01$) and negatively with $\delta^{18}O_{VPDB}$ (r:-0.408; $p<0.01$). When correlation analysis was done separately by subzones, valve lengths exhibited positive correlations with $\delta^{13}C_{VPDB}$ (r: 0.438; $p<0.05$) and with Sr/Ca (r: 0.426; $p<0.05$) at subzone 1a. At subzone 2a valve lengths showed a negative correlation with $\delta^{13}C_{VPDB}$ (r:-0.533; $p<0.05$) and positive correlation with Sr/Ca (r: 0.574; $p<0.05$). However, the correlations obtained at zones 2, 3 and 4 should be interpreted carefully due to the low number of remains. No significant correlations were found at subzones 2b, 3a and 3b, probably due to the low number of data available for these subzones.

All the counted valves were checked for the presence of nodes (Fig. 4.9). The valves found at the bottom of the core, subzone 1a, were smooth and the percentage of noded forms increased slightly to the top of this subzone.

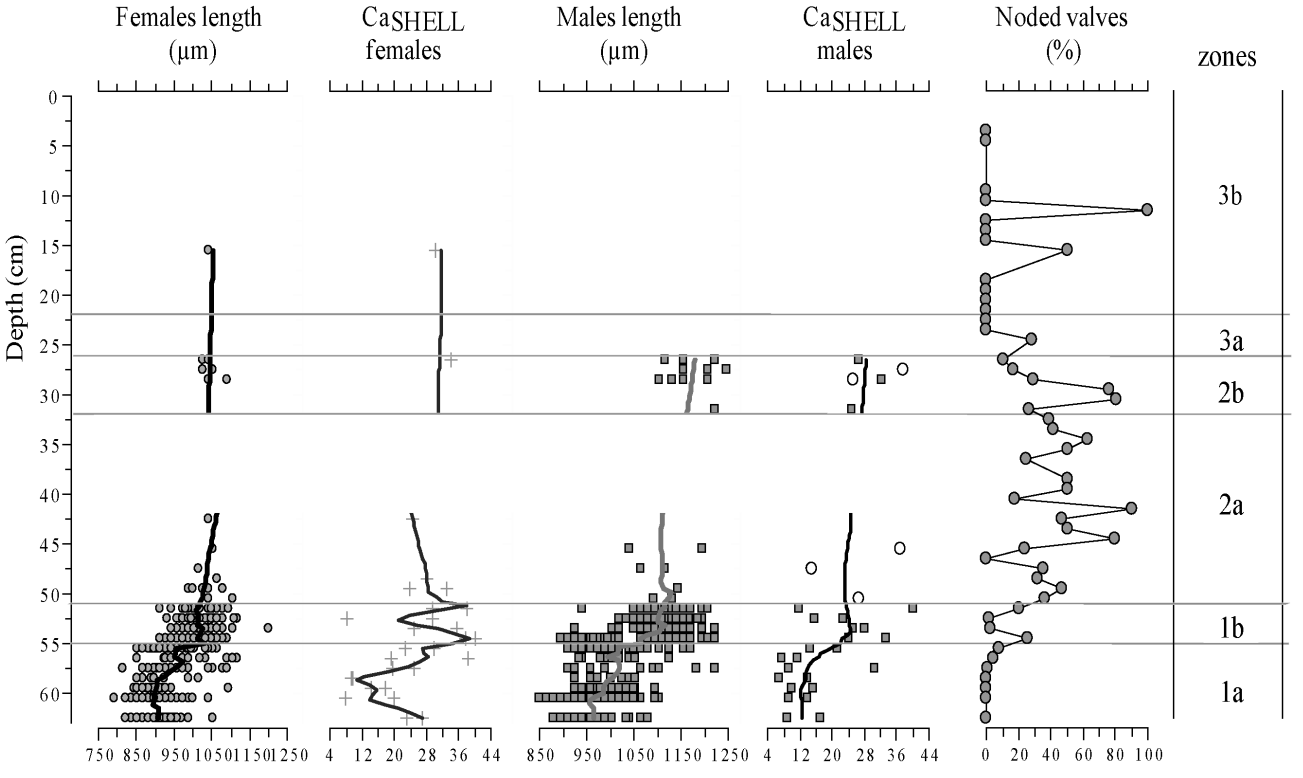

Figure 4.9: *C. torosa* measured lengths for females and males, Ca_{SHELL} per valve for females and males and percentages of noded *C. torosa* valves. LOESS regressions were applied for length values (using average scale of 10 for females and 20 for males) and Ca_{SHELL} values (using average scale of 20 for females and 10 for males). Note: the white circles, at Ca_{SHELL} values for males, indicate samples where males and females were mixed altogether in the analysis.

Figura 4.9*: Longitud de las valvas de hembras y machos de* C. torosa, *Ca_{SHELL} de hembras y machos, el porcentaje de valvas nodadas. La regresión LOESS se aplico sobre los datos de longitudes (factor de escala de 10 para hembras y 20 para machos) y para los valores de Ca_{SHELL} (factor de escala de 20 para hembras y 10 para machos). Notar que los valores de Ca_{SHELL} para machos y hembras con círculos blancos indican muestras donde hembras y machos se mezclaron en el análisis.*

Subzone 1b, showed small peaks at the bottom and at the top of subzone. Subzone 2a showed alternating phases of noded and smoothed forms reaching the highest percentages of noded valves at the bottom half of subzone. Subzone 2b presented high percentages of noded valves at the bottom half of the subzone, however, the percentages decreased to the top of the subzone. Subzone 3a showed a small peak at the bottom. And subzone 3b presented most of the samples with smoothed valves except in two peaks, where the highest percentages were found accounting for the entire core. However, due to the very low number of *C. torosa* valves and probably consisting on reworked remains in zone 3 (especially subzone 3b), these results should be interpreted carefully.

3.2.4 C. torosa *population structure*

Sex-ratio (M:F) at L'Antina core (Fig. 4.10), *C. torosa* M:F, showed values closed to one at subzone 1a with some deviations at the top of this subzone. Some samples at the bottom of subzone 1b showed values displaced to males dominance; however, the population came back to values close to one at the top of subzone 1b. Sex-ratios observed at the other zones showed high deviations from the theoretical distribution (1:1) probably due to the low number of adult remains that were found at these samples. Sex-ratio was not correlated with Juveniles/Adults ratio, valve/carapace ratio or fragments ratio, either analyzing the entire core or each subzone separately.

Juveniles/adults ratio (J/A). We calculated the J/A ratio of L'Antina core (Fig. 4.10). We observed low values at subzone 1a suggesting similar proportions of juveniles and adults valves. Subzone 1b showed slightly higher values and the tendency of the next subzones was to increase at the top of each subzone. J/A ratio was not well correlated with any other estimated taphonomical ratio, when considering the entire core.

Valve/carapace ratio (VCR). We observed a sample with high valve/carapace ratio values at the bottom of subzone 1a, accounting for the highest values in the entire core, suggesting possible rework events. VCR was variable, decreased at the middle of subzone 1a and showed some drastic high peaks at the top of this subzone. Subzone 1b showed changing peaks along the zone, whereas subzone 2a showed relatively low ratios. We observed only three samples with carapaces at subzone 2b, the first two samples located at the bottom presented low ratios and the sample located at the top half presented a high ratio values, suggesting changing depositional conditions to the top. VCR was not well correlated with

any other taphonomical ratio accounting for the entire sequence.

Fragments ratio (FR). The calculated fragments ratio showed high peaks at the bottom half of subzone 1a and low values at the top. We also observed the same pattern at subzone 1b. Subzone 2a presented low values at the bottom half of this subzone, however, some peaks were observed at the top half. These changing peaks were also observed along subzone 2b and 3a. Subzone 3a showed drastic high peaks at the top of this subzone. Subzone 3b showed the highest peaks for the entire core at the bottom half of this subzone. However, the ratio was cero at the top, due to lack of rests.

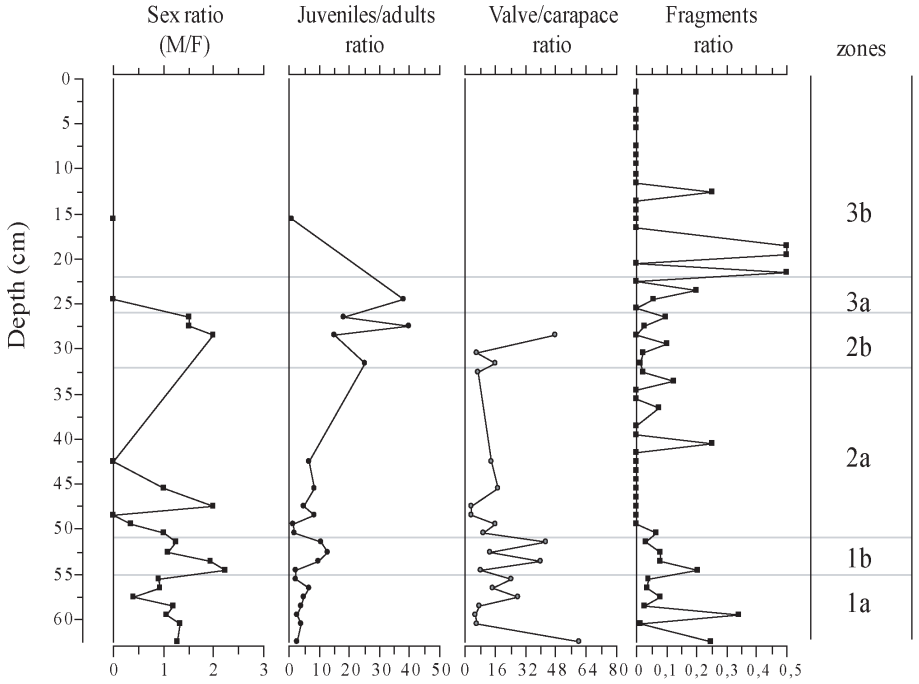

Figure 4.10: Fossil population structure of the ostracod *C. torosa*, and FR (fragments ratio) for the whole ostracod paleoassemblage. Ostracod grouped zones are located on the right column.

Figura 4.10*: Estructura de la población fósil de* C. torosa *y el FR (ratio de fragmentos) para todo el paleoensamblaje de ostrácodos. Las zonas agrupadas para los ostrácodos se sitúan en la columna de la derecha.*

3.3 Trace elements

Trace elements molar ratios for *C. torosa* valves are plotted in figure 4.11. Mg/Ca ranged from 0.0059 to 0.0219 (average value of 0.0114) along the core. Sr/Ca ranged from 3.63 x10^{-3} to 9.58 x10^{-3} (average value of 6.47 x10^{-3}) along the core (Table 3, Fig. 4.11).

Table 4.1: Mean maximum and minimum values of Mg/Ca and Sr/Ca molar ratios from *C. torosa* valves in the different established bio-zones along the L'Antina core.

Tabla 4.1*: Valores mínimos, máximos y medios de los ratios molares de elementos traza (Mg/Ca y Sr/Ca) de* C. torosa *en relación con las biozonas de ostrácodos del sondeo de L'Antina.*

		Mg/Ca (molar) x10^{-3}			Sr/Ca (molar) x10^{-3}		
zones	**nº analyses**	**min**	MEAN±*SD*	**max**	**min**	MEAN±*SD*	**max**
3b	1	8,59	8,59	8,59	7,65	7,65	7,65
3a	4	7,75	9,58 ± *2,1*	12,64	6,25	6,74 ± *0,4*	7,20
2b	23	6,40	9,39 ± *2,9*	18,48	5,83	6,53 ± *0,5*	7,38
2a	23	5,93	11,28 ± *3,8*	19,85	5,46	7,60 ± *0,8*	8,82
1b	16	7,78	11,68 ± *4,0*	21,86	4,22	6,86 ± *1,3*	9,58
1a	28	9,17	13,03 ± *2,0*	16,85	3,63	5,10 ± *1,3*	8,18

Mg/Ca showed low variability at subzone 1a (Table 4.1; Fig 4.10). Zone 1b reported slight lower values for Mg/Ca on average but more variable (average value of 0.012). On the other hand, Sr/Ca showed low variability at the bottom of subzone 1a and increased variability and mean values at the top. The Sr/Ca increased along zone 1b, (average value of 6.9 x10^{-3}) but kept the same standard deviation.

At subzone 2a, Mg/Ca showed values similar for those reported at subzone 1b and the variability increased at the middle of the subzone. However, the results at the top of the subzone showed low variability and were similar to those reported at the bottom. Sr/Ca showed low variability along this subzone (average of 7.6 x10^{-3}). Subzone 2b showed very low variability for Mg/Ca and Sr/Ca. Mg/Ca (average of 0.009) and Sr/Ca (average of 6.53 x10^{-3}) presented low variability compared with the previous subzone (SD: 0.5 and 0.8 respectively) (Table 4.1).

At Subzone 3a due to the low numbers of analyses (4) we can only say that Mg/Ca values were in the range of the previous subzone and with a similar average. The pattern of Sr/Ca values of subzone 3a was also similar to those of subzone 2b. Only one analysis was carried out at subzone 3a; Mg/Ca presented a low value (0.00858) and Sr/Ca a relatively high value (7.65x10^{-3}).

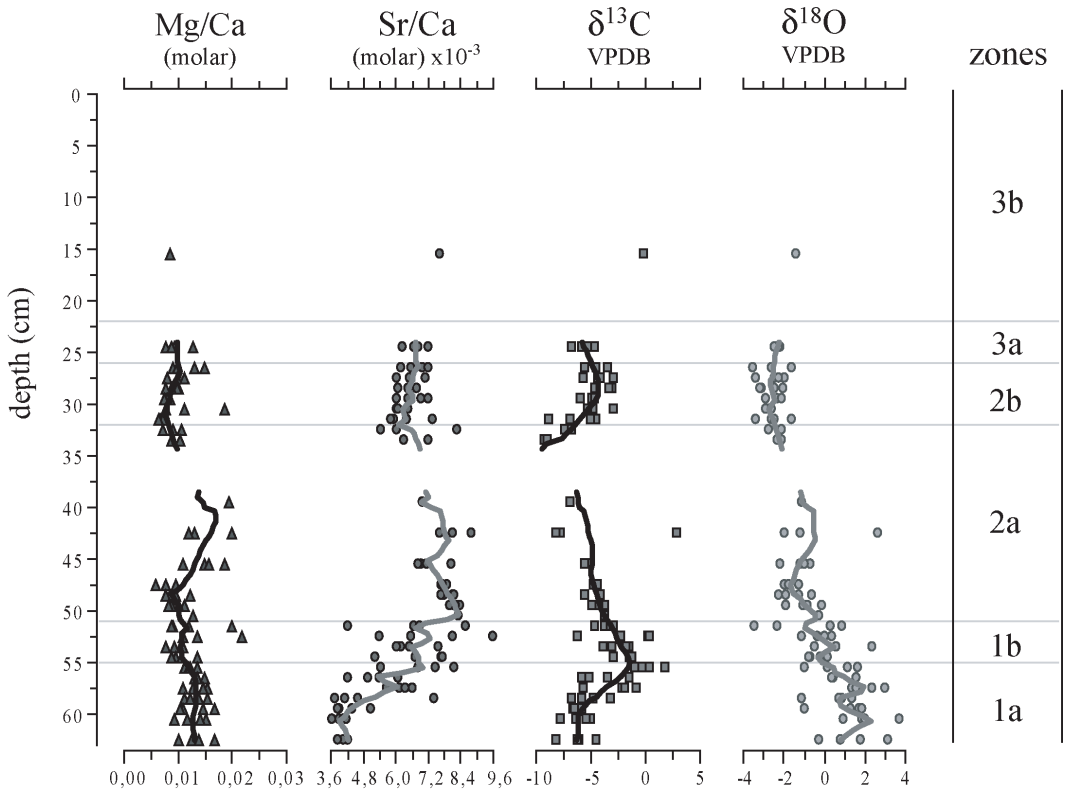

Figure 4.11: Mg/Ca and Sr/Ca molar ratios and isotopic ratios ($^{13}C/^{12}C$ and $^{18}O/^{16}O$) along the sedimentary sequence of L'Antina core, from geochemical analysis performed on *C. torosa* valves. Loess regression was performed for all the variables using average scale of 10 for $\delta^{13}C_{VPDB}$ and Mg/Ca and 20 for $\delta^{18}O_{VPDB}$ and Sr/Ca

Figura 4.11: *Mg/Ca y Sr/Ca ratios molares y ratios isotópicos ($^{13}C/^{12}C$ and $^{18}O/^{16}O$) a lo largo de la secuencia sedimentaria del sondeo L'Antina. La regresión LOESS se aplico a todas las variables usando un factor de escala de 10 para $\delta^{13}C_{VPDB}$ y Mg/Ca y 20 para $\delta^{18}O_{VPDB}$ y Sr/Ca.*

Shell Sr/Ca and Mg/Ca values were negatively correlated (r: -0.37; p<0.01) along the whole core but correlations were not significative separately by subzones suggesting that they were controlled by different factors at each individual subzone.

3.4 Isotope results

C. torosa isotopic results are shown in Figure 4.11, and the ranges and average values for the different bio-zones can be read in Table 4.2. $\delta^{13}C_{VPDB}$ ranged between -9.22 ‰ and 2.95 ‰ (mean value -4.35‰) along the core and $\delta^{18}O_{VPDB}$ ranged between -3.49 ‰ and 3.73 ‰ (mean value of -1.78‰) along the core.

Table 4.2: Minimum, maximum and mean values for isotopical variables ($\delta^{13}C_{VPDB}$ and $\delta^{18}O_{VPDB}$) according to ostracod bio-zones.

Tabla 4.2*: Valores mínimos, máximos y medios de las variables isotópicas ($\delta^{13}C_{VPDB}$ and $\delta^{18}O_{VPDB}$) en relación con las biozonas de ostrácodos.*

		$\delta^{13}C_{VPDB}$ (‰)			$\delta^{18}O_{VPDB}$ (‰)		
zones	**nº analyses**	**min**	MEAN± *SD*	**max**	**min**	MEAN± *SD*	**max**
3b	1		-0,14			-1,35	
3a	4	-6,68	-5,58 ± *0,86*	-4,64	-2,466	-2,31 ± *0,15*	-2,13
2b	23	-8,81	-4,76 ± *1,36*	-2,89	-3,494	-2,57 ± *0,54*	-1,56
2a	23	-9,22	-5,26 ± *2,41*	2,95	-2,724	-1,28 ± *1,08*	2,64
1b	16	-6,18	-2,51 ± *1,69*	0,38	-3,401	-0,30 ± *1,30*	2,35
1a	28	-8,11	-4,29 ± *2,65*	1,81	-1,108	1,23 ± *1,18*	3,73

$\delta^{13}C_{VPDB}$ showed low values at the bottom of subzone 1a but higher variability and higher values towards the top, reaching the highest values for the entire sequence. $\delta^{13}C_{VPDB}$ ranged between -8.11‰ and 1.8‰ (mean: -4.29). On the other hand, $\delta^{18}O_{VPDB}$ showed high variability and the highest values of the entire core at this subzone (mean: 1.23±1.18) descending towards the top. $\delta^{13}C_{VPDB}$ and $\delta^{18}O_{VPDB}$ isotopic ratios were not correlated (p>0.05) at this subzone, suggesting that both variables were affected by different processes. However, $\delta^{13}C_{VPDB}$ was well correlated with Ca_{SHELL} (r: 0.607; p<0.01) and with Sr/Ca (r: 0.706; p<0.01) in this subzone.

The variability of isotopic data at subzone 1b (compared with subzone 1a) was lower for $\delta^{13}C_{VPDB}$ and followed a decreasing trend to the top of the

subzone. $\delta^{18}O_{VPDB}$ was still variable but showed a decreasing trend with respect to subzone 1a (mean: -0.3±1.3 ‰). $\delta^{13}C_{VPDB}$ and $\delta^{18}O_{VPDB}$ isotopic ratios were not correlated ($p>0.05$) at this subzone, but $\delta^{13}C_{VPDB}$ was negatively correlated with Sr/Ca (r: -0.546; $p<0.05$).

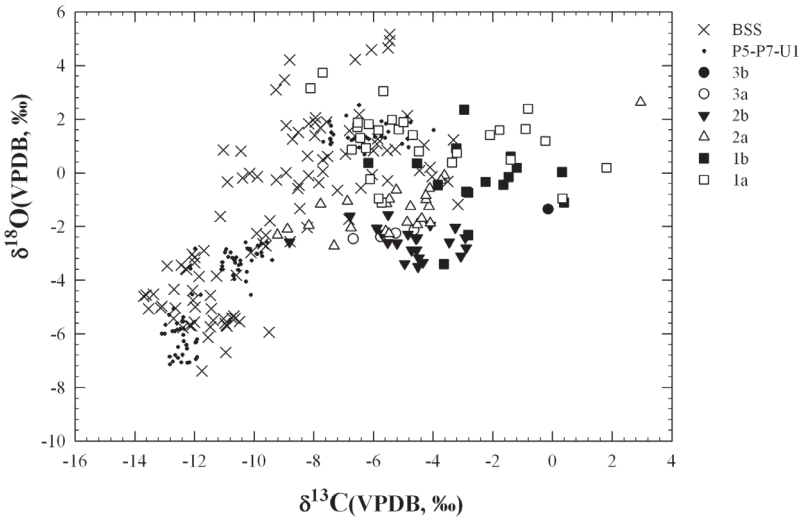

Figure 4.12: Stable isotopic composition ($\delta^{13}C$ and $\delta^{18}O$; VPDB notation) of *C. torosa* calcite valves. The established ostracods biozones samples (1a, 1b, 2a, 2b, 3a, 3b) are plotted over *C. torosa* actual data (Chapter I) recent data (Broad survey: BSS and Monthly survey: P5-P7-U1).

Figure 4.12*: Composición isotópica de la calcita de las valvas de* C. torosa *($\delta^{13}C$ and $\delta^{18}O$; VPDB notación). Las muestras de las biozonas establecidas para los ostrácodos (1a, 1b, 2a, 2b, 3a, 3b) están dibujadas sobre los datos actuales de* C. torosa *(Capitulo I) (Estudio extensivo: BSS y estudio mensual: P5-P7 y U1).*

$\delta^{13}C_{VPDB}$ followed the same decreasing trend at the bottom of subzone 2a as it was observed for the previous subzone (1b) with constant reduction of mean values. The few analyses that were carried out at the middle of subzone 2a showed high variability and the data values for the samples located at the top showed lower values than those at the bottom of this subzone. $\delta^{18}O_{VPDB}$ values obtained at the bottom of subzone 2a were low and presented low variability, the few analyses carried out at the mid part of this subzone showed high variability, whereas the analyzed samples at the top showed low variability and lower values. In general, both oxygen and carbon isotope ratios were lower than at previous zone 1 (Table 4.2, Fig. 4.11). At subzone 2a, $\delta^{13}C_{VPDB}$ and $\delta^{18}O_{VPDB}$ isotopic

ratios were positively correlated between them (r: 0.808; p<0.01). $\delta^{13}C_{VPDB}$ and $\delta^{18}O_{VPDB}$ were also positively correlated with Ca_{SHELL} values for males (r: 0.497; p<0.05 and r: 0.622; p<0.01 respectively).

At the bottom half of subzone 2b, $\delta^{13}C_{VPDB}$ increased and maintained high values until the top of the subzone. $\delta^{13}C_{VPDB}$ was higher on average (mean: -4.76‰) than in subzone 2a. $\delta^{18}O_{VPDB}$, however, presented lower mean values than in the previous subzone (mean: -2.57‰). $\delta^{13}C_{VPDB}$ and $\delta^{18}O_{VPDB}$ were not correlated (p>0.05) for subzone 2b.

The few analyses carried out at subzone 3a showed $\delta^{18}O_{VPDB}$ values similar to the previous subzone and $\delta^{13}C_{VPDB}$ slightly reduced. The only analysis performed at subzone 3b showed slightly higher isotopic ratios than those of the previous subzone.

We plotted, in Fig. 4.12, this core isotopic results altogether with recent data of *C. torosa* shell isotopes (Chapter I). The shells of *C. torosa* of our established ostracod biozones showed similar values of $\delta^{18}O_{VPDB}$ than the shells from brackish and hypersaline places, studied in chapter I. However, $\delta^{13}C_{VPDB}$ values were in general higher than those obtained from the mentioned recent ostracod collections. In general, results from this core compared with data from living ostracods in different localities (Chapter I) fitted well with the expected $\delta^{18}O_{VPDB}$ range in brackish waters but the $\delta^{13}C_{VPDB}$ values exceeded the observed range in living ostracoda and being higher than expected for the corresponding $\delta^{18}O_{VPDB}$ values

3.4 Sr/Ca_{water} and salinity recosntructions

Both past water Sr/Ca and past salinity were inferred from *C. torosa* morphological and geochemical results applying equations of Chapter I. Past water Sr/Ca was reconstructed based in this Sr/Ca ratio from *C. torosa* shells and isotopic results, and salinity reconstruction was based in the prportion of *C. torosa* noded forms and $\delta^{18}O_{VPDB}$. The past water chemistry reconstructions are show in figure 4.13. In general, water Sr/Ca was negatively correlated with salinity (r: -0.687; p<0.01) although both variables were not correlated individually for each different subzones, probably due to the low number of reconstructed water values that were obtained per subzone. The highest salinity values and salinity variability observed for zone 1 were progressively decreasing whereas and simultaneous increase of Sr/Ca was apparent. Reconstructed salinity was high at zone 1, but remained mostly below 10 g/L through the rest of the sequence.

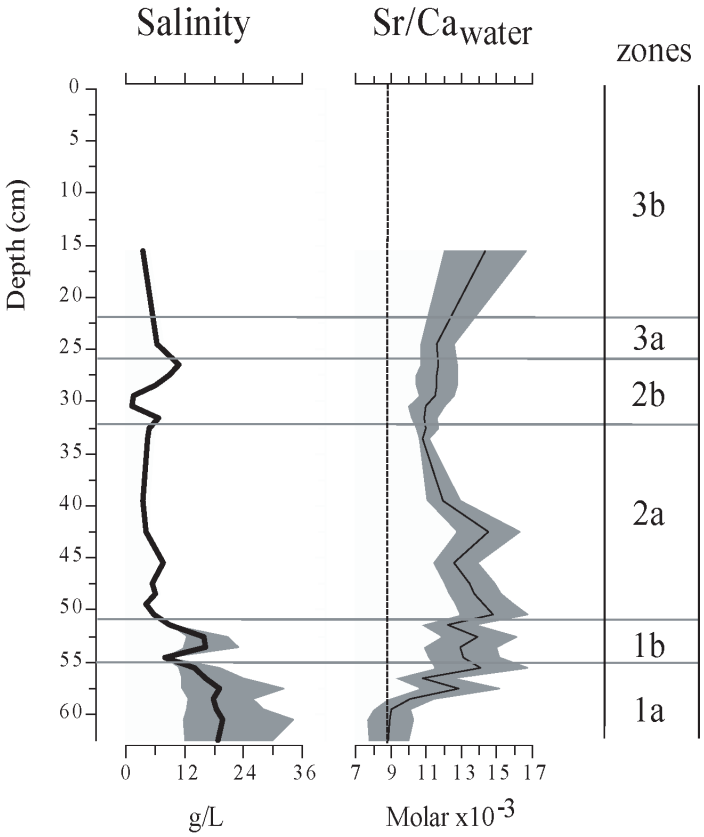

Figure 4.13: Inferred water Sr/Ca and salinity from multivariate regressions (Chapter I). The line indicates the mean estimated value and the shadow parts the minimum and maximum standard errors. The dotted line indicates real sea water Sr/Ca value.

Figura 4.13*: Sr/Ca del agua y salinidades inferidas a partir de las regresiones múltiples (Capitulo I). La línea indica el valor medio estimado y las partes sombreadas los valores de la desviación estándar mínimos y máximos. La Línea de puntos indica los valores reales de Sr/Ca del agua marina.*

4.-Discussion

The Albufera de Valencia ecosystem has been influenced by sea level changes, storm events, flooding, and humid and warm periods along the early mid part of the Holocene (Chapter III; Santiesteban *et al*., in press). In this chapter we will discuss recent changes based on the historical reconstructions focused on the hydrology and landscape evolution of Albufera de Valencia, which has been influenced by humans prior medieval times (Sanchís Ibor, 2001).

Dating sediments in a shallow, productive and largely human controlled system such as the Albufera de Valencia can be highly problematic due to wind-induced resuspension of sediments, diagenetic reactions causing gas generation, washing processes, high sedimentation rates, and bioturbation by benthivorous fish, burrowing insect larvae and humans. For these reasons, L'Antina core was a challenging core to date, but the resulting chronology should be used with caution. However, the statigraphic match between the two cores (L'Antina and core Center) in both LOI and ^{137}Cs, and inferred salinity and water Sr/Ca lends confidence to the overall result. Despite of c:r:s model encompass the last century at L'Antina core (at the bottom: 1900 AD) and contrasting the results with the previous core, we estimated that the year 1900 AD at the bottom of this core is considerably young. Contrasting the different proxies from both cores and the historical archives, we consider that the period located between 1865 and 1927 AD with high hydrological changes should be located around the top of facies A1 (≈52-57 cm) where we distinguished marked statigraphic changes in both cores (around 70-80 cm in core Center).

L'Antina core biozones established based on ostracod paleoassemblages, paleoecological indices and/or geochemical analyses are in concordance with lithological facies descriptions. As we discuss below, the changing ostracod assemblages observed at the different bio-zones are mainly caused by changes in mineral salt composition, pollution increase and loss of macrophyte meadows since the beginning of the last XXth century.

4.1 Core interpretation

In this section, we first discuss the interpretation of the different paleoenvironmental phases that took place in the lake according to bio-zones, based on our multi-proxy data. Finally we relate the recent evolution of the lake in the general context of human's management and salinity changes.

4.1.1. Zone 1

The ostracod paleoassembalges and geochemical analyses along zone 1 (62.5-51cm) represent a changing environment, varying between an Albufera influenced by marine waters and therefore with high salt content (probably mesohaline) to a human controlled oligohaline lake, with waters mostly derived from freshwater inputs (springs, gullies, channels) and minor marine influence to the top of the zone.

Subzone 1a

Subzone 1a (62.5-55cm) is clearly dominated by a brackish ostracod assemblage. *C. torosa*, *L. elliptica* and *X. nitida*. The last one is the most characteristic of this subzone appearing in high abundances at the bottom of it. These species are usually found establishing assemblages that tolerate high salinity fluctuations (transitional environments), mainly in estuaries and coastal lakes with muddy sediments enriched in sands (Ruiz *et al.* 2000a,b, 2006). *L. elliptica* is a brackish phytofagous ostracod species (salinity range: 8-25 g/l; Mezquita *et al.*, 2005) that is adapted to high levels of hydrodynamic energy environment (Carbonel, 1980; Ruiz *et al.*, 2000b). This species can be found in transitional habitats such as coastal lakes or channels, with water currents, close to the transitional zones between the lake and the sea, these places could be zones where mechanical processes such as wave action and wind play an important role. The euryhaline *Cyprideis torosa* (salinity range: 0.2-59 g/l; Mezquita *et al.*, 2005; Chapter I) has slower metabolism and prefers quite zones. *X. nitida* was found at high abundances at this subzone. It is a phytofagus brackish ostracod species although it can tolerate salinities over 30‰ (salinity range: 8-29 g/l; Mezquita *et al.*, 2005) in estuaries and lagoons and usually it is associated with *Zostera* and green algae (Athersuch *et al.*, 1989). The decrease of ostracods and *X. nitida* abundances and the appearance of less halotolerant species such as *C. angulata* could indicate reducing salinities to the top.

Sex ratio values close to one and relatively high juveniles/adults ratio are good indicators that the assemblages represent a natural living population (Kilenyi, 1969; Heip, 1976). Moreover, the VCR ratio was generally low suggesting reduced reworking, except at the first bottom sample where this ratio and FR were high, which could indicate some post-mortem movement of the ostracod carapaces by wave action and resuspension.

Diversity indices (Fig. 4.8) indicated constant environmental conditions at the bottom and the top of this subzone with slight variations at the half bottom. However the increase of *C. torosa* valve lengths, Ca_{SHELL} and the slight increase on the percentage of noded forms at the top of this subzone suggest a reduction in salinity (Van Hartem, 1975; see Chapter I of this thesis).

The high values and the wide scatter of $\delta^{18}O$, and the low $\delta^{13}C$ values (Fig. 4.11) suggest brackish waters with low productivity and low DIC content. The $\delta^{13}C$ of the DIC is influenced (increased) by the input of carbon from different sources, which include atmospheric CO_2, the dissolution of carbon rocks, organic matter mineralization, respiration and photorespiration (Lampert and Sommer, 2007). The $\delta^{13}C$ of the DIC in the water is also influenced by the removal of dissolved inorganic carbon by macrophytes, algae or diatoms during photosynthesis (fixing preferentially ^{12}C) and by carbonate precipitation (Leng and Marshall, 2004).

In Chapters I, we studied *C. torosa* morphological and geochemical traits and their relationships with the surrounding environment in different types of coastal systems and we found that shells of *C. torosa* living in brackish and hypersaline waters influenced by sea waters had similar $\delta^{18}O$ values than those found at this subzone 1a (Fig. 4.12). Thus, we suggest that the bottom of subzone 1a was influenced by sea water or by high evaporation processes that increased salinity. The combination of ostracod paleoassemblages, isotopical data and the historical bibliography suggest that the Albufera was connected and influenced by the sea until the late XIXth century-beginning of the XXth century. $\delta^{18}O$ observed values at the bottom of subzone 1a coincide with values observed for saline or hypersaline places (Chapter I and Fig. 4.12). However, we observed a marked $\delta^{13}C$ increase and a slight $\delta^{18}O$ decrease at the top of subzone 1a. The $\delta^{13}C$ and $\delta^{18}O$ values for autogenic carbonates in closed-basin lakes often covary (Talbot 1990; Li and Ku, 1997). However, for ostracod calcite from L'Antina core at subzone 1a, there is no such correlation and both variables followed opposite trends. In addition, $\delta^{13}C$ was correlated with Ca_{SHELL} and Sr/Ca suggesting

freshwater inputs and similar DIC origin. For that reason, we can attribute $\delta^{13}C$ of DIC increase to a new water source supply, probably the waters with high carbonate contents transported from Júcar River to increase irrigation, and lastly enter in Albufera with an additional increase in $\delta^{13}C$ due to higher primary production. This is in agreement with the slight decrease in the inferred salinity and the occasional appearance apparition oligohaline and freshwater ostracod species such as *C. angulata* and *Herpetocypris* cf *chevreuxi* (salinity tolerance: 0.1-0.4 g/l; Mezquita *et al*., 2005) at the top of this subzone.

The application of different transfer functions to reconstruct past salinities and past Sr/Ca waters based on *C. torosa* (Chapter I) suggest that this subzone had brackish waters (approximately 18g/L) with a salinity decrease to the top. Water Sr/Ca reconstruction suggest that the bottom half of this subzone was influenced by waters, with typical sea water Sr/Ca values (Sr/Ca sea: 8.8 $x10^{-3}$; Renard, 1985; Weinbauer and Velimirov, 1995; de Villiers, 1999). However, Sr/Ca water increased to the top suggesting different water source derived from waters with a higher Sr/Ca ratio. As it was explained in Chapter II, the Sr/Ca increase could be explained by the anomalous high Sr content in the freshwater sources. The waters derived from Júcar river that cross zones of Keuper could explain these anomalies as it was already described for Palmar core and for other cases with similar high Sr anomalies (Müller, 1968, 1969; Anadón and Juliá, 1990). Moreover, historical archives confirm that additional waters from Júcar River were taken at this time to irrigate the increasing extension of rice fields (Sanchís Ibor, 2001). Therefore, both ostracod assemblages and geochemistry results indicate high salinities (brackish) at the bottom half of the subzone 1a and a mixture of waters (possibly from freshwater inputs) to the top. These results are in agreement with the sedimentary descriptions.

Subzone 1b

Subzone 1b (55-51 cm) showed a drastic increase in ostracod abundances at the mid part due to *C. torosa* growth followed by a progressive fall to the top of the subzone. The other brackish species decreased progressively and *X. nitida* almost disappeared at the top of the subzone. The presence of a few valves of the brackish *Leptocythere* cf *porcellanea* usually found in estuaries and bays (Athersuch *et al*., 1989) suggests that there is still some sea water interchange and probably this material was reworked from outflowing channels. In general, at this subzone, ostracod assemblages changed; and an initial increase in permanent freshwater species such as *C. angulata* and *D. stevensoni* was followed by a decrease at the top.

C. angulata is commonly found together with *C. torosa* and other brackish species forming brackish assemblages, it prefers permanent freshwater conditions but it can tolerate some salinity variations (0.2-14‰) (Meisch, 2000). *D. stevensoni* is an ostracod species that can stand salinities of 0.3 to 2.1 g/L (Mezquita *et al.*, 2005) existing a reference of salinity tolerance up to a maximum of 15‰ (Meisch, 2000). These ostracods assemblages are most commonly found in fresh or oligohaline conditions but could also be found in brackish waters. However, the presence of other freshwater species in this zone is remarkable, such as *Bradleystrandensia* cf *reticulata*, *P. psammophila*, *L. inopinata*, *H. chevreuxi* and *Limnocythere* cf *stationis* and more punctually some valves of *Heterocypris* sp. Shannon diversity index (H) and Evenness decreased with respect to the last subzone due to *C. torosa* dominance. The fluctuating index D_o presented values close to cero because of the dominance *C. torosa* with the occurrence of freshwater species is the most representative ostracod composition along this core.

The high number of ostracod remains, relatively high J/A ratio and low FR in the mid of this subzone indicate a low energy environment allowing good preservation, perhaps except the bottom sample were a high FR and sex ratio was observed.

The hypothesis of a higher freshwater input in this subzone consolidating the general salinity reduction observed in the previous subzone was also confirmed by valve morphology and geochemistry. Most proxies indicated that salinity was fluctuant, lower mainly at the bottom and top of the subzone but not so low in the middle. *C. torosa* valve lengths were higher than in the previous subzone, suggesting increasing freshwater input. The weights of Ca_{SHELL}, as well as the percentage of noded valves were also higher than down below, although suggesting increasing freshwater influence at the bottom and at the top of subzone. Finally, the geochemical analysis of *C. torosa* shells showed a general trend of increasing Sr/Ca ratio and decreasing Mg/Ca, $\delta^{18}O$, and $\delta^{13}C$, indicating salinity diminution and lower ratio production/decomposition.

Reconstructed salinity indicated low salinity at the bottom and at the top of subzone 1b, and brackish waters at the half part of subzone similar to these salinities reported for the last subzone, suggesting some salinity influence or evaporation processes although this might be an artifact due to the highest preservation of *C. torosa* compared to freshwater species with thinner valves. Water reconstructed Sr/Ca showed slight variations suggesting a supply of water from similar sources along this period.

4.1.2. Zone 2

A great salinity reduction is supposed to have occurred in this zone indicated by the ostracod paleoassemblages dominated by oligohaline and freshwater species and low values of reconstructed salinity based on *C. torosa* morphology and geochemistry.

Subzone 2a

Subzone 2a (51-32 cm) showed important changes in ostracods assemblages. *C. torosa* is still being the most common species but the increase of *C. angulata* and other oligohaline and freshwater species indicate the establishment of freshwater conditions, specially towards the top. For instance, the cosmopolitan freshwater species *C. vidua* (salinity range=0.3 to 2.3 g/L; Mezquita *et al*., 2005) and *Bradleystrandensia* cf *reticulata* increased at the top. These species can tolerate a wide type of habitats, temporary or semipermanent and they are usually found at high densities related with macrophytes. H and D_o increased at the top, where more freshwater species were found, suggesting changing environments, probably due to the punctual apparitions of different freshwater species (*I. gibba* and *L. inopinata*). *C. torosa* sex ratio, juveniles/adults ratio and % of noded valves at this subzone varied importantly. This together FR, suggest high energy post-mortem environment at the top of this subzone, where more freshwater species were found. Ca_{SHELL} and *C. torosa* valve lengths and percentage of noded animals suggest freshwater conditions similar to those observed at subzone 1b, but no analyses were carried out at the mid part of this subzone.

$\delta^{13}C$ and $\delta^{18}O$ showed a slight progressive decline more pronounced at the bottom of this subzone and both variables were positively correlated. Our data followed the same trend as the waters studied in Chapter I (Fig. 4.12), suggesting salinity reduction. Water Sr/Ca remained constant along the bottom half of this subzone indicating constant water supply from the same sources. Therefore, the big scatter and the low number of ostracod valves observed at the mid part suggest probably reworked material and the few analyses that were carried at the top suggest freshwater conditions. Despite a low number of geochemical analyses in the rest of the subzone, the data suggest maintenance of freshwater conditions.

Inferred salinity suggests a oligohaline environment for the major part of the zone with a small increase fluctuation at the bottom half, where reconstructed water Sr/Ca decreased, suggesting that water came from other sources, probably

due to the important hydrological control by humans that derived waters from the river Júcar through irrigation channels.

Inferred water Sr/Ca indicate two periods of main changes probably due to hydrological modifications, first, between the top of subzone 1a and the bottom of subzone 1b where Sr/Ca increased. And second, between subzone 1b and the bottom of subzone 2a, where salinity and Sr/Ca varied. After the last mentioned period of hydrological control, water Sr/Ca suggests that no controls were exerted at the top of subzone 2a.

Subzone 2b

Subzone 2b showed a slight increase in ostracod abundances, it is characterized by an increase in the euryhaline *C. torosa* and the freshwater species *C. angulata*, *D. stevensoni*, *P. psammophila* (salinity range=0.2 to 1.7 g/L), *L. inopinata* (salinity range=0.8 to 3.7 g/l) and punctually *Bradleystrandensia* cf *reticulata*, *C. vidua*, *Cypria* sp. indicating a more stable freshwater environment (Mezquita *et al*., 2005). The presence of brackish species such as *L. elliptica* and *Cytherois* sp. suggest that this material was reworked from other parts of the lake. Diversity indices decreased slowly to the top of this subzone but these are no important changes, suggesting a stable environment. *C. torosa* sex ratio, juveniles/Adults ratio valve/carapace ratio and FR ratio suggest these were natural living populations at this subzone and not reworked material.

C. torosa valve lengths and Ca_{SHELL} suggest freshwater. Moreover, the percentage of *C. torosa* noded forms suggests freshwater conditions at the bottom and a salinity increase to the top of this subzone. *C. torosa* $\delta^{13}C$ seems to increase from the bottom to the top of this subzone, it coincides with LOI decrease, and the known high phytoplankton photosynthesis (fixing more ^{12}C) and organic matter degradation that probably liberated more CO_2 reducing the $\delta^{13}C$ of DIC (Leng and Marshall, 2004). On the other hand $\delta^{18}O$ and Sr/Ca remained constant, suggesting freshwater conditions and constant freshwater supply along the subzone.

Inferred Sr/Ca seems to be constant along this subzone, suggesting that the waters came from the same sources. Moreover, inferred salinity showed a decrease at the bottom half with oligohaline conditions (≈1.3 g/L).

4.1.3.-Zone 3

Zone 3 was characterized by the abrupt disappearance of ostracod species. At subzone 3a, there were still populations of the dominant species of the previous zone, *C. torosa* and *C. angulata*, but their abundances decreased to the top of subzone and the accompaniment freshwater species were as well present with low abundances. Taphonomical ratios, despite the low number of valves, indicate that most of the valves found were reworked from other parts (high FR). The percentage of *C. torosa* noded forms suggests a freshwater environment at the bottom of this subzone. H and E showed changing fluctuations along this subzone, probably due to the scatter presence of different permanent and temporary freshwater species. A few geochemical analyses were carried out at this zone suggesting similar conditions to the previous subzone. At subzone 3b, if ostracods were present they were composed by the euryhaline *C. torosa*, the brackish *L. elliptica* or by the freshwater cosmopolitan species *L. inopinata*, *S. aculeata* and *I. gibba*. This material probably does not represent natural living populations due to the low number of ostracods valves (Whatley, 1983a,b) and could be reworked from other places (e.g. ricefields surrounding the lake). Inferred salinity and water Sr/Ca was inferred from only one geochemical analysis and the results indicated conditions similar to the previous subzone. The ostracod disappearance could be due to important changes that have occurred in the trophic state of this lake (see below), that drove to the gradual disappearance of ostracods fauna.

4.2.-Evolution of the Albufera Lake during the last century

The study of cores Centre and L'Antina settled the controversy found in the previous studies (Sanchis Ibor, 2001, Sanjaume *et al.*, 1992; Ruiz and Carmona, 2005) about the period of time when humans undertook a high control over the Albufera de Valencia hydrology. The results of these studies confirmed how human influences had an important effect on the solute composition of the Lake, and indirectly on the fauna and submerged flora of the Lake. Ostracod paleointerpretations clearly indicated a previous brackish-marine stage that gradually changed to a freshwater environment from the bottom part of this core to the top in agreement with the previous studies based on other short cores from Albufera de Valencia (Margalef and Mir 1973; Robles *et al.*, 1985).

However, ^{210}Pb and ^{137}Cs dates indicated high sedimentation rates and recent sediments at the bottom of the core, which we hypothesize that they

could be from the first halve of XIX century. On the other hand, we obtained a radiocarbon date at 53-54 cm depth on L'Antina core with a result of 635±5 cal yrs BP. In fact, despite that the analysis was carried out on pollen concentrate material, and although it is supposed that C comes from atmospheric pollen it may be contaminated with other remains coming from subaquatic plants that take C mineral from the water. This altogether with a reservoir effect (Stuiver *et al*., 1986, Stuiver and Becker 1993; Siani *et al*., 2000) could had a high effect in our analysis, giving erroneously older age estimation, for that reason, we applied the Mediterranean correcting factor of 390±85 yrs. However, the result does not fit with our ^{210}Pb and ^{137}Cs age model and we think that the estimated radiocarbon age (635 cal yrs BP=1314 AD) should be interpreted cautiously because the reservoir effect is system specific e.g. such as Gulf of Lyon where the estimated reservoir effect was of 635 years or 480 years in the case of Banyuls (France) at nearby zones of Spanish Mediterranean coast (Siani *et al*., 2000). Concretely, our system was connected to the sea and was irrigated by rivers and gullies and internal springs that cross cretaceous zones, altogether contributing with ^{14}C with different ages.

In agreement with the previous studies based on diatoms and gastropods by Margalef and Mir, (1973) and Robles *et al.* (1985), the initial part of this sequence was characterized by a brackish stage. Moreover, the bottom of the L'Antina core is characterized by the typical sediments of a lagoon-barrier system that suggest that these sediments were influenced by sea waters at that time. Our ostracod paleoecological and geochemical analyses suggest a typical brackish environment (subzone 1a, Fig. 4.5, 4.12 and 4.13) probably due to the mix of waters from rivers, gullies and nearby or internal springs and from Mediterranean Sea. The initial brackish stage (62.5-55 cm) is estimated to occur before the middle of the XIX century. Slow sedimentation rates and a progressive decrease of salinity were observed from the bottom to the top of this interval. Inferred Sr/Ca indicate that the water supply came from the same sources until the mid part of this period where this variable increased rapidly, indicating that water source supply changed. We hypothesized, that this period coincides with the important increase in the control of the hydrology of the lake that occurred in the XX century. In 1865, Spain was under a big economic crisis. This crisis and the high economical expense involved in management the Albufera de Valencia was the reason why the queen Isabel II decided to transfer the property of Albufera of Valencia to the Spanish government (Sanchís Ibor, 2001). The Spanish government decided to allow an agricultural expansion at the area, with the

aim of reducing the economical expenses that supposed the Lake maintenance. The hydrological control by humans started in 1761 with the development of an entire hydrological infrastructure increased between 1865 and 1927 (Sanchís Ibor, 2001). The previous constructed hydrological infrastructures allowed the agricultural rice expansion, and the area of the open lake was importantly reduced, e.g. it lost 5000 ha between 1865 and 1927. Since then, farmers are controlling water supplies and most of the additional waters for irrigation that finally go to Albufera came from the Júcar River. These water inputs provoked the salinity shift of lake waters most probably in the period comprised between 1865 and 1927. Júcar River waters changed the Lake water chemistry, decreasing its salinity and increasing Sr/Ca. Moreover, the salinity reduction favoured the development of big charophyte meadows (*Chara vulgaris*, *Chara hispida*, etc..) and the growth of other freshwater macrophytes which in turn allowed the increase in freshwater ostracod abundances

This changes culminated at the end of subzone 1b (55-51 cm) when the definitive shift from a brackish to a oligohaline lagoon occurred. Our ostracod assemblages and salinity reconstruction indicates that this subzone is an intermediary period with high fluctuations. The euryhaline *C. torosa* increased its abundances, the brackish species disappeared and freshwater species appeared and developed. Inferred water Sr/Ca suggests constant supply from the same sources. At subzone 2a, the low number of ostracod valves and the $\delta^{13}C$ decrease coincide with an oligohaline lagoon with a high development of macrophytes. However, ostracod communities were lost during the las 50 years, and it can be explained by combined reasons (see below). The Albufera suffered an eutrophication process which led first to macrophyte development and later to a turbid state of phytoplankton dominance and macrophyte loss. Eutrophy increased in the Albufera de Valencia which became a turbid hypereutrophic lagoon with a dense phytoplankton population, this change has been documented by different authors to occur in the 1970s (Blanco, 1973; Vicente and Miracle 1992, Romo *et al*., 2008). The loss in macrophytes abundances also allowed the increase of mugilid fish (from 80 to 490 t^{-1} per year; Blanco and Romo, 2006) and the reduction in fish species richness since the decade of 1950, as it was documented by several authors (Docavo, 1979; Blanco and Romo, 2006). Since 1950s, mugilid (*Mugil cephalus* and *Liza aurata*) captures increased in detriment of species such as the predaceous *Anguilla anguilla* or *Dicentrarchus labrax*. Mugilids cannot swim well with dense macrophyte meadows and probably the loss of macrophytes and associated fauna favoured mugilids increase in detriment to

more commercial fishes (Romo, personal communication). The adult mullets are basically herbivorous and detritivorous (Blanco *et al*., 2003), in Albufera they consume superficial sediment, taking also macrozooplankton and zoobenthos, being more benthic with age. The drastic reduction of macrophyte coverage, the increasing benthic disturbance by wind and fishes and the anoxic and reduced conditions of the substrate are main reasons for the drastic reduction of ostracod communities during the last 50 years of Albufera de Valencia (at zone 3), as it was already discussed by Poquet *et al*., (2008) for other Spanish Mediterranean loclaities and particularly by Robles *et al*., (1985) in reference to the reduction of abundance and diversity of gastropods since the late 60's.

The inferred salinity for the next years (≈3g/L) is a little bit higher compared with instrumental data. There are very frequent measurements since 1972 (Blanco, 1973; Vicente and Miracle 1992, Romo *et al*., 2008) and salinity did not reach values over 2 g/L. Due to low ostracod abundances and possibly reworked remains found at these upper samples salinity was over estimated.

Overall, we confirm that the main anthropogenic influence on the Albufera de Valencia started in the last period of the s. XIX and the first period of the last century. The transfer of the Albufera of Valencia to the Central Spanish government by the queen Isabel II and the management, that the government undertook, allowed the development of rice farming and the reduction of the lake area in favor of agriculture. This expansion meant an important hydrologic control of the water inputs and outputs onto the lake. The hydrological control meant increasing input of Júcar River waters (high Sr/Ca content) that drove a salinity reduction. Nevertheless, the new rice farm period also started the use of fertilizers and herbicides/pesticides to fight against weeds and plagues (around 1950s). The use of fertilizers increased the nutrients charge onto the lake that consequently increased the phytoplankton and started the eutrophication process in the coming years (decreasing water DIC too). The loss of macrophyte meadows, the increase of fish filtering superficial sediments and the reduced oxygen content at the substrate provoked a decrease in ostracod abundances. In the last three decades of Albufera de Valencia represent a hypereutrophic lake with consequently loss of ostracod communities (Poquet *et al*., 2008). Several studies have been carried out during this time about hydrology (Soria and Vicente, 2002; Soria, 2006), nutrients loads and eutrophication processes (Soria *et al*., 1987) and phytoplankton tendencies (Romo *et al*., 2008) that showed the high negative human impact suffered by the lake and calling for a more effective water management and reduction of untreated polluted waters input into the lake.

General remarks and conclusions

General remarks and conclusions

The previous chapters illustrate how ostracods can be useful paleoenvironmental proxies in different ways. In the first chapter, we prove how *Cyprideis torosa* morphological and geochemical variables, alone or in combination, can be powerful paleolimnological tools. In the second part, we applied the final conclusions of chapter I to a case of study: the Albufera de Valencia. Three cores were extracted from this lake, one (850 cm long) from the sand bar and two from the middle of the lake (240 cm and 63 cm). The coastal lagoon Albufera de Valencia serves as an example of how to use the shell morphological and geochemical data obtained from a target species (*Cyprideis torosa*), in combination with ostracod paleoassemblages, taphonomical indices and geochemical and sedimentological analyses, to reconstruct the Holocene history of a coastal shallow lake.

C. torosa *calibration* (Part I)

The complexity of paleolimnological studies derives partly from the poor information that is known about concrete aspects of the biology, distribution and morphology of particular biotic proxies and their relationships with the surrounding environmental variables, which may help us to infer past environmental changes. Consequently, a good knowledge of the aquatic systems of the study area is fundamental, including water chemistry, hydrology and geological basin characteristics, which are necessary to understand the functioning of the whole system. We undertook a wide field study which included the analysis of physic-chemical and isotopic composition of the aquatic ecosystems of the Valencia region, and how these traits affect morphological and geochemical ostracod shells traits. The selection of a target species such as *Cyprideis torosa* for its calibration as a paleoenvironmental proxy intended to promote its future use in other similar areas where this species is present. Nevertheless, despite the results of this thesis clarify some previously unanswered doubts (Chapter I) more research is still needed in this field.

Many publications deal with the salinity influence on the morphology of *C. torosa* shells, but we did not find any published comprehensive study that undertook a wider research program testing which particular physic-chemical parameters (e.g. salinity, pH, ionic concentrations...) can affect these morphological variations (carapace lengths, nodes...). Our results show that

morphological variables are good indicators of water chemistry changes, as it was already suggested in the literature (Kilenyi, 1972; Vesper, 1972a,b; Van Harten, 1975, Keyser, 2005). *C. torosa* shell lengths and nodes are influenced by salinity variations. As we observed, comparing our results with the results obtained from the literature (Fig. 1.9), both males and females are smaller at higher salinities. Additionally, shell length and calcium content (Ca_{SHELL}) are positively correlated and animals with the longest shells are also the heaviest regarding to Ca_{SHELL}. Thus, both variables can be used as an indicator of salinity variations and/or of diagenetic processes (non positive correlation between length and Ca), and consequently these could be a useful tool in paleoenvironmental reconstructions. However, we should test if other chemical variables (for instance SO_4 concentration), could affect these morphological variables and *in vitro* experiments should be carried out at different water types to see length and Ca_{SHELL} variations. Furthermore, experiments based on the re-mineralization of the shells to test which diagenetic processes can affect the Ca_{SHELL} should be done (*e.g.* changes in pH may affect the shell calcite).

In the case of *C. torosa* shell nodes, many attempts have been done to establish the relationship between noding and salinity and other variables such as water Ca content (see Sandberg, 1964; Kilenyi, 1972; Vesper; 1972a,b, 1975; Van Harten, 1975, 1996, 2000; Keyser, 2005). Our study suggests that the limiting factor affecting the appearance of nodes is salinity. Moreover, the combination of this variable with the shell $\delta^{18}O$ provides a more accurate tool to reconstruct past salinities than node proportion alone. However, when it comes to apply this equation in sedimentary sequences we should analyse a high number of *C. torosa* shells per sample and discard alocthonous individuals. In addition, this tool presents some deficiencies that should be tested and, in particular, more *C. torosa* recent populations should be analysed to test if this relationship holds in more varied environments and water types.

Many attempts have been made to reconstruct salinity, temperatures or evaporation/precipitation patterns from ostracod Sr/Ca, Mg/Ca, $\delta^{13}C$ and $\delta^{18}O$ during the last years (*e.g.* Engstrom and Nelson, 1991; Von Grafenstein *et al.*, 1992, 1999a,b; Xia *et al.*, 1997a, b; Wansard, 1996b; Wansard *et al.*, 1998; Palacios-Fest and Dettman, 2001; Ito *et al.*, 2002). Regarding to trace elements, we suggest avoiding the use of shell Mg/Ca, Sr/Ca or the Kds from these metals ratios as paleothermometers or paleosalinometers as other authors suggested previously. We saw that *C. torosa* built their shells of low Mg-calcite (with little variation) in a wide gradient of salinities (Chapter I). However, more research should be done

about *C. torosa* shell Mg/Ca composition in waters with Mg/Ca over 6. Further research using *in vitro* experiments with *C. torosa* living in waters with Mg/Ca over 6 and at different temperatures should be performed to test the control of shell Mg/Ca content in the calcification of this species at high Mg/Ca waters.

On the other hand the positive correlation between ostracod Sr/Ca and water Sr/Ca holds at any condition. The lack of covariation of shell Sr concentration with TDS and with other metals concentrations indicates that Sr shell uptake is independent of moulting time or stressful physiological conditions. This variable is a good indicator of different water types supply (waters with different Sr/Ca content) in the system. As we show in chapter I, it seems that this relationship holds for other ostracods, at least from the same genus (Fig. 1.15c). However, future further research should be done to test if this signal works for all ostracod species in general and at any water type.

Our $\delta^{13}C$ results support the use of this variable as an indicator of changes in the isotopic ratio of the dissolved inorganic carbon and indirectly changes of carbon and the productivity of the system may be inferred (Schwalb, 2003; Leng and Marshall, 2004). Our *C. torosa* shells are 2‰ lower than expected from $\delta^{13}C_{DIC}$ reflecting that calcification takes place probably in the infaunal environment. In the future, different experiments should be done testing ostracod shell $\delta^{13}C$ variations in waters with different $\delta^{13}C_{DIC}$ concentrations so as the partitioning of $\delta^{13}C_{DIC}$ in interstitial waters at variable depths.

Oxygen isotopical results support the use of this proxy to reconstruct precipitation/evaporation and salinity changes, as there is a general good match between ostracod and water $\delta^{18}O$ values. However, *C. torosa* seems to incorporate more ^{16}O at salinities over 20 g/L. Stressful conditions at high salinities result in poorly calcified shells with lighter isotopical ratios. For that reason, the use of this proxy to reconstruct past high salinities should be done carefully, and always using other variables that support this proxy.

Paleolimnology of Albufera de Valencia (Part II and III)

The Holocene evolution of the Albufera de Valencia has been interpreted from a multiproxy study of core Palmar with special focus on ostracod paleoassemblages and geochemistry. The location of the core allowed the interpretation of the prograding phases occurred during the early-mid Holocene, as beach barrier systems are suitable for this kind of studies (Zazo *et al.*, 2008). The morpho-sedimentary study carried out by Santiesteban *et al.* (2009) shows the formation of four individual bars that were progressively separating the lake from the sea. The combination of lithological descriptions, paleoecological indices, fossil assemblages and geochemical analyses helped us to understand the Holocene evolution of the Albufera of Valencia, strongly influenced by sea level changes. The Palmar sequence allowed the interpretation of the main marine transgression occurred around 6000 yrs BP and the immediately prograding phase occurred later on, along the Mediterranean Spanish Holocene. In addition, for the first time, our findings showed that the area of Albufera has never been (at least since the mid-Holocene) an open marine system (as thought before), as we did not find any marine-like ostracod paleoassemblage through the entire sequence. However, in order to obtain a better reconstruction of the lower part of the Holocene (Goy *et al.*, 1996), another core close to the bar but in the marine platform should be extracted and a second long core in the middle of the lake, to be able to reconstruct more accurately the chemical water lake changes in this early period. The lack of good sedimentological levels with organic carbon content in this core led us to date pollen concentrates, which usually give older ages because the presence of organic C formed in aquatic environment cannot be avoided. And we had problems to build an accurate age model. Reworking processes and reservoir effects may play also an important role in pollen concentrates and in the likely older resulting ages. For that reason and in future research, the luminescence method should be used to date this kind of sequences highly enriched in sands (Cohen, 2003).

The Palmar sequence encompass an important part of the Holocene probably lacking from one side the earlier sequence and the more recent part from the other side. Thus, to reconstruct the evolution of the lake in historical times, we decided to extract another two short cores, namely core Center and L'Antina core (240 and 67 cm long respectively), in the middle of the lake. Core Center sequence spans overlapping the core El Palmar sequence. Sedimentological composition, geochemical analyses and ostracod assemblages and shell geochemistry interpretations are in concordance with other studies on

Spanish coastal Holocene evolution. We recognize the last marine transgressions *h3* and *h4* (Somoza *et al.*, 1998) occurred during the late Holocene. However, the last one that occurred during the last 500 years (*h5*) is not clearly observed in this record because the lake was highly controlled and exploited by humans during this period. Core data including ostracod paleoassembalges, Sr, Cl and inferred salinity allowed us the interpretation of the changes in solute composition hydrology of the lake that took place during the last 200 years. N, P and LOI also gave us information about macrophytes cover and the indiscriminate use of fertilizers along the last 100 years. The phosphorous load increased markedly in the lake favoring the eutrophication of the lake and completely eliminating the macrophytes cover at the beginning of the 1970 decade.

In L'Antina core, we combine ostracod paleoecology and geochemistry at high resolution to see with more detail the last 200 years of the Albufera evolution. The different extraction location of this core and the good correlation with the previous one, support the general view of our interpretations and suggest that the effects of the heterospatial differences in the lake are of minor importance in this case. This core supports the previous interpretations of salinity reduction and hydrological management during the last 100 years. Furthermore ^{210}Pb and ^{137}Cs dates, as well as radiocarbon dates match well between both cores, however, radiocarbon dates ^{14}C did not fit well with ^{210}Pb chronological models. We used pollen concentrations for radiocarbon dates for all the cores (chapters II, III and IV), and as we explained in chapter III and IV, there may be several effects that give anomalously old ages. For further research in this kind of systems more dating should be done in different kind of material, to compare and precise the dates and the age model for more accurate paleoenvironmental reconstructions.

The main objectives of this thesis have been fully covered. *Cyprideis torosa* calibration demonstrated that ostracods may be useful paleoenvironmental proxies. Our results discourage some previous ideas about the use of ostracod shell geochemistry to reconstruct salinities and temperatures (based on Mg/Ca and Sr/Ca), employed in other paleolimnological studies. We support some other findings such as the salinity influences in ostracod morphological variables (lengths and nodes), oxygen isotopes and ostracod assemblages. Furthermore, we contribute with new information, such as the possibility to reconstruct water Sr/Ca from ostracod Sr/Ca or to infer water isotope composition and salinity from the combination of morphological variables (nodes) and shell isotopic data (δ^{18}O). In addition, we contributed to clarify the Holocene evolution of Albufera de Valencia and to disclose the main factors determining major variations in this

lagoon, such as sea level variation effects, hydrological changes, eutrophication, heavy metal pollution and some other human influences.

Conclusions

The general conclusions of this thesis can be summarized as follows:

1.-Morphology and geochemistry of valves of ostracod target species that are present in a wide physic-chemical gradient can be calibrated to approach possible ways to reconstruct environmental variables. The results should always be used in combination with other paleoenvironmental proxies to avoid possible misinterpretations.

2.-With our sampling program, it was not possible to assess the exact time and the environmental conditions when the ostracods moulted and calcified, because *C. torosa* populations showed overlapping adult generations through the year in the studied sites (P5-P7-U1). Juveniles shell traits, however, might reflect water changes with higher resolution, due to the shorter time interval between moults of juvenile stages, comparing to those of adults. *Cyprideis torosa* individuals with the longest shells are also the heaviest regarding to shell calcium content (Ca_{SHELL}). In addition, shell size is correlated with water chemistry; both males and females are smaller at higher salinities. The low salinities and water Alk/Ca ratio, between 1 and 2, in the studied waters seems the optimal to build more calcified shells.

3.-According to our results salinity reconstruction from *C. torosa* shells cannot be done correctly by geochemistry alone and needs information from shell morphology. It is known that the proportion of noded individuals of *C. torosa* may be one of the best proxies for salinity reconstruction. The combination of noding and $\delta^{18}O$ provides a more accurate quantitative reconstruction model.

4.-There are no differences in geochemical composition (isotopic and trace metal ratios) between sexes in *C. torosa* shells. Subsequently in paleoecological studies there is no need to analyze sexes separately when using these geochemical variables. However, the use of size and Ca_{SHELL} as paleoenvironmental proxies should take into account sex differences.

5.-No effects of either temperature or water Mg/Ca is observed on Mg/Ca assimilation in the ostracod *C. torosa* in waters with a Mg/Ca ratio below 6. *C. torosa* builds shells with low Mg/Ca in a wide salinity gradient. However, in other studies that involved higher water Mg/Ca ratios a direct relationship between these and ostracod Mg/Ca was observed for other particular species (*Cyprideis australiensis*) De Deckker *et al.* (1999), and therefore more research is needed to clarify this response pattern.

6.-Ostracod shell Sr/Ca in *C. torosa* is strongly and significantly related to water Sr/Ca. In fact, regression analyses show that reconstruction of water Sr/Ca from ostracod Sr/Ca is the most accurate (in statistical terms) paleoenvironmental proxy using *C. torosa* shells.

7.-In *C. torosa* there is a significant positive relationship between ostracod $\delta^{18}O$ and water $\delta^{18}O$. However, at high salinities (> 20 g/L) more ^{16}O is incorporated into the shell as observed in previous works studying calcification under stressful conditions (Xia *et al.*, 1997a; Chivas *et al.*, 2002).

8.–$\delta^{13}C_{DIC}$ can be inferred from *C. torosa* $\delta^{13}C$ and indirectly changes of carbon and the productivity of the system may be estimated. $\delta^{13}C$ in *C. torosa* shells are 2‰ lower than expected from $\delta^{13}C_{DIC}$ reflecting that calcification probably takes place in the infaunal environment.

9.-Multiple regressions helped us to reconstruct past hydrochemistry from proxies derived from ostracod shells. The given equations can asses' salinities and water Sr/Ca in a quantitative manner, always with a combination of several paleoenvironmental proxies to avoid the possible errors included in the equations.

10.-The Palmar sequence results corroborated that beach barrier systems are good sedimentological sets to reconstruct sea level Holocene fluctuations. At Palmar core two sedimentary steps can be recognized which coincides with the same sea level changes observed at other Spanish Mediterranean locations (Zazo *et al.*, 2008). This core can be interpreted as a sediment sequence over the main marine transgression and the immediately prograding phase that occurred along the Mediterranean Spanish Holocene, in concordance with other studies on coastal Holocene evolution.

11.-The Albufera was an ancient enclosed bay connected to the sea at the early Holocene. However, our records did not found an established ostracod marine assemblages suggesting that the Palmar sequence corresponds to an elongated lagoon connected to the sea by a outlet, but restricted to its southern end, as derived from historical archives. The ostracod fauna and isotopical ratios are characteristic of a brackish water type environment.

12.-Core Center sediment sequence spans a period corresponding approximately to the last 3400 years, if we could trust the ^{14}C datations at the bottom of this core, but it is probably younger. Sedimentological composition, ostracod assemblages and geochemical analyses interpretations are in concordance with other studies on Spanish coastal Holocene evolution. Here, we recognized the last marine transgressions *h3* and *h4* (Somoza *et al.*, 1998) occurred during the late Holocene and how these affected the ostracod fauna and the salinity of the lake. However, the last marine transgression that occurred during the last 500 years (*h*5) is not clear in this record because the lake was highly controlled and exploited by humans during these years.

13.-From geochemistry and ostracod species composition, we conclude that the main desalinization of the Albufera took place later than thought before, in the last quarter of the XIX century, when rice field expansion occurred, thus leading humans to undertake the control of the lake hydrological system for irrigation (Sanchís Ibor, 2001).

14.-Eutrophication processes increased the nutrient load of the lake, indicated with the higher total P in the upper sedimentation, initially favoring macrophyte abundances, and later provoking a change of state to a phytoplankton dominance and disappearance of submerged macrophytes. The untreated sewage from Valencia city and the surrounding towns increased the nutrients load onto the lake favoring a drastic eutrophication process. The dense macrophyte cover disappeared from the lake by the end of 1960 and the lake sediment was completely bare in the first years of 1970.

15.-The recent loss of ostracod populations in the lake observed in this work may be explained by the lack of oxygen derived from the increasing eutrophication processes (Poquet *et al*., 2008), metal pollution at the bottom sediments, changes in hydrology, macrophyte loss and fish population shifts. From the XRF results, we can conclude that there has been a heavy metals load in the lake from spills of the nearby industries (especially Cu and Zn) in the last

three decades and a older accumulation of lead due probably to intensification of hunting activities with the use of lead bullets.

16.-According to the results from core Center and L'Antina core, during the last 200 years, the Albufera de Valencia showed the typical patterns observed for this kind of systems around the world (Halpern *et al*., 2008); the high human pressure mainly based on the hydrological control of the lake, wastewater and industrial sewage pollution, rice field expansion and hunting affected the whole system droving the lake to a highly deteriorated system.

Conclusiones

A continuación se resumen las conclusiones generales de la presente tesis:

1.-Las variables morfológicas y geoquímicas de especies clave de ostrácodos que ocupan amplios gradientes físico-químicos, pueden ser calibradas como herramientas para reconstruir variables ambientales. Los resultados obtenidos a partir de estas herramientas, siempre deben ser contrastados con otros indicadores paleoambientales para evitar posibles interpretaciones erróneas.

2.-Con nuestro diseño experimental de muestreo, no fue posible detectar el momento preciso y las condiciones ambientales en los que los ostrácodos mudaron y calcificaron, debido a que las poblaciones de la especie *Cyprideis torosa* mostraron diferentes generaciones de adultos solapadas a lo largo del año para los puntos de estudio (P5-P7-U1). Sin embargo, la composición geoquímica de las conchas de los juveniles puede reflejar, con mayor resolución, los cambios químicos del agua. Esto es debido a que los juveniles muestran intervalos más cortos de tiempo entre mudas, comparado con los adultos, pudiendo así reflejar mejor estos cambios. Los individuos de *Cyprideis torosa* más grandes, respecto a la longitud de las valvas, también presentan un mayor contenido en Ca en las valvas. Además, el tamaño de la concha esta correlacionado con la química del agua; machos y hembras son más pequeños a altas salinidades. Las bajas salinidades y la Alk/Ca del agua (entre 1 y 2) en los cuerpos de agua estudiados, parecen ser las condiciones más óptimas para desarrollar conchas más calcificadas en la especie *C. torosa*.

3.-Según los resultados obtenidos de los modelos de reconstrucción de la salinidad a partir de las conchas de *C. torosa*, ésta no puede realizarse correctamente con la geoquímica por sí sola y se necesita la información morfológica de las conchas. Se sabe que la proporción de individuos nodados de *C. torosa* puede ser uno de los mejores indicadores para reconstruir salinidades. La combinación de nodos y $\delta^{18}O$ nos facilita un modelo de reconstrucción cuantitativa más ajustado.

4.-No existen diferencias en la composición geoquímica (isótopos y elementos traza) entre sexos de las conchas de *C. torosa*. Consecuentemente, no es necesario analizar sexos separadamente cuando se requiera utilizar estas variables geoquímicas. Sin embargo, a la hora de utilizar el tamaño y la cantidad de Ca en las valvas como indicadores paleoambientales deberían tenerse en cuenta las diferencias entre sexos.

5.- No se observaron efectos de la temperatura o la concentración de Mg/Ca en el agua sobre la asimilación de Mg/Ca por parte de ostrácodo *C. torosa* en aguas con Mg/Ca<6. *C. torosa* construye conchas de calcita pobre en magnesio en un amplio gradiente de salinidades. Sin embargo, se observaron relaciones directas entre el Mg/Ca del agua y del ostrácodo en estudios realizados con altas concentraciones de esta variable y en la especie *Cyprideis australiensis* (De Deckker *et al*., 1999), por ello es necesario investigar más acerca de este patrón de respuesta.

6.-El Sr/Ca de las conchas de *C. torosa* esta fuertemente y significativamente relacionado con el Sr/Ca del agua. De hecho, el análisis de regresión muestra que la reconstrucción del Sr/Ca del agua a partir del Sr/Ca del ostrácodo es el indicador paleoambiental más fiable (en términos estadísticos) usando las conchas de *C. torosa*.

7.-Existe una relación positiva y significativa entre el $\delta^{18}O$ de los ostrácodos y el $\delta^{18}O$ del agua. Sin embargo a altas salinidades (>20g/L) más ^{16}O es incorporado en las conchas, como se observo en estudios previos estudiando la calcificación bajo condiciones de estrés (Xia *et al*., 1997a; Chivas *et al*., 2002).

8.-El $\delta^{13}C_{DIC}$ puede ser inferido a partir del $\delta^{13}C$ de *C. torosa* e indirectamente los cambios de carbono y la productividad del sistema. El $\delta^{13}C$ de las valvas de *C. torosa* es 2‰ más bajo que lo esperado para el $\delta^{13}C_{DIC}$, reflejando que la calcificación probablemente tiene lugar en zonas intersticiales del sedimento.

9.-Las ecuaciones obtenidas a partir de las regresiones múltiples nos pueden ayudar a reconstruir la hidroquímica del pasado a partir de indicadores derivados de las conchas de ostrácodos. Con las ecuaciones mostradas se pueden inferir salinidades y el Sr/Ca del agua de una manera cuantitativa, pero siempre deberán ser utilizadas en combinación de otros indicadores paleoambientales para evitar posibles errores incluidos en estas.

10.-Los resultados de la secuencia del sondeo Palmar corroboran que los sistemas de playa-barrera-laguna contienen información muy valiosa en sus sedimentos, de tal modo que se pueden reconstruir las variaciones del nivel del mar durante el Holoceno. En el sondeo Palmar se pueden reconocer dos eventos sedimentológicos, los cuales coinciden con los mismos cambios de nivel del mar observados en otras regiones Mediterráneas Españolas (Zazo *et al*., 2008). Este sondeo puede ser interpretado como una secuencia sedimentaria

enclavada sobre la principal transgresión marina ocurrida durante el Holoceno Mediterráneo Español (*h1*) y la inmediata fase de progradación ocurrida después, en concordancia con otros estudios sobre la evolución del Holoceno en la costa Mediterránea Española.

11.-La Albufera de Valencia fue una antigua bahía enclavada y conectada con el mar en el Holoceno temprano. Sin embargo, en nuestros registros no se ha encontrado una asociación marina de ostrácodos bien establecida, sugiriendo que la secuencia del Palmar correspondía con una laguna costera alargada conectada con el mar por un amplio canal, localizado en la zona sur, como se deduce de los archivos históricos. La fauna de ostrácodos y los ratios isotópicos indican ambientes de aguas salobres.

12.-La secuencia de sedimentos del sondeo Centro abarca el periodo correspondiente a aproximadamente los últimos 3400 años, si asumimos la veracidad de las dataciones de ^{14}C, aunque probablemente la base del sondeo se pueda especular como de procedencia más reciente. Las interpretaciones sobre la composición sedimentológica, las asociaciones de ostrácodos y los análisis geoquímicos están en concordancia con otros estudios realizados sobre la evolución Holocena de las costas Mediterráneas Españolas. En este sondeo se reconocen las últimas transgresiones marinas *h3* y *h4* (Somoza *et al.*, 1998) ocurridas durante el Holoceno y cómo estas afectaron a la composición de la fauna de ostrácodos y la salinidad del lago. Sin embargo, la última transgresión marina que ocurrió durante los últimos 500 años (*h5*) no esta clara en está secuencia porque el lago estuvo altamente controlado y explotado por los humanos durante estos años.

13.-De la geochímica y la composición de especies de ostrácodos, concluímos que la principal desalinización del lago de la Albufera ocurrió más tarde de los asumido anteriormente, a finales del siglo XIX, cuando tuvo lugar la expansión del arroz, permitiendo así a los humanos tener el control hidrológico del sistema (Sanchís Ibor, 2001).

14.-Los procesos de eutrofización incrementaron la carga de nutrientes en el lago, indicado por la alta acumulación de fósforo total en el techo del sondeo, favoreciendo inicialmente el incremento de las abundancias de macrófitos y provocando el posterior cambio hacia un estado de dominancia fitoplanctónica, con la consiguiente desaparición de los macrófitos. La aguas, sin tratar, procedentes de la ciudad de Valencia y de las ciudades de alrededor,

incrementaron la carga de nutrientes en el lago favoreciendo los procesos drásticos de eutrofización. La densa capa de macrófitos desapareció del lago hacia finales de los años 60 y completamente del fondo del lago a principios de los años 70. Esto afectó a la comunidad de ostrácodos que vió disminuida su abundancia de manera considerable.

15.-La reciente perdida de las poblaciones de ostrácodos en el lago observadas durante los últimos años pueden ser explicadas por la falta de oxígeno derivada del incremento de los procesos de eutrofización (Poquet *et al*., 2008), contaminación por metales en los sedimentos, cambios en la hidrología del sistema, perdida de macrófitos y cambios en la composición de las poblaciones de peces. De los resultados obtenidos del XRF, podemos concluir que ha habido una acumulación de metales pesados (especialmente Cu y Zn) en el lago debido a los vertidos incontrolados de las empresas cercanas a este en las últimas decadas, y una acumulación más antigua de plomo, probablemente debida a la intensificación de la caza y el uso de munición con alto contenido de este elemento.

16.-Como se deduce del estudio de los sondeos cortos de L'Antina y Centro, durante los últimos 200 años, la Albufera de Valencia há mostrado los típicos patrones de evolución observados para este tipo de sistemas en todo el mundo (Halpern *et al*., 2008); la alta presión humana basada principalmente en el control hidrológico del lago, las aguas residuales y los vertidos industriales, la expansión del arroz y la caza afectaron de manera sustancial al sistema, conduciendo al lago a un estado altamente deteriorado.

References

Ahearn G. A., Duerr J. M., Zhuang Z., Brown R. J., Aslamkhan A., and Killebrew, D. A. 1999. Ion Transport Processes of Crustacean Epithelial Cells. *Physiological and Biochemical Zoology*, **72** (1): 1-18.

Alfonso, M.T. and Miracle, M.R. 1990. Distribución espacial de las comunidades zooplanctonicas de la Albufera de Valencia. *Scientia Gerundesis*, **16** (2): 11-25.

Álvarez-Cobelas, M., Rojo, C. and Angeler, D. 2005. Mediterranean limnology: current status, gaps and future. *Journal of Limnology*, **64** (1): 13–29.

Anadón, P. 2005. Reconstrucción de condiciones ambientales a partir de geoquímica de conchas de moluscos y ostrácodos. In: Alcorlo, P. Redondo, R., Toledo, J. (eds). *Nuevas técnicas metodológicas aplicadas al estudio de los sistemas ambientales: los isótopos estables*. Libro de resúmenes jornadas técnicas: 65-92.

Anadón, P. and Julià, R. 1990. Hydrochemistry from Sr and Mg contents of ostracodes in Pleistocene lacustrine deposits, Baza Basin (SE Spain). *Hydrobiologia*, **197**: 291-303.

Anadón, P., Gliozzi, E. and Mazzini, I. 2002. Paleoenvironmental reconstruction of marginal marine environments from combined paleoecological and geochemical analyses on Ostracods. In: J. Holmes and A. Chivas, Editors, *The Ostracoda: Applications in Quaternary Research*, *Geophysical Monograph*, **131**: 227–247.

APHA. 1992. Standard methods for the examination of water and wastewater. 18th ed. American Public Health Association, Washington, DC. Pp: 1268.

Appleby, P.G. and F. Oldfield. 1978. The calculation of lead-210 dates assuming a constant rate of supply of unsupported ^{210}Pb to the sediment. *Catena* **5**: 1-8.

Arévalo, C. 1916. Introducción al estudio de los Cladóceros del plancton de la Albufera de Valencia. Trabajos del laboratorio de Hidrobiología Española (1). *Anales del instituto General y Técnico de Valencia*, 1(1): 1-66.

Athersuch, J., Horne, D.J., and Whittaker, J.E. 1989. Marine and Brackish water ostracods. Synopses of the British Fauna (new series). n°43. Brill, E.J. London. Pp: 359.

Barbieri, M., Carrara, C., Castorina, F. Dai Pra, G., Esu D., Ghiozzi, E., Paganin, G. and Sadori, L. 1999. Multidisciplinary study of Middle-Upper Pleistocene deposits in a core from the Piana Pontina (central Italy). *Giornale di Geologia*, **61**: 47–73.

Beklioglu, M., Altinayar, G. and Tan, C. O. 2006. Water level control over submerged macrophyte development in five shallow lakes of Mediterranean Turkey. *Archive für Hydrobiology*, **166** (4): 535–556.

Beklioglu, M., Romo, S., Kagalou, I. Quintana, X. and Bécares, E. 2007. State of the art in the functioning of shallow Mediterranean lakes: workshop conclusions. *Hydrobiologia*, **584**: 317–326.

Berger, A. L. 1988. Milankovitch theory and climate. *Reviews of Geophysics*, **26**: 624-657.

Binford, M. W. 1990. Calculation and uncertainty analysis of ^{210}Pb dates for PIRLA project lake sediment cores. *Journal of Paleolimnology*, **3**: 253-267.

Birks, H.J.B. and Gordon, A.D. 1985. Numerical methods in quaternary pollen analysis. Academic Press. Harcourt Brace Jovanovich. Pp: 336.

Blanco, C. 1973. Estudio de los rotíferos de la Albufera de Valencia. Influencia de la contaminación en su distribución. *Tesis de Licenciatura*. Universidad de Madrid. Pp: 51.

Blanco, S. and Romo, S. 2006. Ictiofauna de la Albufera de Valencia: evolución histórica y situación actual. *Boletín de la Real sociedad española de Historia Natural. Sección Biología*, **101** (1-4): 45-56.

Blanco, S., Romo S., Villena, M.J. and Martínez, S. 2003. Fish communities and food web interactions in six shallow Mediterranean lakes. *Hydrobiologia*, **506/509**: 473–480.

Boira, H. 1987. La vegetación de la Albufera de Valencia y sus bioindicadores. Fundación Universitaria San Pablo CEU. Valencia. Pp: 50.

Bolle, H.J. 2003. Mediterranean Climate, Variability and Trends. Springer Verlag, p. Berlin. Heidelberg, New York, Pp: 372.

Boomer, I. 1993. Palaeoenvironmental indicators from Late Holocene and comtemporary ostracoda of the Aral Sea. *Palaeogeography, Palaeoclimatology, Palaeoecology*, **103**: 141-153.

Boomer, I. and Eisenhauer, G. 2002. Ostracod faunas as palaeoenvironmental indicators in marginal marine environments. In: J. Holmes and A. Chivas, Editors, *The Ostracoda: Applications in Quaternary Research, Geophysical Monograph*, **131**: 135–149.

Bowling, L. C. and Tyler, P. A. 1984. Physicochemical differences between lagoons of King and Flinders Island, Bass Strait. *Marine and Freshwater Research*, **35**(6): 655-662.

Boyle, J. F. 2000. Rapid elemental analysis of sediment samples by isotope source XRF. *Journal of Paleolimnology*, **23**: 213–221.

Bronk Ramsey, C. 2005. *OxCalprogamv3.10*. Online: http://www.rlaha.ox.ac.

uk/O/oxcal.php

Bronshtein, Z.S. 1947. Ostracoda Presnykh Vod. Fauna SSSR, Rakoobraznye, Tom 2, Vyp. 1. Moscow; Zoologicheskii Institut, Akademiya Nauk SSSR. [English translation (1988): *Fresh-water Ostracoda*. Fauna of the USSR, Crustaceans, **2**, 1.

Carbonel, P. 1980. Les ostracodes et leur intérêt dans la définition des écosystèms éstuariens et de la plateforme continentale. Essais d'application à des domaines anciens. *Memorie Instute Geologique du Bassin d'Aquitaine*, **2**. Pp: 350.

Carbonnel, G. 1983. Morphométrie et hypersalinité chez Cyprideis torosa (JONES) (Ostracoda, Actuel) dans les Salines de Santa-Pola (Alicante, Espagne). *Sciences Géologiques, Bulletin*, **36**: 211-219.

Carmona, P. and Ruiz, J.M. 1999. Evolución en el Holoceno reciente del delta del rio Turia y la restinga de la Albufera de Valencia. In: Roselló,V.M. (Ed.). *Geoarqueologia i Quaternari litoral*. Memorial M.P.Fumanal. Ed. Universidad de Valencia: 321-330.

Carmona, P. and Ruiz, J.M. 2000. Las inundaciones del los ríos Júcar y Túria. *Serie Geogáfica*, Universidad de Valencia, **9**: 49-69.

Carrión, J.S., Munuera, M., Navarro, C. and Sáez, F. 2000. Paleoclimas e historia de la vegetación cuaternaria en España a través del análisis polínico. Viejas falacias y nuevos paradigmas. *Complutum*, **11**: 115–142.

Chapría, V. E. 1999. Dinamica litoral y sedimentación en las costas Valencianas. *Geoarqueología i Quaternary litoral*. Memorial M.P. Fumanal: 331-342.

Chivas, A. R., De Deckker, P., and Shelley, J. M. G. 1983. Magnesium, strontium, and barium partitioning in nonmarine ostracod shells and their use in paleoenvironmental reconstructions a preliminary study. In: *Applications of Ostracoda* (ed. R. F. Maddocks): 238-249.

Chivas, A. R., De Deckker, P. and Shelley, J. M. G. 1985. Strontium content of ostracods indicates lacustrine palaeosalinity. *Nature*, **316**: 251-253.

Chivas, A. R., De Deckker, P. and Shelley, J. M. G. 1986a Magnesium and strontium in non-marine ostracod shells as indicators of palaeosalinity and palaeotemperature. *Hydrobiologia*, **143**: 135-142.

Chivas, A. R., De Deckker, P. and Shelley, J. M. G. 1986b. Magnesium content of non-marine ostracod shells: a new palaeosalinometer and palaeothermometer. *Palaeogeography, Palaeoclimatology, Palaeoecology*, **54**: 43-61.

Chivas, A. R., De Deckker, P., Wang, S. X. and Cali, J. A. 2002. Oxygen-isotope systematics of the nektic ostracod *Austracypris robusta*. In *The Ostracoda:*

Applications in Quaternary Research, American Geophysical Union (ed. J. A. Holmes and A. R. Chivas), **131:** 301-313.

Clark, I.D. and Fritz, P. 1997. Environmental Isotopes in Hydrology, CRC Press, Boca Raton, FL. Pp: 328.

Cohen, A.S. 2003. Paleolimnology: the history and evolution of lake systems. Oxford University Press, New York. Pp: 500.

Craig, H. and Gordon, L. 1965. Deuterium and oxygen-18 isotope variations in the ocean and marine atmosphere. In *Stable Isotopes in Oceanographic Studies and Paleotemperatures, Spoleto* (ed. E. Tongiorgi): 9-130.

Dabrio, C.J., Zazo, C., Lario, J., Goy, J.L., Sierro, F.J., Borja, F., González, J.A. and Abel Flores, J. 1999. Sequence stratigraphy of Holocene incised-valley fills and coastal evolution in the Gulf of Cádiz (southern Spain). *Geologie en Mijnbouw* , **77**: 263–281.

Danielopol, D.L. and Handl, M. 1990. The carapace preservation of *Cytherissa lacustris*: its possible use for paleoenvironmental reconstructions, *Bulletin de l' Institut de Géologie du Bassin d'Aquitaine,* **47–48**: 239–245.

Danielopol, D.L., Ito, E., Wansard, G., Takahiro, K., Cronin T.M. and Baltanás, A. 2002. Techniques for collection and study of ostracoda. In: J. Holmes and A. Chivas, Editors, *The Ostracoda: Applications in Quaternary Research*, *Geophysical Monograph*, **131**: 227–247.

De Deckker, P. 2002. Ostracod paleoecology. In: Holmes JA, Chivas AR (eds). *The ostracoda: applications in Quaternary research. Geophysical Monograph* **131**, American Geophysical Union , Washington, DC: 121-134.

De Deckker, P., Chivas, A. R. and Shelley, J. M. G. 1999. Uptake of Mg and Sr in the euryhaline ostracod *Cyideis* determined from in vitro experiments. *Palaeogeography, Palaeoclimatology, Palaeoecology*, **148**: 105-116.

De Deckker, P., Chivas, A. R., Shelley, J. M. G. and Torgesten, T. 1988. Ostracod shell chemistry: A new palaeoenvironmental indicator applied to a regressive/transgressive record from the gulf of Carpentaria, Australia. *Palaeogeography, Palaeoclimatology, Palaeoecology*, **66**: 231-241

De Deccker, P. and Forester R.M. 1988. The use of ostracods to reconstruct continental palaeoenvironmental records. In: De Deccker, Colin and Peypouquet (Eds.), *Ostracoda in the earth sciences*, Elsevier: 175-199.

De Villiers, S. 1999. Seawater strontium and Sr/Ca variability in the Atlantic and Pacific oceans. *Earth Planet Science Letters*, **171**: 623–634.

Deer, W.A., Howie, R.A. and J. Zussman. 1996. An Introduction to the

Rock-Forming Minerals. 2nd ed. Upper Saddle River, NJ: Prentice Hall. Pp: 696.

Deines, P., Langmuir, D. and Harmon, R.S. 1974. Stable carbon isotope ratios and the existence of a gas phase in the evolution of carbonate groundwaters. *Geochimica et Cosmochimica Acta*, **38**: 1147–1164.

Docavo, I. 1979. La albufera de Valencia. Sus peces y sus aves. Institución Alfonso el Magnánimo (Eds), Valencia. Pp: 240.

Dorgelo, J. 1976. Salt tolerance in crustacea and the influence of temperature upon it. *Biological Review*, **51**: 255-290.

Dubois, D.M. 1973. An index of fluctuations, D_a, connected with diversity and stability of ecosystems: applications in the Lotka-Volterra model and in an experimental distribution of species. Rapport de sythèse III, Programme National sur l´environment Physique et Biologique, Project Mer. Commision Interministérille de la Politique Scientifique. Liège.

Durazzi, J. T. 1977. Stable isotopes in the ostracod shell: a preliminary study. *Geochimica et Cosmochimica Acta*, **41**: 1168-1170.

Easterling, D.R., Meehl, G.A., Parmesan, C., Changnon, S.A., Kyrsrsrl, T.R. and Mearns, L.O. 2000. Climate extremes: observations, modeling and impacts. *Science*, **289**: 2068– 2074.

Elderfield, H., Bertram, C. J. and Erez, J. 1996. A biomineralization model for the incorporation of trace elements into foraminiferal calcium carbonate, *Earth Planetary Science Letters*, **142**: 409 – 423

Engstrom, D. R. and Nelsom, S. 1991. Paleosalinity from trace metals in fossil ostracods compared with observational records at Devils Lake, North Dakota, USA. *Palaeogeography, Palaeoclimatology, Palaeoecology*, **83**: 295-312.

Eugster, H. P. and Jones, B. F. 1979. Behavior of major solutes during closed-basin brine evolution. *American Journal Science*, **279**: 609-631.

Ferree, M.A. andShannon, R.D. 2001. Evaluation of a second derivative UV/visible spectroscopy technique for nitrate and total nitrogen analysis of wastewater samples. *Water Research*, **35**: 327-332.

Fontes, J.C. and Gasse, F. 1991. Chronology of the major palaeohydrological events in NW Africa during the late Quaternary: PALHYDAF results. *Hydrobiologia*, **214**: 367-72.

Geddes, M.C. and Butler, A.J. 1984. Physicochemical and biological studies on the Coorong Lagoons, and the effect of salinity on the distribution of the macrobenthos, Transactions of the Royal Society of Australia, **108**: 51–62.

Gibbons, W. and Moreno, T. 2002. The geology of Spain. The Geological Society, London, Pp: 649.

Goldsmith, J. R. and Newton, R. C. 1969. *P-T-X* relations in the system $CaCO_3$-$MgCO_3$ at high temperatures and pressures. *American Journal Science*, **267**: 160-90.

Gönenç, I.E. and Wolflin, J.P. 2004. Coastal Lagoons. Ecosystem Processes and Modelling for Sustainable Use and Development. CRC Press, Boca Raton, FL. Pp: 500.

Goy, J.L., Zazo, C., Dabrio, C.J. and Hillaire-Marcel, C. 1987. Evolution des systems de lagoons-iles barriere du Tyrenien a l'actualitea Campo de Dalıas (Almería, Espagne). Travaux et Documents, vol. 197, Editions de l'ORSTOM, Paris: 169–171.

Goy, J.L., Zazo, C., Dabrio, C.J., Lario, J., Borja, F., Sierro, F. and Flores, J.A. 1996. Global and regional factors controlling changes of coastlines in southern Iberia during the Holocene. *Quaternary Science Reviews*, **15** (3–4): 1–8.

Goy, J.L., Zazo, C. and Dabrio, J.D. 2003. A beach-ridge progradation complex reflecting periodical sea-level and climate variability during the Holocene (Gulf of Almería, Western Mediterranean). *Geomorphology*, **50**: 251–268.

Griffiths, H.I. and Holmes, J.A. 2000. Non-marine Ostracods and Quaternary Paleoenvironments (Technical Guide Nº 8). *Quaternary Research Association*: London. Pp: 179.

Grimm, E.C. 1987. CONISS: A FORTRAN 77 program for stratigraphycally constrained cluster analysis by the method of incremental sum of squares. *Computers y Geosciences*, **13**: 13-35.

Grimm, E.C. 1993. TILIA Diagramming Program. Illionis Sate Museum. Springfield.

Halpern, B.S., Walbridge, S., Selkoe, K.A., Kappel, C.V., Micheli, F., d'Agrosa, C., Bruno, J.F., Casey, K.S., Ebert, C., Fox, H.E., Fujita, R., Heinemann, D., Lenihan, H.S., Madin, E.M.P., Perry, M.T., Selig, E.R., Spalding, M., Steneck, R. andWatson, R. 2008. A global map of human impact on marine ecosystems. *Science*, **319**: 948-952.

Hazel, J. 1988. Determining late Neogene and Quaternary paleoclimates and paleotemperature regimes using ostracods. In: P. Deckker, J.P. Colin and J.P. Peypouquet, Editors, *Ostracoda in the Earth Sciences*, Elsevier, Amsterdam: 89–101.

Heip, C. 1976 The life cycle of *Cyprideis torosa* (Crustacea, Ostracoda). *Oecologia*, **24**: 229-245.

Hill, M.O. and Gauch, H.G. 1980. Detrented correspondence analysis: An improved ordination technique. *Plant Ecology*, **42**: 47-58

Holmes, J.A. and Chivas, A.R. 2002. Ostracod Shell Chemistry-Overview In: Holmes, J.A. and Chivas, A.R. (Eds.). *The Ostracoda*: *Applications in Quaternary Research*. American Geophysical Union: 185-204.

Holmes, J.A., Fothergill, P.A., Street-Perrott, F.A. and Perrott, R.A. 1998: A high-resolution Holocene ostracod record from the Sahel Zone of Northeastern Nigeria . *Journal of Paleolimnology*, **20**: 369–380.

Horne, D. J. and Mezquita, F. 2008. Palaeoclimatic applications of large databases: developing and testing methods of palaeotemperature reconstruction using nonmarine ostracods. *Senckenbergiana lethaea*, **88**: 93-112.

Ito, E. 2001. Application of stable isotope techniques to inorganic and biogenic carbonates. In *Tracking Environmental Change Using Lake Sediments.* Physical and Chemical Techniques (ed. W. M. Last and J. P. Smol). Kluwer Academic Publishers, **2**: 351-371.

Ito, E., Bacon, S. W., Smith A. J. and Palmer, D. F. 2002. Geochemistry of ostracod calcite: Empirical calibration of 3 species from page Pond, Ohio, U.S.A. *Geochimica et Cosmochimica Acta*, **66**: A357.

Ito, E., De Deckker, P. and Eggins, S. M. 2003. Ostracods and their shell chemistry: Implications for paleohydrologic and paleoclimatologic applications. In: *Bridging the Gap: Trends in the Ostracod Biological and Geological Sciences.* The Paleontological Society Papers, **9:** 119-151.

Ito, E. and Forester, R.M. 2009, Changes in continental ostracode shell chemistry; uncertainty of cause. *Hydrobiologia*, **620**, n°1.

Jahn, A., Gamenick, I. and Theede, H. 1996. Physiological adaptations of *Cyprideis torosa* (Crustacea, Ostracoda) to hydrogen sulphide. *Marine Ecology Progress Series*, **142**: 215-223.

Jalut, G., Esteban Amat, A., Riera i Mora, S., Fontugne, M., Mook, R., Bonnet, L. and Gauquelin, T. 1997. Holocene climatic changes in the western Mediterranean: installation of the Mediterranean climate. C. R. Acad. Sci., Paris, *Earth Planetery Sciences*, **325**: 327–334.

Jalut G., Amat A.E, Bonnet L., Gauquelin, T. and Fontugne, M. 2000. Holocene climatic changes in the Western Mediterranean, from south-east France to south-east Spain. *Palaeogeography*, *Palaeoclimatology*, *Palaeoecology*, **160**: 255-290.

Jedoui, Y., Kyllel N., Fontugne M.; Ismail H.B., M'Rabet, A. and Montacer, M. 1988. A high relative sea-level stand in the middle Holocene of southeastern Tuisia. *Marine Geology*, **147**, **1**: 123-130.

Jeffrey, S.W. and Humphrey, G.F. 1975. New spectrophotometric equations for determining chlorophylls a, b, and c in higher plants, algae and natural phytoplankton. Biochem. Physiol. Pflanzen: 167-191.

Jeppesen, E., Sondergaard, M. Jensen, J. P., Mortensen, E., Hansen, A. M. and Jorgensen, T. 1998. Cascading trophic interactions from fish to bacteria and nutrients after reduced sewage loading: an 18-year study of a shallow hypertrophic lake. *Ecosystems*, **3**: 250–267.

Jongman, R.H.G., Ter Braak, C.J.F. and Van Tongeren, O.F.R. (eds.) 1995. Data analysis in community and landscape ecology. Pudoc, Wageningen, The Netherlands. Pp: 299.

Keatings, K. W., Hawkes, W., Holmes, J. A., Flower, R. J., Leng, M. J., Abu-Zied, R. H. and Lord, A. R. 2007. Evaluation of ostracod-based palaeoenvironmental reconstruction with instrumental data from the arid Faiyum Depression, Egypt. *Journal of Paleolimnology*, **38**: 261–283.

Keatings, K. W., Heaton, T. H. E. and Holmes, J. A. 2002. Carbon and oxygen isotope fractionation in non-marine ostracods: Results from a 'natural culture' environment. *Geochimica et Cosmochimica Acta*, **66**(10): 1701-1711.

Keyser, D. 2005. Histological peculiarities of the noding process in *Cyprideis torosa* (Jones) (Crustacea, Ostracoda). *Hydrobiologia*, **538**: 95-106

Keyser, D. and Walter, R. 2004. Calcification in ostracodes. *Revista Española de Micropaleontologia*, **36**: 1-11.

Kim, S.T. and O'Neil, J. R. 1997. Equilibrium and nonequilibrium oxygen isotope effects in synthetic carbonates. *Geochimica et Cosmochimica Acta*, **61**: 3461-3475.

Kilenyi, T. I. 1969. The problems of ostracod ecology in the Thames Estuary. In: Neale JW (eds) *The Taxonomy, Morphology and Ecology of Recent Ostracoda*. Oliver and Boyd, Edinburgh: 251-267.

Kilenyi, T. I. 1972. Transient and balanced genetic polymorphism as an explanation of variable noding in the ostracode *C. torosa*. *Micropaleontology*, **148**: 23-35.

Kjerfve, B. 1994. Coastal Lagoon Processes. Elsevier Science Publishers, Amsterdam, Pp: 577.

Lambeck, K., Yokoyama, Y. and Purcell, T. 2002. Into and out of the Last Glacial Maximum: sea-level change during Oxygen Isotope Stages 3 and 2. *Quaternary Sciences Reviews*, **21**: 343–360.

Lampert, W. and Sommer, U. 2007. Limnoecology: The Ecology of Lakes

and Streams. Oxford University Press, New York. Pp: 324.

Lario, J., Zazo, C., Goy, J.L., Dabrio, C.J., Borja, F., Silva, P.G., Sierro, F., González, A. Soler, V. and Yll, E. 2002. Changes in sedimentation trends in SW Iberia Holocene estuaries (Spain). *Quaternary International*, **93–94**: 171–176.

Leng, M. J. and Marshall, J. D. 2004. Palaeoclimate interpretation of stable isotope data from lake sediment archives. *Quaternary Science Reviews*, **23** (7-8): 811-831.

Levin, L.A., Boesch, D.F., Covich, A., Dahm, C., Erseus, C., Ewe, K.C., Kneib, R.T., Moldenke, A., Palmer, M.A., Snelgrove, P., Strayer, D. and Weslawski, J.M. 2001. The function of marine critical transition zones and the importance of sediment biodiversity. *Ecosystems*, **4**: 430–451.

Li, H.-C. and Ku, T.L. 1997. $\delta^{13}C$–$\delta^{18}O$ covariance as a paleohydrological indicator for closed-basin lakes. *Palaeogeography, Palaeoclimatology, Palaeoecology* **133**: 69–80.

López, P. and Tomás, X. 1989. Chemical composition of the small coastal lagoons of the Mediterranean Spanish littoral. *Scientia Marina*, **53**: 591–599.

López-Buendía, A.M., Bastida, J., Querol, X. and Whateley, M.K.G. 1999. Geochemical data as indicators of palaeosalinity in coastal organic-rich sediments. *Chemical Geology*, **157**: 235-254.

Lotze, H.K., Lenihan, H.S., Bourque, B.J., Bradbury, R.H., Cooke, R.G., Kay, M.C., Kidwell, S.M., Kirby, M.X., Peterson, C.H. and Jackson, J.B.C. 2006. Depletion, degradation and recovery potential of estuaries and coastal seas. *Science*, **312**: 1806-1809.

Margalef, R. 1974. Ecología. Ed. Omega. Barcelona, España. Pp: 951.

Margalef, R. and Mir, M. 1973. Indicadors de canvis de salinitat en els sediments de l´Albufera de València. *Treballs Societat Catalana Bioligia*, **32**: 111-117

Martin-Vide, J. and Lopez-Bustins, J. A. 2006. The Western Mediterranean Oscillation and rainfall in the Iberian Peninsula. *International Journal of Climatology*. **26**: 1455-1475.

Martínez-Cortizas, A., Pontevedra-Pombal, X, Nòvoa-Muñoz, J. C. and García-Rodeja Gayoso, E. 1997. Four thousand years of atmospheric Pb, Cd, and Zn deposition recorded by the ombrotrophic peat bog of Penido Vello (Northwestern Spain). *Water, Air, and Soil Pollution*, **100**: 387-403.

Meisch, C. 2000. *Freshwater Ostracoda of the Western and Central Europe.* (Süβwasserfauna von Mitteleuropa 8/3). Spektrum Akademischer Verlag, Heildeberg. Pp: 523.

Mezquita, F., Olmos V. and Oltra R. 2000. Population ecology of *Cyprideis torosa* (Jones, 1850) in a hypersaline environment of the Western Mediterranean (Santa Pola, Alacant). *Ophelia*, **53** (2): 119-130.

Mezquita, F., Roca J. R. and Wansard, G. 1999. Moulting, survival and calcification: the effects of temperature and water chemistry on an ostracod crustacean (*Herpetocypris intermedia*) under experimental conditions. *Archiv fur Hydrobiologie*, **146**(2): 219-238.

Mezquita, F., Roca, J.R., Reed, J.M. and Wansard, G. 2005. Quantifying species-environment for ecological and paleoecological studies: Examples using Iberian data. *Palaeogeography, Palaeoclimatology, Palaeoecology*, **225**: 93-117.

Miracle, M.R. 1978. Organització del zooplàncton d'aigua dolça durant un cicle anual: aplicació d'un índex de fluctuacions. *Col·loquis de la Societat Catalana de Biologia X*: 183–193.

Miracle, M. R., Soria, J.M., Vicente, E. and Romo, S. 1987. Relaciones entre la luz, los pigmentos fotosintéticos y el fitoplancton en la Albufera de Valencia, laguna hipereutrófica. *Limnetica*, **3**: 25-34.

Miracle, M. R., Vicente, E. and Garay, E. 1984. L'Albufera de València i la problemática de la contaminació de les aigües continentals costaneres. *XII Congrés de Metges i Biòlegs en Llengua Catalana*: 135-166.

Mischke, S. 2001. Mid and Late Holocene palaeoenvironment of the lakes Eastern Juyanze and Sogo Nur in NW China, based on ostracod species assemblages and shell chemistry. Thesis.

Mischke, S., Herzschuh, U., Massmann, G. and Zhang, C. 2007. An ostracod-conductivity transfer function for Tibetan lakes. *Journal of Paleolimnology*, **38**: 509–524.

Morse, J. W. and Bender, M. L. 1990. Partition coefficients in calcite: Examination of factors influencing the validity of experimental results and their application to natural systems. *Chemical Geology*, **82**: 265-277.

Moss, B., Stephen, D. Balayla, D. Bécares, E. Collings, S.E. Fernández-Aláez, C. Fernández-Aláez, M. Ferriol, C. García, P. Goma, J., Gyllström, M. Hansson, L.-A. Hietala, J., Kairesalo, T.,. Miracle, M. R., Romo, S., Rueda, J., Russell, V., Stahl-Delbanco, A. , Svennson, M., Vakkilainen, K., Valentin, M., Van de Bund, W. J., Van Donk, E. Vicente E. and Villena, M. J. 2004. Continentalscale patterns of nutrient and fish effects on shallow wetland lakes: synthesis of a pan-European mesocosm experiment. *Freshwater Biology*, **49**: 1633–1650.

Mucci, A. and Morse, J.W. 1983. The incorporation of Mg^{2+} and Sr^{2+} into calcite overgrowths: influences of growth rate and solution composition. *Geochimica et Cosmochimica Acta*, **47**: 217-233.

Müller, G. 1968. Exceptionally high strontium concentrations in fresh water onkolites and mollusk shells of lake Constance. In G. Miller and G. M. Friedman (eds.). *Recent Developments in Carbonate Sedimentology in Central Europe*. Springer. Berlin-Heidelberg-New York: 116-127.

Mülller, G. 1969. High Strontium Contents and Sr/Ca ratios in Lake Constance Waters and Carbonate and their Sources in the Drainage Area of the Rhine River (Alpenrhein). *Mineral Deposita*, **4**: 75-84.

Müller, G., Irion, G. and Förstner, U. 1972. Recent Formation and Diagenesis of Inorganic Ca-Mg Carbonates in the Lacustrine Environment. Naturwissenschaften, **59**: 158-164.

Naselli-Flores, L. and Barone, R. 2005. Water-level fluctuations in Mediterranean reservoirs: setting a dewatering threshold as a management tool to improve water quality. *Hydrobiologia*, **548**: 85–99.

Neale, J.W. 1964. Some factors influencing the distribution of recent British Ostracoda. *Publications of the Station of Zoology*, Napoli, **33**: 247– 307.

Neufeld, D. S. and Cameron, J. N. 1993. Transepithelial movement of calcium in crustaceans. *Journal of Experimental Biology*, **184**(1): 1-16.

Omran, E.F. 1992. Holocene sea level changes at the nile delta coastal zone of Egypt. *GeoJournal*, **26**: 389-394.

Palacios-Fest, M. R. and Dettman, D. L. 2001. Temperature controls monthly variation in Ostracod valve Mg/Ca: *Cypridopsis vidua* from a small lake in Sonora, Mexico. *Geochimica et Cosmochimica Acta*, **65**(15): 2499-2507.

Pardo, L. 1942. La Albufera de Valencia. Bilogía de las aguas continentales II. Instituto forestal de Investigaciones y Experiencias. Madrid, Pp: 263.

Péqueux, A. 1995. Osmotic regulation in crustaceans. *Journal of Crustacean Biology*, **15**: 1-60.

Pirazzoli, P.A. 2005. A review of possible eustatic, isostatic and tectonic contributions in eight late-Holocene relative sea-level histories from the Mediterranean area. *Quaternary Science Reviews*, **24**: 1989–2001.

Poquet, J.M., Mezquita, F., Rueda, J. and Miracle., M.R. 2008. Loss of Ostracoda biodiversity in Western Mediterranean wetlands. *Aquatic conservation: Marine and Freshwater ecosystems*, **18**: 280-296.

Radke, L. C., Howard, K. W. F. and Gell, P. A. 2002. Chemical diversity in south-eastern Australian saline lakes. I: geochemical causes. *Marine and Freshwater Research*, **53**(6): 941-959.

Radke, L. C., Juggins S., Halse S. A., Deckker, P. D., and Finston, T. 2003. Chemical diversity in south-eastern Australian saline lakes II: biotic implications. *Marine and Freshwater Research*, **54**(7): 895-912.

Reddy, M. M. and Wang, K. K. 1980. Crystallization of calcium carbonate in the presence of metal ions. 1. Inhibition by magnesium ion at pH 8.8 and 25° C. *Journal of Crystal Growth*, **50**: 470-480.

Reimer, P.J., Baillie, M.G.L., Bard, E., Bayliss, A., Beck, J.W., Bertrand, C.J.H., Blackwell, P.G., Buck, C.E., Burr, G.S., Cutler, K.B., Damon, P.E., Edwards, R.L., Fairbanks, R.G., Friedrich, M., Guilderson, T.P., Hogg, A.G., Hughen, K.A., Kromer, B ., McCormac, G., Manning, S., Ramsey, C.B., Reimer, R.W., Remmele, S., Southon, J.R., Stuiver, M., Talamo, S., Taylor, F.W., van der Plicht, J. and Weyhenmeyer C.E. 2004. IntCal04 Terrestrial Radiocarbon Age Calibration, 0–26 cal kyrs BP. *Radiocarbon*, **46** (3): 1029-1059.

Renard, M. 1985. Géochimie des carbonates pèlagiques. *Documents de Bureau des Recherches Géologiques et Mineralogiques*, **85**: 1-650.

Robles, F., Collado, M.A. and Borredá, V. 1985. Variaciones en la fauna de moluscos en la Albufera de Valencia: implicaciones paleogeográficas. *Pleistoceno y Geomorfología litoral. Homenaje a Juan Cuerda*. Universidad de València: 123-133.

Roca, J.R. and Wansard, G. 1997. Temperature influence on development and calcification of Herpetocypris brevicaudata Kaufmann, 1900 (Crustacea: Ostracoda) under experimental conditions. *Hydrobiologia*, **347**: 91–95.

Romo, S., Miracle M.R., Villena M.J., Rueda J., Ferriol, C. and Vicente, E. 2004. Mesocosm experiments on shallow lake food webs in a Mediterranean climate. *Freshwater Biology*, **49**: 1593–1607.

Romo, S. and Miracle, M. R. 1993. Long-term periodicity of *Planktothrix agardhii*, *Pseudanabaena galeata* and *Geitlerinema* sp. In a shallow hypertrophic lagoon, the Albufera of Valencia (Spain*). Archive für Hydrobiologie*, **126**: 469–486.

Romo, S. and Miracle, M.R. 1994. Population dynamics and ecology of subdominant phytoplankton species in a shallow hypertrophic lake (Albufera of Valencia, Spain). *Hydrobiologia*, **273**: 37-56.

Romo, S., Murcia, G., Villena, A., Sanchez, M.J. and Ballester, A. 2008. Tendencias del fitoplancton en el lago de la Albufera de Valencia e implicaciones para su ecología, gestión y recuperación. *Limnetica*, **27** (1): 11-27.

Romo, S., Villena, M. J., Sahuquillo, M., Soria, J. M., Gimenez, M., Alfonso, T., Vicente, E. and Miracle, M. R. 2005. Response of a shallow Mediterranean lake to nutrient diversion: does it follow similar patterns as in northern shallow lakes?. *Freshwater Biology*, **50**(10): 1706–1717.

Roselló, V.M. 1995. L´Álbufera de València. Ed: *Publicacions de L´Abadia de*

Montserrat. Barcelona. Pp: 190.

Rosenfeld, A. and Vesper, B. 1976. The variability of the sieve-pores in recent and fossil species of *Cyprideis torosa* (Jones 1850) as an indicator for salinity and palaeosalinity. In: Löffler H, Danielopol D (eds) Aspects of ecology and zoogeography of recent and fossil ostracods. In: *Proceedings of the sixth international ostracod symposium, Saalfelden*. Junk Publishers, The Hague: 55–67.

Rueda J., Aguilar-Alberola, J.A. and Mezquita, F. 2006. Contribución al conocimiento de los crustáceos (Arthropoda, Crustacea) de las Malladas de la Devesa del Parque Natural de la Albufera (Valencia). *Boletín de la Asociación Española de Entomología*, **30**: 9-29.

Ruiz, F., Abad, M., Galán, E., González, I., Aguila, I., Olías, M., Gómez Ariza J.L. and Cantano, M. 2006. The present environmental scenario of El Melah Lagoon (NE Tunisia) and its evolution to a future sabkha. *Journal of African Earth Sciences*, **44**: 289–302.

Ruiz, F., González-Regalado, M.L., Baceta, J.I., Menegazzo-Vitturi, L., Pistolato, M., Rampazzo, G. and Molinaroli, E. 2000a. Los ostrácodos de la laguna de Venecia (NE de Italia). *Geobios*, **33**: 447–454.

Ruiz, F., Gonález-Regalado, M.L., Baceta, J.I. and Muñoz, J.M. 2000b. Comparative ecological analysis of the ostracod faunas from low and high-polluted southwestern Spanish estuaries: a multivariate approach. *Marine Micropaleontolgy*, **40**: 345–376.

Ruiz, J.M. and Carmona, P. 2005. La llanura deltaica de los ríos Júcar y Turia y la Albufera de Valencia. En, Sanjaume, E. and Mateu, J. (Eds.): *Geomorfologia i Quaternari litoral*, Homenaje al Dr. V. Rosselló, Dept. de Geografia, Universitat de València: 399-419.

Sánchez, E., C. Gallardo, M. A. Gaertner, Arribas A. and Castro, M. 2004. Future climate extreme events in the Mediterranean simulated by a regional climate model: a first approach. *Global and Planetary Change*, **44**: 183–180.

Sanchis Ibor, C. 2001. Regadiu i canvi ambiental a l´Álbufera de València. *Publicacions de la Universidad de Valencia*. Pp: 332.

Sandberg, P.A. 1964 The ostracod genus *Cyprideis* in the Americas. Acta Universitatis Stockholmiensis, Contributions in Geology, **12.** Pp: 178.

Sanjaume, E. 1985. Las costas Valencianas. Sedimentología y aspectos de morfología litoral. *Thesis*. Universidad de Valencia. Pp: 505.

Sanjaume, E., Roselló, V.M., Pardo, J. E. , Carmona, P., Segura, F., and Lopez García, M.J. 1996. Recent Coastal Changes in the Gulf of Valencia (Spain). *Zeitch für Geomorphologie*. N. F. lup. Bd, **102**: 95-118.

Sanjaume, E. Segura, F., López M.J. and Pardo, J. 1992. Tasas de sedimentación en L'Albufera de València. *Cuadernos de Geografía*, **51**: 63-81.

Santiesteban, C., Marco-Barba. J. and Miracle, M.R. in press. La evolución Holocena de la Albufera de Valencia. *Geogaceta*.

Schwalb, A. 2003. Lacustrine ostracods as stable isotope recorders of late-glacial and Holocene environmental dynamics and climate, *Journal of Paleolimnology*, **29**: 267–351.

Scheffer, M. 1998. Ecology of shallow lakes. Chapman and Hall, London, Pp: 357.

Scheffer, M., S. H. Hosper, M.-L. Meijer, Moss B. and Jeppesen, E. 1993. Alternative equilibria in shallow lakes. *Trends in Ecology and Evolution*, **8**: 275–279.

Scheffer, M. and Van Nes, E.H. 2007. Shallow lakes theory revisited. Various alternative regimes driven by climate, nutrients, depth and lake size, *Hydrobiologia,* **584**: 455–466.

Schornikov, E.I. 1969. A new family of Ostracoda from the supralittoral zone of Kuril Islands. *Zoologicheskii Zhurnal*, **48**: 494-498.

Shannon, C.E. and Weaver, W. 1963. The Mathematical theory of communication. Univ. Illionis Press, Urbana. Pp: 144.

Shoaf, W.T and Lium B.W. 1976. Improved extraction of chlorophyll *a* and b from algae using dimethyl sulphoxide. *Limnology and Oceanography*, **21**: 926-928.

Siani, G. Paterne, M., Arnold, M., Bard, E., Métivier, B., Tisnerat, N. and Bassinot, F. 2000. Radiocarbon reservoir ages in the Mediterranean Sea and Black Sea coastal waters, *Radiocarbon,* **42** (2): 271–280.

Sivan, D., Wdowinski, S., Lamback, K., Galili, E. and Raban, A. 2001. Holocene sea-level changes along the Mediterranean coast of Israel, based on archaeological observations and Numerical model. *Palaeogeography, Palaeoclimatology, Palaeoecology*, **167**: 101-117.

Smith, A.J. and Horne, D.J. 2002. Ecology of marine, marginal marine and nonmarine Ostracodes, *in*: Holmes, J.A.; Chivas, A.R. Eds. 2002. *The Ostracoda: Applications in Quaternary Research. Geophysical Monograph,* **131**: 37-64

Somoza, L., Barnolas, A., Arasa, A., Maestro, A., Rees, J.G., Hernández-Molina, F.J. 1998. Architectural stacking patterns of the Ebro delta controlled by Holocene high-frequency eustatic fluctuations, delta-lobe switching and subsidence processes. *Sedimentary Geology*, **117**: 11–32.

Soria, J.M. 2006. Past, present and future of Albufera of Valencia Natural Park. *Limnetica*, **25**: 135-142.

Soria, J.M., Miracle, M.R. and Vicente, E. 1987 Aporte de nutrientes y eutrofización de la Albufera de Valencia. *Limnetica*, **3:** 227–242.

Soria, J.M. and Vicente, E. 2002 Estudio de los aportes hídricos al parque natural de la Albufera de Valencia. Limnetica, **21**: 105–115.

Stuiver, M. and Becker, B. 1993. High-precision decadal calibration of the radiocarbon time scale, AD 1950–6000 BC. *Radiocarbon*, **35**(1): 65.

Stuiver, M., Pearson, G.W. and Braziunas, T.F. 1986. Radiocarbon age calibration of marine samples back to 9000 cal yrs BP. In: Stuiver M, Kra RS, editors. *Radiocarbon*, **28**(2B): 980–1021.

Stuiver, M., Reimer, P.J., Bard, E., Beck, J.W., Burr, G.S., Hughen, K.A.,Kromer, B., McCormac, F.G., Plicht, J. and Spurk, M. 1998. INTCAL 98 radiocarbon age calibration, 24,000-0 cal BP. *Radiocarbon*, **40**: 1041–1083.

Talbot, M.R. 1990. A review of the palaeohydrological interpretation of carbon and oxygen isotopic ratios in primary lacustrine carbonates. *Chemical Geology*, **80**: 261–279.

Titterton, R. 1978. Biometric and ontogenetic studies on fossil and Recent *Cyprideis torosa* (Jones, 1850). Pp: 99.

Trigo, I. F., Bigg, G. R., and Davies, T. D. 2002. Climatology of cyclogenesis mechanisms in the Mediterranean. *Monthly Weather Review*, **130**: 549–649.

Turpen, J. B. and Angell, R. W. 1971. Aspects of moulting and calcification in the ostracod Heterocypris. *Biology Bulletin* (Woods Hole, Mass), **140**: 331-338.

Valderrama, J.C. 1981. The simultaneous analysis of total nitrogen and total phosphorus in natural waters. *Marine Chemistry*, **10**: 109-122.

Van Harten, D. 1975. Size and environmental salinity in the modern euryhaline ostracod *Cyprideis torosa* (Jones, 1850) a biometrical study, *Palaeogeography*, *Palaeoclimatology*, *Palaeogeography*, **17**: 35–48.

Van Harten, D. 1996. *Cyprideis torosa* (Ostracoda) revisited. Of salinity, nodes and shell size. In Keen, M. C. (ed.), Proc.2nd European Ostracodologists' Meeting (Glasgow 1993),British Micropalaeontol. Soc. London: 191–194.

Van Harten, D. 2000. Variable noding in *Cyprideis torosa* (Ostracoda, Crustacea): an overview, experimental results and a model from Catastrophe Theory. *Hydrobiologia*, **419**: 131–139.

Vesper, B. 1972a. Zur Morphologie und Ökologie von *Cyprideis torosa* (Jones, 1850) (Crustacea, Ostracoda, Cytheridae) unter besonderer Berücksichtigung seiner Biometrie. *Mitteilungen Hamburger Zoologisches Museum und Institut*, **68**: 21–77.

Vesper, B. 1972b. Um Problem der Buckelbildung bei *Cyprideis torosa* (Jones 1850) (Crustacea, Ostracoda, Cytheridae). *Mitteilungen Hamburger Zoologisches Museum und Institut*, **68**: 79-94.

Vesper, B. 1975. Ein Beitrag zur Ostracodnfauna Schleswig-Holsteins, Mitteilungen Hamburger Zoologisches Museum und Institut, **72**: 97–108.

Viaroli, P., Lasserre, P., and Campostrini P. 2007. Lagoons and coastal wetlands. *Hydrobiologia*, **577**: 1-3.

Vicente, E. and Miracle, M.R. 1992. The coastal laggon Albufera de Valencia Natural Park: an ecosystem under stress. *Limnetica*, **8**: 87-100.

Viehberg, F. A. 2006. Freshwater ostracod assemblages and their relationship to environmental variables in waters from northeast Germany. *Hydrobiologia,* **571**: 213–224.

Villena, M.J. and Romo, S. 2003. Phytoplankton changes in a shallow Mediterranean lake (Albufera of Valencia, Spain) after sewage diversion. *Hydrobiologia,* **506–509**: 281–287.

Vita Finzi, C. 1972. The Mediterranean sea: a natural sedimentation laboratory. *Hutchinson and Ross*: 43-46.

Von Grafenstein U., Erlenkeuser H., Müller J. and Kleinmann-Eisenmann A. 1992. Oxygen isotope records of benthic ostracods in Bavarian lake sediments: reconstruction of late and post glacial air temperatures. *Naturwissenschaften*, **79**: 145-152.

Von Grafenstein, U., Erlenkeuser, H. and Trimborn, P. 1999. Oxygen and carbon isotopes in modern fresh-water ostracod valves: assessing vital offsets and autecological effects of interest for palaeoclimate studies. *Palaeogeography, Palaeoclimatology, Palaeoecology*, **148**: 133–152.

Wagner, G.W. 1957. Sur les ostracodes du quaternaire récent des pays-bas et ley utilisation dans l´étude géologique de depots Holocénes. Editado por Mouton and Co. Pp: 259.

Wansard, G. 1996a. Nouvelle approche de la quantification des paléotempératures à partir du rapport (Mg/Ca) des valves d'ostracodes lacustres. *Comptes Rendús Académie des Sciences de Paris, Sciences de la terre et des planètes*, **323**: 493-500.

Wansard, G. 1996b. Quantification of paleotemperatures changes during

isotopic stage 2 in the La Draga continental sequence (NE Spain) based on the Mg/Ca ratio of freshwater ostracods. *Quaternary Science Reviews*, **15**: 237-245.

Wansard, G., De Deckker, P. and Julià, R. 1998. Variability in ostracod partition coefficients D(Sr) and D(Mg): Implications for lacustrine palaeoenvironmental reconstructions. *Chemical Geology*, **146**: 39-54.

Wansard, G. and Roca, J.R. 1997. Étude expérimentale de l'incorporation du strontium et du magnésium dans les valves d'un ostracode d'eau douce, *Herpetocypris brevicaudata* (Crustacea, Ostracoda). Comptes Rendús Académie des Sciences de Paris, Sciences de la terre et des planètes, **325**: 403-409.

Weinbauer, M.G. and Velimirov, B. 1995. Calcium, Magnesium and strontium concentrations in the calcite sclerites of Mediterranean gorgonians (Coelenterata:Octocorallia). *Estuarine, Coastal and Shelf Science*, **40**: 87–104.

Wetterich, S., Schirrmeister L., Meyer H., Viehberg F. and Mackensen A. 2008. Arctic freshwater ostracods from modern periglacial environments in the Lena River Delta (Siberian Arctic, Russia): geochemical applications for palaeoenvironmental reconstructions. *Journal of Paleolimnology*, **39**(4): 427-449.

Weygoldt, P. 1960. Embryologische Untersuchungen an Ostrakoden: Die Entwicklung von *Cyprideis litoralis* (G. S. Brady) (Ostracoda, Podocopa, Cytheridae). *Zoologische Jahrbücher*, **78**: 369-426.

Whatley, R.C. 1983a. The application of ostracoda to paleoenvironmental analysis. R. F. Maddocks, (ed). *Applications of ostracoda*: 51-57.

Whatley, R.C. 1983b. Some simple procedures for enhancing the use of Ostracoda in paleoenvironmental analysis. *Norgewian Petroleum Directorate*, **2**: 129-146.

Whatley, R.C. 1988. Population structure of ostracods: some general principles for the recognition of paleoenvironments. In: *Ostracoda in the Earth Sciences*, De Deccker, P., J.P. Colin and Peypouquet (eds); Elsevier, Amsterdam: 245-256

Wouters, K. 1973. Quelques ostarcodes du Tyrhénien de Monastir (Tunisise). *Annales de Mines et de la Géologie*, **26:** 379-399.

Xia J., Ito E. and Engstrom D. R. 1997a Geochemistry of ostracod calcite: 1. An experimental determination of oxygen isotope fractionation. *Geochimica et Cosmochimica Acta*, **61** (2): 377-382.

Xia, J., Engstrom, D. R. and Ito, E. 1997b Geochemistry of ostracod calcite: 2. the effects of water chemistry and seasonal temperature variation on *Candona rawsoni*. *Geochimica et Cosmochimica Acta*, **61**(2): 383-391.

Zazo, C. and Goy, J. L. 2000. Geomorfología litoral. In: J. R. de Andrés y F. J Garcia, (Eds.) IGME: 187-197.

Zazo, C., Dabrio., C.J. , Goy, J.L. Lario, J. Cabero, A. Silva, P.G. Bardají, T. Mercier, N., Borja, F. and Roquero, E. 2008. The coastal archives of the last 15 ka in the Atlantic–Mediterranean Spanish linkage area: Sea level and climate changes. *Quaternary International*, **181**: 72–87

Zeebe, R. E. 1999. An explanation of the effect of seawater carbonate concentration on foraminiferal oxygen isotopes. *Geochimica et Cosmochimica Acta* **63**(13-14): 2001-2007.

Plates

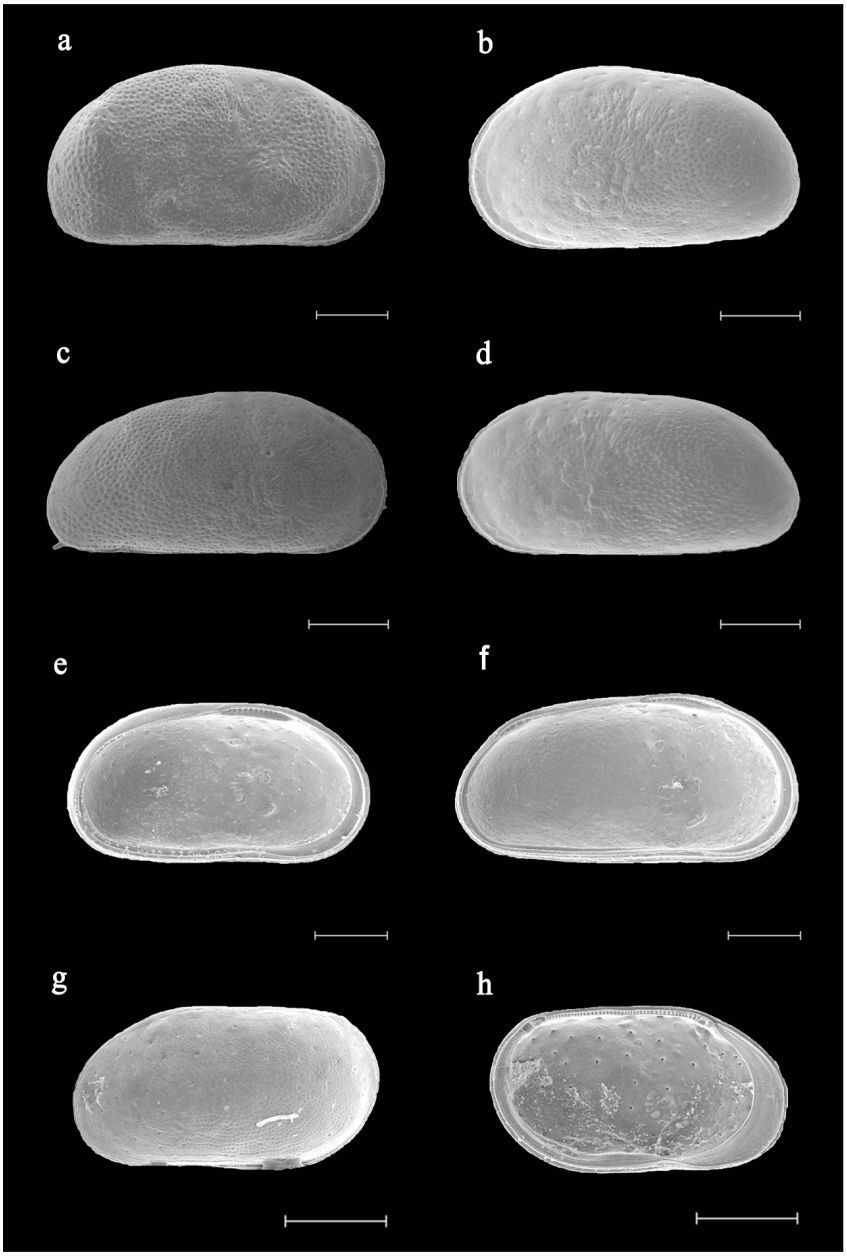

Plate 1.1: SEM photographies of euryhaline and brackish species from Palmar core. The scale is located below each photography and detailed bertween brackets for each specimen. a) *C. torosa* female RV ext. (200 μm), **b)** *C. torosa* hembra LV ext. (200 μm), **c)** *C. torosa* male RV ext. (200 μm), **d)** *C. torosa* male LV ext. (200 μm), **e)** *C. torosa* female LV int. (200 μm), **f)** *C. torosa* male LV int. (200 μm), **g)** *L.elliptica* male LV ext. (200 μm), **h)** *L.elliptica* male LV int. (200 μm).

Lámina 1.1: Fotografías de ME de las distintas especies eurihalinas y de aguas salobre encontradas en el sondeo Palmar. El valor de escala se sitúa debajo de cada valva y se detalla entre paréntesis para cada individuo. **a)** *C. torosa* hembra VD ext. (200 μm), **b)** *C. torosa* hembra VI ext. (200 μm), **c)** *C. torosa* macho VD ext. (200 μm), **d)** *C. torosa* macho VI ext. (200 μm), **e)** *C. torosa* hembra VI int. (200 μm), **f)** *C. torosa* macho VI int. (200 μm), **g)** *L.elliptica* macho VI ext. (200 μm), **h)** *L.elliptica* macho VI int. (200 μm).

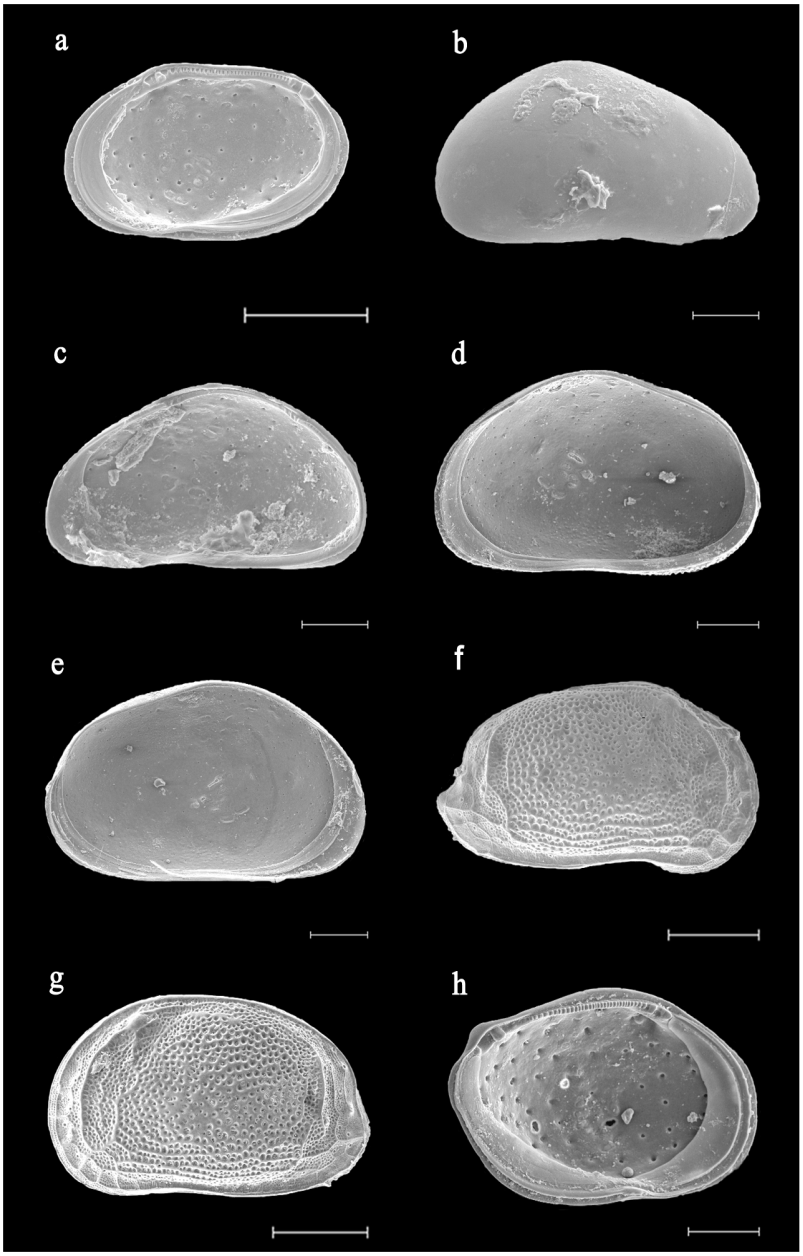

Plate 1.2: SEM photographies of different brackish (a-e) and marine (f-h) species from Palmar core. The scale is located below each photography and detailed bertween brackets for each specimen. **a)** *L. elliptica* female RV int. (200 μm), **b)** *X. nitida* RV ext. (100 μm), **c)** *X. nitida* RV int. (100 μm), **d)** *H. salina* RV int. (200 μm), **e)** *H. salina* LV int. (200 μm), **f)** *A. arborescens* RV ext. (200 μm), **g)** *A. arborescens* LV ext. (200 μm), **h)** *L .rhomboidea* LV int. (100 μm).

Lámina 1.2: Fotografías de ME de las distintas especies encontradas en sondeo Palmar (a-e: afinidades salobres, f-h: afinidades marinas). El valor de escala se sitúa debajo de cada valva y se detalla entre paréntesis por cada individuo. **a)** *L. elliptica* hembra VD int. (200 μm), **b)** *X. nitida* VD ext. (100 μm), **c)** *X. nitida* VD int. (100 μm), **d)** *H. salina* VD int. (200 μm), **e)** *H. salina* VI int. (200 μm), **f)** *A. arborescens* VD ext. (200 μm), **g)** *A. arborescens* VI ext. (200 μm), **h)** *L .rhomboidea* VI int. (100 μm).

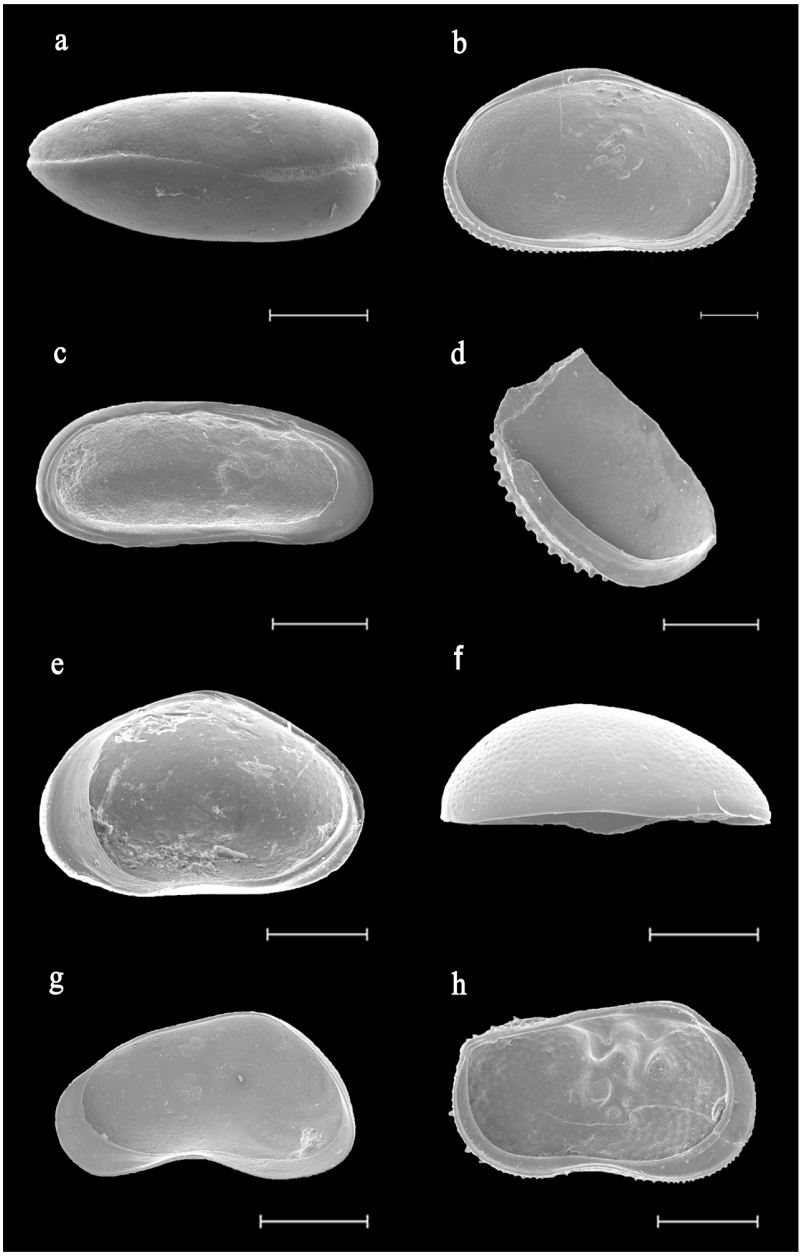

Plate 1.3: SEM photographies of different brackish-marine (a-d) and freshwater (e-h) species from Palmar core. The scale is located below each photography and detailed bertween brackets for each specimen. **a)** *Pontocythere* cf. *turbida* dorsal view (200 μm), **b)** *Hemicypris* sp. LV int. (200 μm), **c)** *Pontocythere* cf. *turbida* LV int. (200 μm), **d)** *Hemicypris* sp. fragment int. (200 μm), **e)** *Cypridopsis vidua* RV int. (200 μm), **f)** *C. vidua* dorsal view LV (200 μm), **g)** *C. angulata* male RV int. (100 μm), **h)** *I. gibba* LV int. (200 μm).

Lámina 1.3: Fotografías ME de las distintas especies encontradas en sondeo Palmar (a y d: afinidades marinas, e-h: agua dulce). El valor de escala se sitúa debajo de cada valva y se detalla entre paréntesis por cada individuo. **a)** *Pontocythere* cf. *turbida* visión dorsal (200 μm), **b)** *Hemicypris* sp. VI int. (200 μm), **c)** *Pontocythere* cf. *turbida* VI int. (200 μm), **d)** Fragmento *Hemicypris* sp. int. (200 μm), **e)** *Cypridopsis vidua* VD int. (200 μm), **f)** *C. vidua* visión dorsal VI (200 μm), **g)** *C. angulata* macho VD int. (100 μm), **h)** *I. gibba* VI int. (200 μm).

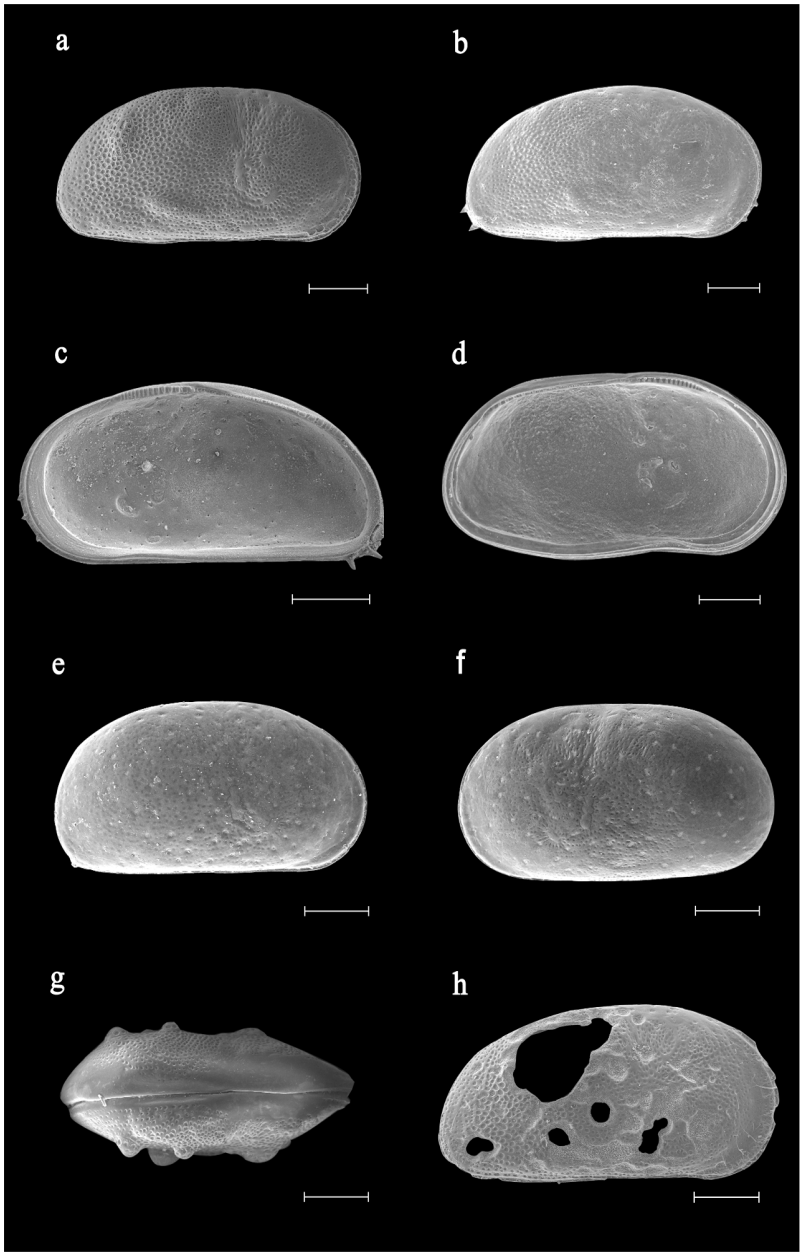

Plate 2.1: SEM photographies of different brackish species from core Center. The scale is located below each photography and detailed between brackets for each specimen. **a)** *C. torosa* male RV ext. noded (200 μm), **b)** *C. torosa* male RV ext. with spines (200 μm) **c)** *C. torosa* male RV int. (200 μm), **d)** *C. torosa* male LV int. deformed (200 μm), **e)** *C. torosa* female RV ext. smoothed (200 μm), **f)** *C. torosa* female LV ext. smoothed (200 μm) **g)** *C. torosa* juvenile, ventral view, noded (200 μm), **h)** *C. torosa* male RV ext. corroded (200 μm) .

Lámina 2.1: Fotografías de ME de las distintas especies de aguas salobre encontradas en el sondeo Centro. El valor de escala se sitúa debajo de cada valva y se detalla entre paréntesis para cada especiemen. **a)** *C. torosa* macho VD ext. nodado (200 μm), **b)** *C. torosa* male VD ext. com espinas (200 μm) **c)** *C. torosa* macho VD int. (200 μm), **d)** *C. torosa* maho VI int. deformado (200 μm), **e)** *C. torosa* hembra VD ext. no nodado (200 μm), **f)** *C. torosa* hembra VI ext. (200 μm) **g)** *C. torosa* juvenil, visión ventral, nodado (200 μm), **h)** *C. torosa* macho VD ext. corroido (200 μm) .

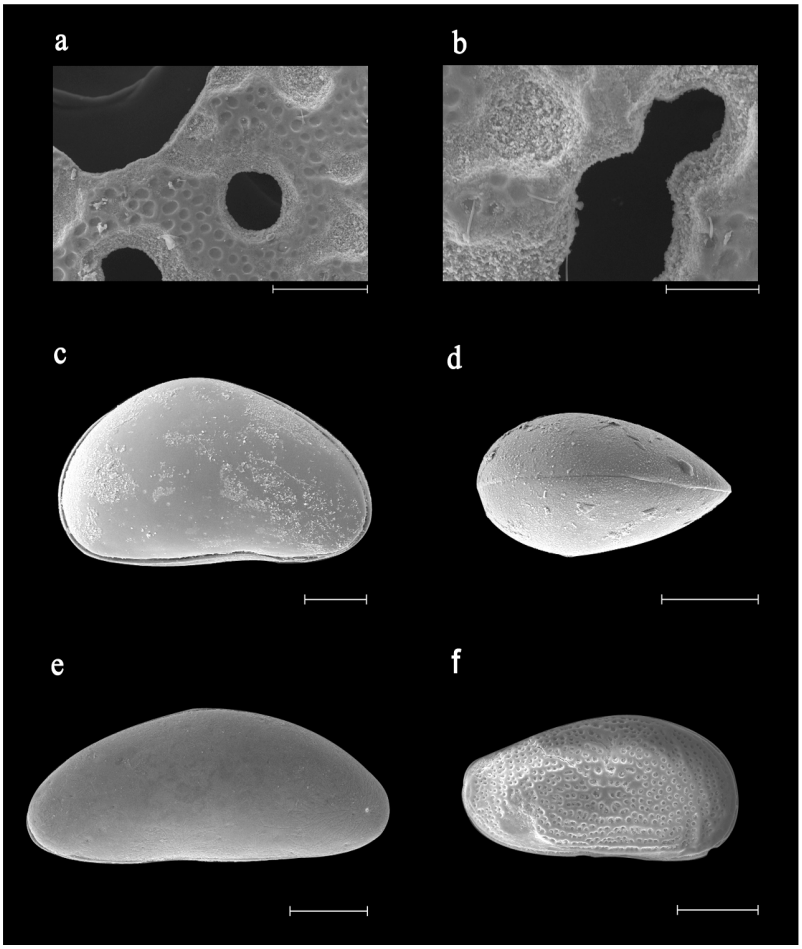

Plate 2.2: SEM photographies of different brackish species from core Center. The scale is located below each photography and detailed between brackets for each specimen. **a)** Detail of the corroded *C. torosa* (plate 2.1h) (100 μm), **b)** Detail of the corroded *C. torosa* (plate 2.1h) (50 μm), **c)** *X. nitida* RV ext. (100 μm), **d)** *X. nitida* dorsal view (200 μm), **e)** *Cytherois* cf *stephanidesi* ext. LV (100 μm), **f)** *Leptocybtere* sp. RV ext. (100 μm).

Lámina 2.2: Fotografías de ME de las distintas especies de aguas salobre encontradas en el sondeo Centro. El valor de escala se sitúa debajo de cada valva y se detalla entre paréntesis para cada epecimen. **a)** Detalle del *C. torosa* corroido (Lámina 2.1h) (100 μm), **b)** Detalle del *C. torosa* corroido (Lámina 2.1h) (50 μm), **c)** *X. nitida* VD ext. (100 μm), **d)** *X. nitida* visión dorsal (200 μm), **e)** *Cytherois* cf *stephanidesi* ext. VI (100 μm), **f)** *Leptocythere* sp. VD ext. (100 μm).

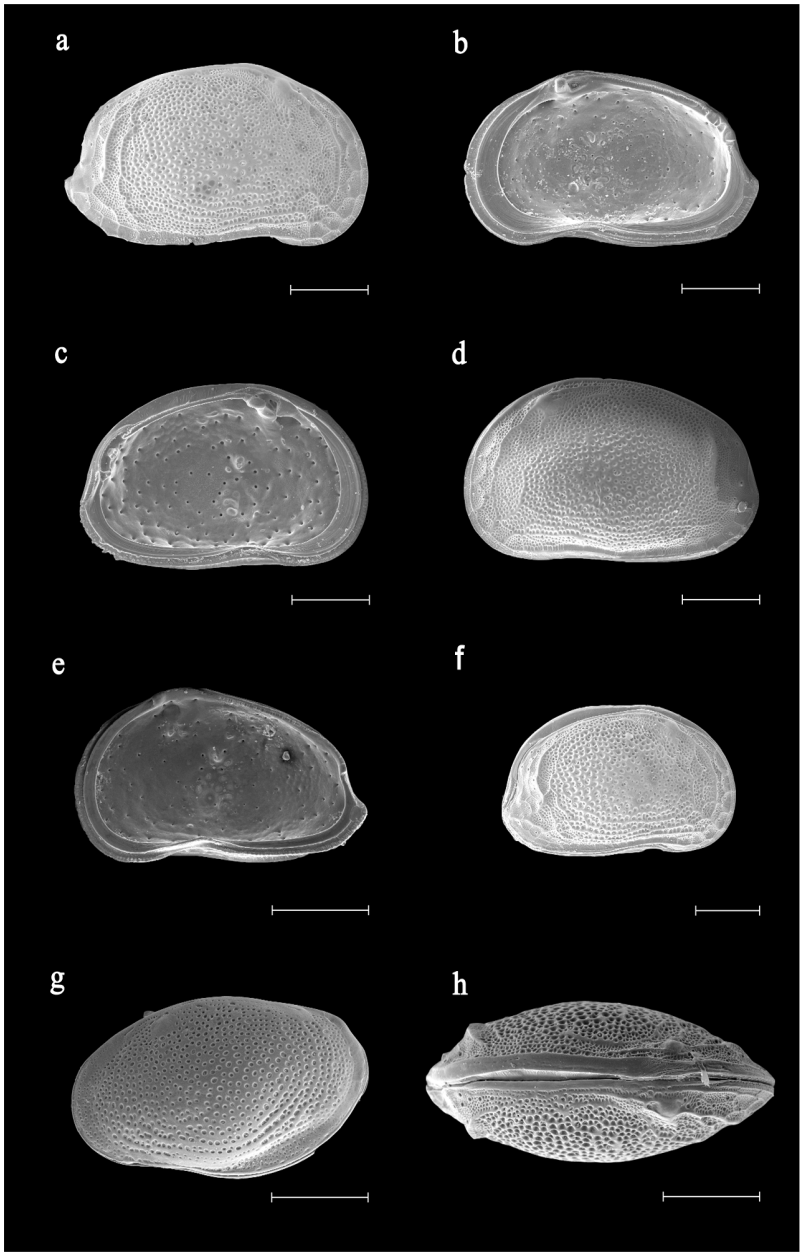

Plate 2.3: SEM photographies of different marine species from core Center. The scale is located below each photography and correspond to 200 μm for all the cases. **a)** *Aurila arborescens* RV ext., **b)** *Aurila arborescens* RV int., **c)** *Aurila arborescens* LV int., **d)** *Aurila arborescens* LV ext., **e)** *Aurila arborescens* RV int., **f)** *Aurila arborescens* juvenile RV ext. **g)** *Loxoconcha rhomboidea* LV ext., **h)** *Loxoconcha rhomboidea* ventral view.

Lámina 2.3: Fotografías de ME de las distintas especies de afinidades marinas encontradas en el sondeo Centro. El valor de escala se sitúa debajo de cada valva y corresponde a 200 μm para todos los casos. **a)** *Aurila arborescens* VD ext., **b)** *Aurila arborescens* VD int., **c)** *Aurila arborescens* VI int., **d)** *Aurila arborescens* VI ext., **e)** *Aurila arborescens* VD int., **f)** *Aurila arborescens* juvenile VD ext., **g)** *Loxoconcha rhomboidea* VI ext., **h)** *Loxoconcha rhomboidea* ventral view.

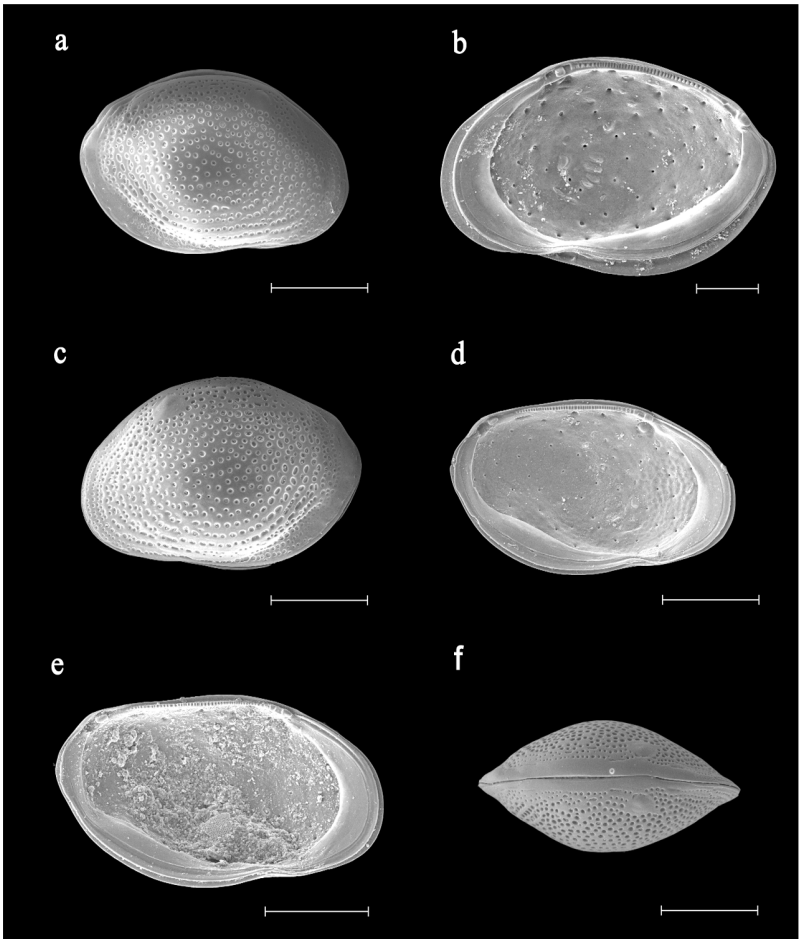

Plate 2.4: SEM photographies of different marine ostracod species from Center core. The scale is located below each photography and detailed between brackets for each specimen. **a)** *Loxoconcha rhomboidea* RV ext. (200 μm), **b)** *Loxoconcha rhomboidea* RV int. (100 μm), **c)** *Loxoconcha rhomboidea* LV ext., **d)** *Loxoconcha rhomboidea* LV int. (200 μm), **e)** *Loxoconcha rhomboidea* LV int. (200 μm), **f)** *Loxoconcha rhomboidea*, juvenile, dorsal view (200 μm).

Lámina 2.4: Fotografías de ME de las distintas especies con afinidades marinas encontradas en el sondeo Centro. El valor de escala se sitúa debajo de cada valva y entre paréntesis para cada especímen. **a)** *Loxoconcha rhomboidea* VD ext. (200 μm), **b)** *Loxoconcha rhomboidea* VD int. (100 μm), **c)** *Loxoconcha rhomboidea* VI ext., **d)** *Loxoconcha rhomboidea* VI int. (200 μm), **e)** *Loxoconcha rhomboidea* VI int. (200 μm), **f)** *Loxoconcha rhomboidea*, juvenil, visión dorsal (200 μm).

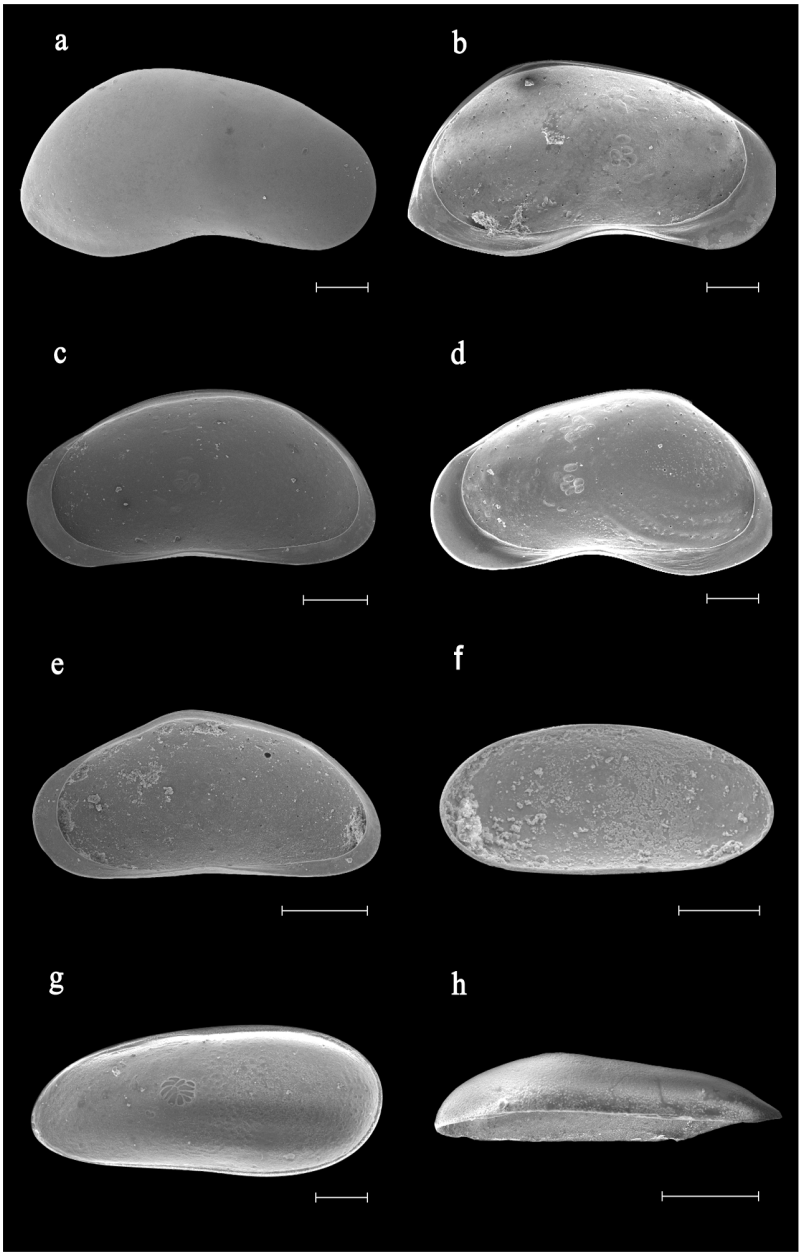

Plate 2.5: SEM photographies of different freshwater species from Center core. The scale is located below each photography and and detailed between brackets for each specimen. **a)** *Candona angulata* male RV ext. (200 μm), **b)** *Candona angulata* male LV int. (200 μm), **c)** *Candona angulata* female RV int. (200 μm), **d)** *Candona angulata* male RV int. (200 μm), **e)** *Candonidae* sp. RV int. (200 μm), **f)** *Candonidae* sp., juvenile int. (100 μm) **g)** *Darwinula stevensoni* RV int. (200 μm), **h)** *Darwinula stevensoni* LV dorsal view (200 μm).

Lámina 2.5: Fotografías de ME de las distintas especies de afinidades marinas encontradas en el sondeo Centro. El valor de escala se sitúa debajo de cada valva y detallada entre paréntesis para cada especimen. **a)** *Candona angulata* macho VD ext. (200 μm), **b)** *Candona angulata* malcho VI int. (200 μm), **c)** *Candona angulata* hembra VD int. (200 μm), **d)** *Candona angulta* macho VD int. (200 μm), **e)** *Candonidae* sp. VD int. (200 μm), **f)** *Candonidae* sp. juvenil int. (100 μm), **g)** *Darwinula stevensoni* VD int. (200 μm), **h)** *Darwinula stevensoni* VI visión dorsal (200 μm).

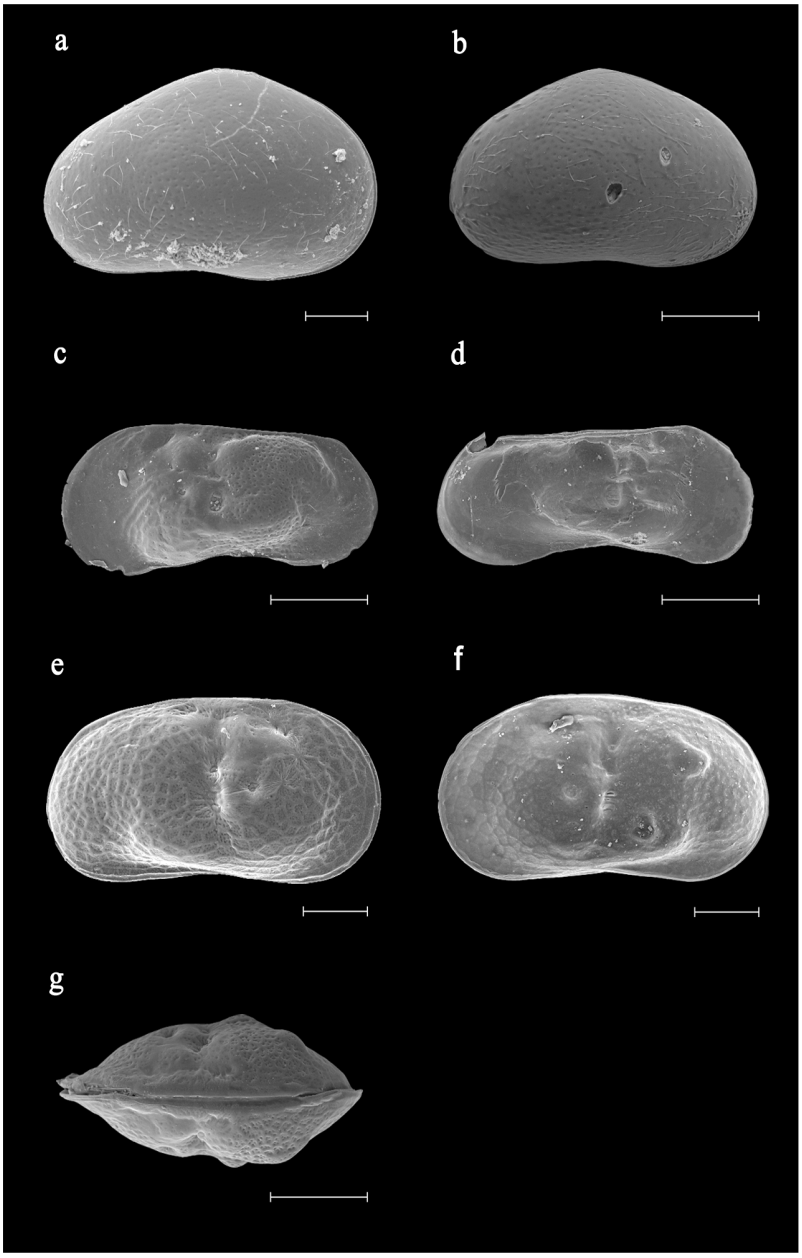

Plate 2.6: SEM photographies of different freshwater species from Center core. The scale is located below each photography and detailed between brackets for each specimen. **a)** *Cypridopsis vidua* RV ext. (100 μm), **b)** *Cypridopsis vidua* RV ext. (200 μm), **c)** *Paralimnocythere psammophila* female LV ext. (200 μm), **d)** *Paralimnocythere psammophila* male RV ext. (200 μm), **e)** *Limnocythre inopinata* RV ext. (100 μm), **f)** *Limnocythre inopinata* LV ext. (100 μm) **g)** *Limnocythre inopinata* dorsal view (200 μm).

Lámina 2.6: Fotografías de ME de las distintas especies de afinidades marinas encontradas en el sondeo Centro. El valor de escala se sitúa debajo de cada valva y detallada entre paréntesis para cada especimen. **a)** *Cypridopsis vidua* VD ext. (100 μm), **b)** *Cypridopsis vidua* VD ext. (200 μm), **c)** *Paralimnocythere psammophila* hembra VI ext. (200 μm), **d)** *Paralimnocythere psammophila* macho VD ext. (200 μm), **e)** *Limnocythre inopinata* VD ext. (100 μm), **f)** *Limnocythre inopinata* VI ext. (100 μm) **g)** *Limnocythre inopinata* visión dorsal (200 μm).

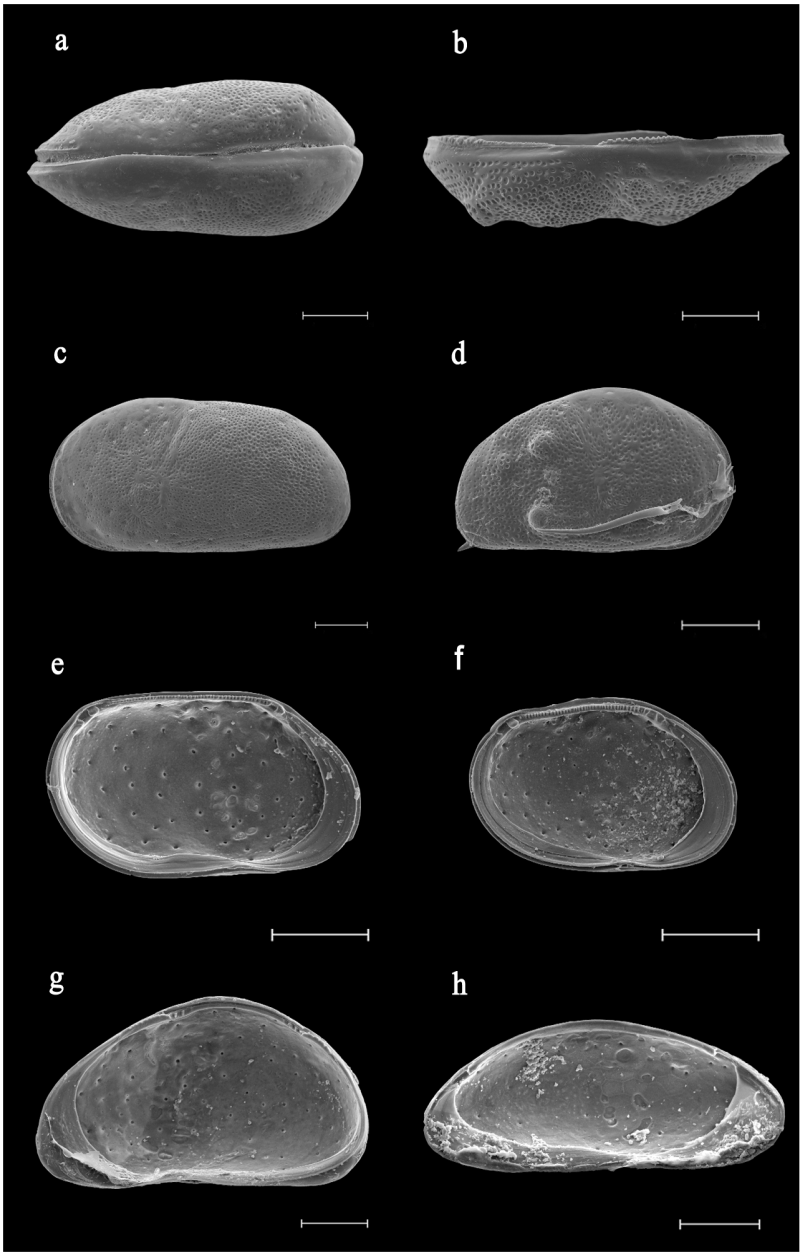

Plate 3.1: SEM photographies of different brackish ostracod species from L'Antina core. The scale is located below each photography and detailed between brackets for each specimen. **a)** *C. torosa* male dorsal view (200 μm), **b)** *C. torosa* male RV, noded, dorsal view (200 μm), **c)** *C. torosa* male LV, **d)** *C. torosa* juvenile, RV ext. noded (200 μm), **e)** *Loxoconcha elliptica* LV int. (200 μm), **f)** *Loxoconcha elliptica* juvenile LV int. (200 μm), **g)** *Xestoleberis nitida* RV int. (100 μm), **h)** *Cytherois* cf *stephanidesi* LV int. (100 μm).

Lámina 3.1: Fotografías de ME de las distintas especies de ostrácodos con afinidades de aguas salobres encontradas en el sondeo de L'Antina. El valor de escala se sitúa debajo de cada valva y se detalla entre paréntesis para cada individuo. **a)** *C. torosa* macho visión dorsal (200 μm), **b)** *C. torosa* macho VD, nodado, visión dorsal (200 μm), **c)** *C. torosa* macho VI, **d)** *C. torosa* juvenil, nodado, VD ext. (200 μm), **e)** *Loxoconch elliptica* VI int. (200 μm), **f)** *Loxoconch elliptica* juvenil VI int. (200 μm), **g)** *Xestoleberis nitida* VD int. (100 μm), **h)** *Cytherois* cf *stephanidesi* VI int. (100 μm).

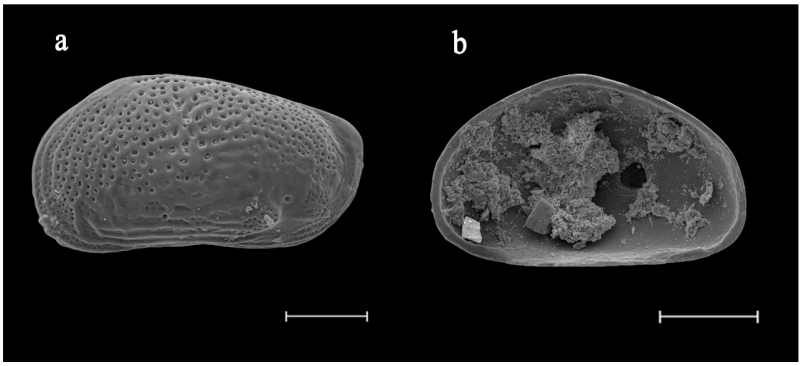

Plate 3.2: SEM photographies of different brackish ostracod species from L'Antina core. The scale is located below each photography and detailed between brackets for each specimen. **a)** *Leptocythere* cf. *porcellanea* LV ext. (100 μm), **b)** *Heterocypris* sp. juvenile RV int. (200 μm).

Lámina 3.2: Fotografías de ME de las distintas especies de ostrácodos con afinidades de aguas salobres encontradas en el sondeo de L'Antina. El valor de escala se sitúa debajo de cada valva y se detalla entre paréntesis para cada individuo. **a)** *Leptocythere* cf. *porcellanea* VI ext (100 μm), **b)** *Heterocypris* sp. juvenil VD int. (200 μm).

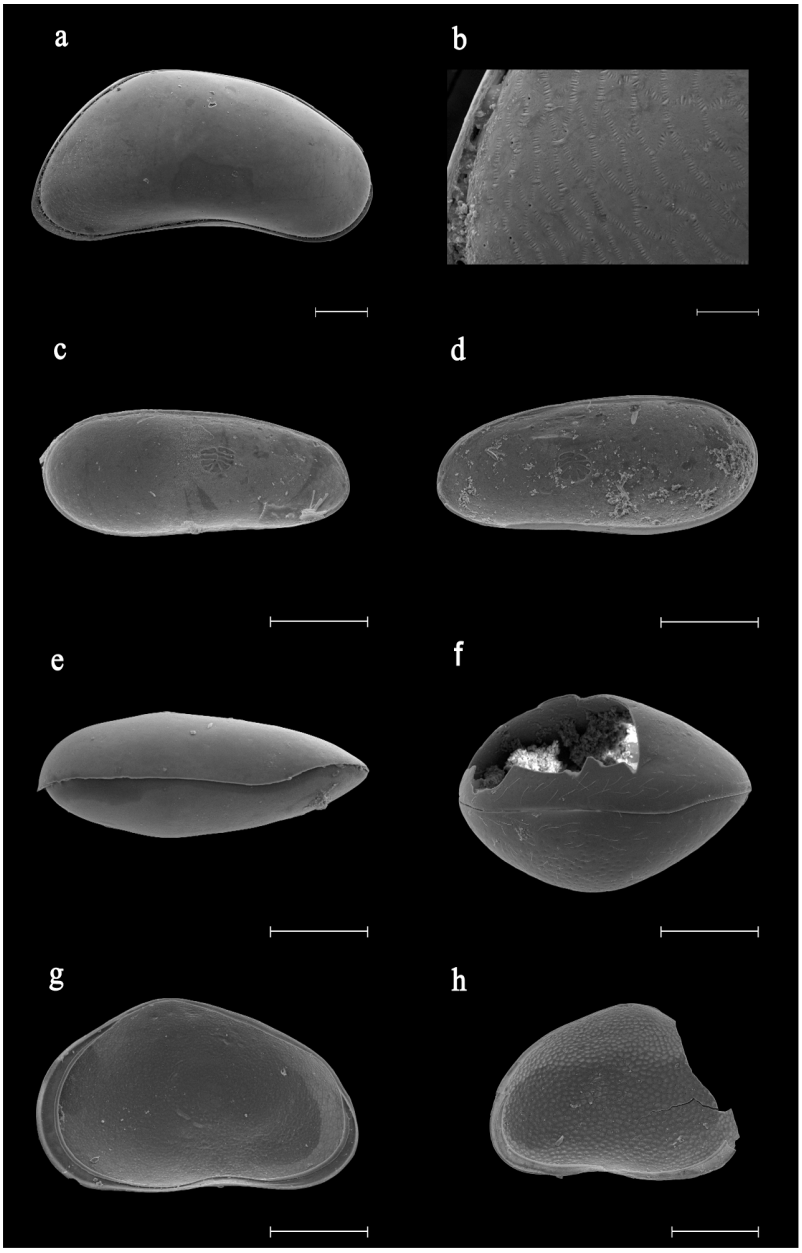

Plate 3.3: SEM photographies of different freshwater ostracod species from L'Antina core. The scale is located below each photography and detailed between brackets for each specimen. **a)** *Candona angulata* female RV ext. (200 μm), **b)** Detail of the posterior part of *Candona angulata* (100 μm), **c)** *Darwinula stevensoni* LV int., **d)** *Darwinula stevensoni* RV int. (200 μm), **e)** *Darwinula stevensoni* ventral view (200 μm), **f)** *Cypridopsis vidua*, dorsal view (200 μm), **g)** *Sarcypridopsis aculeata* RV int. (200 μm), **h)** *Sarcypridopsis aculeata* juvenile RV ext. (100 μm).

Lámina 3.3: Fotografías de ME de las distintas especies de ostrácodos con afinidades de aguas dulces encontradas en el sondeo de L'Antina. El valor de escala se sitúa debajo de cada valva y se detalla entre paréntesis para cada individuo. **a)** *Candona angulata* hembra VD ext. (200 μm), **b)** Detalle de la parte posterior de *Candona angulata* (100 μm), **c)** *Darwinula stevensoni* VI int., **d)** *Darwinula stevensoni* VD int. (200 μm), **e)** *Darwinula stevensoni* visión ventral (200 μm), **f)** *Cypridopsis vidua*, visión dorsal (200 μm), **g)** *Sarcypridopsis aculeata* VD int. (200 μm), **h)** *Sarcypridopsis aculeata* juvenil VD ext. (100 μm).

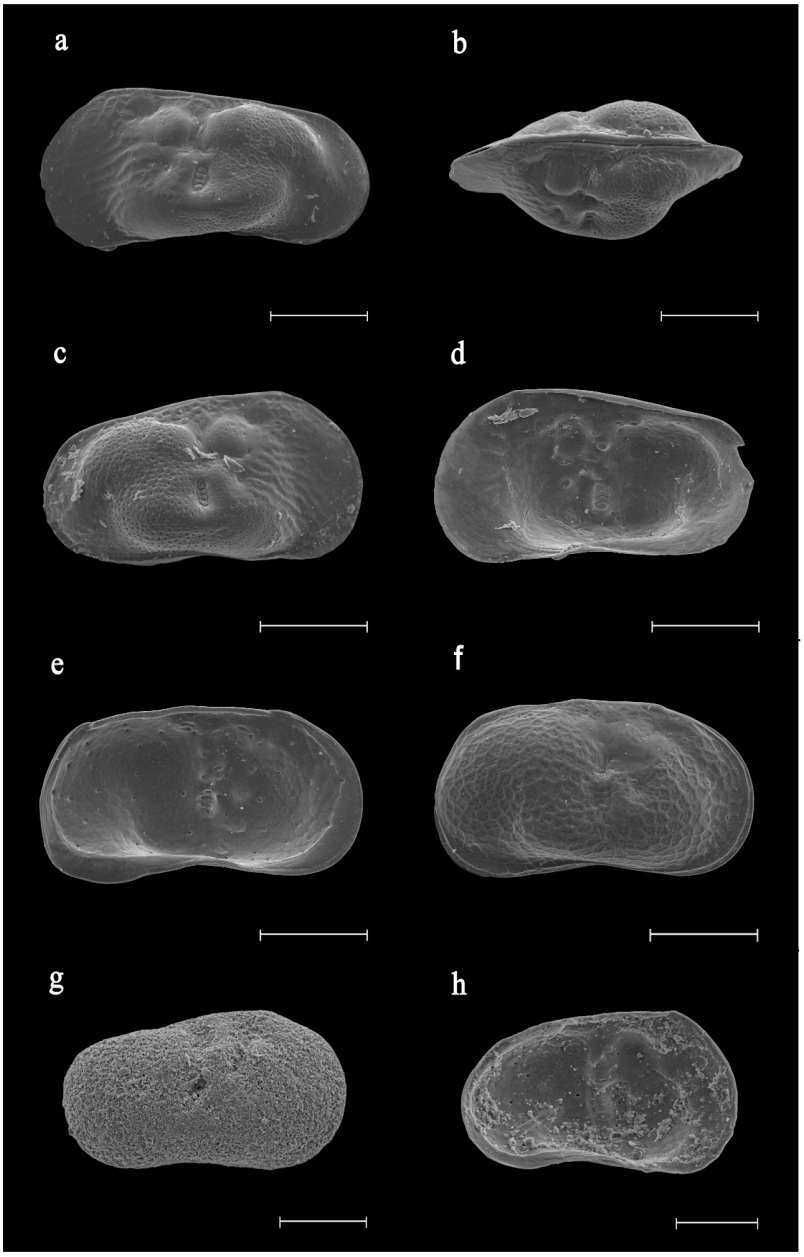

Plate 3.4: SEM photographies of different freshwater ostracod species from L'Antina core. The scale is located below each photography and detailed between brackets for each specimen. **a)** *Paralimnocythere psammophila* female LV ext. (200 μm), **b)** *Paralimnocythere psammophila* dorsal view (200 μm), **c)** *Paralimnocythere psammophila* juvenile RV ext. (200 μm), **d)** *Paralimnocythere psammophila* LV ext. (200 μm), **e)** *Limnocythere inopinata* LV int. (200 μm), **f)** *Limnocythere inopinata* RV ext. (200 μm), **g)** *Iliocypris gibba* RV ext. (200 μm), **h)** *Limnocythere stationis* RV ext. (100 μm).

Lámina 3.4: Fotografías de ME de las distintas especies de ostrácodos con afinidades de aguas dulces, encontradas en el sondeo de L'Antina. El valor de escala se sitúa debajo de cada valva y se detalla entre paréntesis para cada individuo. **a)** *Paralimnocythere psammophila* hembra VI ext. (200 μm), **b)** *Paralimnocythere psammophila* visión dorsal (200 μm), **c)** *Paralimnocythere psammophila* juvenil VD ext. (200 μm), **d)** *Paralimnocythere psammophila* VI ext. (200 μm), **e)** *Limnocythere inopinata* VI int. (200 μm), **f)** *Limnocythere inopinata* VD ext. (200 μm), **g)** *Iliocypris gibba* VD ext. (200 μm), **h)** *Limnocythere stationis* VD ext. (100 μm).

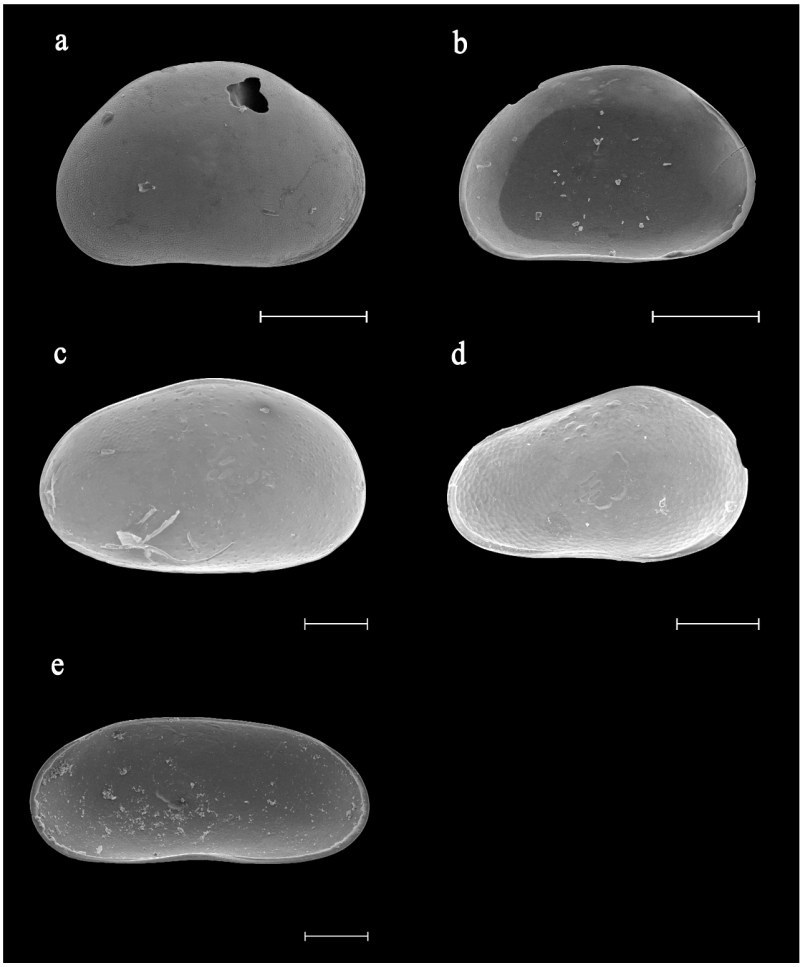

Plate 3.5: SEM photographies of different freshwater ostracod species from L'Antina core. The scale is located below each photography and detailed between brackets for each specimen. **a)** *Cypria* cf *ophtalmica* RV ext. (200 μm), **b)** *Cypria* cf *ophtalmica* LV int. (200 μm), **c)** *Bradleystrandensia* cf *reticulata* int. (200 μm), **d)** *Bradleystrandensia* cf *reticulata* juvenile LV int. (200 μm), **e)** *Herpetocypris* cf *chevreuxi* RV int. (200 μm).

Lámina 3.5: Fotografías de ME de las distintas especies de ostrácodos con afinidades de aguas dulces, encontradas en el sondeo de L'Antina. El valor de escala se sitúa debajo de cada valva y se detalla entre paréntesis para cada individuo. **a)** *Cypria* cf *ophtalmica* VD ext. (200 μm), **b)** *Cypria* cf *ophtalmica* VI int. (200 μm), **c)** *Bradleystrandensia* cf *reticulata* int. (200 μm), **d)** *Bradleystrandensia* cf *reticulata* juvenil VI int. (200 μm), **e)** *Herpetocypris* cf *chevreuxi* RV int. (200 μm).

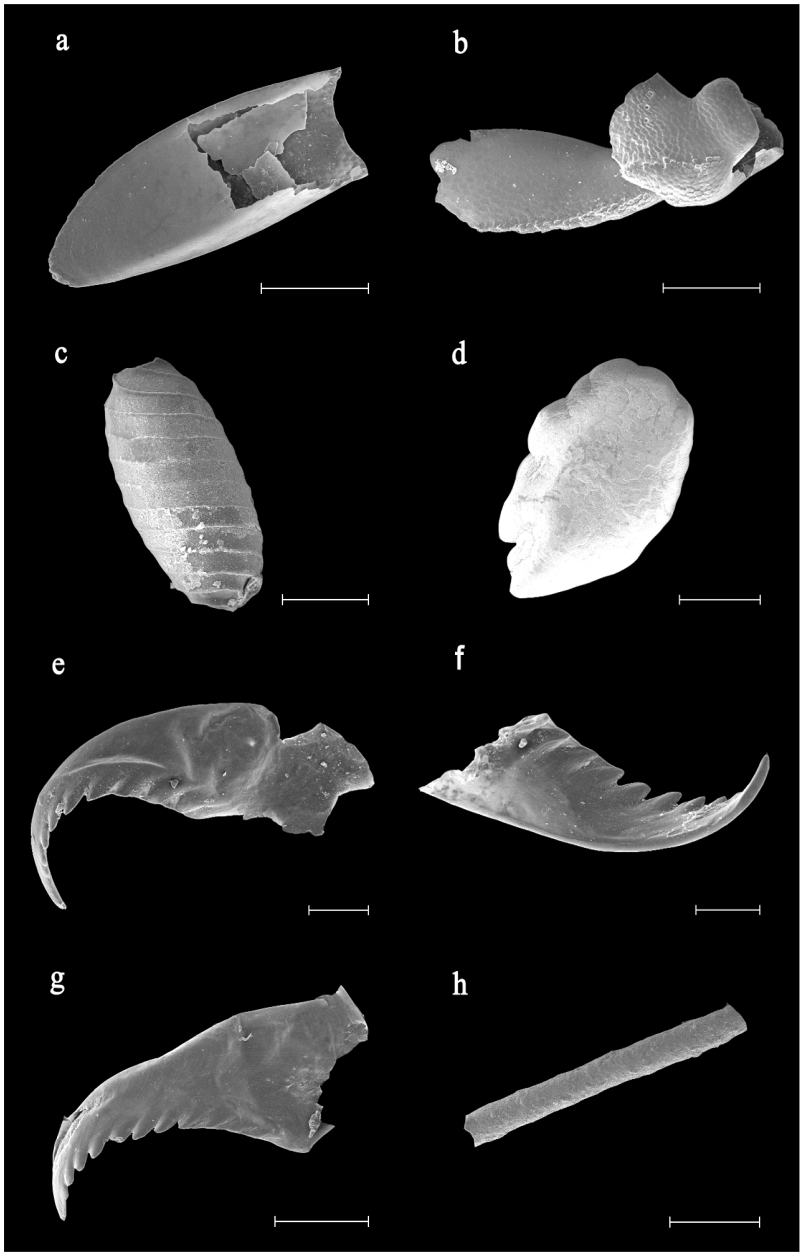

Plate 4.1: SEM photographies of other remains found at cores Center and L'Antina (CA). The scale is located below each photography and detailed between brackets for each specific remain, the depth is also palced. **a)** Unidentified remain, 89.5cm (200 μm), **b)** Unidentified remain, 62cm (200 μm), **c)** Oogonium, 19cm, CA (200 μm), **d)** *Fish otolith*, 81.5cm (500 μm), **e)** *Nereis* mandibule, 79cm (200 μm), **f)** *Nereis* mandibule, 76.5cm (200 μm), **g)** *Nereis* mandibule, 66.5cm (500 μm), **h)** Macrophyte stem, 72.5 cm (1 mm).

Lámina 4.1: Fotografías de ME de las distintas restos encontrados en los sondeos del Centro y de L'Antina (SA). El valor de escala se sitúa debajo de cada resto y se detalla entre paréntesis, la profundidad donde se encontro el resto también esta señalada. **a)** Resto no identificado, 89.5cm (200 μm), **b)** Resto no identificado, 62cm (200 μm), **c)** Oogonio, 19cm, SA (200 μm), **d)** Otolito, 81.5cm (200 μm), **e)** *Nereis* mandibula, 79cm (200 μm), **f)** *Nereis* mandibula, 76.5cm (200 μm), **g)** *Nereis* mandibula, 66.5cm (500 μm), **h)** tallo de macrófito, 72.5cm (1 mm).

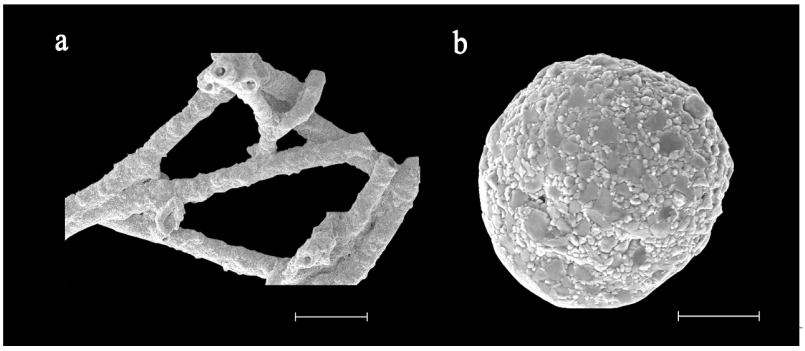

Plate 4.2: SEM photographies of other remains found at the cores Center (CC) and L'Antina (CA). The scale is located below each photography and detailed between brackets for each specific remain, the depth is also palced. **a)** Macrophytes stems, 72.5cm, CC (500 μm), **b)** Unidentified remain, 40.5cm, CA (50 μm).

Lámina 4.2:_Fotografías de ME de las distintas restos encontrados en los sondeos del Centro (SC) y de L'Antina (SA). El valor de escala se sitúa debajo de cada resto y se detalla entre paréntesis, la profundidad donde se encontro el resto también esta señalada. **a)** tallos de macrófitos, 72.5cm, SC (500 μm), **b)** resto sin identificar, 40.5cm, SA (50 μm).

Appendices

Appendix 1.1: BSS water hydrochemistry for the sampled period (March-04).

Apéndice 1.1: *Variables hidroquímicas de las muestras correspondientes al estudio extensivo (BSS) para Marzo-04.*

Sample	Coordenates (º)		TDS	Salinity	Chlorophyll*a*	T	DO	pH	Na^+	Mg^{2+}	K^+	Ca^{2+}	Sr^{2+}	Cl^-	Br^-	SO_4^{2-}	alkalinity	Mg/Ca	Sr/Ca	$\delta^{18}O$	δ^2H
	Longitude	Latitude	(mg/l)	(g/L)	(µg/L)	(ºC)	(mg/L)		(mg/L)	(mg/L)	(mg/L)	(mg/L)	(mg/L)	(mg/L)	(mg/L)	(mg/L)	meq	(molar)	(molar)x10^{-3}	‰	‰
E01	-0,0948	38,8765	613	0,50	0,03	17,80	8,82	7,50	174	30,0	6,67	83,7	0,27	317,6	0,1	66,44	3,9	0,59	1,50	-6,51	-35,2
E02	-0,0837	38,8821	896	0,90	0,33	17,10	8,63	7,48	265	40,7	9,64	100,3	0,39	478,9	1414	91,72	3,5	0,67	1,76	-6,44	-34,7
E06	-0,0821	38,8797	754	1,80	0,23	19,60	10,79	7,83	222	33,8	7,85	89,8	0,34	399,1	1148	77,71	3,5	0,62	1,74	-6,44	-35,8
E07	-0,0376	38,8543	13884	14,20	0,30	19,20	2,60	7,16	4446	503,2	159,50	409,7	3,57	8338	24	1225	4,1	2,03	3,98	-3,27	-17,7
E08	-0,0545	38,8769	4781	5,10	2,64	18,10	8,54	7,46	1508	177,4	50,34	236,6	1,38	2800	7466	418,2	3,6	1,24	2,66	-5,05	-26,7
E21	-0,2355	39,1912	1867	2,00	5,33	20,60	18,17	8,60	568	111,5	21,64	114,9	1,60	1047	2663	454,6	3,1	1,60	6,37	-1,05	-7,3
E28	-0,3168	39,2504	1399	1,50	0,13	19,40	5,62	7,18	406	93,6	10,60	168,9	2,53	715,7	1863	340	5,0	0,91	6,85	-5,72	-37,3
E38	-0,6122	38,1872	41484	41,10	0,52	10,90	8,92	8,30	13880	1733	576,50	519,3	9,24	24688	77	3742	3,6	5,50	8,14	1,70	9,7
E38 BIS	-0,6182	38,1848	48637	47,50	1,16	19,50	18,90	8,82	16510	2055	680,30	597,7	10,67	28689	93	4296	3,8	5,67	8,17	1,80	9,2
E39	-0,6182	38,1941	63153	63,50	8,97	18,50	4,67	7,78	21165	2677	860,55	787,8	14,60	37534	112	5879	4,4	5,60	8,48	2,75	14,6
E39 BIS	-0,6182	38,1941	20310	21,20	2,97	10,00	7,60	7,86	6801	987,7	154,50	749,3	27,45	11568	21	4047	7,9	2,17	16,76	0,06	-7,0
E45	-0,7515	38,1929	8123	9,40	2,60	10,00	8,20	7,65	2895	458,7	56,92	502,0	16,49	4189	3542	2984	7,5	1,51	15,03	-2,36	-20,5
E46	-0,7401	38,1672	7043	8,00	4,37	9,50	8,90	8,10	2447	453,3	47,13	491,7	16,27	3581	4563	2691	7,7	1,52	15,13	-3,66	-27,6
E53	0,2444	40,2022	2469	2,60	6,89	13,90	6,83	7,57	693	103,6	17,53	248,9	1,32	1400	3944	243,5	6,3	0,69	2,43	-4,62	-26,5
E59	0,2229	40,2134	5996	7,20	0,42	10,70	10,35	8,00	1783	248,4	56,37	395,1	3,09	3500	9879	450,8	3,9	1,04	3,58	-3,01	-20,4
RA05	-0,3179	39,3369	10956	11,60	71,50	9,10	11,64	9,23	3663	617,2	173,60	241,5	6,75	6236	17	2065	3,7	4,21	12,78	1,13	-1,9
E70	-0,5336	39,1476	247	0,20	0,32	18,90	8,14	7,01	30	35,5	3,45	124,6	1,49	52,05	0,2	163	4,6	0,47	5,47	-5,94	-36,6

Sample Name	Coodenates	Sampling date	TDS	salinity	T^a	DO	pH	Na^+	Mg^{2+}	K^+	Ca^{2+}	Sr^{2+}	alk/Ca	TIC-HCO_3	Cl^-	Br^-	SO_4^{2-}	Mg/Ca	Sr/Ca	$\delta^{18}O$	δ^2H	DIC–$\delta^{13}C$
	Long. / Lati.	yyyy-mm-dd	mg/L	(g/L)	(ºC)	(mg/L)		(mg/L)	(mg/L)	(mg/L)	(mg/L)	(mg/L)	(meq/L)	(mg/L)	(mg/L)	(mg/L)	(mg/L)	molar	molar x10^{-3}	VSMOW	VSMOW	VPDB
P5		2001-03-22	65909	73	22,3	6,4	8,33	21230	2688	837,6	833,86	15,23	0,09	148,65	40190	114,34	5616,8	5,32	8,35	3,85	1,62	-2,55
Santa Pola	-0,614/38,186	2001-04-30	47719	50	22,9	6,7	8,41	15200	1729	622,2	447,68	10,71	0,24	168,21	29610	100,19	4090,2	6,37	10,94	3,76	18,21	-0,33
		2001-06-05	48278	55	28,9	3,1	8,08	15440	1682	642,1	457,78	10,7	0,13	121,90	29946	99,65	4094,2	6,06	10,69	3,44	30,18	-4,15
		2001-07-26	51428	55	28,9	6	8,4	16500	1798	635,2	472,68	11,53	0,23	88,63	31904	106,39	4309,2	6,27	11,16	3,74	19,83	-3,15
		2001-09-07	50445	55	28,5	4,2	8,55	16170	1847	652,4	480,88	11,07	0,18	91,18	31180	104,29	4255,2	6,33	10,53	3,50	28,15	-3,11
		2001-10-11	45204	48	24,3	8,8	8,48	14540	1811	584,8	585,77	10,49	0,2	121,77	27596	76,45	3747,2	5,1	8,19	1,89	-0,09	-5,30
		2001-11-09	43823	46	15,5	7	8,77	14330	1736	541,3	486,58	10,23	0,23	103,29	26628	91,1	3651,7	5,88	9,62	0,97	7,12	-3,81
		2001-12-13	45676	50	11,8	10,3	8,87	15420	1853	658,4	525,17	10,56	0,16	112,92	27109	100,49	3692,2	5,82	9,20	1,41	12,58	-3,42
		2002-01-15	40010	43	13,9	9,9	8,84	12810	1606	499,8	473,08	9,54	0,22	120,23	24528	83,95	3412,2	5,6	9,22	0,24	12,51	-3,42
		2002-02-15	45472	45	12,9	14,5	9,0	15160	1889	580,4	552,37	10,81	0,14	106,37	27191	88,45	3771,7	5,64	8,95	1,73	21,48	-3,35
		2002-03-12	48478	50	16,6	12,1	9,0	15830	1994	592,4	569,17	11,77	0,15	99,33	29371	110,59	4044,2	5,78	9,46	2,71	32,40	-5,08
P7		2001-03-22	9484	10,3	24,8	17	8,32	3206	469	55,76	528,37	15,92	0,28	303,02	5204	5,01	2835,1	1,46	13,78	-3,38	-13,74	-7,36
Santa Pola	-0,614/38,181	2001-04-30	7979	9,0	23,5	17,3	9,59	2757	292	48,99	294,69	11,02	0,43	246,99	4570,5	4,88	2038,6	1,63	17,11	-3,00	-14,53	-3,51
		2001-06-05	8241	9,2	30,5	12,9	8,23	2724	386	50,69	351,08	14,85	0,42	313,01	4707,5	7,23	2258,6	1,81	19,35	-3,40	-17,04	-8,20
		2001-07-26	8099	9,0	32,9	12,5	9,15	2679	396	51,58	342,28	14,66	0,31	242,99	4608,5	7,29	2288,1	1,91	19,59	-3,20	-19,39	-7,00
		2001-09-07	3058	4,5	30,4	4,3	8,32	1025	111	41,96	127,39	4,13	0,99	151,32	1746,5	2,22	738,8	1,43	14,84	-3,85	-17,06	-10,93
		2001-10-11	6251	7,2	23,7	12,7	8,24	2077	321	44,72	327,58	9,9	0,29	223,99	3468	3,63	2027,6	1,61	13,82	-4,46	-30,47	-9,42
		2001-11-09	7542	8,5	16,6	3,9	7,67	2588	396	51,25	360,78	13,76	0,26	301,77	4126	6,1	2314,6	1,81	17,45	-4,29	-23,61	-9,43
		2001-12-13	7125	7,8	14,5	15,2	8,0	2555	372	47,29	374,08	12,93	0,39	392,88	3757,5	6,22	2027,6	1,64	15,81	-4,38	-29,19	-8,76
		2002-01-15	7033	8,2	13,3	7,7	7,72	2362	383	42,38	386,78	13,21	0,37	364,98	3840	5,35	2051,1	1,63	15,62	-3,96	-14,41	-8,67
		2002-02-15	7616	6,9	16,5	17,4	8,39	2607	427	49,5	384,38	14,05	0,37	305,98	4128,5	5,69	2166,6	1,83	16,72	-3,06	-8,12	-7,38
		2002-03-12	7534	8,7	17,3	11,8	8,3	2515	409	50,05	380,98	13,83	0,34	325,98	4159	6,11	2146,1	1,77	16,60	-2,88	-12,62	-7,04
U1		2001-03-22	177	0,3	21,9	9,9	8,0	22,5	26,6	1,46	85,84	0,33	1,24	267,53	40,34	0,112	66,38	0,51	1,75	-6,08	-50,01	-10,61
"Ullal fosc"	-0,391/39,294	2001-04-30	139	0,1	23,2	6,9	7,6	18,3	20,9	1,02	66,5	0,23	1,57	247,17	31,63	0,102	46,37	0,52	1,61	-6,20	-45,25	-10,89
spring		2001-06-05	172	0,4	27,9	10,3	8,1	27,5	27	3,37	69,03	0,41	1,63	243,99	44,74	0,126	81,82	0,65	2,7	-6,16	-51,02	-9,53
		2001-07-26	206	0,1	28,3	13,2	8,0	38,6	28,2	2,65	68,92	0,47	1,25	224,47	67,09	0,174	97,04	0,68	3,15	-6,16	-50,00	-9,25
		2001-09-07	176	0,4	27	8,4	8,0	27,7	26,1	3,29	70,76	0,42	1,36	244,43	47,54	0,141	88,74	0,61	2,69	-6,65	-43,50	-10,4
		2001-10-11	199	0,1	22,6	5,8	7,7	28	29,9	1,86	90,74	0,41	1,06	280,58	48	0,101	79,57	0,54	2,08	-6,99	-36,19	-10,6
		2001-11-09	195	0,3	16	9,2	8,2	27,3	28,8	1,9	88,49	0,41	1,15	271,73	48,07	0,151	82,19	0,54	2,09	-5,87	-37,36	-9,86
		2001-12-13	228	0,1	17,7	11,7	7,7	37,6	29,8	14,87	92,82	0,36	1,08	281,36	52,64	0,139	90,82	0,53	1,76	-5,53	-30,49	-12,15
		2002-01-15	209	0,4	18,8	7,8	7,6	37	29,5	4,05	86,01	0,38	1,19	274,10	51,78	0,139	73,56	0,57	2,02	-5,95	-43,48	-11,44
		2002-02-15	180	0,1	19,1	12	7,6	22,5	27,9	1,51	87,78	0,32	1,14	265,27	39,75	0,159	68,69	0,52	1,68	-5,58	-25,96	-10,92
		2002-03-12	173	0,1	19,5	8,7	7,8	21,9	26,6	1,56	83,72	0,29	1,29	275,33	38,63	0,141	64,58	0,52	1,6	-5,77	-30,79	-11,18

Appendix 1.2: Hydrochemical variables during the sampling period from March-01 to March-02 for the monthly survey samples (MSS). Note that the water data from of July 3rd is absent.

Apéndice 1.2: *Variables hidroquímicas de las muestras mensuales del estudio intensivo (MSS) desde Marzo-01 a Marzo-02. Notar, que no se realizaron análisis para el día 3 Julio-01 por lo que no están incluidos.*

Appendix 1.3: Ostracod data set for the broad survey samples (BSS). The average values for females (f), males (m), and juveniles (y) are given for: valve length (CL), Ca content (Ca_{SHELL}), isotopic values ($\delta^{18}O_{VPDB}$ and $\delta^{13}C_{VPDB}$), cation ratios (Mg/Ca and Sr/Ca), Kd(Mg/Ca) ($Mg/Ca_{ostracod}/Mg/Ca_{water}$), and Kd(Sr/Ca) ($Sr/Ca_{ostracod}/Sr/Ca_{water}$).

Apéndice 1.3*: Datos del ostrácodo para el estudio extensivo (BSS). Los valores medios para hembras(f), machos (m) y juveniles (j) se muestran para: longitud de la valva (CL), contenido en Ca (Ca_{SHELL}), isótopos ($\delta^{18}O_{VPDB}$ and $\delta^{13}C_{VPDB}$), ratio de cationes (Mg/Ca and Sr/Ca), Kd(Mg/Ca) ($Mg/Ca_{ostracod}/Mg/Ca_{water}$), and Kd(Sr/Ca) ($Sr/Ca_{ostracod}/Sr/Ca_{water}$).*

Samples	#carapaces	Length♀	Ca_{SHELL}♀	$\delta^{18}O$♀	$\delta^{13}C$♀	Mg/Ca♀	Sr/Ca♀	Mg/Ca_{valve} / Mg/Ca_{water}	Sr/Ca_{valve} / Sr/Ca_{water}
		µm	µgCa/carapace	‰ VPDB	‰ VPDB	molar ($x10^{-2}$)	molar ($x10^{-3}$)	$x10^{-2}$	$x10^{-1}$
E01									
E02									
E06	7	1053,0	35,57	-5,87	-11,00	0,94	1,85	1,52	10,67
E07	6	949,7	24,42	-3,54	-12,33	1,14	2,00	0,56	5,03
E08	8	1079,0	34,44	-4,90	-13,16	0,69	1,76	0,56	6,61
E21	3	1001,0	17,09	-0,18	-5,78	1,02	4,70	0,63	7,39
E28	4	1105,0	24,30	-5,61	-10,71	0,80	4,29	0,88	6,26
E38	4	1004,3	22,97	-0,75	-3,33	1,50	2,97	0,27	3,65
E38 BIS	7	983,1	17,98	-2,25	-9,70	1,51	5,84	0,27	7,15
E39	8	997,8	20,53	1,01	-5,24	1,19	2,78	0,21	3,28
E39 BIS	8	979,9	18,31	1,75	-7,91	1,29	8,97	0,60	5,35
E45	8	955,5	22,11	0,06	-10,14	1,00	9,44	0,66	6,28
E46	8	950,6	17,63	-2,42	-9,47	1,88	9,64	1,23	6,37
E53	5	1087,7	40,98	-4,31	-11,99	0,99	1,87	1,44	7,70
E59	8	1009,1	23,93	0,11	-8,15	1,48	2,26	1,43	6,33
RA05	8	955,5	13,46	3,75	-8,41	1,41	5,80	0,34	10,59
E70	2	1001,0	25,33	-5,77	-12,38	0,92	3,27	1,97	2,56

Samples	#carapaces	Length♂	Ca_{SHELL}♂	$\delta^{18}O$♂	$\delta^{13}C$♂	Mg/Ca♂	Sr/Ca♂	Mg/Ca_{valve} / Mg/Ca_{water}	Sr/Ca_{valve} / Sr/Ca_{water}
		µm	µgCa/carapace	‰ VPDB	‰ VPDB	molar ($x10^{-2}$)	molar ($x10^{-3}$)	$x10^{-2}$	$x10^{-1}$
E01	1	1209,0	23,2	-7,38	-11,74	1,79	1,07	3,04	7,16
E02	2	1267,5	34,4	-6,13	-11,53	0,78	1,39	1,17	7,90
E06	8	1212,3	28,3	-5,68	-10,94	0,83	1,87	1,34	10,78
E07	5	1077,9	15,4	-3,19	-12,03	0,97	2,08	0,48	5,23
E08	3	1277,3	32,4	-5,01	-13,31	0,93	1,54	0,75	5,79
E21	8	1225,3	29,9	-0,51	-7,48	0,79	4,41	0,50	6,92
E28	3	1202,5	14,2	-5,38	-10,85	1,13	4,76	1,24	6,95
E38	2	1066,0	16,7	-0,15	-4,03	1,33	2,55	0,24	3,13
E38 BIS	2	1105,0	16,4	-4,78	-11,97	1,61	7,12	0,28	8,72
E39	8	1063,4	14,1	1,38	-6,03	1,18	2,70	0,21	3,19
E39 BIS	8	1061,1	16,7	1,75	-8,29	1,39	9,10	0,64	5,43
E45	8	1014,0	16,8	-0,25	-9,45	1,40	10,20	0,93	6,79
E46	8	1053,0	15,9	-2,14	-9,44	1,65	10,05	1,09	6,64
E53	5	1180,8	23,6	-4,68	-11,65	1,10	1,96	1,61	8,05
E59	5	1061,7	24,6	0,64	-7,98	1,23	2,20	1,19	6,16
RA05	8	1048,1	11,6	4,83	-5,62	1,89	6,35	0,45	11,61
E70	1	1105,0	9,10	-5,67	-12,16	1,58	3,27	3,36	2,55

Samples	#carapaces	$Length_{juv}$	$Ca_{SHELL juv}$	$\delta^{18}O_{juv}$	$\delta^{13}C_{juv}$	Mg/Ca_{juv}	Sr/Ca_{juv}	Mg/Ca_{valve} / Mg/Ca_{water}	Sr/Ca_{valve} / Sr/Ca_{water}
		µm	µgCa/carapace	‰ VPDB	‰ VPDB	molar ($x10^{-2}$)	molar ($x10^{-3}$)	$x10^{-2}$	$x10^{-1}$
E07	8	687,4	3,40	-3,31	-12,44	0,99	2,07	0,49	5,21
E08	5	894,8	9,93	-4,78	-13,25	0,62	1,64	0,50	6,15
E28	4	760,5	5,44	-5,40	-10,75	0,54	4,64	0,59	6,77
E38	8	825,1	7,06	0,50	-3,95	1,65	3,07	0,3	3,77
E53	6	877,5	9,26	-2,57	-10,80	0,83	1,74	1,22	7,17

Sample	Collection Date dd/mm/yyy	Instar	# carapaces	Ca_{SHELL} µgCa/carapace	$\delta^{13}C_{VPDB}$ ‰	$\delta^{18}O_{VPDB}$ ‰	Mg/Ca molar x10^{-2}	Sr/Ca molar x10^{-2}	Mg/Ca_{valve} / Mg/Ca_{water} same month x10^{-2}	Sr/Ca_{valve} / Sr/Ca_{water} same month x10^{-1}	Mg/Ca_{valve} / Mg/Ca_{water} month before x10^{-2}	Sr/Ca_{valve} / Sr/Ca_{water} month before x10^{-1}
P5	22/03/2001	f	7	14,63 ± *2,9*	-7,43 ± *1,95*	1,07 ± *2,15*	1,11 ± *0,73*	2,55 ± *0,5*	0,209 ± *0,138*	3,037 ± *0,609*		
		m	7,5	12,20 ± *3*	-7,48 ± *0,58*	1,92 ± *0,56*	0,83 ± *0,29*	2,59 ± *0,1*	0,156 ± *0,055*	3,084 ± *0,123*		
		y	14,5	5,80 ± *1,7*	-7,69 ± *1,22*	1,16 ± *1,53*	0,79 ± *0,29*	3,41 ± *0,4*	0,149 ± *0,046*	4,061 ± *0,544*		
	30/04/2001	f	9	13,05 ± *4,3*	-6,91 ± *0,7*	2,14 ± *0,38*	0,93 ± *0,28*	2,79 ± *0,3*	0,146 ± *0,044*	2,561 ± *0,248*	0,175 ± *0,052*	0,332 ± *0,032*
		m	8,5	10,19 ± *3,7*	-6,48 ± *0,81*	2,53 ± *0,32*	0,93 ± *0,19*	2,80 ± *0,2*	0,146 ± *0,029*	2,570 ± *0,205*	0,174 ± *0,035*	0,333 ± *0,027*
		y	14,5	7,02 ± *1,4*	-6,16 ± *0,65*	1,27 ± *0,38*	1,31 ± *0,25*	3,11 ± *0,3*	0,206 ± *0,040*	2,854 ± *0,249*	0,246 ± *0,047*	0,370 ± *0,032*
	05/06/2001	f	6	17,88 ± *3,4*	-7,43 ± *1,27*	1,76 ± *1,06*	0,80 ± *0,24*	2,79 ± *0,2*	0,133 ± *0,040*	2,611 ± *0,194*	0,126 ± *0,038*	0,256 ± *0,019*
		m	8	11,53 ± *2,7*	-7,41 ± *0,67*	1,13 ± *0,23*	1,03 ± *0,31*	2,97 ± *0,2*	0,169 ± *0,052*	2,772 ± *0,145*	0,161 ± *0,049*	0,272 ± *0,014*
		y	13,5	6,98 ± *0,8*	-7,44 ± *0,51*	1,24 ± *0,1*	0,98 ± *0,18*	3,09 ± *0,1*	0,162 ± *0,029*	2,891 ± *0,135*	0,154 ± *0,028*	0,284 ± *0,013*
	03/07/2001	f	11	11,35 ± *2,9*	-7,35 ± *0,48*	1,52 ± *0,65*	0,97 ± *0,31*	3,14 ± *0,2*	0,160 ± *0,051*	2,933 ± *0,223*	0,160 ± *0,051*	0,293 ± *0,022*
		m	10	13,98 ± *4,3*	-7,35 ± *0,5*	1,43 ± *0,63*	1,13 ± *0,17*	3,05 ± *0,1*	0,186 ± *0,028*	2,854 ± *0,093*	0,186 ± *0,028*	0,285 ± *0,009*
		y	15,5	5,37 ± *0,6*	-7,45 ± *0,4*	1,28 ± *0,09*	0,95 ± *0,09*	3,28 ± *0*	0,157 ± *0,015*	3,070 ± *0,025*	0,157 ± *0,015*	0,307 ± *0,002*
	26/07/2001	f	12	12,02 ± *3,2*	-6,73 ± *0,57*	1,22 ± *0,21*	1,04 ± *0,18*	3,09 ± *0,2*	0,166 ± *0,029*	2,770 ± *0,158*	0,172 ± *0,030*	0,289 ± *0,017*
		m	12	16,03 ± *7,5*	-6,68 ± *0,31*	1,25 ± *0,33*	1,00 ± *0,18*	3,01 ± *0,2*	0,160 ± *0,028*	2,698 ± *0,159*	0,165 ± *0,029*	0,282 ± *0,017*
		y	16	6,48 ± *1,3*	-6,85 ± *0,58*	1,31 ± *0,15*	1,27 ± *0,51*	3,19 ± *0,1*	0,203 ± *0,082*	2,857 ± *0,082*	0,210 ± *0,085*	0,298 ± *0,009*
	07/09/2001	f	10,5	13,14 ± *3,7*	-6,20 ± *0,49*	1,30 ± *0,23*	2,78 ± *2,31*	3,22 ± *0,3*	0,439 ± *0,365*	3,056 ± *0,241*	0,444 ± *0,368*	0,288 ± *0,023*
		m	10	18,61 ± *4,8*	-6,62 ± *0,32*	1,30 ± *0,21*	2,51 ± *2,01*	2,98 ± *0,1*	0,396 ± *0,318*	2,834 ± *0,124*	0,400 ± *0,321*	0,267 ± *0,012*
		y	16,5	6,03 ± *2,3*	-6,16 ± *0,76*	1,04 ± *0,36*	5,04 ± *3,21*	3,20 ± *0,1*	0,796 ± *0,507*	3,036 ± *0,098*	0,803 ± *0,512*	0,287 ± *0,009*
	11/10/2001	f	10,5	12,08 ± *1,8*	-6,26 ± *0,8*	1,34 ± *0,56*	1,11 ± *0,29*	3,00 ± *0,1*	0,218 ± *0,057*	3,666 ± *0,175*	0,176 ± *0,046*	0,285 ± *0,014*
		m	12,5	14,10 ± *1,6*	-5,96 ± *1,42*	1,69 ± *0,45*	0,94 ± *0,12*	3,00 ± *0,3*	0,185 ± *0,023*	3,659 ± *0,319*	0,149 ± *0,019*	0,285 ± *0,025*
		y	12,5	7,01 ± *3,3*	-6,48 ± *1,14*	0,94 ± *0,29*	1,12 ± *0,21*	2,96 ± *0,2*	0,220 ± *0,041*	3,610 ± *0,209*	0,177 ± *0,033*	0,281 ± *0,016*
	09/11/2001	f	12	12,16 ± *1,8*	-5,73 ± *1,64*	1,43 ± *0,87*	1,20 ± *0,32*	3,14 ± *0,3*	0,205 ± *0,055*	3,264 ± *0,271*	0,236 ± *0,063*	0,383 ± *0,032*
		m	12	16,94 ± *3,1*	-5,51 ± *1,2*	1,54 ± *0,71*	1,20 ± *0,26*	3,12 ± *0,2*	0,203 ± *0,044*	3,245 ± *0,221*	0,234 ± *0,050*	0,381 ± *0,026*
		y	19,5	6,80 ± *3,4*	-5,61 ± *1,35*	1,31 ± *0,62*	1,23 ± *0,38*	3,19 ± *0,3*	0,210 ± *0,065*	3,318 ± *0,331*	0,242 ± *0,075*	0,390 ± *0,039*
	13/12/2001	f	11,5	12,26 ± *3,4*	-4,86 ± *1,61*	1,28 ± *0,69*	1,15 ± *0,27*	3,08 ± *0,2*	0,198 ± *0,046*	3,345 ± *0,233*	0,195 ± *0,046*	0,320 ± *0,022*
		m	11	19,28 ± *4,6*	-5,58 ± *1,76*	1,83 ± *0,42*	1,13 ± *0,31*	3,09 ± *0,3*	0,194 ± *0,052*	3,358 ± *0,268*	0,192 ± *0,052*	0,321 ± *0,025*
		y	20	7,87 ± *3,7*	-5,94 ± *1,72*	1,34 ± *0,96*	1,18 ± *0,56*	3,21 ± *0,4*	0,202 ± *0,096*	3,488 ± *0,451*	0,200 ± *0,095*	0,334 ± *0,043*
	15/01/2002	f	11,5	13,71 ± *2*	-4,75 ± *1,63*	1,88 ± *0,35*	1,31 ± *0,18*	3,28 ± *0,2*	0,235 ± *0,031*	3,552 ± *0,226*	0,226 ± *0,030*	0,356 ± *0,023*
		m	11	20,75 ± *3,4*	-3,98 ± *1,42*	1,60 ± *0,57*	1,32 ± *0,41*	3,34 ± *0,8*	0,237 ± *0,072*	3,620 ± *0,854*	0,228 ± *0,070*	0,363 ± *0,086*
		y	20	5,81 ± *2,9*	-5,73 ± *1,83*	1,35 ± *0,79*	1,28 ± *0,44*	3,22 ± *0,3*	0,229 ± *0,078*	3,496 ± *0,320*	0,221 ± *0,075*	0,351 ± *0,032*
	15/02/2002	f	11	13,72 ± *3,2*	-5,04 ± *2,07*	1,08 ± *0,85*	1,18 ± *0,35*	3,06 ± *0,4*	0,209 ± *0,062*	3,419 ± *0,439*	0,211 ± *0,062*	0,332 ± *0,043*
		m	12	18,86 ± *4,8*	-5,04 ± *1,71*	1,55 ± *0,73*	1,17 ± *0,43*	2,96 ± *0,3*	0,208 ± *0,076*	3,302 ± *0,341*	0,210 ± *0,077*	0,320 ± *0,033*
		y	19	5,83 ± *3*	-5,74 ± *1,38*	1,93 ± *0,69*	1,46 ± *0,38*	3,36 ± *0,4*	0,260 ± *0,068*	3,752 ± *0,482*	0,262 ± *0,069*	0,364 ± *0,047*
	12/03/2002	f	11,5	14,86 ± *2,6*	-4,87 ± *0,95*	2,08 ± *0,85*	1,39 ± *0,35*	3,25 ± *0,3*	0,241 ± *0,060*	3,441 ± *0,309*	0,247 ± *0,062*	0,364 ± *0,033*
		m	10,5	15,19 ± *4*	-4,83 ± *1,61*	0,96 ± *0,58*	1,19 ± *0,27*	2,93 ± *0,3*	0,206 ± *0,047*	3,101 ± *0,359*	0,211 ± *0,048*	0,328 ± *0,038*
		y	18	6,31 ± *2*	-6,30 ± *1,77*	0,70 ± *1,1*	1,25 ± *0,38*	3,47 ± *0,6*	0,216 ± *0,066*	3,673 ± *0,629*	0,222 ± *0,068*	0,388 ± *0,066*

Appendix 1.4: Ostracod data set for the monthly survey samples (P5-P7-U1). The average values for females (f), males (m), and juveniles (y) are given for: Ca_{SHELL}, isotopic values ($\delta^{13}C_{VPDB}$ and $\delta^{18}O_{VPDB}$), cation ratios (Mg/Ca and Sr/Ca), Kd(Mg/Ca):($Mg/Ca_{ostracod}/Mg/Ca_{water}$), and Kd(Sr/Ca):($Sr/Ca_{ostracod}/Sr/Ca_{water}$). The Kds were calculated using the water data from the same month and also with the data from previous months. Note that the standard deviation is located to the right of each mean value.

Apéndice 1.4: *Datos del ostrácodo para las muestras mensuales* (P5-P7-U1). *Los valores medios para hembras (f), machos (m) y juveniles (j) se muestran para: contenido en Ca (Ca_{SHELL}), isótopos ($\delta^{18}O_{VPDB}$ and $\delta^{13}C_{VPDB}$), ratio de cationes (Mg/Ca and Sr/Ca), K_d(Mg/Ca):($Mg/Ca_{ostracod}/Mg/Ca_{water}$), and K_d(Sr/Ca):($Sr/Ca_{ostracod}/Sr/Ca_{water}$). El Kd se calculo usando el dato del agua de la misma fecha de muestreo y con el dato del mes anterior. Notar que la desviación estándar para cada variable está colocada a la derecha de la misma.*

	Collection Date		#	Ca_{SHELL}	$\delta^{13}C_{VPDB}$	$\delta^{18}O_{VPDB}$	Mg/Ca	Sr/Ca	Mg/Ca_{valve} / Mg/Ca_{water}	Sr/Ca_{valve} / Sr/Ca_{water}	Mg/Ca_{valve} / Mg/Ca_{water}	Sr/Ca_{valve} / Sr/Ca_{water}
Sample	**dd/mm/yyy**	Instar	carapaces	µgCa/carapace	‰	‰	molar x10^{-2}	molar x10^{-2}	same month x10^{-2}	same month x10^{-1}	month before x10^{-2}	month before x10^{-1}
P7	22/03/2001	f	7	14,87 ± *6*	-10,94 ± *0,2*	-2,84 ± *0,3*	1,017 ± *0,3*	8,013 ± *0,6*	0,697 ± *0,209*	0,581 ± *0,040*		
		m	7	13,80 ± *3*	-10,64 ± *0,5*	-3,34 ± *0,5*	1,391 ± *0,4*	8,631 ± *0,9*	0,953 ± *0,254*	0,625 ± *0,066*		
		y	6	7,16 ± *2*	-11,09 ± *0,4*	-3,6 ± *0,8*	1,006 ± *0*	7,271 ± *1,6*	0,689 ± *0,016*	0,527 ± *0,117*		
	30/04/2001	f	10	17,96 ± *3*	-10,87 ± *1,0*	-3,13 ± *0,4*	1,245 ± *0,6*	8,651 ± *0,8*	0,764 ± *0,375*	0,506 ± *0,049*	0,853 ± *0,418*	0,627 ± *0,061*
		m	10	11,10 ± *5*	-10,6 ± *0,5*	-3,14 ± *0,2*	1,556 ± *0,4*	8,85 ± *0,9*	0,955 ± *0,242*	0,518 ± *0,054*	1,066 ± *0,270*	0,642 ± *0,066*
		y	9	7,30 ± *3*	-11,98 ± *1,1*	-2,82 ± *0,6*	0,835 ± *0,2*	8,893 ± *0,2*	0,512 ± *0,095*	0,520 ± *0,013*	0,572 ± *0,106*	0,644 ± *0,016*
	05/06/2001	f	8	17,77 ± *5*	-10,98 ± *1,0*	-2,99 ± *0,5*	1,40 ± *0,3*	8,428 ± *0,7*	0,773 ± *0,161*	0,437 ± *0,039*	0,858 ± *0,179*	0,493 ± *0,044*
		m	8	13,17 ± *4*	-12,12 ± *1,1*	-3,57 ± *0,5*	1,473 ± *0,5*	8,588 ± *0,9*	0,814 ± *0,287*	0,445 ± *0,044*	0,904 ± *0,319*	0,430 ± *0,195*
		y	8,5	6,49 ± *2*	-10,27 ± *0,8*	-4,04 ± *0,2*	1,415 ± *0,6*	10,15 ± *0,5*	0,782 ± *0,315*	0,526 ± *0,025*	0,868 ± *0,350*	0,445 ± *0,298*
	03/07/2001	f	10,5	14,27 ± *3*	-10,53 ± *0,6*	-3,61 ± *0,5*	1,484 ± *0,3*	9,539 ± *0,9*	0,820 ± *0,167*	0,493 ± *0,046*	0,820 ± *0,167*	0,494 ± *0,046*
		m	10	16,38 ± *6*	-11,05 ± *0,9*	-3,59 ± *0,7*	1,773 ± *0,2*	9,803 ± *0,6*	0,979 ± *0,116*	0,507 ± *0,032*	0,980 ± *0,116*	0,508 ± *0,032*
		y	17,5	6,37 ± *1*	-10,11 ± *0,5*	-4,54 ± *0,2*	1,211 ± *0,2*	10,88 ± *0,4*	0,669 ± *0,097*	0,563 ± *0,018*	0,669 ± *0,097*	0,564 ± *0,018*
	26/07/2001	f	11,5	15,89 ± *4*	-9,576 ± *2,1*	-2,23 ± *1,4*	1,59 ± *0,3*	9,12 ± *1,5*	0,810 ± *0,142*	0,458 ± *0,077*	0,853 ± *0,150*	0,464 ± *0,078*
		m	10,5	17,78 ± *5*	-10,66 ± *1,0*	-2,47 ± *1,3*	1,43 ± *0,2*	9,038 ± *1,8*	0,748 ± *0,128*	0,461 ± *0,090*	0,788 ± *0,134*	0,467 ± *0,091*
		y	16	7,60 ± *3*	-8,763 ± *2,4*	-2,91 ± *1,2*	1,645 ± *0,6*	8,43 ± *2,2*	0,863 ± *0,320*	0,430 ± *0,111*	0,908 ± *0,337*	0,436 ± *0,113*
	07/09/2001	f	10	15,14 ± *4*	-9,73 ± *1,0*	-3,10 ± *0,9*	1,661 ± *0,6*	9,79 ± *0,6*	1,161 ± *0,410*	0,660 ± *0,037*	0,872 ± *0,308*	0,500 ± *0,028*
		m	10	20,68 ± *6*	-9,922 ± *1,2*	-2,67 ± *1,4*	1,492 ± *0,3*	9,224 ± *1,6*	1,043 ± *0,238*	0,622 ± *0,110*	0,783 ± *0,178*	0,471 ± *0,083*
		y	17	8,56 ± *2*	-10,24 ± *1,4*	-3,68 ± *0,8*	1,657 ± *0,5*	9,51 ± *1,1*	1,159 ± *0,358*	0,641 ± *0,073*	0,870 ± *0,268*	0,485 ± *0,056*
	11/10/2001	f	10	16,29 ± *3*	-10,28 ± *0,7*	-2,59 ± *1,9*	1,437 ± *0,3*	9,08 ± *0,6*	0,890 ± *0,185*	0,657 ± *0,041*	0,955 ± *0,143*	0,624 ± *0,041*
		m	10	21,14 ± *6*	-10,51 ± *0,8*	-3,43 ± *0,7*	1,366 ± *0,2*	9,25 ± *0,6*	0,846 ± *0,127*	0,669 ± *0,044*	1,004 ± *0,208*	0,612 ± *0,038*
		y	18	9,08 ± *6*	-10,67 ± *1,2*	-3,96 ± *0,8*	1,272 ± *0,3*	8,643 ± *1,3*	0,788 ± *0,207*	0,625 ± *0,095*	0,889 ± *0,233*	0,583 ± *0,088*
	09/11/2001	f	12,5	15,69 ± *4*	-9,897 ± *0,9*	-3,02 ± *0,9*	1,37 ± *0,2*	8,771 ± *0,9*	0,685 ± *0,254*	0,457 ± *0,159*	0,984 ± *0,180*	0,593 ± *0,219*
		m	11	21,21 ± *5*	-10,13 ± *1,4*	-2,83 ± *2,0*	1,59 ± *0,3*	8,943 ± *1,6*	0,804 ± *0,296*	0,470 ± *0,173*	0,846 ± *0,134*	0,577 ± *0,201*
		y	18	7,67 ± *4*	-9,757 ± *1,7*	-2,97 ± *1,5*	1,35 ± *0,3*	8,793 ± *1*	0,745 ± *0,158*	0,504 ± *0,057*	0,837 ± *0,177*	0,636 ± *0,072*
	13/12/2001	f	10,5	15,54 ± *4*	-10,45 ± *0,5*	-3,4 ± *0,6*	1,73 ± *0,6*	9,238 ± *0,8*	1,054 ± *0,337*	0,584 ± *0,048*	0,955 ± *0,305*	0,530 ± *0,043*
		m	12,5	17,07 ± *5*	-10,71 ± *0,6*	-3,81 ± *0,8*	1,692 ± *0,5*	9,634 ± *0,7*	1,031 ± *0,288*	0,609 ± *0,045*	0,934 ± *0,261*	0,552 ± *0,041*
		y	20	4,16 ± *5*	-11,06 ± *1,1*	-3,33 ± *0,5*	1,276 ± *0,3*	8,91 ± *0,5*	0,777 ± *0,202*	0,564 ± *0,032*	0,704 ± *0,183*	0,511 ± *0,029*
	15/01/2002	f	10	17,33 ± *4*	-10,08 ± *1,0*	-3,26 ± *0,4*	1,493 ± *0,2*	9,107 ± *0,6*	0,914 ± *0,148*	0,583 ± *0,035*	0,909 ± *0,147*	0,576 ± *0,035*
		m	11	19,39 ± *5*	-10,73 ± *1,4*	-3,15 ± *0,8*	1,511 ± *0,3*	9,252 ± *0,5*	0,925 ± *0,177*	0,592 ± *0,031*	0,921 ± *0,176*	0,585 ± *0,030*
		y	18	4,32 ± *2*	-10,79 ± *1,1*	-2,96 ± *1,3*	1,411 ± *0,2*	9,053 ± *1,1*	0,864 ± *0,149*	0,579 ± *0,068*	0,860 ± *0,149*	0,573 ± *0,067*
	15/02/2002	f	12	16,93 ± *3*	-10,47 ± *0,9*	-3,27 ± *0,8*	1,341 ± *0,4*	9,254 ± *0,6*	0,733 ± *0,237*	0,554 ± *0,038*	0,821 ± *0,266*	0,592 ± *0,040*
		m	11,5	17,12 ± *4*	-11,07 ± *0,8*	-3,19 ± *1,1*	1,393 ± *0,3*	8,099 ± *1,1*	0,698 ± *0,270*	0,444 ± *0,154*	0,853 ± *0,184*	0,475 ± *0,165*
		y	17,5	8,40 ± *5*	-9,566 ± *1,6*	-2,59 ± *0,8*	1,407 ± *0,3*	8,819 ± *1,8*	0,769 ± *0,183*	0,527 ± *0,106*	0,861 ± *0,205*	0,565 ± *0,114*
	12/03/2002	f	11	15,42 ± *4*	-9,757 ± *0,5*	-2,63 ± *1,0*	1,191 ± *0,6*	9,721 ± *0,6*	0,673 ± *0,317*	0,585 ± *0,036*	0,651 ± *0,307*	0,581 ± *0,035*
		m	11	17,76 ± *5*	-10,13 ± *0,9*	-2,89 ± *0,9*	1,237 ± *0,3*	9,126 ± *0,9*	0,699 ± *0,168*	0,550 ± *0,056*	0,676 ± *0,162*	0,546 ± *0,055*
		y	20	6,55 ± *3*	-9,87 ± *0,9*	-2,70 ± *0,8*	0,891 ± *0,4*	9,532 ± *0,9*	0,503 ± *0,199*	0,574 ± *0,053*	0,487 ± *0,193*	0,570 ± *0,053*

	Collection Date		#	Ca_{SHELL}	$\delta^{13}C_{VPDB}$	$\delta^{18}O_{VPDB}$	Mg/Ca	Sr/Ca	Mg/Ca_{valve} / Mg/Ca_{water}	Sr/Ca_{valve} / Sr/Ca_{water}	Mg/Ca_{valve} / Mg/Ca_{water}	Sr/Ca_{valve} / Sr/Ca_{water}
Sample	**dd/mm/yyy**	Instar	carapaces	µgCa/carapace	‰	‰	molar x10^{-2}	molar x10^{-2}	same month x10^{-2}	same month x10^{-1}	month before x10^{-2}	month before x10^{-1}
U1	22/03/2001	f	6	23,01 ± *7,0*	-12,6 ± *0,5*	-5,8 ± *0,3*	0,8 ± *0,1*	1,1 ± *0,1*	1,523 ± *0,267*	0,626 ± *0,031*		
		m	6	20,35 ± *7,2*	-12,1 ± *1,5*	-4,5 ± *1,3*	1 ± *0,2*	4,1 ± *3,6*	2,025 ± *0,391*	2,323 ± *2,047*		
		y	8	6,67 ± *2,3*	-11,4 ± *0,9*	-3,8 ± *1,5*	0,9 ± *0,2*	5,4 ± *3,9*	1,800 ± *0,337*	3,088 ± *2,235*		
	30/04/2001	f	5,5	30,02 ± *3,5*	-12,7 ± *0,7*	-5,8 ± *0,3*	0,8 ± *0,1*	1,1 ± *0*	1,582 ± *0,149*	0,700 ± *0,016*	1,613 ± *0,152*	0,644 ± *0,014*
		m	7	27,67 ± *9,9*	-12,9 ± *0,4*	-5,6 ± *0,3*	1,1 ± *0,2*	1,40 ± *0,9*	2,143 ± *0,416*	0,872 ± *0,550*	2,185 ± *0,424*	0,802 ± *0,506*
		y	1	3,40 ± *3,4*	-12,7 ±	-5,9 ± *-5,9*	0,7 ± *0,7*	0,9 ± *0,9*	1,388 ± *1,388*	0,546 ± *0,546*	1,415 ± *1,415*	0,502 ± *0,502*
	05/06/2001	f	5,5	24,84 ± *8,5*	-12,7 ± *0,5*	-5,9 ± *0,9*	0,83 ± *0,1*	1,8 ± *2*	1,282 ± *0,205*	0,674 ± *0,735*	1,603 ± *0,256*	1,130 ± *1,233*
		m	5	26,54 ± *8,2*	-13,2 ± *0,6*	-5,9 ± *0,3*	1 ± *0,1*	1 ± *0,1*	1,594 ± *0,226*	0,385 ± *0,031*	1,993 ± *0,282*	0,646 ± *0,052*
		y	8	3,57 ± *1,9*	-12,6 ± *0,5*	-6,8 ± *0,1*	0,9 ± *0,2*	1,3 ± *0,2*	1,457 ± *0,342*	0,491 ± *0,065*	1,821 ± *0,428*	0,824 ± *0,109*
	03/07/2001	f	5	26,05 ± *4,9*	-12,3 ± *1,7*	-6 ± *2,6*	1,1 ± *0,1*	1,6 ± *0,6*	1,567 ± *0,215*	0,500 ± *0,184*	1,640 ± *0,225*	0,593 ± *0,218*
		m	4,5	22,00 ± *4,6*	-12,7 ± *0,5*	-7 ± *0,1*	1,1 ± *0,1*	1,5 ± *0,1*	1,679 ± *0,166*	0,476 ± *0,016*	1,757 ± *0,174*	0,564 ± *0,019*
		y	18,5	5,41 ± *1,3*	-12,8 ± *0,4*	-7,1 ± *0,1*	1,1 ± *0,2*	1,6 ± *0,3*	1,677 ± *0,290*	0,491 ± *0,082*	1,754 ± *0,304*	0,582 ± *0,097*
	26/07/2001	f	5,5	27,16 ± *4,4*	-12,2 ± *0,3*	-7,1 ± *0,3*	1,1 ± *0,1*	1,5 ± *0,1*	1,642 ± *0,217*	0,461 ± *0,030*	1,642 ± *0,217*	0,461 ± *0,030*
		m	5,5	20,97 ± *5,5*	-12,6 ± *0,5*	-6,9 ± *0,2*	1,21 ± *0,2*	1,4 ± *0,1*	1,777 ± *0,316*	0,444 ± *0,039*	1,777 ± *0,316*	0,444 ± *0,039*
		y	17	6,48 ± *1,2*	-12,4 ± *0,3*	-7,1 ± *0,1*	1,1 ± *0,1*	1,5 ± *0*	1,673 ± *0,204*	0,482 ± *0,015*	1,673 ± *0,204*	0,482 ± *0,015*
	07/09/2001	f	5,5	27,28 ± *4,7*	-12,16 ± *0,4*	-7,06 ± *0,2*	1,2 ± *0,2*	1,5 ± *0*	1,957 ± *0,250*	0,540 ± *0,015*	1,756 ± *0,225*	0,456 ± *0,012*
		m	5,5	18,92 ± *6,8*	-12 ± *0,5*	-6,94 ± *0,2*	1,4 ± *0,2*	1,4 ± *0*	2,282 ± *0,325*	0,520 ± *0,016*	2,047 ± *0,291*	0,439 ± *0,014*
		y	17,5	4,37 ± *1,7*	-12,4 ± *0,2*	-6,8 ± *0,1*	1,1 ± *0,2*	1,53 ± *0*	1,736 ± *0,364*	0,568 ± *0,013*	1,558 ± *0,327*	0,479 ± *0,011*
	11/10/2001	f	6,5	22,69 ± *7,3*	-11,9 ± *0,3*	-6,9 ± *0,3*	1,1 ± *0,2*	1,48 ± *0,1*	1,974 ± *0,388*	0,711 ± *0,027*	1,762 ± *0,347*	0,548 ± *0,021*
		m	5	17,42 ± *4,6*	-12,2 ± *0,5*	-6,5 ± *0,3*	1,1 ± *0,2*	1,44 ± *0,1*	1,842 ± *0,640*	0,637 ± *0,197*	1,781 ± *0,299*	0,532 ± *0,036*
		y	18	6,37 ± *1,5*	-12,5 ± *0,4*	-6,5 ± *0,1*	0,9 ± *0,1*	1,4 ± *0*	1,613 ± *0,227*	0,668 ± *0,019*	1,440 ± *0,202*	0,515 ± *0,015*
	09/11/2001	f	6,5	21,41 ± *4,9*	-12 ± *0,6*	-6,3 ± *0,7*	0,96 ± *0,3*	1,5 ± *0,1*	1,796 ± *0,545*	0,695 ± *0,064*	1,787 ± *0,552*	0,696 ± *0,065*
		m	5	18,32 ± *7,6*	-11,9 ± *0,8*	-6,2 ± *0,5*	1,05 ± *0,5*	1,2 ± *0,4*	1,665 ± *1,136*	0,491 ± *0,292*	2,129 ± *0,710*	0,642 ± *0,097*
		y	19	5,60 ± *1,9*	-12,4 ± *0,3*	-5,8 ± *0,2*	0,7 ± *0,1*	1,4 ± *0*	1,368 ± *0,191*	0,666 ± *0,022*	1,368 ± *0,191*	0,666 ± *0,022*
	13/12/2001	f	5,5	21,13 ± *6,5*	-12,4 ± *0,7*	-5,5 ± *0,9*	0,9 ± *0,3*	1,3 ± *0,1*	1,628 ± *0,500*	0,751 ± *0,065*	1,606 ± *0,493*	0,632 ± *0,055*
		m	5,5	13,69 ± *4,5*	-11,9 ± *0,6*	-6,3 ± *0,6*	1 ± *0,4*	1,2 ± *0,5*	1,971 ± *0,759*	0,703 ± *0,259*	2,139 ± *0,400*	0,651 ± *0,101*
		y	18	5,04 ± *2,5*	-12,7 ± *0,4*	-5,1 ± *0,3*	0,7 ± *0,1*	1,2 ± *0,1*	1,293 ± *0,137*	0,671 ± *0,045*	1,275 ± *0,135*	0,565 ± *0,038*
	15/01/2002	f	5,5	19,87 ± *8,2*	-12,4 ± *0,6*	-5,5 ± *0,7*	0,9 ± *0,2*	1,3 ± *0,1*	1,579 ± *0,310*	0,632 ± *0,071*	1,691 ± *0,332*	0,723 ± *0,082*
		m	5,5	15,54 ± *4,7*	-12,4 ± *0,5*	-5,37 ± *0,9*	1 ± *0,4*	1,2 ± *0,4*	1,721 ± *0,734*	0,578 ± *0,200*	2,028 ± *0,521*	0,728 ± *0,068*
		y	18	5,05 ± *1,3*	-12,8 ± *0,3*	-5,3 ± *0,4*	0,7 ± *0,1*	1 ± *0,1*	1,236 ± *0,164*	0,501 ± *0,073*	1,324 ± *0,176*	0,574 ± *0,084*
	15/02/2002	f	6,5	23,29 ± *7,2*	-12,6 ± *0,5*	-5,6 ± *0,8*	0,9 ± *0,2*	1,2 ± *0,2*	1,577 ± *0,651*	0,645 ± *0,235*	1,606 ± *0,379*	0,591 ± *0,086*
		m	5,5	21,46 ± *6,6*	-12,4 ± *0,7*	-6 ± *0,6*	1,1 ± *0,2*	1,3 ± *0,3*	1,693 ± *0,939*	0,608 ± *0,351*	1,916 ± *0,440*	0,620 ± *0,168*
		y	16,5	6,32 ± *1,0*	-12,5 ± *0,7*	-5,8 ± *0,3*	0,8 ± *0,1*	1 ± *0,2*	1,473 ± *0,204*	0,621 ± *0,113*	1,364 ± *0,189*	0,518 ± *0,094*
	12/03/2002	f	5	23,22 ± *4,8*	-12,4 ± *0,6*	-5,5 ± *0,6*	0,8 ± *0,3*	1,1 ± *0,5*	1,468 ± *0,654*	0,657 ± *0,294*	1,711 ± *0,218*	0,729 ± *0,098*
		m	7,5	19,62 ± *6,0*	-12,3 ± *0,8*	-6,4 ± *0,7*	1,3 ± *0,2*	1,3 ± *0,2*	2,519 ± *0,429*	0,805 ± *0,136*	2,517 ± *0,428*	0,765 ± *0,129*
		y	17,5	5,88 ± *1,7*	-12,37 ± *0,5*	-6,27 ± *0,6*	1 ± *0,1*	1,1 ± *0,2*	1,996 ± *0,217*	0,686 ± *0,126*	1,994 ± *0,217*	0,653 ± *0,120*

Appendix 2.1: Ostracod abundance species of Palmar core without SP type C. Note that the total number of valves and the number of species (spp.) per sample is also placed.

Apéndice 2.1*: Abundancias de los ostrácodos del sondeo Palmar sin incluir las valvas con estados de preservación (SP) tipo C. Notar que el número total del valvas y el número de especies (spp.) por muestra también se muestra en la tabla.*

Depht(cm)	*Cyprideis torosa*	*Loxoconcha elliptica*	*Loxoconcha rhomboidea*	*Aurila arborescens*	*Candona angulata*	*Cypridopsis vidua*	*Darwinula stevensoni*	*Ilyocypris gibba*	*Xestoleberis nitida*	*Heterocypris salina*	*Pontocythere*	*Hemycipris*	TOTAL (x10g/dw)	*n° spp*
63	47	4	0	3	0	3	0	0	0	0	0	0	57	3
68	17	1	0	0	0	1	0	0	0	0	0	0	19	2
88	150	17	0	5	5	24	1	2	2	2	0	0	208	8
96	282	130	0	3	7	5	0	2	15	3	0	0	447	7
99	266	141	0	3	3	3	0	0	36	0	0	0	452	5
112	51	11	0	2	6	1	0	0	4	2	0	0	77	6
118	236	30	0	4	130	1	0	0	12	2	0	0	415	6
178	339	48	0	27	23	2	0	0	3	0	0	0	442	5
192	521	58	0	20	23	1	0	0	4	0	0	0	628	5
196	293	46	0	17	7	2	0	0	1	0	0	0	366	5
209	198	38	0	8	1	0	0	0	0	0	0	0	246	3
223	332	55	0	12	2	2	0	0	2	0	0	0	406	5
233	30	10	0	1	0	2	0	0	0	0	0	0	43	3
245	195	49	0	0	0	2	0	2	0	0	0	0	249	3
258	305	40	0	0	33	1	0	0	11	0	0	0	389	4
269	675	95	0	27	44	0	0	0	3	0	1	0	845	5
274	22	10	0	1	0	0	0	0	0	0	0	0	33	2
288	1	6	0	0	0	0	0	0	0	0	1	0	8	2
300	238	54	0	5	20	9	0	1	0	0	1	0	328	6
312	262	54	0	5	18	1	0	0	1	0	0	0	340	5
319	165	32	0	4	2	0	0	0	0	0	0	0	203	3
326	123	32	0	9	2	0	0	0	0	0	0	0	165	3
333	134	20	0	3	2	1	0	0	0	0	0	0	160	4
341	84	9	0	2	0	0	0	0	0	0	2	0	98	3
355	20	4	0	7	0	1	0	1	0	0	0	0	33	4
360	35	2	0	0	0	1	0	1	0	0	0	0	40	3
371	31	9	0	0	0	0	0	0	0	0	0	0	40	1

Depht(cm)	*Cyprideis torosa*	*Loxoconcha elliptica*	*Loxoconcha rhomboidea*	*Aurila arborescens*	*Candona angulata*	*Cypridopsis vidua*	*Darwinula stevensoni*	*Ilyocypris gibba*	*Xestoleberis nitida*	*Heterocypris salina*	*Pontocythere*	*Hemycipris*	TOTAL (x10g/dw)	*n° spp*
385	11	0	0	0	0	1	0	0	0	0	0	0	12	1
398	16	8	0	0	0	0	0	0	0	0	0	0	24	1
420	2	0	0	0	0	0	0	0	0	0	0	0	2	0
436	1	0	0	0	0	0	0	0	0	0	0	0	1	0
451	18	0	0	0	0	0	0	0	0	0	0	0	18	0
488	0	0	0	0	0	0	0	0	0	0	0	0	0	0
503	5	0	0	0	0	0	0	0	0	0	0	0	5	0
519	4	1	0	0	0	0	0	0	0	0	0	0	5	1
537	40	14	0	3	0	0	0	0	0	0	0	0	56	2
550	19	4	0	0	0	0	0	0	0	0	0	0	23	1
560	53	4	0	0	0	0	0	0	0	0	0	0	57	1
572	109	25	0	2	2	1	0	0	0	0	0	0	139	4
581	207	39	0	5	0	1	0	1	0	0	0	0	253	4
593	18	5	0	3	0	0	0	0	0	0	1	0	28	3
616	34	0	0	1	0	2	0	0	0	0	0	0	37	2
628	30	11	0	2	0	0	0	0	0	0	0	0	42	2
634	30	10	0	1	0	0	0	0	0	0	0	0	41	2
643	3	1	0	1	0	0	0	0	0	0	0	0	5	2
655	5	2	0	0	0	0	0	0	0	0	0	0	7	1
666	7	0	0	0	0	0	0	0	0	0	0	0	7	0
680	56	13	0	1	0	0	0	0	0	0	0	0	70	2
698	48	8	0	1	0	0	0	0	0	0	0	0	57	2
701	16	6	0	0	0	0	0	0	0	0	0	0	22	1
709	11	0	0	0	0	0	0	0	0	0	0	0	11	0
717	3	0	0	0	0	0	0	0	0	0	0	0	3	0
726	5	0	0	0	0	0	0	0	0	0	0	0	5	0
736	0	0	0	0	0	0	0	0	0	0	0	0	0	0
745	26	1	0	0	0	0	0	0	0	0	0	0	27	1
753	43	8	1	0	0	1	0	0	0	0	0	0	52	3
761	26	4	0	0	0	0	0	0	0	0	0	0	30	1
770	51	7	0	0	0	0	0	0	0	0	0	0	59	1
775	65	8	0	0	0	0	0	0	0	0	0	0	73	1
794	181	3	0	0	1	0	0	0	0	0	0	0	185	2
808	52	6	0	1	2	0	0	0	0	0	0	0	60	3
822	1637	170	0	0	0	0	0	0	0	0	0	0	1807	1
824	980	7	0	0	0	0	0	0	0	0	0	0	988	1
844	2199	184	0	0	0	0	0	0	0	0	0	0	2383	1
												min	0	0
												max	2383	8
												Total	13332	12

Appendix 2.2: Morphological information of *Cyprideis torosa*: SP (states of preservation), number of valves of each stage (f=females, m=males, j=juveniles), valve length for females and males, % noded forms, the % of pores type and number of transparent/opaque valves.

Apéndice 2.2*: Información morfológica de* Cyprideis torosa*: SP (estados de preservación), número de valvas de cada estadio (f=hembras, m=,machos, j=juveniles), longitud de las valvas para hembras y machos, porcentaje de formas nodadas, porcentaje del tipo y número de valvas transparentes/opacas.*

depth (cm)	Total of valves ($10gdw^{-1}$)	A	F	M	J	SP type B	SP type A	length f (µm)	# Valves measured	length m (µm)	# Valves measured	Round pores (%)	Elongate pores (%)	Irregular pores (%)	Sieved pores	nº selected valves	%TOTAL opaque	nº transparent valves	nº valves meassured	*Pn*	nº valves meassured for nodes
63	58	19	17	2	28	2	45	866 ± *34*	**13**	983 ± *32*	**3**	52	25	23	202	7	75	4	4	0,4	22
68	25	0	0	0	17	15	2	921 ± *51*	**6**								100	0	0	0,3	41
88	159	49	37	12	101	6	144	970 ± *82*	**14**	994 ± *79*	**5**	28	29	43	384	12	56	7	7	0,4	27
96	409	50	38	12	232	75	207	936 ± *89*	**12**	1042 ± *110*	**7**	38	39	23	457	10	13	13	13	0,4	24
99	430	53	33	20	213	88	178	942 ± *69*	**11**	968 ± *59*	**13**						6	18	18	0,0	27
112	139	18	14	5	33	12	39	894 ± *43*	**13**	952 ± *56*	**6**						15	11	11	0,2	25
118	333	26	19	8	210	74	162	953 ± *90*	**15**	1066 ± *40*	**5**						35	11	11	0,7	24
178	645	63	48	15	276	175	165	910 ± *59*	**19**	949 ± *64*	**6**	**56**	**10**	**34**	193	10	42	11	11	0,3	30
192	926	115	85	30	406	188	334	922 ± *60*	**22**	958 ± *44*	**9**						27	20	20	0,2	33
196	462	59	48	11	234	125	168	906 ± *44*	**18**	980 ± *38*	**5**						26	14	14	0,1	27
209	336	39	33	6	159	78	121	889 ± *47*	**28**	973	**1**	**52**	**25**	**23**	175	6	0	24	24	0,1	39
223	550	47	34	13	285	188	145	896 ± *51*	**23**	930 ± *38*	**10**						0	29	29	0,1	33
233	56	16	15	1	14	27	2	908 ± *81*	**9**	973	**1**						100	0	0	0,6	13
245	426	36	33	3	159	159	36	888 ± *73*	**15**	940	**1**	**57**	**36**	**7**	14	1	91	1	1	0,3	20
258	393	47	36	12	257	94	211	870 ± *28*	**15**	1064 ± *90*	**6**						36	10	10	0,2	30
269	1151	121	74	47	554	345	330	916 ± *54*	**10**	1033 ± *85*	**12**	38	24	38	381	11	20	16	16	0,3	26
274	57	14	11	2	8	16	6	862 ± *28*	**10**								57	3	3	0,1	13
288	6	0	0	0	1	1	0	884 ± *39*	**7**								67	1	1	0,3	12
300	337	61	44	17	177	72	166	921 ± *47*	**13**	986 ± *24*	**7**	**56**	**23**	**21**	347	10	40	9	9	0,2	30
312	353	84	71	12	178	57	205	910 ± *48*	**13**	1003 ± *64*	**2**						80	2	2	0,2	33
319	356	36	32	4	129	75	90	911 ± *45*	**14**	926 ± *50*	**4**						67	4	4	0,1	32
326	281	19	16	2	104	82	41	887 ± *54*	**18**								90	1	1	0,0	28
333	263	49	39	10	86	11	124	941 ± *37*	**10**	966 ± *51*	**5**	**59**	**23**	**17**	277	9	86	2	2	0,1	31
341	184	21	19	2	64	32	52	881 ± *57*	**17**	910	**1**						91	1	1	0,3	18
355	54	13	11	2	7	16	4	897 ± *41*	**11**	958	**1**						67	3	3	0,4	12
360	38	15	11	4	21	16	19	902 ± *28*	**10**	954 ± *8*	**2**						64	4	4	0,2	13
371	38	17	15	2	14	18	13	877 ± *42*	**15**	980 ± *32*	**2**						80	2	2	0,3	23
385	11	9	7	2	2	11	0	836 ± *15*	**3**	935 ± *11*	**2**						50	2	2	0,6	10

depth (cm)	Total of valves ($10gdw^{-1}$)	**A**	F	M	J	SP type B	SP type A	**length f (µm)**	# Valves measured	**length m (µm)**	# Valves measured	**Round pores (%)**	**Elongate pores (%)**	**Irregular pores (%)**	Sieved pores	**nº selected valves**	%TOTAL opaque	nº transparent valves	nº meassured	*Pn*	nº valves meassured for nodes
398	16	9	5	3	8	13	3	845 ± *26*	**4**	943 ± *85*	**2**						33	2	2	0,4	9
420	2	2	1	1	0	0	2	942	**1**	958	**1**						0	1	1	0,0	2
436	1	1	0	1	0	1	0			970	**1**						100	0	0	0,0	1
451	18	5	0	5	13	0	19			939 ± *34*	**4**						0	4	4	0,0	15
488	0	0	0	0	0	0	0										0		0		
503	6	4	2	2	1	0	7	836	**1**	920 ± *11*	**2**						33	2	2	0,2	5
519	4	0	0	0	4	2	2										0		0		
537	45	16	14	2	23	13	27	855 ± *32*	**12**	963 ± *32*	**3**						45	6	6	0,4	15
550	23	8	8	0	11	4	15	879 ± *37*	**7**								25	3	3	0,5	10
560	64	17	12	4	36	12	41	880 ± *47*	**15**	1009 ± *70*	**3**						50	5	5	0,0	27
572	112	39	34	5	69	7	102	881 ± *23*	**18**	1013 ± *87*	**3**						50	9	9	0,2	23
581	211	59	42	16	148	0	228	909 ± *39*	**17**	979 ± *61*	**7**	**64**	**22**	**14**	425	12	15	17	17	0,1	27
593	33	8	6	2	10	6	12	942 ± *64*	**6**	935 ± *32*	**2**						29	5	5	0,2	10
601	44	14	10	4	18	14	18	892 ± *57*	**7**	968 ± *50*	**4**						36	7	7	0,4	13
616	51	17	11	5	18	3	31	913 ± *53*	**12**	949 ± *81*	**4**						69	4	4	0,1	24
628	38	16	13	3	14	16	14	849 ± *43*	**12**	958 ± *26*	**3**						70	3	3	0,0	24
634	36	16	14	2	15	15	16	879 ± *53*	**14**	965 ± *49*	**2**						40	6	6	0,1	18
643	7	3	2	1	1	1	3			1010	**1**						0	1	1	0,0	3
655	6	4	3	1	1	0	6	880 ± *20*	**3**	920	**1**						0	1	1	0,0	5
666	20	3	2	1	4	1	6	838 ± *31*	**4**								50	1	1	0,0	8
680	75	18	17	1	38	30	26	863 ± *34*	**16**	910 ± *42*	**2**	**52**	**32**	**17**	311	9	45	6	6	0,0	22
698	49	16	11	5	32	16	32	856 ± *32*	**10**	922 ± *25*	**6**						11	10	10	0,0	25
701	37	13	9	4	3	11	5	877 ± *28*	**8**	943 ± *46*	**4**						18	9	9	0,1	14
709	44	6	6	0	5	7	4	838 ± *48*	**6**								0	4	4	0,1	10
717	8	2	2	0	1	0	5	890 ± *14*	**2**								0	1	1	0,0	2
726	11	4	4	0	1	3	2	887 ± *32*	**3**								100	0	0	0,0	4
736	3	0	0	0	0	0	0										0		0		
745	29	12	11	1	14	21	5	857 ± *41*	**10**	980	**1**						100	0	0	0,2	12
753	43	14	11	3	28	13	29	852 ± *44*	**9**	957 ± *38*	**3**						44	5	5	0,0	22
761	28	4	2	2	22	19	7	916 ± *44*	**5**	943 ± *58*	**3**						63	3	3	0,1	11
770	54	16	13	3	35	21	30	862 ± *43*	**12**	970 ± *36*	**3**						70	3	3	0,0	24
775	66	22	18	4	42	23	41	873 ± *54*	**14**	947 ± *40*	**3**						86	2	2	0,1	17
794	183	15	15	0	166	47	134	905 ± *24*	**18**	1026 ± *54*	**2**						47	8	8	0,0	26
808	52	16	14	2	36	31	21	879 ± *29*	**14**	968 ± *59*	**3**						50	6	6	0,0	27
822	1637	340	261	79	1297	101	1738	923 ± *35*	**15**	1010 ± *19*	**10**	**42**	**39**	**19**	77	6	28	15	15	0,0	29
824	981	192	142	50	789	65	1045	916 ± *38*	**29**	992 ± *20*	**10**						46	14	14	0,0	42
844	2201	197	136	61	2002	20	2179	919 ± *38*	**19**	980 ± *21*	**6**	**49**	**38**	**13**	160	12	38	12	12	0,0	28

Appendix 3.1: ^{210}Pb and ^{137}Cs dates for core Center. a) ^{210}Pb results, inferred age and sediment accumulation rate from c:r:s model. b) ^{210}Pb and ^{214}Pb corrected to alpha results.

Apéndice 3.1: *Datos de ^{210}Pb y ^{137}Cs del sondeo Centro. a) Resultados de ^{210}Pb, edad inferida y tasas de sedimentación basadas en el modelo c:r:s; b) Datos de ^{210}Pb y ^{214}Pb corregidos por los resultados alfa.*

a

Top of Interval (cm)	Base of Interval (cm)	Cum. Dry Mass (g/cm2)	Unsup. Activity (pCi/g)	Cum. Act. below Int. (pCi/cm2)	Age: Base of Int. (yr)	**Date A.D.**	Sediment Accumulation (g/cm2 yr)
0	0,5	0,1	1,60 ± *0,08*	11,7	0,37 ± *2,65*	2006,8	0,23 ± *0,02*
4	4,5	1,0	1,15 ± *0,07*	10,5	3,95 ± *2,75*	2003,3	0,29 ± *0,02*
8	8,5	2,3	0,83 ± *0,04*	9,2	8,11 ± *2,90*	1999,1	0,35 ± *0,03*
14	15	4,7	1,08 ± *0,06*	6,9	17,43 ± *3,29*	1989,8	0,20 ± *0,02*
18	19	6,4	0,87 ± *0,04*	5,3	25,55 ± *3,88*	1981,7	0,20 ± *0,02*
24	25	9,2	0,75 ± *0,04*	3,0	43,64 ± *6,00*	1963,6	0,13 ± *0,02*
30	31	12,2	0,44 ± *0,04*	1,4	69,42 ± *9,19*	1937,8	0,10 ± *0,03*
34	35	14,0	0,47 ± *0,03*	0,5	100,13 ± *23,34*	1907,1	0,04 ± *0,03*
40	41	16,1	0,07 ± *0,03*	0,1	169,44 ± *65,92*	1837,8	0,03 ± *0,06*

b

Interval	Depth	tube ht	Supported Pb-214	**Supported Pb corrected**	Cs-137	**Cs-137 corrected**
	cm	cm	pCi/g	pCi/g	pCi/g	pCi/g
16-17	16,5	4,65	0,440	**0,46**	0,17	**0,18**
22-23	22,5	4,65	0,520	**0,54**	0,21	**0,22**
28-29	28,5	4,65	0,640	**0,66**	0,22	**0,23**
32-33	32,5	4,65	0,500	**0,52**	0,26	**0,27**
36-37	36,5	4,65	0,45	**0,47**	0,93	**0,96**
42-43	42,5	4,65	0,50	**0,52**	0,00	**0,00**

Appendix 3.2: Ostracod abundance species of core Center without SP type C. Note that the total number of fragments, total of valves and the number of species (spp) per sample are also placed.

Apéndice 3.2*: Abundancias de los ostrácodos del sondeo Centro sin incluir las valvas con estados de preservación (SP) tipo C. Notar que el número total de fragmentos, de valvas y el número de especies (spp) por muestra también se muestra en la tabla.*

Depth (cm)	*Cyprideis torosa*	*Loxoconcha elliptica*	*Xestoleberis nitida*	*Aurila arborescens*	*Loxoconcha rhomboidea*	*Leptocythere* sp.	*Cytherois* cf *stephanidesi*	*Candona angulata*	*Candona* sp.	*Cypridopsis vidua*	*Cypria ophtalmica*	*Darwinula stevensoni*	*Ilyocypris gibba*	*Herpetocypris* sp.	*Limnocythere inopinata*	*Limnocythere stationis*	*Parilimnocythere psamophila*	*Potamocypris* sp.	*fragments*	Total	nº de spp
3	0	0	0	0	0	0	0	0	0	0	0	0	0	0	0	0	0	0	0	0	0
5	4	0	0	0	0	0	0	0	0	2	0	0	0	0	0	0	0	0	2	6	**2**
8	2	0	0	0	0	0	0	0	0	0	0	0	0	0	0	0	0	0	0	2	**1**
10	7	0	0	0	0	0	0	0	0	2	0	0	0	0	0	0	0	0	0	9	**2**
13	2	0	0	0	0	0	0	0	0	0	0	2	0	0	0	0	0	0	0	4	**2**
15	5	0	0	0	0	0	0	0	0	0	0	0	0	0	0	0	0	0	0	5	**1**
17	3	0	0	0	0	0	0	1	0	2	0	0	0	0	2	0	0	0	0	8	4
20	0	0	0	0	0	0	0	0	0	0	0	0	0	0	0	0	0	0	0	0	0
22	0	0	0	0	0	0	0	0	0	2	0	0	0	0	0	0	0	0	0	2	**1**
24	1	0	0	0	0	0	0	0	1	0	0	0	0	0	1	0	0	0	0	4	**3**
27	1	0	0	0	0	0	0	0	0	0	0	1	0	0	0	0	0	0	0	3	**2**
29	2	0	0	0	0	0	0	0	0	0	0	0	0	0	0	0	0	0	0	2	**1**
31	10	0	0	0	0	0	0	0	4	1	0	2	0	0	2	0	0	0	0	20	5
33	7	0	0	0	0	0	0	0	1	4	0	0	0	0	0	0	0	0	0	12	**3**
35	8	0	0	0	0	0	0	1	0	0	0	0	0	0	0	0	0	0	0	9	**2**
37	16	0	0	0	0	0	0	3	0	5	0	9	0	0	0	0	0	0	0	33	4
40	49	0	0	0	0	0	0	7	0	8	2	19	0	0	4	0	6	0	2	94	7
42	30	0	0	0	0	0	0	8	0	7	0	46	0	0	18	0	2	0	2	110	6
45	402	21	0	0	0	0	0	14	0	21	0	274	0	0	21	11	64	0	11	828	8
47	55	0	0	0	0	0	0	31	0	0	0	0	0	0	0	0	43	0	43	129	**3**
49	40	0	0	0	0	0	0	33	0	3	0	59	0	0	3	0	28	0	22	166	6
52	28	0	0	0	0	0	0	40	0	14	0	47	0	0	0	0	25	0	3	154	5
54	103	0	0	0	0	0	0	120	0	57	0	170	0	0	0	0	99	0	0	548	5
57	323	30	0	0	0	0	0	301	0	30	0	183	0	0	0	0	61	0	4	929	6
59	27	0	0	0	0	0	0	179	0	14	0	82	0	0	0	0	0	0	3	302	4
61	62	12	6	0	0	0	0	160	0	0	0	37	0	0	0	0	0	0	0	277	5
64	78	0	0	0	0	0	0	112	0	0	0	69	0	0	0	0	0	0	0	259	**3**
66	128	0	20	0	0	0	0	82	0	0	0	49	0	0	0	0	0	0	0	279	4
69	2435	40	0	0	0	0	0	60	0	0	0	180	0	0	0	0	0	10	20	2725	5
71	4541	191	177	0	0	0	0	161	0	4	0	44	7	0	0	0	0	0	449	5126	7
73	509	783	973	0	0	12	9	8	0	0	0	6	0	0	0	0	0	0	31	2301	7
76	1187	958	2858	0	0	0	0	10	0	0	0	0	0	3	0	0	0	0	13	5016	5
78	827	1473	2883	3	0	0	0	1	0	0	0	0	0	0	0	0	0	0	6	5186	5
81	566	850	1270	3	0	0	0	1	0	0	0	0	0	0	0	0	0	0	48	2690	5
83	328	375	492	0	0	0	0	0	0	0	0	0	0	0	0	0	0	0	2	1195	**3**
86	852	450	754	0	0	0	0	0	0	0	0	0	0	0	0	0	0	0	32	2056	**3**
89	4522	2323	2747	36	0	0	3	0	0	0	0	0	0	0	0	0	0	0	260	9631	5
92	1725	850	1193	96	0	0	0	0	0	0	0	0	0	0	0	0	0	0	12	3865	4
94	2142	514	139	94	0	0	0	0	0	0	0	0	0	0	0	0	0	0	57	2889	4
96	3770	773	310	358	0	0	0	0	0	0	0	0	0	0	0	0	0	0	110	5210	4
99	2183	659	148	189	0	0	0	0	0	0	0	0	0	0	0	0	0	0	52	3179	4

Depth (cm)	*Cyprideis torosa*	*Loxoconcha elliptica*	*Xestoleberis nitida*	*Aurila arborescens*	*Loxoconcha rhomboidea*	*Leptocythere* sp.	*Cytherois* cf *stephanidesi*	*Candona angulata*	*Candona* sp.	*Cypridopsis vidua*	*Cypria ophtalmica*	*Darwinula stevensoni*	*Ilyocypris gibba*	*Herpetocypris* sp.	*Limnocythere inopinata*	*Limnocythere stationis*	*Parlimnocythere psamophila*	*Potamocypris* sp.	*fragments*	Total	nº de spp
101	3794	1457	334	100	0	0	0	0	0	0	0	0	0	0	0	0	0	0	44	5685	4
104	2384	928	239	57	1	0	0	0	0	0	0	0	0	0	0	0	0	0	65	3609	5
106	4489	216	0	11	0	0	0	0	0	0	0	0	0	0	0	0	0	0	41	4716	3
108	2392	0	0	0	0	0	0	0	0	0	0	0	0	0	0	0	0	0	29	2392	1
116	351	65	0	89	0	0	0	0	0	0	0	0	0	0	0	0	0	0	7	505	3
123	553	185	1	26	3	0	0	0	0	0	0	0	0	0	0	0	0	0	11	768	5
128	937	189	6	73	17	0	0	0	0	0	0	0	0	0	0	0	0	0	6	1222	5
133	2720	1313	43	693	33	0	0	0	0	0	0	0	0	0	0	0	0	0	3	4802	5
138	2609	1427	16	548	0	0	0	0	0	0	0	0	0	0	0	0	0	0	19	4601	4
144	3873	1216	0	454	4	0	0	0	0	0	0	0	0	0	0	0	0	0	59	5547	4
149	792	220	0	84	0	0	0	0	0	0	0	0	0	0	0	0	0	0	10	1096	3
154	673	265	5	16	0	0	0	0	0	0	0	0	0	0	0	0	0	0	15	959	4
159	470	302	0	6	0	0	0	0	0	0	0	0	0	0	0	0	0	0	7	777	3
164	319	186	0	10	0	0	0	0	0	0	0	0	0	0	0	0	0	0	9	515	3
166	849	258	0	23	1	0	0	0	0	0	0	0	0	0	0	0	0	0	21	1131	4
171	575	470	1	100	5	0	0	0	0	0	0	0	0	0	0	0	0	0	1	1152	5
176	315	133	0	17	3	0	0	0	0	0	0	0	0	0	0	0	0	0	9	468	4
181	533	104	0	1	0	0	0	0	0	0	0	0	0	0	0	0	0	0	11	638	3
186	413	102	0	2	0	0	0	0	0	0	0	0	0	0	0	0	0	0	0	517	3
190	175	35	0	0	0	0	0	0	0	0	0	0	0	0	0	0	0	0	6	209	2
195	202	10	0	0	0	0	0	0	0	0	0	0	0	0	0	0	0	0	1	211	2
200	167	2	0	1	0	0	0	0	0	0	0	0	0	0	0	0	0	0	1	171	3
205	9	0	0	0	0	0	0	0	0	0	0	0	0	0	0	0	0	0	3	9	1
210	52	23	0	0	0	0	0	0	0	0	0	0	0	0	0	0	0	0	5	75	2
215	683	237	0	0	0	0	0	0	0	0	0	0	0	0	0	0	0	0	19	920	2
220	200	135	0	0	1	0	0	0	0	0	0	0	0	0	0	0	0	0	2	336	3
225	398	96	0	0	0	0	0	0	0	0	0	0	0	0	0	0	0	0	14	495	2
229	731	104	0	0	0	0	0	0	0	0	0	0	0	0	0	0	0	0	2	835	2
234	1129	195	0	3	0	0	0	0	0	0	0	0	0	0	0	0	0	0	0	1327	3

min	0	0
max	9631	8
nº total	100952	18
con 1spp		6
con 2-3pp		27

Appendix 3.3: Morphological information of *Cyprideis torosa*: nºtotal of valves, SP (states of preservation), number of valves of each stage (f=females, m=males, j=juveniles), total number of valves (Tdv), number of black valves, valve length for females and males (noted that SD is also placed) and % noded forms.

Apéndice 3.3*: Información morfológica de* Cyprideis torosa*: nº total de valvas, SP (estados de preservación), número de valvas de cada estadio (f=hembras, m=,machos, j=juveniles),nºtotal de dobles valvas (Tdv), nº de valvas negras, longitud de las valvas para hembras y machos (notar que la SD esta puesta), porcentaje de formas nodadas.*

Depth (cm)	Number Total ($10gdw^{-1}$)	Adults	Females	Males	Juveniles	Tdv	SP type B	SP type C	# Noded valves	*black*	FEMALES length (µm)	Valves measured	MALES length (µm)	Valves measured
3	0	0	0	0	0	0	0	0	0	0				
5	4	0	0	0	4	0	0	0	0	0				
8	2	0	0	0	2	0	0	0	0	0				
10	7	0	0	0	7	0	0	0	2	0				
13	2	0	0	0	2	0	0	0	0	0				
15	5	0	0	0	5	0	0	0	0	0				
17	3	0	0	0	3	0	0	0	0	0				
20	0	0	0	0	0	0	0	0	0	0				
22	0	0	0	0	0	0	0	0	0	0				
24	1	0	0	0	1	0	0	0	0	0				
27	1	0	0	0	1	0	0	0	0	0				
29	2	0	0	0	2	0	0	0	0	0				
31	10	0	0	0	10	0	1	0	1	0				
33	7	0	0	0	7	0	0	0	0	0				
35	8	0	0	0	8	0	0	0	0	0				
37	16	0	0	0	16	0	0	0	2	0				
40	49	2	2	0	47	0	0	0	0	0	972,8 ± 43,0	2	1048,8 ±	1
42	30	0	0	0	30	0	0	0	0	0				
45	402	0	0	0	402	0	0	11	29	0	1040,0	1		
47	55	0	0	0	55	0	0	0	52	0			1048,8	1
49	40	3	0	3	37	0	0	0	22	0	972,8	1	1079,2	1
52	28	11	6	6	17	0	0	0	0	0	1007,5 ± 36,8	2	1131,0 36,8	2
54	103	46	25	21	57	0	4	14	0	0	1018,8 ± 35,8	5	1088,3 23,6	2
57	323	0	0	0	323	15	0	0	19	0			1014,0	1
59	27	0	0	0	27	0	0	0	0	0				
61	62	9	3	6	53	0	0	0	6	0	1040,0	1	1183,0	1
64	78	3	3	0	75	0	0	0	37	0	1018,4	1		

Depth (cm)	Number Total (10gdw^{-1})	Adults	Females	Males	Juveniles	Tdv	SP type B	SP type C	# Noded valves	*black*	FEMALES length (µm)	Valves measured	MALES length (µm)	Valves measured
66	128	0	0	0	128	0	0	0	49	0	995,6 ± 33,1	3	1079,2 ±	1
69	2435	100	30	70	2336	75	10	10	362	0	969,0 ± 42,1	14	1099,8 79,3	17
71	4543	648	280	368	3896	570	22	63	394	103	992,4 ± 43,1	22	1103,5 62,9	34
73	509	31	12	18	479	21	6	0	25	0	950,8 ± 49,2	16	994,8 62,9	27
76	1189	332	145	187	856	135	3	0	6	26	955,5 ± 28,3	3	1109,3 15,0	3
78	827	135	71	65	691	68	0	3	6	0	935,7 ± 34,4	20	978,2 39,7	27
81	566	95	57	37	472	40	3	11	5	0	934,6 ± 31,6	24	985,8 58,1	22
83	328	34	7	27	294	29	0	0	0	0	920,3 ± 46,1	16	984,5 47,7	20
86	852	70	12	58	782	28	5	9	30	0	924,5 ± 27,2	19	966,8 51,7	36
89	4522	127	44	83	4394	338	75	55	3	0	929,2 ± 47,1	37	981,8 64,3	30
92	1725	170	56	114	1555	145	3	0	0	0	935,9 ± 46,3	16	975,0 45,6	29
94	2142	419	134	285	1722	268	22	15	0	0	922,3 ± 27,0	28	963,9 40,7	27
96	3770	660	289	371	3110	358	8	5	3	0	926,3 ± 38,0	29	957,3 47,4	35
99	2183	189	93	96	1994	98	3	0	0	0	922,8 ± 28,3	28	949,7 45,3	32
101	3794	430	206	225	3363	336	13	0	0	0	920,5 ± 38,4	28	954,3 37,5	36
104	2384	162	68	94	2222	79	26	5	0	0	927,5 ± 35,7	33	951,9 42,4	44
106	4489	1122	533	589	3367	0	44	16	0	0	929,2 ± 36,9	68	972,4 31,4	69
108	2392	482	190	293	1910	10	34	14	0	0	1012,7 ± 29,9	5	1019,2 11,6	5
116	351	85	49	36	266	19	3	3	0	0	929,5 ± 37,9	21	989,9 52,4	21
123	553	46	27	19	507	38	5	9	0	0	932,2 ± 38,9	32	987,9 37,7	26
128	937	160	83	76	777	83	4	8	0	0	941,8 ± 40,9	22	951,1 45,3	32
133	2720	269	126	143	2451	269	20	17	0	0	942,8 ± 45,6	26	981,1 45,6	29
138	2609	244	97	147	2366	263	14	27	0	0	929,5 ± 50,3	27	952,3 42,2	31
144	3873	344	114	230	3529	252	61	57	0	0	942,8 ± 50,8	27	975,1 33,8	33
149	792	61	26	35	731	55	0	0	0	0	937,0 ± 37,0	23	990,0 51,7	30
154	673	91	30	61	582	10	8	10	0	0	958,8 ± 50,4	20	993,1 53,5	28
159	470	76	39	37	394	46	2	6	0	0	922,4 ± 39,6	22	1000,1 46,4	30
164	319	42	23	18	277	22	1	6	0	0	935,7 ± 35,5	23	984,2 48,5	21
166	849	118	52	66	730	73	3	6	0	0	938,7 ± 40,6	23	1005,1 46,5	32
171	575	127	59	68	449	83	1	2	0	2	920,2 ± 32,3	21		
176	315	54	32	22	261	30	6	9	0	0	951,3 ± 41,8	22	978,1 40,5	54
181	533	93	55	38	440	36	7	6	0	0	954,8 ± 41,0	25	998,9 43,4	24
186	413	97	44	53	316	25	2	1	0	2	915,4 ± 47,7	16	966,0 41,2	26
190	175	55	40	14	120	5	2	4	0	0	951,3 ± 36,6	26	990,6 46,0	14
195	202	39	22	18	163	8	2	6	0	0	940,8 ± 36,6	28	991,2 40,7	26
200	167	41	22	19	127	2	0	2	0	0	946,9 ± 42,8	30	1034,7 40,7	20
205	9	4	3	1	5	0	0	0	0	0	959,8 ± 12,6	4	1001,0 36,8	2
210	52	10	5	5	41	3	1	0	0	0	948,0 ± 55,3	9	1004,4 50,9	7
215	683	145	83	61	539	55	23	61	0	7	925,3 ± 27,0	25	991,9 34,1	31
220	200	32	17	15	168	18	1	1	0	1	941,3 ± 38,9	16	988,1 44,7	20
225	398	83	53	29	316	39	1	6	0	5	946,6 ± 37,0	26	986,4 34,7	24
229	731	117	65	53	614	66	0	5	0	0	952,7 ± 49,7	13	997,1 42,3	19
234	1129	221	149	72	909	108	8	7	0	6	948,3 ± 43,5	27	1006,3 24,2	24

Appendix 4.1: Ostracod abundance species of L'Antina core core without SP type C. Note that the total number of fragments, total of valves and the number of species (spp) per sample are also placed.

Apéndice 4.1: *Abundancias de los ostrácodos del sondeo L'Antina sin incluir las valvas con estados de preservación (SP) tipo C. Notar que el número total de fragmentos, de valvas y el número de especies (spp) por muestra también se muestra en la tabla.*

Depth (cm)	*Cyprideis torosa*	*Loxoconcha elliptica*	*Xestoleberis nitida*	*Bradleystandensia* cf *reticulata*	*Cypria* cf *ophtalmica*	*Candona angulata*	*Cypridopsis vidua*	*Paralimnocythere psammophila*	*Limnocythere inopinata*	*Lymnocythere* cf *stationis*	*Ilyocypris gibba*	*Darwinula stevensoni*	*Sarcypridopsis aculeata*	*Herpetocypris* cf *chevreuxi*	*Leptocythere* cf *porcellanea*	*Heterocypris* sp.	*Cypris* sp.	*Cytheridae* sp.	Fragments	nº Total	nº of spp
2	0	1,9	0	0	0	0	0	0	0	0	0	0	0	0	0	0	0	0	0	2	1
4	1,6	0	0	0	0	0	0	0	0	0	0	0	0	0	0	0	0	0	0	2	1
5	0,7	0	0	0	0	0	0	0	0	0	0	0	0	0	0	0	0	0	0	1	1
6	0	0	0	0	0	0	0	0	1,7	0	0	0	0	0	0	0	0	0	0	2	1
7	0	0	0	0	0	0	0	0	0	0	0	0	0	0	0	0	0	0	0	0	0
8	0	0	0	0	0	0	0	0	3,3	0	0	0	0,8	0	0	0	0	0	0	4	2
9	0	0	0	0	0	0	0	0	0	0	0,8	0	0	0	0	0	0	0	0	1	1
10	0,7	0	0	0	0	0	0	0	1,4	0	0	0	1,4	0	0	0	0	0	0	4	3
11	0,7	0	0	0	0	0	0	0	2	0	0	0	2	0	0	0	0	0	0	5	3
12	0,7	0	0	0	0	0	0	0	0	0	0	0	0,7	0	0	0	0	0	0	1	2
13	0,7	0	0	0	0	0	0	0	0	0	0	0	1,4	0	0	0	0	0	0,7	2	2
14	0,8	0	0	0	0	0	0	0	0	0	0	0	0	0	0	0	0	0	0	1	1
15	1,5	0	0	0	0	0	0	0	0	0	0	0	0	0	0	0	0	0	0	1	1
16	1,4	0	0	0	0	0	0	0	0	0	0	0	0	0	0	0	0	0	0	1	1
17	0	0	0	0	0	0,7	0	0	0	0	0	0	0	0	0	0	0	0	0	1	1
18	0	0	0	0	0	0	0	0	0	0	0	0	0	0	0	0	0	0	0	0	0
19	1,5	0	0	0	0	0	0	0	0	0	0	0	0	0	0	0	0	0	1,5	1	1
20	1,5	0	0	0	0	0	0	0	0	0	0	0	0	0	0	0	0	0	1,5	1	1
21	2,8	0	0	0	0	1,4	0	0	0	0	0	0	0	0	0	0	0	0	0	4	2
22	1,5	0	0	0	0	0	0	0	0	0	0	0	0	0	0	0	0	0	1,5	1	1
23	5,2	0	0	0	0	1,5	0	0	0	0	0	1,5	0,7	0	0	0	0	0	0	9	4
24	9,4	0	0	0	0	5,1	0	0	0	0	0	0	0	0	0	0	0	0	3,6	15	2
25	31	0,8	0	1,6	0	17	0	0,8	0,8	0	0	0	0	0	0	0	0	0	3,2	52	6
26	0	0	0	0	0	4,7	0	0	0	0	0	0	0	0	0	0	0	0	0	5	1
27	66,4	2,1	0	0	0	133	0	1,4	0,7	0	0	6,2	0	0	0	0	0	0	22,8	210	6
28	216	0	0	1,1	0	39	0	13	4,2	0	0	37,9	0	0	0	0	0	0	8,4	311	6
29	77,4	0	0	0	0	130	0	8	1,6	0	0	12	0	0	0	0	0	0	0	229	5
30	36,1	0	0	0	0	69	0,9	2,8	0,9	0	0	5,7	0	0	0	0	0	0,9	13,3	117	7
31	16	0	0	0,8	3,8	43	0	0,8	3,8	0	0	4,6	0	0	0	0	0	0	1,5	73	7
32	42,9	0	0	0,8	0	45	3,3	1,6	1,6	0	0	12,4	0	0	0	0	1,6	0,8	1,6	110	9
33	17,2	0	0	6	3	29	0,7	6	0	0	0	4,49	0	0	0	0	0	0	1,5	67	7
34	9,3	0	0	7,8	3,1	15	1,6	0,8	0	0	0	0,78	0	0	0	0	0	0	5,4	38	7
35	8,3	0	0	17	0	17	1	0	0	0	0	0	0	0	0	0	0	0	0	43	4
36	1,8	0	0	1,8	0	0,9	0,9	0	0	0	0	0	0	0	0	0	0	0	0	5	4

Depth (cm)	*Cyprideis torosa*	*Loxoconcha elliptica*	*Xestoleberis nitida*	*Bradleystandensia* cf *reticulata*	*Cypria* cf *ophtalmica*	*Candona angulata*	*Cypridopsis vidua*	*Paralimnocythere psammophila*	*Limnocythere inopinata*	*Lymnocythere* cf *stationis*	*Ilyocypris gibba*	*Darwinula stevensoni*	*Sarcypridopsis aculeata*	*Herpetocypris* cf *chevreuxi*	*Leptocythere* cf *porcellanea*	*Heterocypris* sp.	*Cypris* sp.	*Cytheridae* sp.	Fragments	n° Total	n° of spp
37	7,4	1,8	0	12	0	1,8	0	0	0	0	0	0	0	0	0	0	0	0	1,8	23	4
38	0	0	0	0	0	0	0	0	0	0	0	0	0	0	0	0	0	0	0	0	0
39	3,4	0	0	0	0	0	3,4	0	0	0	0	0	0	0	0	0	0	0	0	7	2
40	7,9	0	0	0	0	3,9	0,8	0	0	0	0	0	0	0	0	0	0	0	0	13	3
41	12,8	0	0	0	0	2,3	0,8	0	0	0	0	0	0	0	0	0	0	0	5,3	16	3
42	8	0	0	0	0	2,4	0	0	0	0	0	0	0	0	0	0	0	0	0	10	2
43	14,4	0	0	0	0	7,7	0	0	0	0	1	0	0	0	0	0	0	0	0	23	3
44	14,2	0	0	0	0	10	0	0	2	0	2	0	0	0	0	0	0	0	0	28	4
45	4	0	0	0	0	7,2	0	0	0	0	0	3,2	0	0	0	0	0	0	0	14	3
46	33,6	0	0	0	0	15	0	0	0	0	0,9	0	0	0	0	0	0	0	0	49	3
47	4,7	0	0	0	0	0,8	0	0	0	0	0	1,6	0	0	0	0	0	0	0	7	3
48	13,5	0	0	0	0	0	0	0	0	0	0	0	0	0	0	0	0	0	0	14	1
49	13,9	0	0	0	0	0	0	0	0	0	0	0	0	0	0	0	0	0	0	14	1
50	14,6	0	0	0	0	0	0	0	0	0	0	0	0	0	0	0	0	0	0	15	1
51	9,4	0	0	0	0	0,9	0	0	0	0	0	1,7	0	0	0	0	0	0	0,85	12	3
52	566	5,3	1,5	0	0	80	0	0	0	0	0	14,4	0	0	0	0,8	0	0	21,16	668	6
53	2556	20	0	0	0	373	0	0,8	0,8	0,8	0	78,5	0	3,1	0,8	0	0	0	265,4	3034	9
54	3483	61	4,3	0,9	0	358	0	0	0,9	1,7	0	58,1	0	0	0	1,7	0	0	351	3970	9
55	802	80	13,7	0	0	141	0	0,9	0	0,9	0	10,3	0	2,6	0	0	0	0	265	1050	8
56	225	70	36,4	0	0	1,6	0	0	0	0	0	0	0	0,8	0	0	0	0	13,4	333	5
57	210	174	96,6	0	0	3,3	0	0	0	0	0	0	0	0	0	0	0	0	17,2	484	4
58	177	122	50,3	0	0	0	0	0	0	0	0	0	0	0	0	0	0	0	29,7	349	3
59	107	136	88,4	0	0	0	0	0	0	0	0	0	0	0	0	0	0	0	8,5	332	3
60	204	126	224	0	0	0	0	0	0	0	0	0	0	0	0	0	0	0	286,4	555	3
61	696	295	1225	0	0	0	0	0	0	0	0	0	0	0	0	0	0	0	27,6	2217	3
64	232	44	114	0	0	0	0	0	0	0	0	0	0	0	0,6	0	0	0	128,0	390	4

n°total	1488	14943	
min	0	0	0
max	351	3970	9
n°max spp			**18**
con 1spp			16
con 2-3pp			20

Appendix 4.2: Morphological information of *Cyprideis torosa*: nºtotal of valves, SP (states of preservation), number of valves of each stage (f=females, m=males, j=juveniles), total number of valves (Tdv), number of black valves, valve length for females and males (noted that SD is also placed) and % noded forms.

Apéndice 4.2*: Información morfológica de* Cyprideis torosa*: nº total de valvas, SP (estados de preservación), número de valvas de cada estadio (f=hembras, m=,machos, j=juveniles),nºtotal de dobles valvas (Tdv), nº de valvas negras, porcentaje de formas nodadas, longitud de las valvas para hembras y machos (notar que la SD esta puesta).*

Depth (cm)	Number Total of valves ($10gdw^{-1}$)	Adults	Females	Males	Juveniles	Tdv	SP type B	# Noded valves	black	FEMALES length (µm)	Valves measured	MALES length (µm)	Valves measured
2		0											
4	2	0			2								
5	1	0			1								
6		0											
7		0											
8		0											
9		0											
10	1	0			1								
11	1	0			1								
12	1	0			1			1					
13	1	0			1								
14	1	0			1								
15	2	0			2								
16	2	1	1		1			1		1040	1		
17		0			0								
18		0			0								
19	2	0			2								
20	2	0			2								
21	4	0			4								
22	2	0			2								
23	7	0			7								
24	13	0			13								
25	39	1	1		38			11					
26		0			0								
27	96	5	2	3	91			10		1033,5 ± *9,2*	2	1165,7 ± *52,5*	3
28	205	5	2	3	200			34		1040 ± *18,4*	2	1204,7 ± *45,7*	3
29	97	6	2	4	91	2		28		1066 ± *36,8*	2	1150,5 ± *44,4*	4
30	38	0			38			29					
31	21	0			21	3		17					
32	52	2		2	50	3		14				1222,0	1
33	23	0			23	3		9					
34	12	0			12			5					
35	8	0			8			5					
36	2	0			2			1					

Depth (cm)	Number Total of valves ($10gdw^{-1}$)	Adults	Females	Males	Juveniles	Tdv	SP type B	# Noded valves	black	FEMALES length (µm)	Valves measured	MALES length (µm)	Valves measured
37	8	0			8			2					
38		0			0								
39	2	0			2			1					
40	10	0			10			5					
41	17	0			17			3					
42	10	0			10			9					
43	15	2	2		13	1		7		1040	1		
44	14	0			14			7					
45	5	0			5			4					
46	37	4	2	2	33	2		9		1053	1	1118 ± *110,3*	2
47	6	0			6								
48	17	3	1	2	14	4		6		1014	1	1092 ± *36,8*	2
49	19	2	2	0	17	4		6		1066	1		
50	17	8	6	2	9	1		8		1027 ± *35,6*	5	1144	1
51	11	4	2	2	7	1		4		1072,5 ± *46,0*	2	1111,5 ± *27,6*	2
52	749	65	29	36	684	17	22	152	43	1008,1 ± *45,2*	25	1116,2 ± *53,4*	31
53	3323	240	115	125	3083	228	55	71	94	1015,2 ± *40,7*	44	1100,0 ± *43,9*	45
54	4078	375	128	247	3703	100	78	121	346	1020,2 ± *54,2*	36	1103,9 ± *55,5*	37
55	935	300	93	207	635	96	96	240	138	1011,3 ± *43,2*	35	1065,3 ± *86,6*	43
56	284	87	46	41	197	11	15	22	15	953,9 ± *52,6*	50	1013,9 ± *77,9*	37
57	256	33	17	16	223	16	9	11	3	984,3 ± *87,6*	13	1017,5 ± *52,9*	12
58	232	39	28	11	193	8	4	3	0	946,7 ± *66,9*	28	1039,2 ± *108,1*	11
59	114	22	10	12	92	13	1	0	0	910,0 ± *54,6*	10	992,0 ± *45,1*	8
60	214	58	28	30	156	31	8	0	1	897,9 ± *49,2*	24	985,5 ± *42,6*	26
61	832	167	72	95	665	115	25	0	0	896,4 ± *51,2*	45	963,7 ± *58,4*	59
63	368	102	45	57	266	6	26	0	0	908,7 ± *44,0*	43	959,1 ± *45,1*	55